Bulletin

of

The Geological Society of America

VOLUME 68 March 1957 NUMBER 3

CONTENTS

	Pages
Geomorphology of Cima Dome, Mojave Desert, California. By Robert P. Sharp	273–290
Interrelated Precambrian granitic rocks, northwest Adirondacks, New York. By A. F. Buddington	291–306
Disconformity between Lower and Upper Cretaceous in western Colorado and eastern Utah. By William D. Carter	307–314
San Andreas fault zone in San Gorgonio Pass, southern California. By Clarence R. Allen	315–350
Solution-subsidence troughs, Castile Formation of Gypsum Plain, Texas and New Mexico. By Wilds W. Olive	351–358
Geophysical investigations in the Eastern Caribbean: Venezuelan basin, Antilles island arc, and Puerto Rico trench. By C. B. Officer, J. I. Ewing, R. S. Edwards, and H. R. Johnson	359–378
Short Notes	
Test on the possible chondritic composition of the earth's mantle and its abundance of uranium, thorium, and potassium. By Patrick M. Hurley	379–382
Appraisal of Ridgway and Gunnison "tillites," southwestern Colorado. By Franklyn B. Van Houten	383–388
Evidence of a pre-Taconic orogeny in southeastern Quebec. By P. H. Riordon	389–394

Subscription $15.00 per year.

Printing Office: Mt. Royal & Guilford Aves., Baltimore 2, Md.

Communications for publications should be addressed to The Geological Society of America, Dr. H. R. Aldrich, Secretary, 419 West 117 Street, New York, N. Y.

Please give notice of change of address 4 weeks in advance. Claims for non-receipt of the Bulletin of a given month must be sent to the Secretary of the Society before the end of the second succeeding month.

Entered as second-class matter at the Post Office at Baltimore, Md.
under the Act of Congress of July 16, 1894.
Accepted for mailing at special rate of postage provided for in Section 1103
Act of October 3, 1917, authorized on July 8, 1918.

PAPERS IN PRESS FOR FORTHCOMING ISSUES

Origin of Marine-Terrace Deposits in the Santa Cruz Area, California. By W. C. Bradley

Frenchman Formation of Eastern Cypress Hills, Saskatchewan, Canada. By W. O. Kupsch

Fault Structures in the Foothills and Eastern Rocky Mountains of Southern Alberta. By G. S. Hume

Volcanic Structures in Chuska Mountains, Navajo Reservation, Arizona-New Mexico. By C. R. Appledorn and H. E. Wright, Jr.

Paleocurrents of Lake Superior Precambrian Quartzites. By F. J. Pettijohn

Lithofacies of the Salt Wash Member of the Morrison Formation, Colorado Plateau. By T. E. Mullens and V. L. Freeman

Geology of Mount Holyoke Quadrangle, Massachusetts. By Robert Balk

BULLETIN OF THE GEOLOGICAL SOCIETY OF AMERICA
VOL. 68, PP. 273-290, 7 FIGS., 2 PLS. MARCH 1957

GEOMORPHOLOGY OF CIMA DOME, MOJAVE DESERT, CALIFORNIA

BY ROBERT P. SHARP

ABSTRACT

Cima Dome, a remarkably smooth symmetrical alluvium-fringed rock dome in the desert of southeastern California, is the prototype of Davis' granitic desert dome, supposedly convex and presumably developed by backwearing of a granitic fault block. Transit-stadia profiles across Cima Dome show concave or essentially straight slopes and demonstrate that it is not convex except to a slight degree in the uppermost 25 feet.

Geophysical explorations by resistivity, gravity, and seismic methods on the southeastern flank reveal no boundary fault or any form unequivocably identifiable as the convex suballuvial bench deduced by Lawson. At its deepest point the granitic rock floor is buried by 1300 feet of overburden composed of 550 feet of alluvium, or geophysically comparable material, and 650 feet of more coherent rock, presumably welded rhyolitic tuff.

Cima Dome is primarily a regraded part of an extensive late Pliocene-early Pleistocene erosion surface, Hewett's Ivanpah upland, now buried by Pleistocene volcanic rocks immediately to the west. The dome may be an erosion residual on that surface or it may have been created largely by subsequent deformation, primarily warping. Evidence cited favors the warping hypothesis. The present profile of Cima Dome is due to erosion and regrading in the current cycle, and in most places the smoothness of slope and the symmetry are due to uniform debris yielded by granular disintegration of homogeneous quartz monzonite composing the dome. The relations at Cima Dome and elsewhere suggest that the role of recent warping merits consideration with regard to the origin of closed basins, broad divides, disintegrated drainages, areas of dissection and related landscape features in the desert of southeastern California.

CONTENTS

TEXT

	Page
Introduction	274
General statement	274
Location	274
Work and acknowledgments	274
Morphological relations	274
General	274
Profile	274
Surface relief	276
Geological relations	278
Pre-Tertiary crystalline rocks	278
Tertiary(?) rhyolitic tuff	278
Cenozoic fanglomerate	278
Quaternary basaltic volcanic rocks	279
Nature of the pre-volcanic surface	280
Alluvium	280
Faults	282
Geophysical explorations	282
Testimony of Cimacito	283
Origin of Cima Dome	286
Concluding statement	288
References cited	289

ILLUSTRATIONS

Figure	Page
1. Location map	275
2. Map of pertinent geological relations at Cima Dome	276
3. Transit-stadia profiles across Cima Dome	277
4. Subsurface relations as interpreted from geophysical explorations	281
5. Transit-stadia profiles across Cimacito	284
6. Map of pertinent geological relations at Cimacito	285
7. Contour map of surface buried by older volcanic rocks west of Cima Dome	287

Plate	Facing page
1. Views of Cima Dome	276
2. Rock floor and volcanic rocks in Cima Dome area	277

Introduction

General Statement

Cima Dome has attracted the attention of arid-region geomorphologists for 40 years. Initially described by Lawson (1915, p. 26, 33) as approaching a panfan (all fan), the upper part of the dome was later shown to be bare rock (Thompson, 1929, p. 550; Blackwelder, 1931, p. 138). More recently, through the writings of Davis (1933, p. 240–243; 1936, p. 706–707; 1938, p. 1388, Pl. 1), Cima Dome has become in effect the prototype of a granitic dome supposedly evolved from a Basin-Range fault block by backwearing. A regional geological reconnaissance by Hewett (1956, p. 9, 62, 101) throws more light on the nature and origin of Cima Dome than all the earlier studies which are largely inferential or deductive.

Location

Cima Dome lies near the California-Nevada border, 175 airline miles east-northeast of Los Angeles (Fig. 1), and takes its name from the village of Cima, a section station on the Union Pacific Railroad. The summit is clearly visible 6 miles north of the railroad and 12 miles southeast of U. S. Highway 91, about 25 miles east of Baker, California. The topographic setting and form of the dome are shown in T. 14 N., R. 13 E., of the old Ivanpah quadrangle (1/250,000) and upon the newer quadrangles Mescal Range and Kelso (1/62,500).

Work and Acknowledgments

A total of 48 days was spent in the field from 1950 through 1956. The following people have contributed to this study: A. R. Sanford, C. H. Dix, D. F. Hewett, G. W. Potapenko, William Otto, C. G. Engel, C. R. Allen, R. L. Nelson, J. R. Reese, C. W. Faessler, Pierre St. Amand, G. I. Smith, G. P. Eaton, Carel Otte, and J. T. Sharp. Appreciation is expressed for their aid and counsel. The manuscript has been improved by the critical reading and constructive suggestions of the late J. L. Rich, A. D. Howard, and H. E. Wright, Jr.

Morphological Relations

General

Cima Dome covers an area of 75 square miles, the summit altitude is 5750 feet, and the base lies at 5000, 4400, and 4200 feet on the northeast, northwest, and south respectively. The dome thus rises 750 to 1550 feet above its surroundings. It lies along the axis of a highland extending from Ivanpah Mountain on the northeast to Kelso Peak on the southwest. Slopes of the dome drain east to Ivanpah Valley, north to Kingston Wash and Amargosa River, and south to Kelso Valley and Soda Playa.

Profile

The profile form of Cima Dome is critical. From a distance it appears convex (Pl. 1, figs. 1, 2) and has been so described. Davis (1936, p. 707; 1938, p. 1341, 1389) emphatically states that the upper 700 feet is convex, but Bryan (1940, p. 261–262) notes that this apparent convexity is not confirmed by the topographic map (Ivanpah quadrangle, 1/250,000). To ascertain the profile shape accurately, two transit-stadia traverses were surveyed across Cima Dome in a west-northwesterly and in a northerly direction (Fig. 2). These show clearly that the dome consists of concave or nearly straight slopes intersecting in a slightly blunted crest (Fig. 3). Essentially no summit convexity is recorded in the northward-bearing profile, and convexity appears only in the uppermost 25 feet of the northwestward-bearing profile. No topographic inflection point exists 700 feet below the summit or at the rock-alluvium contact as earlier stated (Davis, 1936, p. 706; 1938, p. 1413). New topographic maps available as preliminary blue-line prints (Mescal Range and Kelso, 1/48,000) confirm conclusions derived from the transit-stadia profiles. The several explanations advanced for convex pediments and domes may be valid (Davis, 1933, p. 220–222; 1936, p. 706; 1938, p. 1391–1392; Rich, 1935, p. 1022; Howard, 1942, p. 107–109; Fair, 1948, p. 116), but they are not needed at Cima Dome.

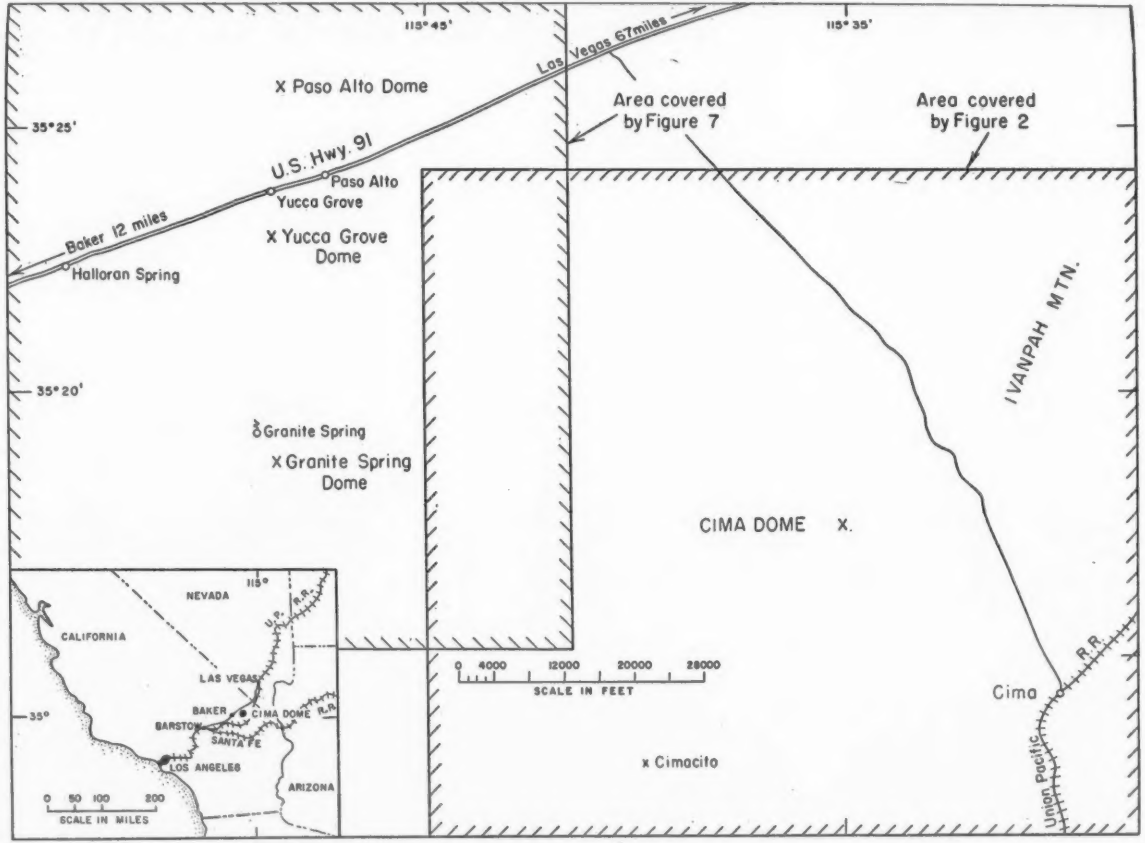

FIGURE 1.—LOCATION MAP

Surface Relief

Relief on the dome is of two varieties: (1) that resulting from residual knobs, hillocks, and ridges held above the general level by resistant rock, and (2) that due to dissection by channeled runoff.

The half dozen major knobs and hillocks rising 50–450 feet above the slopes of Cima Dome are underlain by rocks other than the predominant quartz monzonite. These include Teutonia Peak (Pl. 1, fig. 1), a group of three knobs at the northwest base of the dome (Fig. 2, *E*), a short ridge on the southwest flank (Fig. 2, *F*), and a prominent knob on the south slope (Fig. 2, *G*). The largest, Teutonia Peak, is almost as high as the dome and is actually part of a 2-mile ridge. At scattered places, dikes and silicified

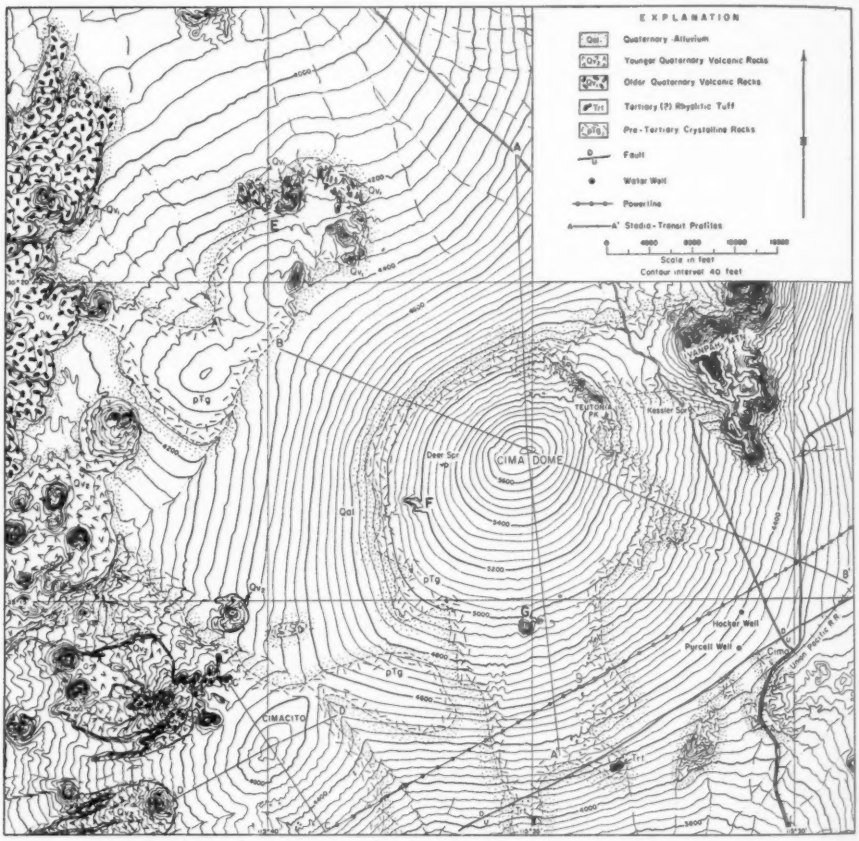

FIGURE 2.—MAP OF PERTINENT GEOLOGICAL RELATIONS AT CIMA DOME

PLATE 1.—VIEWS OF CIMA DOME

FIGURE 1.—Cima Dome from the north; erosion residual at left is Teutonia Peak.

FIGURE 2.—Cima Dome from the southwest; erosion residuals *F* at left and *G* (barely visible) at right

FIGURE 3.—Uppermost eastern slope of Cima Dome looking toward summit. Residual knobs are massive outcrops of the quartz monzonite composing the bulk of the dome.

FIGURE 1

FIGURE 2

FIGURE 3

VIEWS OF CIMA DOME

FIGURE 1

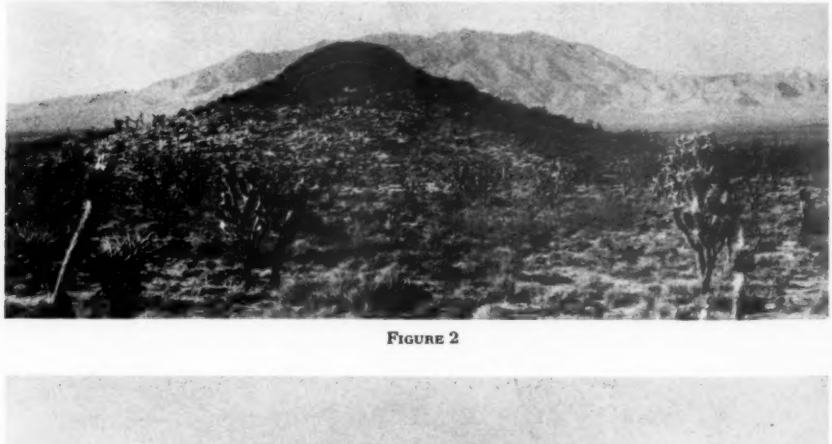

FIGURE 2

FIGURE 3

ROCK FLOOR AND VOLCANIC ROCKS IN CIMA DOME AREA

zones in the quartz monzonite form linear ridges or abrupt risers a few to 25 feet high interrupting the otherwise relatively smooth slopes. Low on the south flank a varied topography having 25 feet of relief is related to the discontinuous and are seemingly due to channelization of runoff between the residuals.

More significant than the features of relief are areas of remarkably smooth rock surface extending over hundreds of acres on the flanks

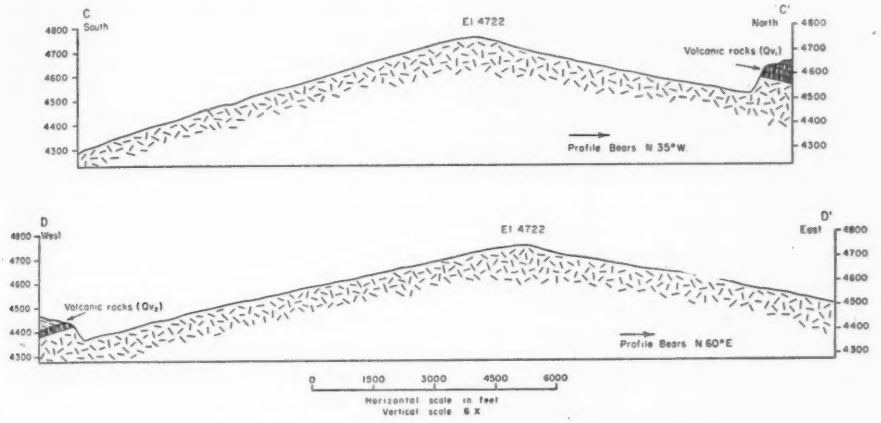

FIGURE 3.—TRANSIT-STADIA PROFILES ACROSS CIMA DOME
Slopes not true owing to 6× exaggeration of vertical scale.

variety of rocks there exposed. On upper parts of the dome are numerous knobs and hillocks, as much as 35 feet high (Pl. 1, fig. 3), composed of exceptionally massive quartz monzonite.

Dissection has been greatest on the east and southeast slopes which drain to Ivanpah Valley. A wash near Kessler Spring at the east base has cut 30 feet into granitic rock, and gullies higher on the dome in this area are intrenched 10–15 feet. This dissection is probably related to concentration of runoff between Cima Dome and Ivanpah Mountain to the east as suggested by Davis (1933, p. 242). Other parts of the dome, particularly the upper slopes (Pl. 1, fig. 3) and the lower south flank, have washes between residual knobs and ridges. These are of the dome. Good examples are on the south flank 1–3 miles east of the residual ridge at *F* (Fig. 2) and on the west flank north of Deer Spring (Pl. 2, fig. 1).

With the possible exception of the smooth rock floor, the sheet-flood robbing deduced by Davis (1933, p. 222; 1938, p. 1391–1392) is prevented by the channels on the upper slopes of Cima Dome. Some of the lowermost smooth alluvial slopes have small channels as much as 1 foot deep, 2–3 feet wide, and 100–200 feet long that start abruptly and end in a lobate tongue of loose gruss. Although these channels somewhat resemble features attributed to sheet floods by McGee (1897, p. 102), they look more like the product of local concentrated flow here, as they are not part of a braided network.

PLATE 2.—ROCK FLOOR AND VOLCANIC ROCKS IN CIMA DOME AREA

FIGURE 1.—Rock floor on quartz monzonite high on west slope of Cima Dome. Three-quarters of a mile northeast of Deer Spring.

FIGURE 2.—Outlier of older lava resting on smooth rock floor, 50 feet above surface currently graded to Cima Dome. Near *E* (Fig. 2) at northwest base, looking north.

FIGURE 3.—Younger volcanic cones and flows west of Cima Dome, looking west.

Geological Relations

Pre-Tertiary Crystalline Rocks

The rock most widely exposed on Cima Dome is light-gray homogeneous coarsely crystalline quartz monzonite, locally porphyritic (Hewett, 1956, p. 61–65). This material weathers rapidly by granular disintegration and is one of the least resistant "hard" rocks exposed in this desert region. The smooth gentle slopes, low relief, and symmetry of Cima Dome are clearly due in large part to the uniform weathering of this rock which yields debris of a grain size that can be transported on such slopes.

The principal knobs and hillocks rising above the smooth flanks of Cima Dome are composed of medium-grained uniform biotite granite, medium-grained muscovite and biotite quartz monzonite, aplite, pegmatite, quartz veins, a gneissic granitic porphyry containing abundant phenocrysts, and a contorted gneiss. The last two rock types appear to be older than the quartz monzonite and are probably inclusions or roof pendants in it. The others may be genetically related to the quartz monzonite but are more resistant to weathering because they contain more quartz and are of finer texture. An area of rough topography on the southern slope below the knob *G* (Fig. 2) is underlain by masses of gneissic porphyry, fine-grained granitic rocks, and a dark microgabbro or diabase. The quartz monzonite is cut by small dikes of aplite and of hornblende trachyte porphyry which are of minor topographic significance.

The quartz monzonite has a well-defined wide-spaced joint system which, because it shows no genetic relation to the present form of the dome, is presumably earlier. Weathering and erosion along the joints determine minor topographic forms such as drainage courses and the shape of rock exposures.

Tertiary (?) Rhyolitic Tuff

Low on the south slope of the dome, 3.5 and 5.5 miles southwest of Cima, are two small exposures of welded rhyolitic tuff (Fig. 2), unlike any other rock seen in the area. The easternmost and larger exposure covers 2–3 acres. Comparable material may be buried beneath the alluvium, for rhyolitic tuff was reported in cuttings from a well near Cima (D. F. Hewett, personal communication), and geophysical explorations on the southeast flank indicate a suballuvial rock layer which has a seismic velocity appropriate for welded rhyolitic tuff.

In outcrops the rhyolitic tuff rests with sharp depositional contact on a complex of crystalline rocks resembling the Precambrian units south of Cima (Hewett, 1956, Pl. 1). Crude layering at the eastern exposure strikes approximately N. 70° E. and dips 5°–10° SE. The tuff ranges from buff to pink and shows various degrees of density and coherence. Some of the most firmly welded material contains fragments and crystals of quartz and feldspar in a glassy tuffaceous matrix. Other less dense and less coherent layers consist predominately of glass and welded pumice fragments. Fragments of calcic plagioclase (labradorite to andesine) and of granitic rock suggest that the tuff picked up considerable foreign material in transit.

The age of the rhyolitic tuff is not known. It is probably older than Quaternary basaltic materials west of Cima Dome. Hazzard (1936, p. 57, 59) reports somewhat similar Quaternary or Tertiary rhyolitic tuffs in the Bengal quadrangle immediately to the south and tuffs of doubtful Miocene age in the nearby Providence Mountains (Hazzard, 1954, p. 28). The material on Cima Dome is possibly Tertiary (?).

Cenozoic Fanglomerate

This formation is not exposed on Cima Dome, but it represents a significant episode in the evolution of the region and may be present within material on the southeast flank of the dome interpreted as alluvium on the basis of geophysical data. These deposits are best seen 15 miles to the northwest in the Yucca Grove-Halloran Spring area (Fig. 1). Because most of the fanglomerate is buried by volcanic rocks the areal extent cannot be determined accurately, but it is not less than 25 square miles. As expected in deposits of this type, the constitution changes rapidly within short distances from coarse bouldery fanglomerate to sand, silt, and mudstone. Beds of reworked granitic gruss are characteristic and constitute as much as 60–70 per cent of some sections.

The best exposures are along the north face of a high, lava-capped tableland 3 miles south of U. S. Highway 91 near Yucca Grove (Fig. 1). The predominate material here is reworked granitic gruss containing scattered granitic boulders, most of which are 1–5 feet and some up to 10 feet in diameter. Also present are bouldery layers with a sparse sandy to gravelly matrix, and beds of fine gravel, sand, silt, mudstone, and at least one layer of white china clay.

The composition of boulders in the fanglomerate varies with location, although granitic types predominate; and in some of the western and central exposures only one granitic rock is represented. To the east, in addition to granitic boulders, gneiss, schist, basic igneous types, aplite, and a few limestone fragments are present. As these lithologies are represented in the bedrock of the vicinity, the formation is clearly of local derivation.

Most of these deposits are loose and unconsolidated, and exposures are poor except in steep faces protected by a capping of lava. Locally, well-cemented arkose beds form small outcrops. Predominate colors range from nearly white in the south through light gray and tan, to pink and reddish in the north. The maximum thickness seen in continuous exposure is about 500 feet.

The deposits are well stratified, and dips are as great as 50°. The basal contact of the formation has not been seen, but from general relations the fanglomerate is inferred to be nonconformable with underlying pre-Tertiary crystalline rocks. Overlying Quaternary volcanic materials make an angular unconformity as great as 55°. Exposures of the fanglomerate are generally so poor that details of structure cannot be worked out, but warping or folding in addition to possible faulting is inferred from topographic forms. The drainage pattern in low hills underlain by fanglomerate on the southeast, east and northeast flanks of the Yucca Grove Dome (Fig. 1) suggests a concentric structure in the fanglomerate conformable with the dome. This impression could not be confirmed by measurements of attitude owing to lack of outcrops. The fanglomerate is clearly younger than the pre-Tertiary crystalline rocks and older than mid-Pleistocene volcanic materials. It may be late Tertiary or more likely early Quaternary.

Quaternary Basaltic Volcanic Rocks

Immediately west of Cima Dome is a volcanic field of 26 well-defined cones, at least a dozen other vents, and plugs, dikes, and flows covering about 75 square miles (Hewett, 1956, p. 103). Two stages of volcanism are represented, both probably Quaternary, and the younger includes activity possibly no more than a few thousand years old. These volcanic rocks extend to the base of Cima Dome on the west (Pl. 2, fig. 3) and northwest (Pl. 2, fig. 2).

The older volcanic rocks consist chiefly of olivine basalt flows, layers of compact agglomerate, and beds of loose pyroclastics. The aggregate thickness is 25–50 feet in many places, but close to vents it approaches 200–400 feet (Hewett, 1956, p. 104). The flows are thin, dense to vesicular, locally contain large crystals of clear vitreous olivine and feldspar, and display a modest range in color, texture, and possibly composition.[1]

Most of the older volcanic materials have been extruded from at least 12 separate vents. The cones formerly surrounding these vents are extensively eroded, and the vents are identified principally by a greater thickness of volcanic materials, an abundance and coarseness of pyroclastic debris, steeply inclined layering, plugs of lava or agglomerate, and associated dikes. The vent nearest Cima Dome lies among the knobs at the dome's northwest base (Fig. 2, *E*). This vent has a central breccia plug containing large granitic boulders mixed with volcanic fragments. The surrounding pyroclastic deposits contain much granitic gruss and are at least 200 feet thick. Other vents lie to the west; one, at an altitude of 4954 feet could have supplied the highest flows in the area.

The older volcanic rocks have been dissected to a maximum depth of 1000 feet in an area 15 miles northwest of Cima Dome and have been widely stripped from the surface onto

[1] On the basis of field and thin-section identification the lavas are termed basalts primarily because they contain olivine. A chemical analysis of a flow in this series near Halloran Spring by Celeste G. Engel, however, shows that the rock has the composition of an andesite.

which they were extruded. This dissection affords many good exposures of the basal contact, and a wide variety of stratigraphic relationships have been observed. The basal volcanic materials differ from place to place among: flows, firm agglomerate, breccia, or loose pyroclastic debris. Early phases of the volcanism must have been intermittent and must have preceded the principal eruptions by a sufficient time to allow for the transportation and mixing of early pyroclastic debris with gruss and granitic gravel. Erosion of some early flows also provided components for a basalt-cobble gravel which was spread across parts of the pre-volcanic surface before burial by later eruptions.

The younger volcanic series lies principally south of the older volcanic rocks but locally overlaps them. It is represented by cinder cones 200–400 feet high (Pl. 2, fig. 3), and in most places lava flows have an aggregate thickness of 20–25 feet but attain a maximum of 74 feet locally. Individual flows are a few feet thick and are dense to vesicular.

The younger flows rest upon a smooth granitic rock surface a maximum of 25 feet above washes graded to the slopes of Cima Dome. The granitic rock below these younger flows is relatively fresh and thinly mantled with weathered or transported debris. This rock surface was developed along broad channels cut below the older volcanic series. The younger volcanic rocks have been dissected 25–35 feet and locally have been removed by stripping. Their age is probably late Pleistocene, although some eruptions possibly occurred within the last few thousand years (Hewett, 1956, p. 104).

The exposures of basalt closest to Cima Dome are at the northwest base, 4.5 miles from the summit (Fig. 2, *E*). More extensive remnants lie 6 miles to the west and southwest. Searches for volcanic rocks on Cima Dome yielded only four small fragments of basalt at widely separated points. Two of these were clearly Indian grinding stones, and they all may have been artificially transported. No argument for a former covering of lava on Cima Dome can be made on the basis of these fragments. A number of hornblende trachyte dikes intrude the quartz monzonite composing the dome but are not of proper composition to have served as the feeding channels of the Quaternary basalts.

Nature of the Pre-Volcanic Surface

The older lavas were erupted onto a surface of low relief cut largely upon granitic rocks but locally truncating fanglomerate. In most places the underlying granitic rock shows extensive weathering; a residual mantle of gruss a few feet thick rests upon 10–75 feet of oxidized and partly disintegrated rock. In some places the uppermost gruss is calichified, and locally it is overlain by a brown calichified clayey soil, locally reddened by contact with the lavas. Veinlets of caliche project many feet downward along fractures into the underlying rock. In a few exposures the volcanic and granitic rocks are separated by a conformable mantle of 50–75 feet of transported but poorly bedded gruss containing fragments of crystalline rock and much intermixed pyroclastic material. Bedded pyroclastic debris containing large granitic boulders was also seen along the contact, and at one locality 10–20 feet of gravel consisting of well-worn cobbles of basalt underlies the basal lava flows.

Much of the pre-volcanic surface is exceedingly smooth, and the local relief does not exceed a few tens of feet (Pl. 2, fig. 2). On a larger scale, the surface exhibits a rolling topography (Fig. 7) featuring smooth domes and rounded ridges which rise with slopes of 1°–4° above the surrounding terrain and attain elevations from a few hundred to nearly 2000 feet higher. In addition, knobs of non-granitic "hard" rocks rise more abruptly above the surface.

Alluvium

The alluvium mantling the lower slopes of Cima Dome is gruss produced by granular disintegration of the quartz monzonite. It consists of crystal aggregates, individual crystals, and crystal fragments, chiefly of feldspar and quartz, averaging 1.8 mm in diameter and ranging from 15 mm to smaller than 0.35 mm. Particles smaller than 0.35 mm compose from 7 to 40 per cent of samples of this material. The mean grain size, as determined by mechanical analysis of samples from a radial profile down the southeast flank, decreases downslope, seemingly in closer relation to the distance of transport than to the degree of slope. The

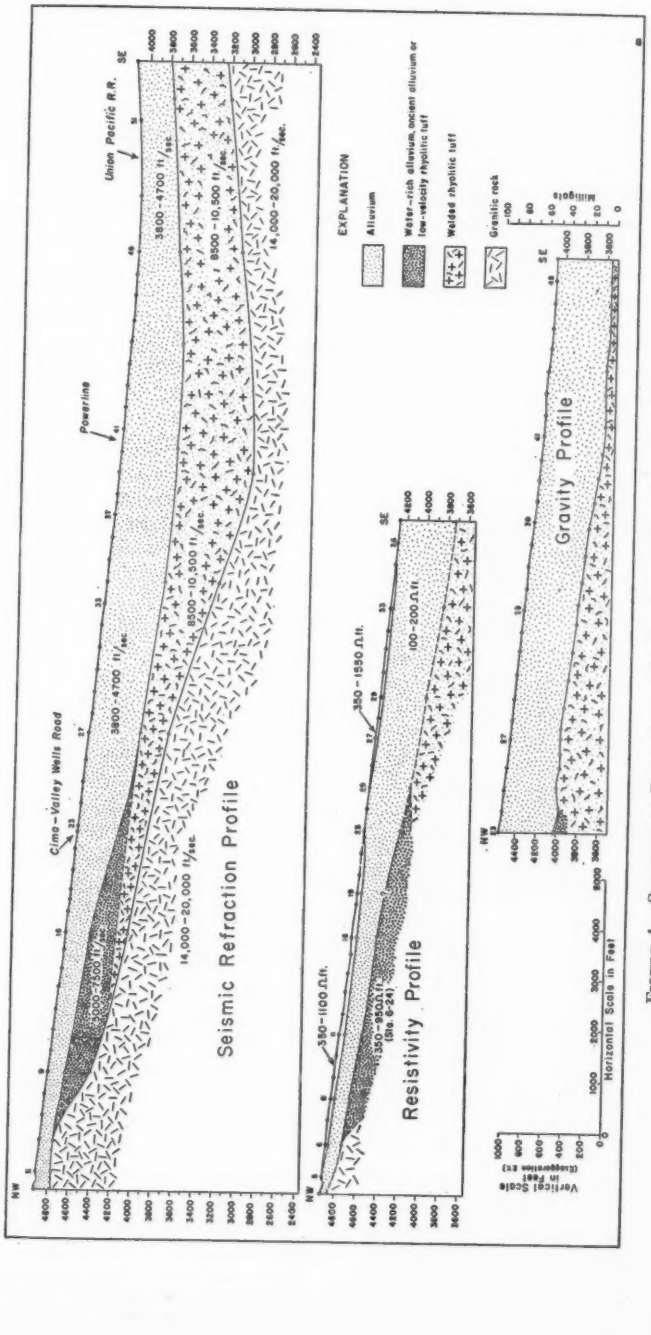

FIGURE 4.—SUBSURFACE RELATIONS AS INTERPRETED FROM GEOPHYSICAL EXPLORATIONS
Location is along profile BB′ (Fig. 2) on lower southeast flank of Cima Dome.

surface layer is enriched in coarser particles owing to removal of fines by rain wash and perhaps to some degree by wind. The alluvium includes a few cobbles of aplite, trachyte, silicified quartz monzonite, and vein quartz. Near residual hillocks of resistant rock stones are more abundant, although gruss is still the predominant component.

The exposed alluvium is crudely layered and has been deposited intermittently, as shown by zones of reddish somewhat clayey soil, underlain by calichified material, that were penetrated by the 12- to 14- foot seismic shot holes. In thickness the alluvium, or geophysically comparable deposits, ranges from a feather edge at the exposed bedrock to at least 550 feet near station 33 on the geophysical profile (Fig. 4). A well on the Purcell property 0.8 mile west of Cima is said to penetrate 700 feet of unconsolidated material without striking rock. Judging from rock exposures, the alluvium is probably not this thick on other parts of the dome, especially the western, eastern, and possibly some parts of the northern and southern slopes. The 550 feet of unconsolidated material on the southeast flank may include deposits older than the surface alluvium, for the contact between these materials and the granitic basement is truncated at a small angle by the present surface in a manner suggestive of erosion and regrading (Fig. 3). The bedrock-alluvium contact has been mapped in some detail on air photos and is represented in generalized fashion on Figure 2. This contact lies 600–700 feet below the crest, about half way down the flank of the dome.

Faults

The only significant fault on the south side of Cima Dome inferred from surface relations extends west-southwestward through Cima (Fig. 2). The fault trace is indicated by aligned bedrock knobs and ridges on the south side in the area mapped and to the east. The rocks south of the fault are considered Precambrian (Hewett, 1956, Pl. 1), and that side is inferred to be upthrown. The existence of the fault and this direction of displacement are confirmed by the Purcell well which penetrates 700 feet of unconsolidated deposits, 0.5 mile north of Precambrian outcrops south of the fault. The patches of rhyolitic tuff south of the fault farther west may seem inconsistent with the inferred displacement; but if such material is buried under alluvium to the north as suggested by the geophysical explorations farther east, these exposures indicate upward displacement of the south side.

Geophysical data give no indication of other faults low on the southeast flank of Cima Dome, and there is no known evidence supporting Davis' (1933, p. 240) inference that Cima Dome is the remnant of an uplifted fault block. His statement as to the faulted nature of Kelso Peak may be sound, however, for a Union Pacific Railroad well at Kelso, 18 miles west-southwest of Cima, in the valley south of Kelso Mountain penetrates 1970 feet of sand, gravel, clay, and conglomerate.[2] Displacement along the Cedar Canyon fault (Hewett, 1956, p. 105–106) could account for these relations.

Geophysical Explorations

The form of the suballuvial rock surface under the lower slopes of the dome is of interest with respect to the postulated fault-block nature of the Cima Dome mass (Davis, 1933, p. 240), the possible existence of a convex suballuvial bench of the type deduced by Lawson (1915, p. 34), and the evolution of the dome. Three geophysical methods were used to determine the depth and configuration of the buried rock surface along the southeastern third of profile *BB'* (Fig. 2). A resistivity survey was made in the spring of 1950, seismic explorations were carried out in 1951, 1952, and 1953; and C. H. Dix and A. R. Sanford made a gravimetric traverse along part of the same profile in 1954.

Although the resistivity data are difficult to interpret, they seem to give a reasonable indication of the depth of alluvium as judged by other means (Fig. 4). These data do not permit a distinction between welded tuff and granitic rock, but they indicate variations within the alluvium (Fig. 4) that are possibly caused by differences in moisture content.

[2] Log of well kindly furnished through the courtesy of William Reinhardt, Vice President, Union Pacific Railroad Company.

Seismic explorations were carried out wholly by refraction, except for one doubtful reflection recorded near station 49 (Fig. 4). Portable six-trace Century Geophysical equipment was used. Shot holes were dug by hand auger to a maximum depth of 14 feet, calichified layers in the alluvium making even this shallow penetration difficult, and charges, up to 10 pounds of 60 per cent seismic dynamite, were tamped by water, wet gruss, or cemented into the holes.

Figure 4 presents an interpretation made from the seismic records by A. R. Sanford. The pertinent points are: (1) There is no indication of a major boundary fault along the south side of Cima Dome as inferred by Davis. (2) Some suggestion of upward convexity on the submerged granitic surface is seen under station 27 (Fig. 4) and more markedly between stations 5 and 9. Faint convexity is seen along the contact between alluvium and water-rich alluvium (?) between stations 16 and 19. The data points are so few, the convexity except between stations 5 and 9 so faint in relation to the accuracy of the measurements, and explanations such as regrading so plausible, that a strong case cannot be made for the existence of a convex suballuvial bench of the Lawson type on the southeast flank of Cima Dome. (3) The maximum thickness of alluvium, or equivalent unconsolidated deposits, is 550 feet. Wells on the C. A. Purcell property 0.8 mile west of Cima and on the Earl Hocker ranch 1 mile northwest of Cima (Fig. 2) are reported to penetrate 700 feet and 200 feet of unconsolidated material respectively without reaching bedrock. These wells are 1–2 miles southwest of the geophysical profile line. (4) A layer of material with a maximum thickness of 650 feet and seismic velocities of 8500 to 10,500 feet per second lies between the alluvium and the granitic bedrock over most of the profile. This layer is probably composed of welded rhyolitic tuff of the type observed 3.5 and 5.5 miles southwest of Cima (Fig. 2) and reported to have been brought up in well cuttings at Cima (D. F. Hewett, personal communication). The seismic velocities are suitable for such a rock and too high for almost any type of alluvium or unconsolidated material. Laboratory[3] measurements on specimens of rhyolitic tuff from the small exposures on the south flank of the dome indicate seismic velocities ranging from 8570 to 10,075 feet per second under a pressure of 500 pounds per square inch, dry. These figures support the inference that the buried rock layer is welded rhyolitic tuff. It is unlikely that this layer is composed of Quaternary basaltic materials like those west of Cima Dome, because the thickness is too great and the seismic velocities are too low for any series containing considerable solid lava. (5) A layer of material with seismic velocities of 5000–7500 feet per second near the northwest end of the profile (Fig. 4) may be water-rich alluvium, moistened by springs and seeps higher on the dome. This possibility is supported by the report of some water at a depth of 390 feet in the Purcell well near Cima. The possibility that this layer may be less firmly welded rhyolitic tuff is not supported by laboratory tests showing seismic velocities of 8500 feet per second for specimens of relatively soft tuff. It might possibly consist of fanglomerate such as that found under the basaltic flows west of Cima Dome, although the velocity seems high for such material. (6) The granitic rock surface is buried most deeply, about 1300 feet, near station 40 which is approximately 0.75 mile northwest of the topographic axis of the present valley.

An interpretation of the gravity survey has been made by A. R. Sanford (Fig. 4). The gravity data do not provide independent determinations of depth, but they do reveal minor variations in the configuration of the buried bedrock surface. They confirm the seismic results, especially the general smoothness and lack of consistent convexity in the suballuvial rock surface, and the absence of any major fault along the southeast flank of the dome. The local relief on the suballuvial rock surface nowhere exceeds 35–50 feet along the profile line (Fig. 2, *BB'*), judging from the gravity data.

Testimony of Cimacito

Seven miles southwest from the top of Cima Dome is a much smaller granitic dome herein called Cimacito for purposes of identification (Fig. 2). With some exceptions Cimacito is a

[3] Made through the courtesy and co-operation of California Research Corporation.

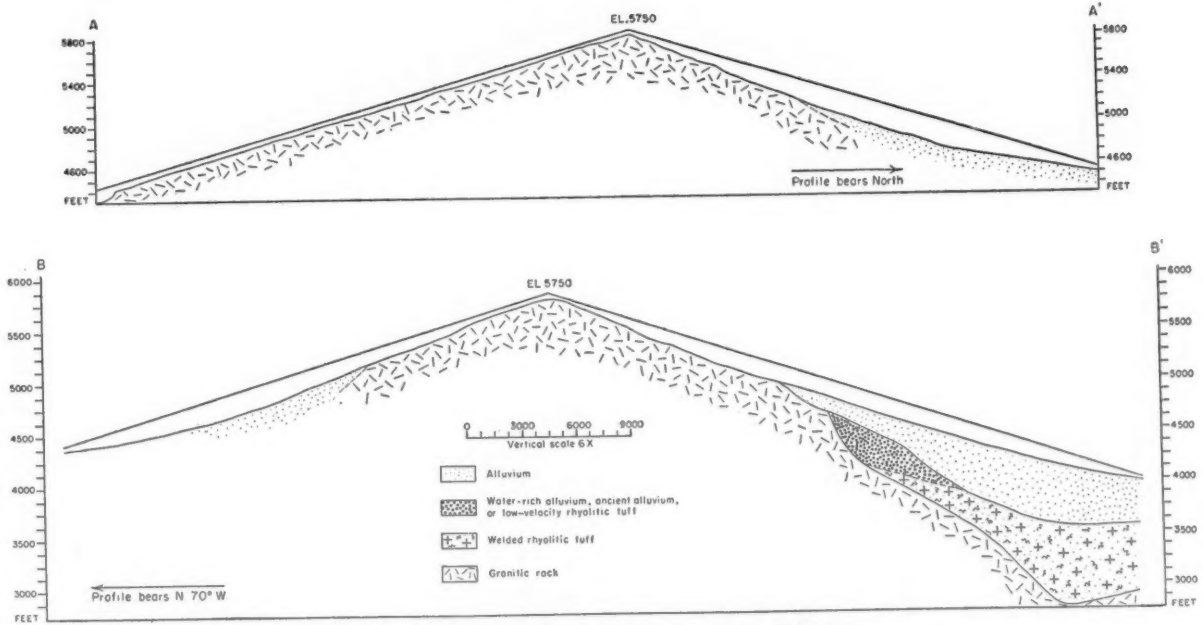

FIGURE 5.—TRANSIT-STADIA PROFILES ACROSS CIMACITO
Slopes and dips in lavas not true owing to 6× exaggeration of vertical scale.

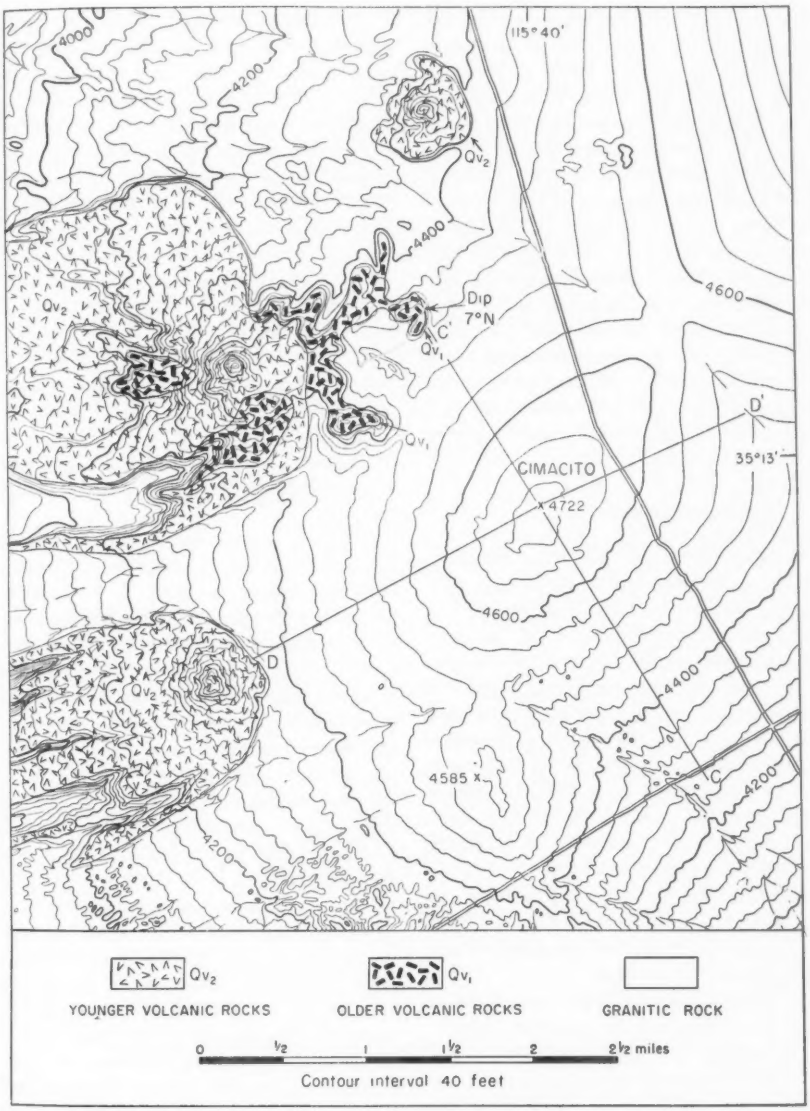

FIGURE 6.—MAP OF PERTINENT GEOLOGICAL RELATIONS AT CIMACITO

small-scale replica of Cima Dome. It covers 6 square miles and rises 200–300 feet to an altitude of 4722 feet. The smooth slopes of Cimacito are almost straight in profile and intersect without perceptible crestal convexity, as shown on transit-stadia profiles (Fig. 5). Relief almost nowhere exceeds 5 feet, and the cover of detrital gruss is thin even on the lower flanks. Cimacito is reasonably symmetrical except for longer slopes to the west and south and for the fact that it is but one of two rounded summits on a ridge 4 miles long (Fig. 6).

The significance of Cimacito lies in the fact that remnants of Quaternary basalt are perched

on low hills along its southwestern, western, and northwestern flanks (Figs. 5, 6). At the north base, flows and pyroclastic debris of the older series dip as much as 7° away from the dome and rest on a smooth granitic rock floor 50–75 feet above the present surface of Cimacito. The lavas to the west are of the younger series and slope westward from Cimacito at a more gentle angle. These relations suggest that Cimacito was once partly or perhaps wholly covered by volcanic rocks which were subsequently dissected and removed by stripping. During this process at least 50–100 feet of granitic material was removed, and the slopes were regraded. No volcanic fragments were found on Cimacito more than 200 feet from the present volcanic outcrops, even though the dome may have once been covered by volcanic rocks.

Origin of Cima Dome

Cima Dome is thought to be a regraded part of the Ivanpah upland (Hewett, 1956, p. 101–102), an extensive erosion surface of late Pliocene to early Pleistocene age covering several hundred square miles in the eastern Mojave Desert. It may have been a residual feature on that surface, or it may have been created by subsequent deformation. In either instance, erosion and regrading in the present cycle have modified it considerably. Nothing found during this study suggests that Cima Dome evolved from a fault block by backwearing in the present cycle or earlier.

Four smaller but similar granitic domes, some partly buried by lava, lie immediately west of Cima Dome (Fig. 1). For purposes of this report, they have been named the Paso Alto, Yucca Grove, Granite Spring, and Cimacito domes. The first three are domelike summits along a broad north-south ridge (Fig. 7). Cimacito lies farther southeast and is one of two summits on a shorter ridge which is perhaps part of a much larger northeast ridge that includes Cima Dome and Ivanpah Mountain (Fig. 1).

Fully 80–90 per cent of the Ivanpah upland in this area truncates granitic rocks. The associated fanglomerates, the weathered mantle, the caliche, and the general topographic form suggest that this surface was developed under arid conditions, possibly under conditions of through-flowing drainage rather than of closed basins and local base levels as at present (Hewett, 1956, p. 101). The recession of steep granitic faces undoubtedly played a major part in producing the smooth gently sloping surfaces characterizing the upland. Thus, the domes and ridges could represent the sites of residual high areas last consumed by the process of slope retreat. The form and distribution of these features and the bedrock structure suggest that the retreating faces were not fault scarps but steep slopes created by dissection of a large uplifted granitic mass. Areas displaying this type of development in a less-advanced stage are found today in other parts of the southern California deserts. If this picture is correct, Cima Dome might be simply the largest of the residual features on the Ivanpah upland in this area.

Although the idea that Cima and the other domes of the Ivanpah upland are residual forms has an appealing simplicity, it is desirable to inquire into the possible role of deformation in the development of these features. The Ivanpah upland presumably evolved under arid conditions at a considerable distance from the sea, so it could have been formed at its present altitude of 4000–5000 feet, but uplift to that elevation is just as likely. Under any circumstances, considerable deformation subsequent to the development of the upland was necessary to produce troughs as deep as Ivanpah and Kelso valleys (Hewett, 1956, p. 105). Furthermore, warping of the Ivanpah upland is suggested by the following relations: (1) The older volcanics at the north base of Cimacito dip away from the dome at an angle greater than the present slopes of the dome. (2) Dips up to 7° have been measured on a smooth granitic surface, part of the Ivanpah upland, where preserved under a capping of lava. The slopes on corresponding surfaces on similar rock in the present topography do not exceed 4° and are generally less. (3) The buried rock surface as traced by geophysical explorations on the southeast flank of Cima Dome is more steeply inclined than the present near-by graded alluvial and rock surfaces (Fig. 4). If the buried rock surface were graded, there is little reason for it to be steeper unless subsequently deformed. (4) The rock

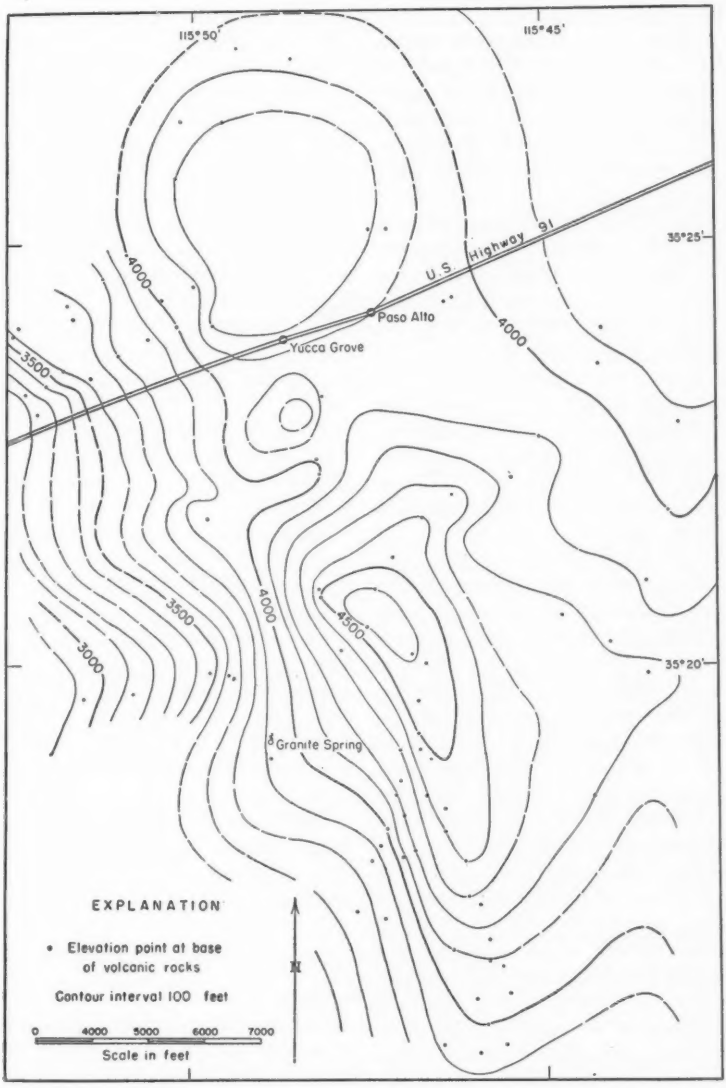

FIGURE 7.—CONTOUR MAP OF SURFACE BURIED BY OLDER VOLCANIC ROCKS WEST OF CIMA DOME

underlying Cima Dome weathers with comparative rapidity and ease, and there is no apparent reason why it should constitute a high-standing erosional remnant. (5) The highest part of the pre-volcanic surface, now preserved under the older lavas, is underlain by relatively soft unconsolidated fanglomerates which stand higher than near-by areas of granitic rock. It is difficult to find a source for these fanglomerates or to understand why they compose a high-standing mass unless uplifted. (6) No consistent thickening of lavas in present lower areas or thinning over higher areas is noted as might be expected if the flows

had been erupted onto a rolling landscape having a relief as great as that of the present surface. The vertical distribution of older lavas does not require warping, however, for one of the older vents at an elevation of 4954 feet is high enough to supply by gravity flow any of the lava remnants in the area west of Cima Dome.

If warping occurred, it need not have been severe, for broad areas are involved, and the inclinations produced by warping need not have exceeded 3° or 4°. Although the present features suggest local domical warping, an alignment along a north axis in one instance and possibly along a northeast axis in another is apparent. Warping of a large granitic mass with little overburden might be accomplished by small displacements along pre-existing joints and fractures. A study of joints on Cima Dome revealed none that seem genetically related to the form of the dome.

Warping may have occurred more than once. Relations suggesting warping following eruption of the older volcanic rocks have already been cited. In addition, the inferred domical structure in fanglomerates on the east flank of Yucca Grove dome and the angular unconformity between these fanglomerate beds and the older lavas suggest an earlier period of deformation which possibly created the Yucca Grove dome. This earlier warping may have been considerably more severe than the younger stage, and either or both might have played a part in creating Cima Dome.

A firm conclusion as to whether Cima Dome is primarily a residual feature on the Ivanpah upland or the product of subsequent warping cannot perhaps be drawn from the available data, and to some degree both explanations may apply. However, the possibility of warping is here favored. The existing form of Cima Dome is the product of regrading in the present cycle no matter what its origin. In the process of regrading, not less than 100–150 feet of granitic rock has been removed from the upper slopes of the dome.

The sequence of events in the evolution of Cima Dome is as follows:

(1) Late Pliocene to early Pleistocene erosion produced an extensive surface of low relief on granitic rocks in the eastern Mojave Desert. This surface may or may not have had domelike residual forms.

(2) During or following this period some slopes were locally steep enough to supply granitic gruss and boulders for the formation of fanglomerate deposits several hundred feet thick in the Yucca Grove-Halloran Spring area.

(3) The fanglomerate beds were deformed, possibly in part by warping, which may have created one or more low domes or ridges on the granitic erosion surface.

(4) Subsequent erosion truncated the deformed fanglomerates, removed them from some areas, and further smoothed the granitic surface.

(5) In the middle Pleistocene, volcanic eruptions spread a mantle of basaltic lava and pyroclastic debris across much of the erosion surface.

(6) Further deformation, presumably warping, gently deformed the volcanic rocks and the underlying surface and created or accentuated granitic domes and ridges (Fig. 7).

(7) Erosion dissected the volcanic rocks, stripped them from extensive areas, removed part of the underlying materials, and regraded local surfaces to lower levels.

(8) Further volcanic eruptions built cones and spread lavas over parts of these lower surfaces.

(9) Erosion shallowly dissected the younger lavas, stripped them from small areas, and further regraded the landscape to its present condition.

Concluding Statement

There is no evidence here, or insofar as known elsewhere in the Mojave Desert, which indicates that desert domes normally evolve into convex forms. Longitudinal convexity of pediments (Gilluly, 1937, p. 333) and pediment passes (Howard, 1942, p. 95, 99) has been described, but it is said to be an exception (Tator, 1952, p. 302) and may even reflect a two-cycle history (King, 1949, p. 246). If the evidence from Cima Dome, Cimacito, and other granitic domes observed in the Mojave Desert is representative, the efforts to explain

convex desert domes may have been pointless as it is yet to be shown that domes of any marked convexity exist.

Cima Dome directs attention to the possible role of recent warping in determining some aspects of the present landscape in the Mojave Desert. Baker (1911, p. 367), Noble (1927, p. 32; 1932, p. 360), and Hewett (1954, p. 18) have recognized the possibility of warping in this region, and Noble (1941, p. 989–990) and Bowen (1954, p. 102–103) have clearly demonstrated its significance in the Death Valley and Barstow areas, respectively. If the warps are broad and gentle, they are extremely difficult to recognize unless associated with some geological unit giving a pre-warp datum surface. Much of the disintegrated drainage, some of the topographic basins and divides, some of the dissection, and some of the alluvial fills of the Mojave Desert may be more the products of warping than of faulting or climatic change.

References Cited

Baker, C. L., 1911, Notes on the later Cenozoic history of the Mojave Desert region in southeastern California: Univ. Calif. Pub., Bull. Dept. Geol. Sci., v. 6, p. 333–383

Blackwelder, Eliot, 1931, Desert plains: Jour. Geology, v. 39, p. 133–140

Bowen, O. E., 1954, Geology and mineral deposits of Barstow quadrangle, San Bernardino County, California: Calif. Div. Mines Bull. 165, 185 p.

Bryan, Kirk, 1940, The retreat of slopes: Assoc. Am. Geographers Annals, v. 30, p. 254–268

Davis, W. M., 1933, Granitic domes of the Mohave Desert, California: San Diego Soc. Nat. Hist., v. 7, p. 211–258

—— 1936, Geomorphology of mountainous deserts: 16th Internat. Geol. Congr. Rept., Washington, v. 2, p. 703–714

—— 1938, Sheetfloods and streamfloods: Geol. Soc. America Bull., v. 49, p. 1337–1416

Fair, T. J. D., 1948, Slope form and development in the interior of Natal, South Africa: Geol. Soc. S. Africa Trans., v. 50, p. 103–118

Gilluly, James, 1937, Physiography of the Ajo Region, Arizona: Geol. Soc. America Bull., v. 48, p. 323–348

Hazzard, J. C., 1936, Notes on the Cambrian rocks of the eastern Mojave Desert, California: Univ. Calif. Pub., Bull. Dept. Geol. Sci., v. 23, p. 57–80

—— 1954, Rocks and structure of the northern Providence Mountains, San Bernardino County, California: Calif. Div. Mines Bull. 170, Chap. IV, p. 27–35

Hewett, D. F., 1954, General geology of the Mojave Desert region, California: Calif. Div. Mines Bull. 170, Chap. II, p. 5–20

—— 1956, Geology and mineral resources of the Ivanpah quadrangle, California and Nevada: U. S. Geol. Survey Prof. Paper 275, 172 p.

Howard, A. D., 1942, Pediment passes and the pediment problem: Jour. Geomorphology, v. 5, p. 3–31, 95–136

King, L. C., 1949, The pediment landform: some current problems: Geol. Mag., v. 86, p. 245–250

Lawson, A. C. 1915, The epigene profiles of the desert: Univ. Calif. Pub., Bull. Dept. Geol. Sci., v. 9, p. 23–48

McGee, W J, 1897, Sheetflood erosion: Geol. Soc. America Bull., v. 8, p. 87–112

Noble, L. F., 1927, The San Andreas rift and some other active faults in the desert region of southeastern California: Seismol. Soc. America Bull., v. 17, p. 25–39

—— 1932, The San Andreas rift in the desert region of southern California: Carnegie Inst. Wash. Yearbook 31, p. 355–372

—— 1941, Structural features of the Virgin Spring area, Death Valley, California: Geol. Soc. America Bull., v. 52, p. 941–1000

Rich, J. L., 1935, Origin and evolution of rock fans and pediments: Geol. Soc. America Bull., v. p. 999–1024

Tator, B. A., 1952, Pediment characteristics and terminology: Assoc. Am. Geographers Annals, v. 42, p. 295–317

Thompson, D. G., 1929, The Mohave Desert region, California: U. S. Geol. Survey Water-Supply Paper 578, 759 p.

California Institute of Technology, Pasadena, California

Manuscript Received by the Secretary of the Society, February 7, 1956

BULLETIN OF THE GEOLOGICAL SOCIETY OF AMERICA
VOL. 68, PP. 291-306, 1 FIG., 1 PL. MARCH 1957

INTERRELATED PRECAMBRIAN GRANITIC ROCKS, NORTHWEST ADIRONDACKS, NEW YORK

BY A. F. BUDDINGTON

ABSTRACT

Twenty-one new chemical analyses of granitic rocks of the northwest Adirondacks are presented; three of the predominant hornblende microperthite granite and equivalent gneiss, nine of alaskite to confirm that the quartz content of the alaskite is less than 42 per cent, eight of microcline-rich granitic gneisses to further elucidation of the problem of their origin, and one of sodium granitic gneiss. The compositions of the granitic rocks as a whole are plotted and their interrelationships discussed. Three additional analyses of biotite-quartz-plagioclase gneiss are also included; this gneiss is the major raw material which has formed the host rock for migmatites and for granitization to yield much porphyroblastic granite gneiss and microcline-rich granitic gneiss.

CONTENTS

TEXT

	Page
Acknowledgments	291
Types and ages of granitic rocks in general	292
Hornblende-microperthite granite and equivalent gneiss	292
Alaskite and equivalent gneiss	295
Inequigranular granite gneiss, microcline-rich granitic gneiss and migmatite	295
Microcline-rich granitic rocks	297
Interrelationships of granitic rocks	299
Migration of mafic constituents in metasomatism	302
Contrasts between younger and older granites	303
Magmatic history of Adirondack Precambrian	304
Conclusion	305
References cited	305

ILLUSTRATIONS

Figure	Page
1. Norm ratios of quartz, orthoclase, and albite + anorthite recomputed to 100 per cent and plotted for granitic rocks and pertinent metasedimentary rocks of the northwest Adirondack Precambrian area	294

Plate	Facing page
1. Biotite-quartz-plagioclase gneiss, microcline-rich granitic gneiss and intermediate granitized facies	302

TABLES

Table	Page
1. Chemical composition and norms of hornblende-micorperthite granite and equivalent gneiss	293
2. Cheimical analyses and norms of alaskite gneiss from phacoliths in belt of metasedimentary rocks, northwest Adirondacks, and of a sodium granite	296
3. Chemical analyses and norms of alaskite and alaskite gneiss from main igneous complex of Adirondacks	298
4. Chemical analyses and norms of biotite-quartz-plagioclase gneiss and migmatites, main belt of metasedimentary rocks	299
5. Chemical analyses of microcline-rich granitic gneisses and biotite-quartz-plagioclase gneiss	300
6. Comparison of mafic constituents in gneisses	303

ACKNOWLEDGMENTS

All the chemical analyses of rocks for this paper, except those quoted from the literature, were made at the Rock Analysis Laboratory of the University of Minnesota. The cost of the analyses and of the collection of a part of the specimens was borne by a grant of funds from the Eugene Higgins Trust allocated to Princeton University. Several of the samples were collected incidental to a study of the St. Lawrence County magnetite district for the U. S. Geological Survey. I am indebted to Richard H. Jahns, B. F. Leonard Jr. and A. E. J. Engel for pertinent suggestions for revision of the manuscript; and to Ada Swineford for a sample of potassium-rich vitric tuff from Kansas.

Types and Ages of Granitic Rocks in General

Five major types of granitic rocks in the northwest Adirondack Precambrian area are (1) hornblende-microperthite granite and its metamorphic equivalent gneiss, (2) microperthite alaskite and its metamorphic equivalent gneiss, (3) microcline-rich granitic gneiss, (4) inequigranular granite and equivalent gneiss (Hermon type), and (5) a veined gneiss, a migmatite of alternating laminae of granitic material and schist. The nature and origin of these rocks have been much discussed in recent years (Buddington, 1939; 1948; 1955; unpublished manuscript; Prucha, 1949, Ph.D. thesis, Princeton Univ.; Engel and Engel, 1953). General agreement is that the first two types are of magmatic origin, that the inequigranular facies (Hermon type) is in part or wholly the product of granitization of biotite-quartz-plagioclase gneiss and to a minor extent of amphibolite, and that the veined gneiss has resulted in part from metasomatic granitization along selected foliation planes of the biotite-quartz-plagioclase gneiss and may in part represent introduction of highly fluid magmatic material. A widespread microcline-rich granitic gneiss in substantial part with accessory sillimanite has been interpreted (Buddington, 1948, p. 36–39) as the products of granitization and invasion of biotite-quartz-plagioclase gneiss by potassium-rich fluids. The inequigranular granitic gneiss (Hermon type) occurs wholly within a great belt where metasedimentary material is predominant, whereas almost all the microcline-rich granitic gneisses are restricted to the main igneous complex where igneous rocks are overwhelmingly predominant. The inequigranular granitic rock is predominantly an augen gneiss resulting from deformation of a porphyroblastic rock and in small part a porphyroblastic granitic gneiss or porphyritic granite.

The granitic rocks belong to at least two periods.

Hornblende-microcline-oligoclase granite gneiss forms a facies of a complex (Diana) of which pyroxene syenite and pyroxene-quartz syenite gneiss are the major part. Such granite gneiss has been interpreted as a differentiated upper facies of intensely deformed and folded great stratiform sheets whose average composition is that of a quartz-bearing syenite. The texture of these gneisses implies a very coarse initial grain except for thin sheets in metasedimentary rocks.

Microcline-rich hornblende or biotite granoblastic granitic gneiss forms a mass on the Lake Bonaparte quadrangle where it was originally called the Carroll School granosyenite gneiss (Buddington, 1926, 62; 1939, p. 137, Nos. 7 and 8). The relationships of this gneiss to the rocks of the Diana complex have not been ascertained.

The foregoing deformed gneissic granoblastic granitic rocks are intruded by metadiabase dikes, in part with granoblastic structures, which crosscut the foliation of the granitic gneisses. The metadiabase dikes are inferred to have had fine-grained borders appropriate to emplacement under hypabyssal conditions.

All of the foregoing rocks were in turn intruded by great masses of magma now represented by hornblende-microperthite granite and equivalent gneiss and by microperthite alaskite and equivalent gneiss. The development of the inequigranular granitic rock and veined gneiss (Hermon type) and the microcline-rich granitic gneisses may also belong to this period of intrusion though there is little evidence upon which to base any interpretation.

Hornblende-Microperthite Granite and Equivalent Gneiss

Hornblende-microperthite granite and equivalent hornblende-microcline-oligoclase gneiss form great batholithic masses within the main igneous complex that constitutes the core of the Adirondack area. They occupy at least two-thirds of the area of younger granitic rocks; and, because a much greater extension than that of the other facies is inferred at depth, they probably constitute more than three-fourths of the total volume of granitic rocks.

If microperthite is considered to be a potassium feldspar or an end member in rock classification, then the hornblende-microperthite granite and microperthite alaskite are orthogranites. On metamorphism the feldspar unmixes to a granoblastic aggregate of micro-

TABLE 1.—CHEMICAL COMPOSITION AND NORMS OF HORNBLENDE-MICROPERTHITE GRANITE AND EQUIVALENT GNEISS

	1	2	3	4	5	6	7
SiO_2	70.11	69.30	70.44	69.27	69.40	70.72	69.70
Al_2O_3	14.11	14.94	13.28	13.87	15.54	13.11	13.29
Fe_2O_3	1.14	1.02	2.07	1.86	1.41	1.85	2.90
FeO	2.62	1.92	2.16	2.23	1.27	1.97	2.07
MgO	.24	.46	.43	.47	.17	.50	.41
CaO	1.66	1.46	1.57	1.97	1.43	1.36	1.55
Na_2O	3.03	3.60	2.95	3.57	3.69	3.35	3.14
K_2O	6.03	5.94	5.57	5.70	6.30	5.60	5.51
H_2O+	.23	.25	.42	.54	.40	.37	.32
H_2O-	.07	.09	.06	.13	.11	.06	.03
TiO_2	.42	.43	.57	...	...	.41	.51
P_2O_5	.09	.12	.14	...	...	.23	.13
MnO	.06	.05	.07	...	...	...	.08
F	.09	.09	.13	...	...	...	n.d.
BaO	...	...	.06	...	...	...	.10
Total	99.90	99.67	99.92	99.61	99.72	99.53	99.94*
Less 0 for F	.04	.04	.05	...	...	...	...
Total	99.86	99.63	99.87	...	...	...	...

* Contains 0.20 per cent CO_2.

Norms

Quartz	23.19	21.33	27.60	21.5	19.6	26.46	26.76
Orthoclase	35.58	35.03	33.36	33.9	37.3	33.36	32.80
Albite	28.03	30.39	25.15	30.4	31.4	28.30	26.72
Anorthite	5.70	6.39	6.12	4.7	7.0	4.17	5.56
Hypersthene	3.40	3.28	2.55	1.6	1.6	2.25	1.69
Magnetite	1.74	1.39	3.02	2.2	2.1	2.65	4.18
Ilmenite	.76	.82	1.06	...	...	.77	.97
Apatite	.20	.27	.34	...	...	.58	.34
Fluorite	.19	.19	.26	...	...	...	...
Corundum	...	.25	...	...	...	...	...
Diopside	1.02	...	.09	4.3	...	0.93	.11

(1) Ferrohastingsite-microperthite granite; 0.5 mile north of Cranberry Lake State Park, Cranberry Lake quadrangle. Analyst, Lee C. Peck.

(2) Hornblende-microperthite granite; road crossing of creek 0.4 mile southeast of High Rock, Cranberry Lake quadrangle. Analyst, Lee C. Peck.

(3) Femaghastingsite-microcline-oligoclase granite gneiss; 1 mile south of Palmerville, Blanchard Hill, Russell quadrangle. Analyst, Lee C. Peck.

(4) Hornblende granite; 0.25 mile west of Jerden Falls, Lake Bonaparte quadrangle (Buddington and Smyth, 1926, p. 41).

(5) Hornblende granite; 1.75 miles east of Jerden Falls, Lake Bonaparte quadrangle (Buddington and Smyth, 1926, p. 41).

(6) Femaghastingsite granite; 1.2 miles north-northeast of Bush's Corners, Lowville quadrangle. Analyst, R. B. Ellestad. (Buddington, 1939, p. 138).

(7) Hornblende granite gneiss; small road-metal quarry on south side of State road, 0.15 mile west of intersection of Waverly, Dickinson and Hopkinton townships, Nicholville quadrangle. Analyst, T. Kameda. (Buddington, 1939, p. 138).

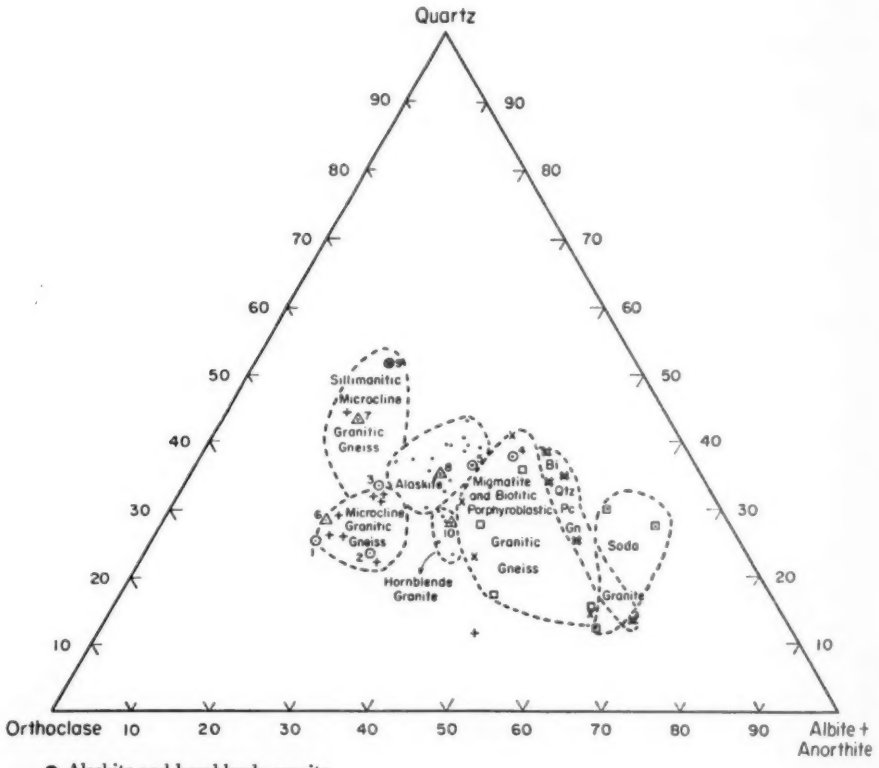

- ● Alaskite and hornblende granite
- \+ Microline-rich granitic gneisses; granitized and migmatitized metasediment
- ⊡ Soda granite
- □ Porphyroblastic biotite granite gneiss (Hermon type)
- × Biotite-quartz-plagioclase gneiss migmatitic with thin granitic veinings
- ⁂ Biotite-quartz plagioclase gneiss
- ⊙ Composition of granite pegmatite in general and of ternary eutectic (No. 5)
- △ Composition of certain volcanics

FIGURE 1.—NORM RATIOS OF QUARTZ, ORTHOCLASE AND ALBITE + ANORTHITE RECOMPUTED TO 100 PER CENT AND PLOTTED FOR GRANITIC ROCKS AND PERTINENT METASEDIMENTS OF THE NORTHWEST ADIRONDACK PRECAMBRIAN AREA

Average composition of several rock types from outside this area are also plotted for comparison.

(1) Average of 11 graphic granites (Washington, 1917).
(2) Average of 5 granite pegmatites with normative quartz between 15 and 28 per cent. (Washington, 1917).
(3) Granite pegmatite lense in metalimestone, Wildcat Branch, N. J. (Lodding, W., 1951, p. 32).
(4) Average composition of 5 granite pegmatites with 32–36 per cent normative quartz. (Washington, 1917).
(5) Ternary eutectic for quartz, albite and orthoclase at 1000 atmospheres pressure H_2O and 720°C., approximated from diagram of Tuttle and Bowen (1952, p. 39).
(6) Average of 5 rhyolites (omeose) with normative corundum. (Washington, 1917).
(7) Average of 25 analyses of 25 specimens from 8 different beds of vitric tuff with K_2O 5.52–6.85 per cent, Na_2O 0.93–2.01 per cent and SiO_2 70.05–74.82 per cent. (Swineford, Frye and Leonard, 1955, p. 252).
(8) Average of 22 calc-alkali rhyolite and rhyolite-obsidian (Nockolds, 1954, p. 1012). Also corresponds to approximate average of 2 "complex" and "zoned" granite pegmatites (Jahns, 1953).
(9) Average composition of 3 microcline granite gneisses with sillimanite quartz nodules from Canada, Sweden, and Norway.
(10) Average composition of 2 rhyolites and 1 perlite (Washington 1917, Nos. 221, 95, and 120).

cline and plagioclase, and the equivalent rock would then be classified as a quartz monzonite gneiss. This classification makes for confusion, and the gneissic equivalent of the microperthite granites is here called granite gneiss. The microperthite of the primary gneissoid granite contains plagioclase and orthoclase members in about equal amounts, and presumably it initially crystallized as sanidine. The microperthite of the primary alaskite had a similar history.

The composition of most of the hornblende granite and gneiss has a narrow range as indicated by the chemical analyses (Table 1); and the plot of all available chemical analyses (Fig. 1). The hornblende ranges from femaghastingsite to ferrohastingsite, with a concomitant decrease of magnetite and increased ratio of FeO to Fe_2O_3. Magnetite is the major to exclusive accessory oxide in the femaghastingsite facies, and ferricilmenite is the predominant to exclusive accessory oxide in the ferrohastingsite facies.

Alaskite and Equivalent Gneiss

Alaskite or equivalent gneiss occurs as many isolated masses within a broad belt of predominantly metasedimentary rocks in the northwest Adirondack area, as local facies of hornblende granite, and as separate sheets in minor belts of metasedimentary rocks within the main igneous complex of the core of the Adirondacks. The term alaskite is here used for granitic rocks with less than 5 per cent dark minerals.

A recent determination (Dietrich, 1954, p. 516) of the modal mineral composition of rock from one of the alaskite bodies in the predominantly metasedimentary belt gives 48–50 per cent quartz. Modal determinations (Dale, 1935, p. 47) of rock samples from alaskite and granite bodies within the main igneous complex are given as more than 45 per cent quartz. These percentages of quartz, if representative, are high enough to raise serious question as to whether the alaskite is really an igneous rock and had the igneous origin ascribed to it by geologists working in this area. The writer determined to investigate this matter thoroughly.

Many modal mineral determinations have been made and fifteen chemical analyses of alaskite from the Adirondack area have been obtained and are presented herewith.

The modal percentage of quartz has been determined in 55 samples of alaskite and alaskite gneiss from the main igneous complex; it ranges between 22 and 42 per cent; about 90 per cent of the specimens contain 30–40 per cent quartz. Most of these rocks carry a few tenths of a per cent of fluorite. No sample was found to contain more than 42 per cent quartz.

The samples (Tables 2 and 3) were chosen at random and are believed to reflect the general range in composition of the alaskite and equivalent gneiss. The normative quartz is between 30 and 38 per cent in 11 of the 15 samples and exceeds 40 per cent in only 1. The modal percentage of quartz may be slightly greater than the norm percentage because of the presence of a little biotite instead of potassium feldspar and will be very slightly less if the norm is recalculated to volume percentage. The normative and modal percentages of quartz in alaskite should therefore be about the same within a range of at most 2 or 3 per cent.

As a result of these data and of field experience it is believed that none of the normal alaskite has quartz in excess of 42 per cent. Rock from the alaskite bodies containing substantially more than 42 per cent quartz is rare indeed and of complex origin, is an included layer of metasedimentary rock, or has been incorrectly analyzed mineralogically. It is urged that any inference that a facies of the alaskite has substantially more than 42 per cent quartz be most carefully checked by detailed field work and supported by a chemical analysis.

Inequigranular Granite Gneiss, Microcline-Rich Granitic Gneiss, and Migmatite

The inequigranular granite gneiss, biotitic or sillimanitic microcline-rich granitic gneiss, and migmatite are thought to be at least in part the product of granitization. The raw material which has been granitized to form each of the three facies has in large part been the same kind of rock, a biotite-quartz-plagioclase gneiss.

Buddington (1939, p. 70, No. 78-L) and Engel

TABLE 2.—CHEMICAL ANALYSES AND NORMS OF ALASKITE GNEISS FROM PHACOLITHS IN BELT OF METASEDIMENTARY ROCKS, NORTHWEST ADIRONDACKS, AND OF A SODIUM GRANITE

	1	2	3	4	5	6	7	8	9	10
SiO_2	72.19	73.10	75.63	75.98	76.80	77.86	76.98	77.26	76.45	64.25
Al_2O_3	12.86	14.29	12.03	11.92	11.97	11.25	11.94	12.05	12.19	16.05
Fe_2O_3	2.64	1.04	1.16	1.24	1.22	1.41	1.24	.81	1.32	1.80
FeO	.47	1.04	1.33	1.26	.86	.90	.69	.63	.75	1.80
MgO	.27	.53	.29	.29	.17	.18	.05	.16	.10	1.31
CaO	.49	1.18	.31	.18	.53	.51	.26	.45	.39	3.30
Na_2O	3.52	3.08	3.69	3.67	3.53	3.20	3.63	3.32	3.27	5.56
K_2O	5.99	5.36	4.77	4.69	4.38	4.08	4.59	4.90	4.84	3.69
H_2O+	.26	.54	.12	.14	.08	.06	.12	.11	.10	.30
H_2O-	.03	.07	.05	.04	.06	.04	.01	.02	.03	.10
CO_2	.34	n.d.	.06	.06	.04	n.d.	.08	...	.02	.63
TiO_2	.56	.18	.25	.26	.18	.20	.16	.16	.19	.64
P_2O_5	.20	.03	.07	.02	.02	.03	...	.01	...	.22
MnO	.01	.07	.04	.04	.03	.01	...	.01	.04	.06
BaO	...	...	...	.03	...	...	...	...	...	...
Cl	...	.03	...	...	...	...	...	...	...	...
F	...	.02	...	...	...	...	...	...	...	...
S	...	.02	...	...	...	...	...	...	...	...
Total	99.83	100.58	99.80	99.82	99.87	99.73	99.75	99.89	99.69	99.71
Norms										
Quartz	28.50	30.40	34.89	35.89	38.22	41.88	37.80	38.16	37.84	11.28
Orthoclase	35.50	31.69	28.36	27.80	26.13	24.46	27.24	28.91	28.58	21.68
Albite	29.87	26.20	30.92	30.65	29.34	27.25	30.39	27.77	27.77	47.16
Anorthite	.28	5.00	.70	.50	2.64	2.50	1.28	2.22	1.95	8.06
Corundum	...	1.50	.61	.68	.56	.61	.55	.56	.87	3.06
Hypersthene	.35	2.46	1.64	1.52	.66	.47	.10	.67	.31	2.55
Magnetite	...	1.67	1.62	1.86	1.86	2.09	1.86	1.16	1.86	1.22
Ilmenite	1.06	.31	.46	.50	.35	.38	.30	.30	.37	0.50
Hematite	2.64	...	...	...	...	...	...	...	...	...
Apatite	.47	.07	.17	.05	.05	.07	...	.02	...	0.52
Calcite	.80*	...	.14	.14	...	...	...	...	...	1.40
Diopside	...	...	...	...	...	...	...	...	...	2.44

* Dolomite.

(1) Alaskite; 0.5 mile southwest of California School, Hyde School phacolith, Hammond quadrangle. Analyst, R. B. Ellestad. Original biotite is altered to chlorite and carbonate, magnetite is altered to hematite. Gneissoid structure. Feldspar includes microperthite, microcline, and albite in about equal proportions.

(2) Biotite-muscovite alaskite gneiss; 0.25 mile south of Alexandria Bay, Alexandira quadrangle (Cushing et al., 1910, p. 177). Analyst, E. W. Morley. Feldspar is exclusively microcline and albite as a granoblastic aggregate.

(3) Augite alaskite; small road-metal quarry, 0.2 mile northeast of Benchmark 484, on road from Gouverneur to Rock Island Bridge, Gouverneur phacolith, Gouverneur quadrangle. Analyst, T. Kameda. Augite is product of contamination from included schliere of amphibolite. Feldspar includes microperthite, albite, and microcline in about equal proportions.

(4) Hornblende alaskite; southwest end of Reservoir Hill phacolith. Gouverneur quadrangle. Analyst, A. Willman. Gneissoid rock with feldspar almost exclusively microperthite.

(5) Augite-microperthite alaskite gneiss; 1 mile northeast on road from its junction with road from Pope Mills to Edwardsville, 1.2 miles east-southeast of Edwardsville, Brier Hill quadrangle. Fish Creek phacolith. A little accessory augite, sphene, and metallic oxides. Analyst, Doris Thaemlitz.

and Engel (1953, p. 1063) give several chemical analyses of the inequigranular granite gneiss and of the biotite-quartz-plagioclase gneiss. New analyses of the biotite-quartz-plagioclase gneiss, migmatite, and microcline-rich granitic gneisses are in Tables 4 and 5.

Microcline-Rich Granitic Rocks

The microcline-rich granitic rocks are characterized by the predominance of microcline over plagioclase. The accessory minerals of the microcline granitic gneisses vary consistently with the nature of included lenses or layers of country rock. Biotite, almandite, or quartz-sillimanite aggregates occur where the schilieren of country rock are of biotite-quartz-plagioclase gneiss; hornblende where included lenses are of amphibolite and pyroxene, or andradite where relic skarn lenses occur.

Chemical analyses and norms of the microcline-rich granitic rocks are given in Table 5.

Plate 1 shows at the left the relatively homogeneous biotite-quartz-plagioclase gneiss that forms the raw material which through granitization and migmatization results in a nearly homogeneous microcline granite gneiss such as the core at the farthest right. The cores between the two extremes represent intermediate stages of granitization and migmatization. The core of microcline granite gneiss at the extreme right has a relic ghost structure of plicated biotitic gneiss and is metasomatic, but similar facies of the uniform microcline granitic gneiss could be of magmatic origin. In particular, the rock of analysis No. 10 (Table 5) seems to be of magmatic origin. No evidence that it is of replacement origin was seen. It is associated with normal hornblende-microperthite granite and is perhaps gradational into it. Microcline-rich granitic gneiss develops in part without accompanying sillimanite in the migmatization and granitization of the biotite-quartz-plagioclase gneiss.

Microcline-rich granitic gneiss containing sillimanitic quartz lenses or nodules and similar to that from the northwest Adirondacks has been described from numerous localities in the Precambrian elsewhere in the world. Chemical analyses of such rock have been given by Adams (1898, p. 169) from Pine Lake, Ontario, by Per Geijer (1930, p. 61) from the Gällivare iron-ore field, Sweden, and by Brøgger (1934, p. 81) from Norway. All are similar. The Swedish rock is described as a leptite altered by solutions accompanying formation of tourmaline pegmatite veins, and the Norwegian rocks have been described by Bugge (1943, p. 103–114) as resulting from penetration of original pelitic sediments by a potassium-rich ichor which has transformed them metasomatically. Other examples of microcline-rich granitic gneiss with similar nodules have been described by Geijer (1911, p. 322–323), Sederholm (1928, p. 80–81), and Coetzee (1942, p. 91–112). The country rock, which is modified to the quartz-sillimanite nodular microcline granitic gneiss, is characteristically a biotite-quartz-plagioclase gneiss.

The sillimanitic and almanditic microcline-rich granitic gneiss of the Adirondack area, on

---

Table 2.—*Continued*

(6) Biotite-microperthite alaskite gneiss; 4.7 miles northeast of Pope Mills (Hammond quadrangle) on Brier Hill quadrangle, 3.6 miles east northeast of Edwardsville. Alaskite contains amphibolite inclusions. Fish Creek phacolith. Some cataclastic granulation. Accessory metallic oxides. Analyst, Doris Thaemlitz.

(7) Alaskite gneiss; 2.7 miles northeast of bridge at Canton, 0.2 miles southwest of Benchmark 378, Canton phacolith, Canton quadrangle. Granoblastic microcline and albite with long quartz pencils. Very little accessory metallic oxide. Analyst, Doris Thaemlitz.

(8) Alaskite gneiss; 1.3 miles southeast of Eddy on road toward Pyrites, Canton phacolith, Canton quadrangle. Granoblastic aggregate of microcline and albite with associated pencil quartz and about 0.2 per cent accessory biotite. Analyst, Doris Thaemlitz.

(9) Alaskite gneiss; 1.7 miles southwest of crossing of Eddy-Pyrites road, Ogdensburg quadrangle, Canton phacolith. Adjacent to amphibolite inclusion. Quartz pencils, granoblastic aggregate of albite and microcline, accessory garnet. Analyst, Doris Thaemlitz.

(10) Oligoclase granite; 0.5 mile east of Jarvis Bridge or 2 miles east of Newton Falls, Cranberry Lake Quadrangle. Analyst, Lee C. Peck.

TABLE 3.—CHEMICAL ANALYSES AND NORMS OF ALASKITE AND ALASKITE GNEISS FROM MAIN IGNEOUS COMPLEX OF ADIRONDACKS

	1	2	3	4	5	6
SiO_2	76.20	76.41	75.42	75.71	70.38	70.99
Al_2O_3	12.54	12.41	11.76	12.68	14.45	14.28
Fe_2O_3	.90	1.01	1.98	.96	1.30	1.19
FeO	.56	.50	1.19	.32	1.46	2.30
MgO	.08	.46	.15	.13	.39	.53
CaO	.73	.78	.83	.67	1.37	1.12
Na_2O	3.57	3.34	3.34	3.29	3.72	2.80
K_2O	5.23	4.33	4.32	5.49	5.59	5.97
H_2O+	.27	.34	.24	.24	.28	.30
H_2O-	.06	.13	.10	.09	.04	.08
S	.....	.01	.....	.....	.....	.....
TiO_2	.....	.03	.20	.18	.42	.26
P_2O_5	.....	.....	.01	.02	.08	.02
MnO	.....	.06	.03	.01	.05	.....
F	.....	.01	.29	.19	.20	.09
BaO	.....	.....	.....	.02	.....	.....
Total	.....	99.84*	99.86	100.00	99.73	99.93
Less 0 for F	.....	.....	.12	.08	.08	.....
Total	100.14	.....	99.74	99.92	99.65	.....
Norms						
Quartz	33.6	37.95	38.25	34.44	24.06	27.42
Orthoclase	31.1	25.58	25.58	32.80	33.36	35.58
Albite	30.4	28.30	28.30	27.77	31.44	23.58
Anorthite	2.5	3.89	1.95	1.81	4.73	5.42
Hypersthene	.....	1.23	.60	.30	2.05	3.94
Magnetite	1.4	1.39	3.02	.53	1.86	1.86
Ilmenite	.....	.....	.38	.35	.76	.46
Apatite	.....	.....	.02	.04	.20	.04
Fluorite	.....	.....	.62	.39	.39	.....
Corundum	.....	.82	.92	.66	.51	1.17
Hematite	.....	.....	.....	.59	.....	.....
Diopside	0.9	.....	.....	.....	.....	.....

* Also includes 0.02 ZrO_2.

† Also includes 0.03 Cl.

(1) Biotite alaskite; Bisha's Mill, Lake Bonaparte quadrangle, (Buddington and Smyth, 1926, p. 43).

(2) Alaskite; Mount Morris, Long Lake quadrangle. (Cushing, 1907, p. 510–512). Analyst, E. W. Morley.

(3) Biotite-fluorite alaskite; southeast of Dead Creek, near Bench Mark 1901, Cranberry Lake quadrangle. Analyst, Lee C. Peck. A little of the magnetite has probably been introduced by ore-forming solutions.

(4) Biotite-fluorite alaskite gneiss; 1.3 miles southeast of Star Lake, north of Alice Brook, Oswegatchie quadrangle. Analyst, Lee C. Peck.

(5) Biotite-fluorite alaskite gneiss; road cut 2.5 miles east of Pond Settlement, Russell quadrangle. Coarser-grained than normal. Analyst, Lee C. Peck.

(6) Garnet alaskite; a facies contaminated from metasedimentary rocks; 0.4 mile south of southwest end of Horseshoe Lake, Tupper Lake quadrangle. Analyst, Lee C. Peck.

the basis of field evidence, appears to be the product of invasion and incomplete granitization of biotite-quartz-plagioclase gneiss by potassium-rich fluids. The fluid effecting this transformation, however, can be best interpreted as much richer in potassium than that of the alaskitic magma. The microcline-rich granitic gneisses with accessory hornblende, pyroxene, andradite, or biotite in large part are so homogeneous that it can be inferred that a magma was involved in their formation. Transitional gradations to country rock such as are common between the microcline-rich granitic gneiss and biotite-quartz-plagioclase gneiss are lacking where the accessory minerals are mafic; though layers of amphibolite characteristically occur in the hornblende-microcline-rich granitic gneiss, and layers of pyroxene or andradite skarn occur in the pyroxene or andradite-microcline-rich granitic gneiss. There are gradational facies between alaskite and microcline-rich granite. The metallic oxides in the hornblende granite and the alaskite are ilmenomagnetite and ilmenite, whereas the metallic oxides in the microcline-rich granitic gneisses are a more oxidized assemblage—magnetite, titanhematite, ilmenohematite, hemoilmenite, or combinations of these minerals. The potassium-rich fluids which are responsible for the microcline-rich granitic gneisses could have been pegmatitic comparable to those represented by numbers 1, 2, and 3, and by the rhyolitic magma of numbers 6 and 7 in Figure 1. Granite pegmatites as discrete bodies of substantial size are relatively uncommon where the microcline gneisses occur but are abundant in the belt of predominantly metasedimentary rocks where the inequigranular granite gneiss (Hermon type) is found.

Interrelationships of Granitic Rocks

Quartz, plagioclase (albite plus anorthite), and orthoclase compose more than 85 per cent of the normative minerals in the granitic rocks with few exceptions. The norm ratios for these three minerals have been recalculated on the basis of 100 per cent for all the pertinent chemical analyses and are plotted in Figure 1.

The locations of the compositions of four types of granite pegmatites (1, 2, 3, 4), four types of rhyolitic rocks (6, 7, 8, 10), and the experimentally determined ternary eutectic (5) for quartz, albite, and orthoclase at 720°C. and 1000 atm. pressure H_2O are given for comparison. The composition of the alaskite and

Table 4.—Chemical Analyses and Norms of Biotite-Quartz-Plagioclase Gneiss and Migmatites, Main Belt of Metasedimentary Rocks

	1	2	3
SiO_2	70.90	67.18	72.49
Al_2O_3	12.17	15.65	13.82
Fe_2O_3	1.31	.13	.13
FeO	4.12	3.31	2.97
MgO	2.32	1.25	1.01
CaO	1.55	1.70	1.48
Na_2O	3.74	3.42	3.08
K_2O	2.87	5.24	3.22
H_2O+	.21	.99	.65
H_2O-	.05	.06	.06
TiO_2	.32	.62	.50
P_2O_5	nd	.10	.06
MnO	.04	.06	.03
	99.60	99.71	99.50
Norms			
Quartz	28.77	19.98	35.88
Orthoclase	16.68	30.86	18.90
Albite	31.70	28.82	26.20
Anorthite	7.78	7.78	7.23
Corundum	.15	1.53	2.55
Hypersthene	11.80	8.12	7.12
Magnetite	1.86	.23	.23
Ilmenite	.61	1.22	.91
Apatite	...	.24	.13
Diopside	...	...	...

(1) Biotite-quartz-plagioclase gneiss; composite sample of 24 specimens across 2000 feet at right angles to strike, along line traverse from West Branch of Oswegatchie River north to Oswegatchie River; 0.9 mile east of Emeryville, Gouverneur quadrangle (Engel and Engel 1953, p. 1063).

(2) Biotite-quartz-plagioclase gneiss with a little garnet and somewhat modified by migmatization. Road cut 2.5 miles west northwest of Colton, Potsdam quadrangle. Analyst, Eileen H. Kane.

(3) Migmatitic garnetiferous biotite-quartz-feldspar gneiss; 0.4 mile southwest of No. 2. Analyst, Eileen H. Kane.

TABLE 5.—CHEMICAL ANALYSES OF MICROCLINE-RICH GRANITIC GNEISSES AND BIOTITE-QUARTZ-PLAGIOCLASE GNEISS

	1	2	3	4	5	6	7	8	9	10	11
SiO_2	63.01	65.28	63.95	70.10	69.40	71.44	70.99	70.99	67.89	68.03	71.29
Al_2O_3	16.60	17.58	17.07	14.14	14.46	14.89	13.54	13.34	13.11	14.63	13.53
Fe_2O_3	3.14	1.29	.96	2.30	2.76	2.40	4.14	2.71	3.32	2.72	2.56
FeO	3.42	1.76	2.36	1.33	1.36	1.38	.54	1.15	2.24	1.77	1.47
MgO	1.41	1.02	.86	.34	.26	.30	.23	.24	.56	.66	.29
CaO	3.50	2.50	1.75	1.39	1.43	.50	.31	.78	1.45	.65	.70
Na_2O	3.62	5.94	4.19	2.11	2.18	1.36	2.71	2.06	1.85	3.00	2.72
K_2O	3.02	2.93	6.08	6.72	6.58	5.99	6.63	7.83	7.88	7.24	6.60
H_2O+	.34	.28	.39	.23	.24	.52	.12	.22	.27	.36	.44
H_2O-	.03	.00	.01	.02	.02	.08	.08	.09	.03	.08	.04
TiO_2	1.06	.59	.49	.59	.74	.65	.45	.43	.72	.52	.37
MnO	.07	.07	.16	.05	.04	.03	.07	.05	.08	.05	.01
P_2O_5	.35	.22	.17	.18	.27	.22	n.d.	.09	.15	.12	.06
BaO	n.d.	.07	n.d.	.08	n.d.	.09	.06	n.d.	n.d.	.10	n.d.
FeS_2	n.d.	n.d.	1.01	n.d.	n.d.	n.d.	n.d.	n.d.	n.d.	n.d.	n.d.
CO_2	n.d.	.15	.18	.15	.08	n.d.	n.d.	n.d.	n.d.	n.d.	n.d.
	99.57	99.74*	99.63	99.73	99.82	99.88†	99.87	99.98	99.54	99.93	100.08
Norms											
Quartz	21.63	12.60	10.05	29.37	28.95	36.18	29.24	27.39	23.67	20.52	27.96
Orthoclase	17.79	17.24	36.14	39.48	38.92	35.58	38.92	46.15	46.70	43.37	38.02
Albite	30.39	50.30	35.63	17.82	18.34	11.53	23.06	17.29	15.72	25.15	23.06
Anorthite	15.29	11.26	7.64	5.84	5.28	1.11	..	3.39	3.89	2.50	3.20
Hypersthene	7.50	3.80	5.32	.85	.65	.80	.60	.60	.73	1.85	.77
Magnetite	2.89	1.86	1.39	2.67	2.32	2.55	1.74	2.67	4.87	3.94	3.71
Hematite	..	..	..	.40	1.28	0.64	2.96	.88	..	..	..
Ilmenite	2.05	1.14	.75	1.14	1.37	1.22	..	.84	1.37	.99	.68
Apatite	.84	.50	.40	.44	.67	.50	.17	.20	.34	.27	.13
Sillimanite**	..	..	..	..	..	9.07**	..	..	..	..	..
Corundum	.82	.46	.76	1.27	1.79	..	1.89	.20	..	.82	.66
Sphene	..	..	..	..	..	..	1.08	..	..	..	..
Diopside	..	..	..	..	..	..	..	..	1.97	..	..

* Contains 0.6 per cent Cl.

† Corrected for .06 per cent fluorine in rock.

** Excess Al_2O_3 calculated as sillimanite instead of as the usual corundum.

(1) Gray biotite-rich quartz-plagioclase gneiss; Spruce Mountain; northwest corner Cranberry Lake quadrangle. Analyst, Lee C. Peck.

(2) (SC-1-436′) Gray biotite-quartz-plagioclase gneiss; from diamond drill hole of Skate Creek ore body, Oswegatchie quadrangle, N. Y. Analyst, Doris Thaemlitz.

(3) (SC-1-22′) Gray biotite-quartz-plagioclase gneiss, with pinkish partly granitized portions; from diamond drill core for Skate Creek ore body, Oswegatchie quadrangle, N. Y. Analyst, Doris Thaemlitz.

(4) (SC-1-26′) Pink schlieren-type biotite-microcline granitic gneiss; from diamond drill core for Skate Creek ore body, Oswegatchie quadrangle, N. Y. Analyst, Doris Thaemlitz.

(5) (SC-1-115′) Pink heterogeneous layered biotite-microcline-rich granitic gneiss; rare sillimanite film; from diamond drill core for Skate Creek ore body, Oswegatchie quadrangle, N. Y. Analyst, Doris Thaemlitz.

(6) (SC-1-120′) Microcline-rich granitic gneiss with thin laminae of quartz-sillimanite aggregate; from diamond drill core for Skate Creek ore body, Oswegatchie quadrangle, N. Y. Analyst, Lee C. Peck.

(7) Microcline-rich biotitic granitic gneiss; road cut 0.8 mile north of Shurtleff, Childwold quadrangle. Analyst, Eileen H. Kane.

part of the microcline-rich granitic gneisses corresponds to the range of composition of granite pegmatite. The composition of the microcline-rich granite gneisses (except those especially rich in quartz-sillimanite aggregates) and the alaskite also corresponds to the range of composition of certain rhyolitic rocks (6, 7, 8). The latter are of magmatic origin which indicates the possibility, though it does not prove, that the alaskite and much of the microcline-rich granitic gneiss is of magnatic origin. There are also rhyolitic rocks (Fig. 1, no. 10) which correspond to the hornblende granites in composition.

The data of Figure 1 clearly demonstrate hat the compositions of the granitic rocks inferred to be of magmatic origin lie within the composition range of volcanic rocks demonstrably of magmatic origin, and that the composition of the alaskite approaches the experimentally determined ratio for the eutectic of albite, orthoclase, and quartz.

An alternative interpretation that the near-eutectic ratio of some granites should also be expected as a product of metasomatism has been argued by De Vore (1946, p. 31–55). This theory is based on the assumption that some granites with a near-eutectic ratio are of metasomatic origin, and that, although the interface energy of a mineral assemblage is a small fraction of the total energy of a rock, it is considered to have a large effect on mineral distribution and mineral ratio. His conclusion is (p. 48) that "the approximately 30 per cent quartz in a rock can be considered as the volumetric expression of that ratio of quartz-feldspar contacts at which the lower energy of quartz, resulting from the quartz-feldspar contact is counteracted and reversed by the increased energy of the feldspar." De Vore further assumes (p. 46) that in many metasomatic granites quartz is almost always the last mineral to form, that feldspars commonly form earlier than the amphibole-mica accessory minerals; and that plagioclase feldspars in most cases form earlier than the K feldspars.

The specific quantitative physiochemical data necessary to predict what the approximate mineral ratio should be in a granite of metasomatic origin where an open system is involved are not available. Hence, in the foregoing hypothesis, the composition of granites inferred to be metasomatic is also inferred to have the ratio which would be approached if the appropriate physicochemical data were known. This of course may or may not be true. Also, in the metasomatic hypothesis, different minerals are inferred to be introduced in a series for which no rational basis has been proposed. The writer does not understand why the final mineral ratio should be the same for a cotectic liquid and for a product of metasomatism controlled by interfacial energies. It may also be noted that the primary feldspar of the Adirondack alaskite was sanidine and not potassium feldspar and albite. The magmatic hypothesis is certainly on a much firmer experimental physiocochemical basis than the metasomatic one, and the burden of proof must rest with the geologist who advocates a metasomatic origin for normal mesoperthite granites.

The field data are consistent with the hypothesis of a magmatic origin for the hornblende-microperthite granite and for the alaskite and much experimental and theoretical physicochemical evidence supports this hypothesis. (Buddington, 1948, p. 34–36).

The plot (Fig. 1) and the field evidence may

TABLE 5.—*Continued*

(8) Augitic microcline-rich granitic gneiss; 0.7 mile north-northeast of Clark, Stark quadrangle. Analyst, Eileen Kane.

(9) Femaghastingsite-microcline-rich granitic gneiss; abandoned crushed stone quarry, north side of Dead Creek, Tupper Lake quadrangle. Analyst, Eileen H. Kane.

(10) Ferrohastingsite-microperthitic microcline granitic gneiss; 0.5 mile southwest of Windfall Pond, Childwold quadrangle. Analyst James J. Engel.

(11) Chloritic microcline-rich granitic gneiss; 0.4 mile west-northwest of Tinney Corners, Lake Bonaparte quadrangle. Analyst, C. O. Ingamells. The granoblastic microcline-rich granitic gneiss is cut by a granoblastic metadiabase dike.

be interpreted on the basis that the porphyroblastic granitic gneiss and the migmatite gneiss have formed through the interaction of fluids related to the alaskitic granite magma with the biotite-quartz plagioclase gneiss. Equigranular alaskite occurs in subordinate masses associated with the porphyroblastic and migmatitic gneisses. Engel and Engel (1953, p. 1067) suggest that such equigranular alaskite is dominantly of igneous origin, although there is clearly no unequivocal basis for such a conclusion. This appears a reasonable statement. The coarse feldspars of the equigranular gneiss clearly appear to be porphyroblastic in much of such rock.

The granitic and pegmatitic vein matter of the migmatite is usually so contaminated with assimilated material, largely in the form of almandite, that its primary nature cannot be ascertained.

Hornblende granite and equivalent gneiss form more than three-fourths of the younger granitic rocks of the main igneous complex. It is inferred that a magma somewhat richer in silica and potassium than that now represented by the hornblende granite gave rise to the formation of the hornblende granite, the alaskite, and to the potassium-rich fluids which invaded the country rock to form the microcline-rich granitic gneisses in the main igneous complex and the equigranular granite gneiss and granite pegmatites within the predominantly metasedimentary belt. The potassium-rich fluids can be considered a volatile-rich magma or ichor, a hydrothermal solution, a cloud of dispersed ions, or a combination of all three. The writer prefers to believe that they are a combination but puts great emphasis on the first in general, but with varying ratio for each particular case. Similarly, the degree to which the potassium-rich fluids are emplaced as injections or as replacements is highly variable. The relationships of the hornblende granite and alaskite to the microcline-rich granitic gneisses, however, have not been definitely ascertained.

The sodium-rich oligoclase granitic rocks are but a very minor part of the granitic rocks of the northwest Adirondack area. In part they occur systematically in the junction zone between amphibolite and alaskite in phacoliths and may be interpreted as a partial melt of the amphibolite modified by material introduced from the alaskite magma. In part, as within the area of the main igneous complex, they are small isolated lenses and sheets of oligoclase granite. It is reasonable to think that the sodium of these rocks originated from the fluid which effected the granitization of the biotite-quartz-plagioclase gneiss to yield the microcline-rich granitic gneisses modified in such a way that potassium was introduced into the solid and sodium acquired in its place along with such other modifications as are required. Dietrich (1954, p. 526) has ascribed the quartz-oligoclase granitic rock of the phacoliths to development from a portion of the alaskite magma contaminated by calcareous country rock. It is difficult to visualize the details of this process.

Migration of Mafic Constituents in Metasomatism

As indicated by the previous discussion, biotite-quartz-plagioclase gneiss was the major raw material that was modified by granitizing fluids to yield a porphyroblastic granite gneiss, a migmatite, and a sillimanitic microcline-rich granitic gneiss. It has been generally inferred

---

Plate 1.—BIOTITE-QUARTZ-PLAGIOCLASE GNEISS, MICROCLINE-RICH GRANITIC GNEISS AND INTERMEDIATE FACIES

Successively from left to right, cores are: (1) (SC-1-436′) gray biotite-quartz-plagioclase gneiss; (2) (SC-1-22′) gray biotite-quartz-plagioclase gneiss with some lighter colored granitized layers; (3) (SC-1-126′) pink microcline-rich granitized gneiss with schlieren of biotite quartz plagioclase gneiss; (4) (SC-1-115′) pink microcline-rich granitized gneiss with schlieren of partly granitized biotite-quartz-plagioclase gneiss; (5) (SC-1-120′) pink microcline-rich granitic gneiss with thin laminae of quartz-sillimanite aggregates; (6) (SM-3-24′) uniform pink microcline-rich granitic gneiss with a relic ghost structure of plicated biotitic gneiss.

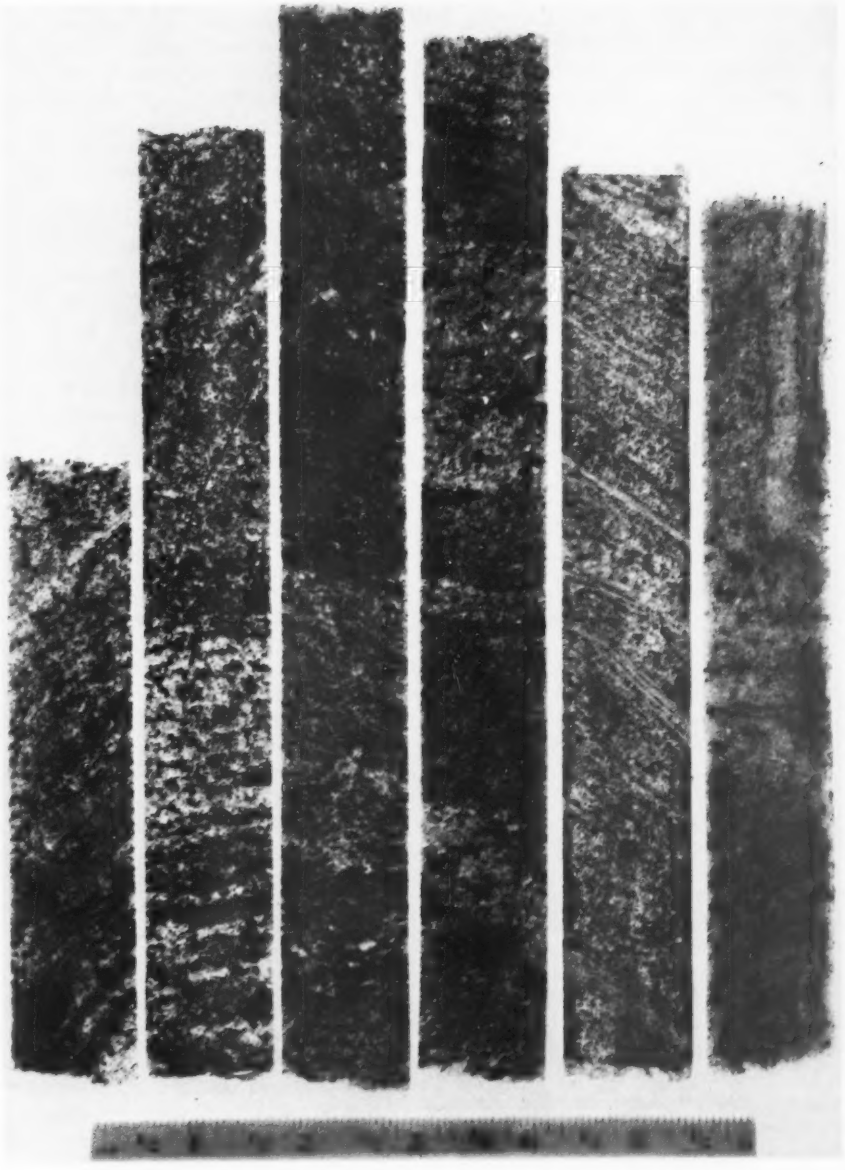

BIOTITE-QUARTZ-PLAGIOCLASE GNEISS, MICROCLINE-RICH GRANITIC GNEISS AND INTERMEDIATE FACIES

that du
iron and
the hos
olds, 19
11).

Average
in ma
Engel
Average
granit
Average
gneiss
rocks
Average
quart
rocks
Average
gneiss

* Perc
only. Th
greater.

The p
the bio
pared
Table 6
imate th
into ac
Further
the am
biotite-
the dep
placed
compar
product
of the
part, be
of the r
as magn
microcl
There h
from r
gneiss
granitiz
degree
ever, is

that during granitization much or most of the iron and magnesium have been driven out from the host rock to yield a "basic front" (Reynolds, 1947) or a "basic behind" (Read, 1951, p. 11).

such a wide range of possibilities that the subject will not be further discussed here. The TiO_2 content of the granitized rocks is uniformly higher than that of the composite biotite-quartz-plagioclase gneisses, but this difference may be due in large part to the fact that the equivalent of the unmodified granitized rock contained more TiO_2 (Cf. Table 5, nos. 1 and 2.)

TABLE 6.—COMPARISON OF MAFIC CONSTITUENTS IN GNEISSES

	MgO	FeO	Fe_2O_3	TiO_2	Total FeO + Fe_2O_3
Average of 24 samples of biotite-quartz-plagioclase gneiss in main belt of metasedimentary rocks, (Engel and Engel 1953, p. 1063)	2.32	4.12	1.31	0.32	5.43
Average of 32 samples of sillimanitic microcline-rich granitic gneiss, main igneous complex*	n.d.	0.64	4.34	0.64	4.98
Average of 8 samples of biotitic porphyroblastic granite gneiss (Hermon type), main belt of metasedimentary rocks	1.11	2.15	1.39	0.45	3.54
Average of 3 samples of migmatitic garnetiferous biotite-quartz-plagioclase gneiss. Main belt of metasedimentary rocks	1.48	3.42	0.71	0.49	4.13
Average of 3 samples of microcline-rich migmatitic biotite gneiss, main igneous complex	0.30	1.36	2.49	0.66	3.85

* Percentage of iron and titanium oxides based on percentage of magnetite and titaniferous hematite only. The iron and titanium of the small amount of biotite present would make the total oxides slightly greater.

The percentage of MgO and FeO + Fe_2O_3 in the biotite-quartz-plagioclase gneiss compared with that in the granitized rocks in Table 6. The comparative data are so approximate that it does not seem worth while to take into account the effect of changes in density. Furthermore, anyone attempting to estimate the amount of material expelled from the biotite-quartz-plagioclase gneiss must consider the degree to which material has been emplaced by injection and consequent inflation as compared with the degree to which it is the product of emplacement by replacement. Iron of the biotite-quartz-plagioclase gneiss has, in part, been retained in the almandite and biotite of the migmatite, and in large part or in whole as magnetite and especially as hematite in the microcline-rich sillimanitic granitic gneiss. There has certainly been some MgO driven out from much of the biotite-quartz-plagioclase gneiss to varying degrees consequent to granitization and migmatization. The relative degree of movement and fixation of iron, however, is so dependent on assumptions that have

CONTRASTS BETWEEN YOUNGER AND OLDER GRANITES

The alaskite and hornblende granite and equivalent gneisses so far discussed are inferred to belong to a series that transects an older belt of hornblende granite gneiss. This older granite gneiss is believed to be the upper facies of a gravity-differentiated thick sheet of orthogneiss which grades from feldspathic pyroxenite (rich in ilmenomagnetite and ilmenite) near the base through pyroxene syenite, pyroxene-quartz syenite, and hornblende-quartz syenite into hornblende granite at the top. These rocks have been described as the Diana and Stark complexes (Buddington, 1939, p. 73–109; 1948, p. 24–48). The older hornblende granite gneiss has a slightly higher ratio of plagioclase to potassium feldspar than

does the younger hornblende granitic rocks, and the quartz content is almost exclusively less than 24 per cent. The hornblende of both ages of granite may range from femaghastingsite to ferrohastingsite, both of which have normal fluorine content.

The origin of the members of the Diana and Stark complexes contrasts with that of the younger granites. The magma of the Diana and Stark complexes is inferred to have been emplaced as a sheet in only gently deformed rocks, whereas the younger granitic magmas were intruded contemporaneous with orogeny as phacoliths and batholiths in intensely deformed rocks.

Phenomena exhibited by the pyroxene-quartz syenite of the Diana complex indicate that the complex developed at higher temperatures than did the younger granites. The titaniferous magnetite of two specimens contained 7 and 7.4 per cent TiO_2 respectively, whereas the ilmenomagnetite of the younger hornblende-microperthite granites generally have only 5–6 per cent TiO_2 (Buddington, Fahey, and Vlisidis, 1955, p. 508). The higher percentage of TiO_2 is probably due to its greater solubility in the magnetite at higher temperature. Pyrrhotite is characteristically a minor accessory in the pyroxene syenite and quartz syenitic gneisses, whereas pyrite is the equivalent in the younger hornblende granites. This relationship is likewise indicative of a higher temperature (Kullerund and Yoder, 1956, p. 42). The crystallization of pyroxene in place of hornblende suggests a relatively more anhydrous magma which in turn would require a higher melting temperature than the magma which yielded the younger hornblende granites and alaskite. The younger hornblende granite and alaskite magma must have carried a substantial percentage of volatiles in solution, for minerals such as scapolite (Cl), chondrodite (F, OH), phlogopite (F, OH) and tourmaline (B) are widely disseminated in the marble where it is associated with younger granite masses.

The silicates in marble at contact with members of the Diana complex (Agar, 1923, p. 157–173) are characteristically of a higher-temperature group than those in association with the younger granites. For example, in the zones of contract with pyroxene-quartz syenite, the characteristic minerals are microperthite, diopside-augite, diopside, meionite, wernerite, and locally wollastonite. In contrast with the mineral assemblage at contact with the younger granites, the feldspar may be more strongly microperthitic, the pyroxene be more augitic and the scapolite more meionitic. Amphiboles and phlogopite, so normal at contact with the younger granites, are rare or absent adjacent to pyroxene-quartz syenite.

Wollastonite has not been found in zones of contact with the younger hornblende granite but occurs with the pyroxene-quartz syenite (Agar, 1923, p. 148–156) and with the hornblende granite of the Stark Complex at the Clifton magnetite mine. The wollastonite at the base of the Diana complex must have formed under a pressure of at least 2000 bars. If an equivalent pressure of CO_2 is inferred, the temperature must have been above 700°C. (Harker and Tuttle, 1956). Occurrence of wollastonite in zones of contact with the hornblende granite of the Stark complex and not in zones of contact with the younger hornblende granites may indicate that the Stark sheet was intruded in relatively brittle rocks at moderate depths where the CO_2 pressure was moderate and the temperature at which wollastonite formed was somewhat less than 700°C. These conditions contrast to the plutonic plastic-flow environment in which the younger granites were emplaced. The CO_2 pressure was high in this environment, and the temperature required for formation of wollastonite was not reached.

Magmatic History of Adirondack Precambrian

The major igneous rocks within the Grenville series of the Adirondacks point to a magmatic history which, as is now well known, has no equivalent in post-Precambrian time and which, though not uncommon in the Precambrian shields, is nevertheless absent from many orogenic structures of Precambrian age. In common with orogenic structures in general there are several periods of intrusion of magma of basaltic composition but these are relatively small in quantitative importance.

The three major kinds of magmas have

successively the composition of (1) gabbroic anorthosite; (2) pyroxene syenite, pyroxene-quartz syenite, and charnockite type (relatively rich in hypersthene of syenite and granite; and (3) normal hornblende granite and biotite alaskite. The first two are inferred to have been introdued as sheetlike masses under pre-orogenic conditions, and the third is synorogenic. A very long period of time and a period of diabase dike intrusion with the development of chill facies separate the first two sets of intrusives from the third. The gabbroic anorthosite magma may have been relatively rich in volatiles as indicated by recent data (Yoder, 1955, p. 1638) and by the associated geological phenomena. The syenitic-charnockitic magmas on the contrary were relatively dry. The pyroxene syenite (allied to mangerite), pyroxene-quartz syenite, and the charnockitic syenite and charnockitic granite may each have been intruded as separate sheets or may have formed differentiated facies within thick sheets.

By contrast with the most common types of rocks in orogenic structures there are no normal tonalites, quartz diorites, or granodiorites and no peridotites or lamprophyres.

Conclusion

New chemical data are interpreted to be consistent with the hypotheses that the hornblende-microperthite granite, biotite-microperthite alaskite, and their equivalent gneisses of the northwest Adirondacks are initially of magmatic origin; and that an inequigranular granite gneiss and sillimanitic microcline-rich granitic gneiss result in part at least from granitization of biotite-quartz-plagioclase gneiss.

References Cited

Adams, F. D., 1898, Nodular granite from Pine Lake, Ontario: Geol. Soc. America Bull., v. 9, p. 163–172

Agar, W. M., 1913, Contact metamorphism in the western Adirondacks: Am. Philos. Soc. Proc., v. LXII, p. 95–174

Brøgger, W. C., 1934, On several Archean rocks from the south coast of Norway. I Nodular granites from the environs of Kragerø; Vid. Akad. Skr. Math. Natur. Kl. (1933)

Buddington, A. F., 1934, Geology and mineral resources of the Hammond, Antwerp and Lowville quadrangles, N. Y. State Mus. Bull. No. 296

——1939, Adirondack igneous rocks and their metamorphism: Geol. Soc. America Mem. 7, 354 p.

——1948, Origin of granitic rocks of the northwest Adirondacks, p. 21–43 *in* Gilluly, James, *Editor*: Origin of granite: Geol. Soc. America Mem. 28, 139 p.

Buddington, A. F., and Smyth, C. H., 1926, Geology of the Lake Bonaparte quadrangle: N. Y. State Mus. Bull. No. 269

Buddington, A. F., Fahey, Joseph, and Vlisidis, Angela, 1955, Thermometric and petrogenic significance of titaniferous magnetite: Am. Jour. Sci., v. 253, p. 497–532

Bugge, J. A. W., 1943, Geological and petrological investigations in the Kongsberg-Bamble formation: Norges Geologiska Undersökelse, nr. 160, p. 103–114

Coetzee, C. B., 1942, Metamorphosed sediments from the Goodhouse-Pella area, Namaqualand, South Africa: Royal Soc. S. Africa, p. 91–112

Cushing, H. P., 1907, Geology of the Long Lake quadrangle, N. Y.: N. Y. State Mus. Bull. No. 115

Cushing, H. P., *et al.*, 1910, Geology of the Thousand Islands region: N. Y. State Mus. Bull. No. 145

Dale, N. C., 1935, Geology of the Oswegatchie quadrangle: N. Y. State Museum Bull. no. 302

DeVore, G. W., 1956, Surface chemistry as a chemical control on mineral association: Jour. Geol., v. 64, p. 31–55

Dietrich, R. V., 1954, Fish Creek phacolith northwestern New York: Am. Jour. Sci., v. 252, p. 513–531

Engel, A. E. J., and Engel, C. G., 1953, Greenville series in the northwest Adirondack Mountains, New York: Geol. Soc. America Bull., v. 64, p. 1049–1097

Geijer, Per, 1911, Contributions to the geology of the Sydvaranger iron ore deposits: Geol. fören Stockholm Förh., Bd. 33, p. 322–323

——1930, Geology of the Gällivare iron ore field: Sveriges Geol. Undersokning, Ser. Ca. no. 22, p. 112

Harker, R. I., and Tuttle, O. F., 1956, Experimental data on the PCO_2-I curve for the reaction: calcite + quartz wollastonite + carbon dioxide: Am. Jour. Sci., v. 254, p. 239–256

Jahns, R. H., 1953, The genesis of pegmatites: Am. Mineralogist, v. 38, p. 1078–1112

Kullerud, G., and Yoder, H. S., 1956, Upper stability curve of pyrite: Am. Geophys. Union Abstracts p. 42

Lodding, W., 1951, New Jersey's potential feldspar resources: Mineral Technology and Economic Evaluation: Bull. 5, pt. II, p. 32

Nockolds, S. R., 1954, Average chemical composition of some igneous rocks: Geol. Soc. America Bull., v. 65, p. 1007–1032

Read, H. H., 1951, Metamorphism and granitization: Geol. Soc. S. Africa Trans., v. 54, annexure, p. 1–27

Reynolds, D. L., 1947, The association of basic "fronts" with granitization: Sci. Progress, v. XXXV, p. 205–219

Sederholm, J. J., 1928, On orbicular granites: Comm. geol. Finlande Bull, 83, p. 80–81

Swineford, Ada, Frye, J. C., and Leonard, A. B., 1955, Petrography of the late Tertiary volcanic ash falls in the central Great Plains: Jour. Sed. Petrology, v. 25, p. 243–261

Tuttle, O. F., and Bowen, N. L., 1952, Annual report of Director of the Geophysical Laboratory for the year 1951–1952, no. 1205, p. 39

Washington, H. S., 1917, Chemical analyses of igneous rocks published from 1884 to 1913, inclusive: U. S. Geol. Survey Prof. Paper 99

Yoder, H. S., 1955, Diopside-anorthite-water system at 5000 bars: Geol. Soc. America Bull., v. 66, p. 1638–1639

PRINCETON UNIVERSITY, PRINCETON, N. J.

MANUSCRIPT RECEIVED BY THE SECRETARY OF THE SOCIETY, MAY 24, 1956

BULLETIN OF THE GEOLOGICAL SOCIETY OF AMERICA
VOL. 68, PP. 307-314, 3 FIGS., 1 PL. MARCH 1957

DISCONFORMITY BETWEEN LOWER AND UPPER CRETACEOUS IN WESTERN COLORADO AND EASTERN UTAH

BY WILLIAM D. CARTER

ABSTRACT

In a part of western Colorado and eastern Utah the contact between the Burro Canyon formation (Lower Cretaceous) and the Dakota sandstone (Upper Cretaceous) is a broadly undulating erosional surface. Angular and subangular pebbles, cobbles, and boulders of sandstone, chert, and quartzite derived from the Burro Canyon have been found in the basal part of the Dakota sandstone. These fragments and a thin quartzite bed at the top of the Burro Canyon indicate that the formation was lithified, probably under subaerial conditions, before its erosion and before deposition of the Dakota sandstone. On the basis of fossil plants R. W. Brown (1950) placed the boundary between the Lower and Upper Cretaceous at the top of the Burro Canyon. The field evidence described here supports this division and further suggests a hiatus between the deposition of Lower and Upper Cretaceous sediments in part of the Colorado Plateau.

CONTENTS

TEXT

	Page
Introduction	307
Burro Canyon formation	308
Dakota sandstone	309
Burro Canyon-Dakota contact	311
Conclusions	313
References cited	313

ILLUSTRATIONS

Figure	Page
1. Index map of part of the Colorado Plateau	309
2. Generalized section of strata above and below the Burro Canyon-Dakota contact	310
3. Diagrammatic cross section of a typical channel of the Dakota sandstone	312
Plate	**Facing page**
1. Quartzite and sandstone boulders in conglomerate of the Dakota sandstone	312

INTRODUCTION

The age of the Dakota sandstone and its relationship with underlying formations in western Colorado and eastern Utah have been the subject of discussion among geologists for many years. Early workers described the contact as an erosional unconformity having angular relationships between the beds above and below the erosion surface. Some describe wedging out of the underlying beds or of entire formations. Coffin (1921, p. 109), in a discussion of the Post-McElmo (as defined by him) and the Dakota relationships, described thinning of the upper beds of the Post-McElmo which he thought "could be due to either non-deposition or deposition and subsequent erosion." He described the lowermost unit of the Dakota as "the first sandstone or conglomerate which underlies the lowest carbonaceous shale or coal horizon." Gilluly and Reeside (1927, p. 82) mention that "the Dakota(?) sandstone rests unconformably on the eroded surface of the Morrison formation" around the northern part of the San Rafael Swell. Gregory and Moore (1931, p. 94) state that "Throughout the Kaiparowits region the Dakota(?) sandstone rests with more or less marked unconformity on the Morrison or on Upper Jurassic sandstones." In that region the unconformity is indicated by (1) a wedging out of the beds beneath the Dakota(?); (2) marked irregularities in the surface covered by the Dakota(?); (3) a marked change in the character of sedimentation at the base of the Dakota(?) sandstone. A general description of this unconformity is given by Baker (1946, p. 91) in his discussion of the Dakota sandstone and its

basal contact with the Morrison formation. Stokes (1950, p. 93) also briefly describes the same unconformity in his discussion of the conglomerates of the Shinarump, Buckhorn, and Dakota.

It is possible that much of the difficulty in mapping the contact stems from the disagreement of early workers in defining and correlating the formations below the Dakota sandstone. This difficulty dates back at least to Holmes (1875, p. 243), who included beds in what he called the Upper Dakota strata that are now considered Dakota and Burro Canyon. He placed the beds now called Morrison in his Lower Dakota group. At one time the McElmo formation contained all strata from the base of the Carmel of Middle and Late Jurassic age up to the base of the Dakota sandstone. Cross and others (1899), in the Telluride and La Plata folios, describe a conglomeratic sandstone bed in what they called the McElmo formation that is lithologically similar to the Dakota but lies 50–100 feet below the Dakota sandstone.

In assigning an age to the Dakota it is well to observe comments by J. B. Reeside, Jr. (Personal communication), who states that, "The reference of Dakota sandstone to an Early(?) and Late Cretaceous age . . . was intended to be used only in areas where a Lower Cretaceous unit is not recognized as a separate entity and is presumably included in the 'Dakota' of local usage." Similar diversity of opinion has arisen over the age and stratigraphic limits of the Morrison formation. For example, Gilluly and Reeside (1927, p. 81) included the Morrison formation in the Lower Cretaceous(?) series, which, as mapped, it may have been at least in part. Stratigraphic limits, as then defined, may have included beds that are now considered to be of Late Jurassic and Early Cretaceous ages.

Geologic mapping in the Mt. Peale No. 1 quadrangle (Fig. 1), east of the La Sal Mountains near the Utah-Colorado line, led to the recognition of the unconformity and certain features heretofore undescribed. It is hoped that the subsequent discussion will aid the field geologist and lead to further studies, more regional in scope. The geologic mapping in that quadrangle, upon which this study is based, was conducted by the U. S. Geological Survey on behalf of the Division of Raw Materials of the U. S. Atomic Energy Commission.

Burro Canyon Formation

The unit now called the Burro Canyon formation, originally described as a separate formation by Coffin (1921) who called it Post-McElmo, was named by Stokes (1948) to designate the beds separating the Morrison formation of Jurassic age from the Dakota sandstone of Late Cretaceous age in southwestern Colorado and southeastern Utah. Stratigraphic position and fossil evidence (Brown, 1950; Katich, 1951; Stokes, 1952) indicate that the Burro Canyon is of Early Cretaceous age.

West of the Colorado River in Utah are beds of somewhat similar lithology and the same age as the Burro Canyon that Stokes (1944) named the Buckhorn conglomerate and Cedar Mountain shale. Stokes (1944, p. 968) believes that these beds were included in the McElmo and Morrison described by earlier workers.

The Burro Canyon formation contains a basal unit, approximately 110 feet thick, composed of light-gray to light-brown medium- to coarse-grained cross-bedded sandstone containing pebble conglomerate lenses and sparse silicified logs. This basal unit conformably overlies the variegated shale and mudstone units of the Brushy Basin shale member of the Morrison formation (Fig. 2). Commonly exposed as a prominent cliff and forming mesas, this sandstone unit in most places is overlain by light-green mudstone, siltstone, and shale containing thin beds of siliceous limestone, limestone conglomerate, limy sandstone, chert, and quartzite, which have an aggregate thickness of 150 feet. Where present, these strata distinguish the Burro Canyon formation from the overlying Dakota sandstone. The maximum measured thickness of the Burro Canyon formation in the Mt. Peale No. 1 quadrangle is about 260 feet. At localities within the quadrangle where complete sections of the formation are preserved, a thin (1–8 feet thick) bed of light-gray well-indurated quartzite constitutes the uppermost unit.

In the quartzite bed, spheroidal structures with concentric crack systems, covering areas

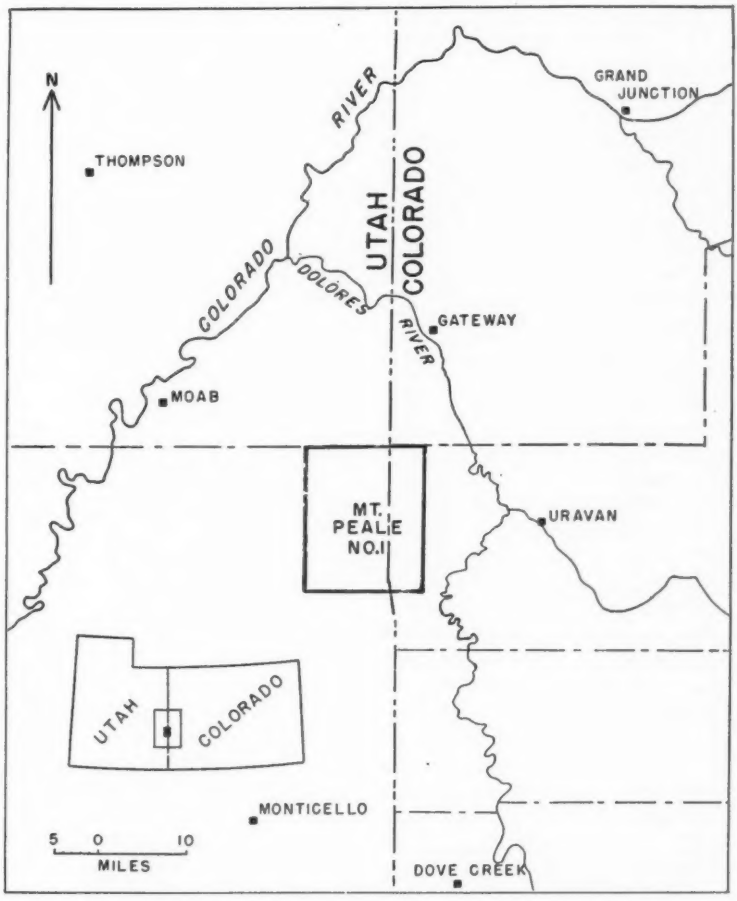

FIGURE 1.—INDEX MAP OF PART OF THE COLORADO PLATEAU

up to several feet in diameter, are common. Several of these have irregular nodular cores of light-blue-gray chert, which accoring to Pettijohn (1949, p. 149–150) result from local concentrations of silica during epigenetic relacement of carbonate cement, common in the Burro Canyon, by silica within the sandstone unit. Later dehydration caused the quartzite to shrink and created concentric crack systems known as contraction spheroids. This phenomenon is common in the quartzite bed, around chert nodules and elsewhere in the unit.

Silicification of the sandstone to quartzite came before deposition of the overlying formations. As this is the uppermost unit of the Burro Canyon formation, it is presumed that lithifying processes were active during a period of nondeposition under subaerial weathering conditions. The duration of this hiatus is not yet determined.

DAKOTA SANDSTONE

The Dakota sandstone in the Mt. Peale No. 1 quadrangle rests on the eroded surface of the Burro Canyon formation and separates it from the Mancos shale of Late Cretaceous age. The strata constituting the Dakota sandstone can generally be divided into three parts: (1) a basal unit of sandstone and conglomerate, (2)

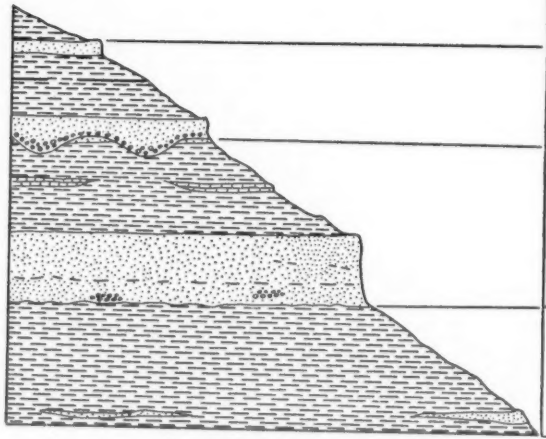

SERIES	FORMATION	THICKNESS	CHARACTER
UPPER CRETACEOUS	Mancos shale	300 ? feet	GREENISH-GRAY TO DARK GRAY SHALE AND SILTSTONE; FOSSILIFEROUS. FORMS SLOPES.
	Dakota sandstone	90-200? feet	LIGHT-BROWN SANDSTONE. GRAY CARBONACEOUS SHALE, MUDSTONE. THIN COAL SEAMS. CARBON AND LIMONITE REPLACED PLANT FOSSILS. FORMS SLOPE.
	Disconformity		
LOWER CRETACEOUS	Burro Canyon formation	Absent-150 feet	SANDSTONE AND CONGLOMERATE. GRAY-GREEN MUDSTONE. THIN DISCONTINUOUS BEDS OF LIMESTONE, CHERTY LIMESTONE, AND CALCAREOUS SANDSTONE. FORMS SLOPES.
		60-110 feet	LIGHT-BROWN SANDSTONE. MASSIVE AND CROSSBEDDED. PEBBLE CONGLOMERATE LENSES. FORMS PROMINENT CLIFFS.
UPPER JURASSIC	Morrison formation	700-760 feet	Brushy Basin shale member: VARICOLORED MUDSTONE AND SILTSTONE WITH DISCONTINUOUS SANDSTONE AND CONGLOMERATE LENSES. UPPER 200 FEET SHOWN. FORMS SLOPES.

FIGURE 2.—GENERALIZED SECTION OF STRATA ABOVE AND BELOW BURRO CANYON-DAKOTA CONTACT
Mt. Peale No. 1 Quadrangle, San Juan County, Utah, and Montrose County, Colorado

a middle unit of gray carbonaceous shale with discontinuous coal seams, (3) an upper unit of sandstone. Where all three units are present the formation has an aggregate thickness of approximately 200 feet. The upper contact with the overlying Mancos is obscure in most places.

The basal unit ranges from a few inches to more than 60 feet in thickness and crops out as a ledge which commonly forms the cap of mesas. It is composed of yellow-brown to light-orange-brown medium-grained sandstone which is characterized in many places by thin lentils of sandstone, 4 inches–2 feet thick. These lentils frequently contain inclined beds of sandstone which dip from 20° to 40° in a northeasterly direction. The basal sandstone unit contains sparse to abundant carbonaceous and limonite-replaced plant debris which are considered to be of Late Cretaceous age (Brown, 1950, p. 47). These, and the carbonaceous shale and coal beds of the middle unit, are diagnostic of the Dakota and distinguish it from the Burro Canyon formation.

In many places sandstone of this unit contains or rests upon discontinuous lenses of coarse conglomerate and sandstone. The conglomerate is composed of rounded and subrounded pebbles of gray and black chert, milky quartz, and gray quartzite ranging in diameter from 5 mm to 5 cm. Local concentrations of angular and subangular cobbles and boulders of sandstone, quartzite, and chert are found at the base of the sandstone or conglomerate. In places the conglomerate is very poorly cemented and extremely friable; elsewhere it contains great quantities of silica cement and is well indurated. Where present this distinctive conglomerate forms the bottom of the sequence of beds constituting the Dakota.

The basal unit grades upward into, and in places interfingers with, light-gray carbonaceous shale, siltstone, and mudstone which may have a total thickness of approximately 100 feet. Coal seams, generally less than 3 feet thick, are found at various levels throughout the unit.

The upper unit is a light-brown medium- to fine-grained sandstone which forms ledges that range from 10 to 30 feet in thickness. Both inclined and flat bedding are common throughout the upper sandstone unit.

Burro Canyon-Dakota Contact

The Burro Canyon-Dakota contact in the Mt. Peale No. 1 quadrangle is extremely undulatory. Where the quartzite bed at the top of the Burro Canyon formation is present it is conformably overlain by lenses of conglomerate and sandstone constituting the basal unit of the Dakota sandstone. Following the outcrop from such a locality it is observed that the base of the conglomerate comes in contact with progressively lower beds of the Burro Canyon defining the edge of a channel. Broad channels filled with conglomerate of the Dakota have been observed in contact with the light-green mudstone, limestone, and chert of the Burro Canyon, and, in many places, with the thick sandstone with conglomerate lenses which comprises the basal unit of the Burro Canyon. Included in the basal unit of the Dakota are angular and subangular fragments of rock from the beds through which the channels have been scoured (Pl. 1). These fragments are composed of the more resistant quartzite, chert, and sandstone of the Burro Canyon. The fragments of quartzite in the conglomerate are identical to the quartzite at the top of the Burro Canyon. The mudstone and limestone of the upper part of the Burro Canyon are less resistant to stream action and are represented by fragments that are generally smaller than the chert and quartzite pebbles of the conglomerate.

In the channels, most of the quartzite of the Burro Canyon and the sandstone below it is represented by angular and subangular boulders ranging from a few cubic inches to 15 or 20 cubic feet. The larger boulders, although less abundant, seem to indicate deposition of coarser material along the channel axes (Fig. 3).

Here the relationships between the beds above and below the erosion surface are considerably different from those described elsewhere on the Colorado Plateau.

As no angular relationship or wedging out was observed, except on a local basis, in the Mt. Peale No. 1 quadrangle the term "discon-

formity" is used herein to describe the contact in this area.

In outcrop, the disconformity between the Burro Canyon formation and the Dakota sandstone is in places obscured, and because of its undulatory nature is difficult to trace. Where cemented and extremely friable. Where the contact is stratigraphically higher—that is, on the mudstone and limestone of the upper Burro Canyon, the conglomerate forms a ledge 1–20 feet thick, and on dip slopes it is found as outliers capping knolls.

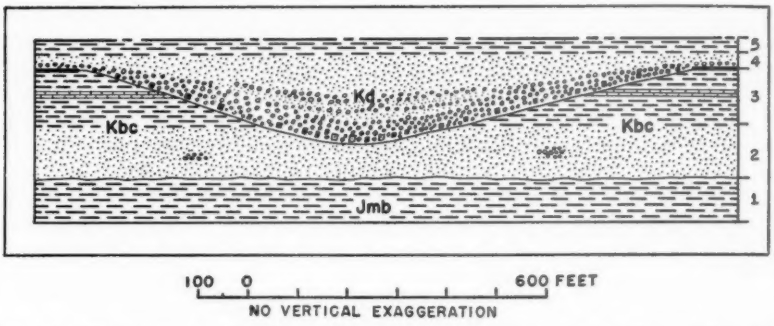

FIGURE 3.—DIAGRAMMATIC CROSS SECTION OF A TYPICAL CHANNEL OF THE DAKOTA SANDSTONE

1. Variegated mudstones of the Brushy Basin member of the Morrison formation of Jurassic age.
2. Basal sandstone and conglomerate unit of the Burro Canyon formation of Cretaceous age.
3. Light-gray-green shale, siltstone, mudstone and limestone containing thin sandstone beds capped by light-gray quartzite (heavy black line) which constitute the upper unit of the Burro Canyon formation.
4. Basal conglomerate and sandstone bed of the Dakota sandstone of Cretaceous age, filling channel scour and also resting on the quartzite bed of the Burro Canyon. Black squares indicate quartzite blocks of the Burro Canyon included in the conglomerate. Dotted squares indicate fragments of the basal Burro Canyon. Distribution and frequency of blocks are approximate.
5. Light-gray shale and mudstone overlain by thin, discontinuous carbonaceous shales and coal seams of the Dakota sandstone.

resting on basal sandstone of the Burro Canyon, conglomerate of the Dakota may be distinguished from a distance by a color contrast—that is, the somber gray sandstone of the Burro Canyon is overlain by conglomerate beds in the Dakota that range from yellow brown to pale orange brown. To an observer near the outcrop this color contrast is less conspicuous; in hand specimen it is indiscernible except where the Burro Canyon is bleached immediately below its contact with the Dakota. Bleached zones range from a few inches to several feet in thickness and are typified by rock that is poorly

These basal conglomerates of the Dakota fill broad depressions or channels in the Burro Canyon formation that are over 100 feet deep in many places, several thousands of feet wide, and of unknown length. Measurements of current lineation, cross-beds, and festoons indicate that the trend of these channels varies, but in general is N. 30° E. Poorly preserved fossils in the chert pebbles of the conglomerate have been tentatively identified as of Permian or Pennsylvanian age. Some forms are similar to fossils found in the Kaibab limestone and suggest a source that lies to the southwest (L. C.

PLATE 1.—QUARTZITE AND SANDSTONE BOULDERS IN CONGLOMERATE OF THE DAKOTA SANDSTONE

FIGURE 1.—Dakota sandstone and conglomerate resting on the basal sandstone unit of the Burro Canyon formation. Locality is on Wray Mesa, north of Coyote Wash, San Juan County, Utah.

FIGURE 2.—Exceptionally large sandstone boulders comprise the basal conglomerate of the Dakota sandstone at Peter's Hill near Monticello, Utah. Man's hammer indicates contact with the basal sandstone of the underlying Burro Canyon formation. Photograph by J. C. Warman.

FIGURE 1

FIGURE 2

QUARTZITE AND SANDSTONE BOULDERS IN CONGLOMERATE
OF THE DAKOTA SANDSTONE

Craig, personal communication). This source agrees with measurements of sedimentary structures found in the conglomerate beds at the base of the Dakota sandstone.

Other localities where boulder fragments of the Burro Canyon are imbedded in the base of sandstone and conglomerate of the Dakota are: Peters Hill (Pl. 1, fig. 2); Browns Hole and other areas near Lisbon Valley, Utah, reported by G. W. Weir (personal communication); near the Abajo Mountains, Utah, reported by I. J. Witkind (personal communication); and observed by the writer at Spring Creek Mesa near Uravan, Colorado. Although fragments of cobble and boulder size are not always present, an erosional contact is being mapped as far south as the Great Sage Plain (L. C. Huff, personal communication) and the Ute Mountains (E. B. Ekren, personal communication) in southwestern Colorado and southeastern Utah. Craig and others (1955) state that in northeastern Arizona and northwestern New Mexico the Dakota sandstone overlies progressively older formations to the south and west.

Reworked fragments derived from the Burro Canyon are notably absent in the Dakota at the type locality of the Burro Canyon formation and over a large area of Disappointment Valley in San Miguel County, Colorado. Light-green mudstone, siltstone, and shale beds of the Burro Canyon are separated from the gray carbonaceous shale of the Dakota by a sandstone bed which is a few feet thick, somewhat quartzitic, and contains minor amounts of carbonaceous debris. It is probable that this area remained as a slight highland area, around which early Dakota streams entrenched and meandered, and was buried by later Dakota deposition. Several similar though probably smaller highland areas are present in the Mt. Peale No. 1 quadrangle and may represent a greater time lapse in deposition than in areas where channels are present.

Conclusions

A disconformity is present between the Burro Canyon formation of Early Cretaceous age and the Dakota sandstone of Late Cretaceous age in the Mt. Peale No. 1 quadrangle. It is represented by an undulatory erosional surface separating the sandstone, and light-green limestone, mudstone, and shale of the Burro Canyon from the overlying conglomerate, sandstone, gray carbonaceous shale, and coal beds of the Dakota sandstone. The beds above and below the contact are concordant, in contrast to the conditions in certain other areas of the Colorado Plateau where an angular unconformity exists locally.

A quartzite bed is the uppermost unit of the Burro Canyon formation, and angular blocks of this and lower units are found in the basal conglomerate and sandstone of the Dakota. This evidence indicates that the Burro Canyon was lithified before erosion and deposition of the Dakota sandstone and that a hiatus separates the two formations. It further suggests that the Dakota sandstone of Early (?) and Late Cretaceous age may be Early (?) only where the Burro Canyon formation of Early Cretaceous age is present but undifferentiated.

References Cited

Baker, A. A., 1946, Geology of the Green River desert—Cataract Canyon region, Emery, Wayne, and Garfield Counties, Utah: U. S. Geol. Survey Bull. 951, 122 p.

Brown, R. W., 1950, Cretaceous plants from southwestern Colorado: U. S. Geol. Survey Prof. Paper 221-D, p. 45–66

Coffin, R. C., 1921, Radium, uranium, and vanadium deposits of southwestern Colorado: Colorado Geol. Survey Bull. 16, 227 p.

Craig, L. C., Holmes, C. N., Cadigan, R. A., Freeman, V. L., 1955, Stratigraphy of the Morrison and related formations, Colorado Plateau region, A preliminary report: U. S. Geol. Survey Bull. 1009–E, p. 125–168

Cross, C. W., and Purington, C. W., 1899, Description of the Telluride quadrangle: U. S. Geol. Survey Geol. Atlas, folio 57

Cross, C. W., Spencer, A. C., and Purington, C. W., 1899, Description of the La Plata quadrangle: U. S. Geol. Survey Geol. Atlas, folio 60

Gilluly, James, and Reeside, J. B., Jr., 1927, Sedimentary rocks of the San Rafael Swell and some adjacent areas in eastern Utah: U. S. Geol. Survey Prof. Paper 150, p. 61–110

Gregory, H. E., and Moore, R. C., 1931, The Kaiparowits region, a geographic and geologic reconnaissance of parts of Utah and Arizona: U. S. Geol. Survey Prof. Paper 164, 157 p.

Holmes, W. H., 1875, Geological report on the San Juan district: U. S. Geol. and Geog. Survey Terr. 9th Ann. Rept. (1877), p. 237–277

Katich, P. J., Jr., 1951, Recent evidence for Lower Cretaceous deposits in Colorado Plateau: Am. Assoc. Petroleum Geologists Bull., v. 35, p. 2093–2094

Pettijohn, F. J., 1949, Sedimentary Rocks: N. Y., Harper and Brothers, 526 p.

Stokes, W. L., 1944, Morrison formation and related deposits in and adjacent to the Colorado Plateau: Geol. Soc. America Bull., v. 55, p. 951–992

—— 1950, Pediment concept applied to Shinarump and similar conglomerate: Geol. Soc. America Bull., v. 61, p. 91–98

—— 1952, Lower Cretaceous in Colorado Plateau: Am. Assoc. Petroleum Geologists Bull., v. 36, p. 1766–1776

Stokes, W. L., and Phoenix, D. A., 1948, Geology of the Utah-Colorado Salt Dome region with emphasis on Gypsum Valley, Colorado: U. S. Geol. Survey Prelim. Oil and Gas Inv. Map 93

U. S. Geological Survey, Grand Junction, Colorado

Manuscript Received by the Secretary of the Society, July 20, 1956

Publication Authorized by the Director, U. S Geological Survey

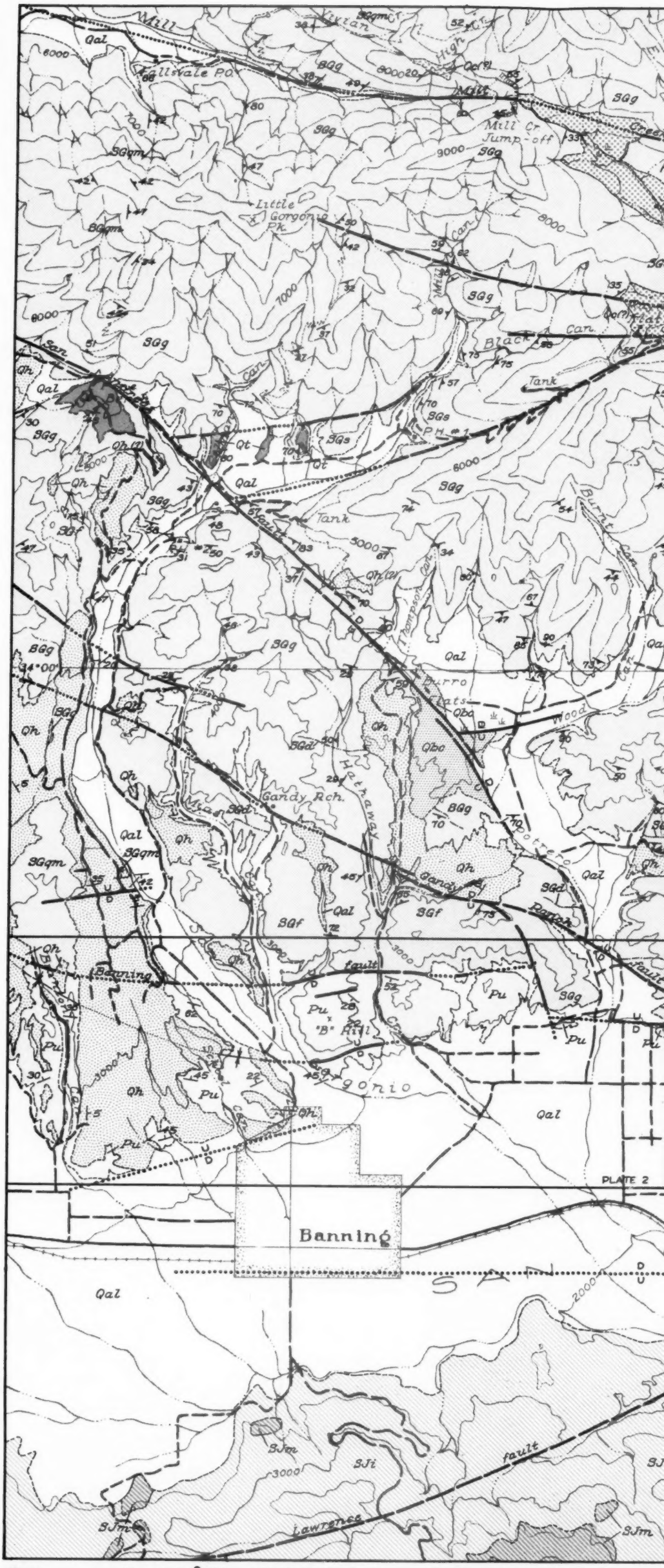

Base map south of 34°00′ modified from Corps of Engineers, U. S. Army, 1
Base map north of 34°00′ from air photographs; topography adapted from U
Geological Survey, 1902. Accuracy: poor.

y, 1943-1944
om U. S.

1 0.5 0 1 2 3 4 5

Contour interval 500 feet

GEOLOGIC MAP OF THE SAN GORGONIO PASS AREA, SOU

1944

Geology north of San Gorgonio P
Geology south of San Gorgonio P

0.5 0 1 2 3 4 5 Miles

Contour interval 500 feet

GIC MAP OF THE SAN GORGONIO PASS AREA, SOUTHERN CALIFORNIA

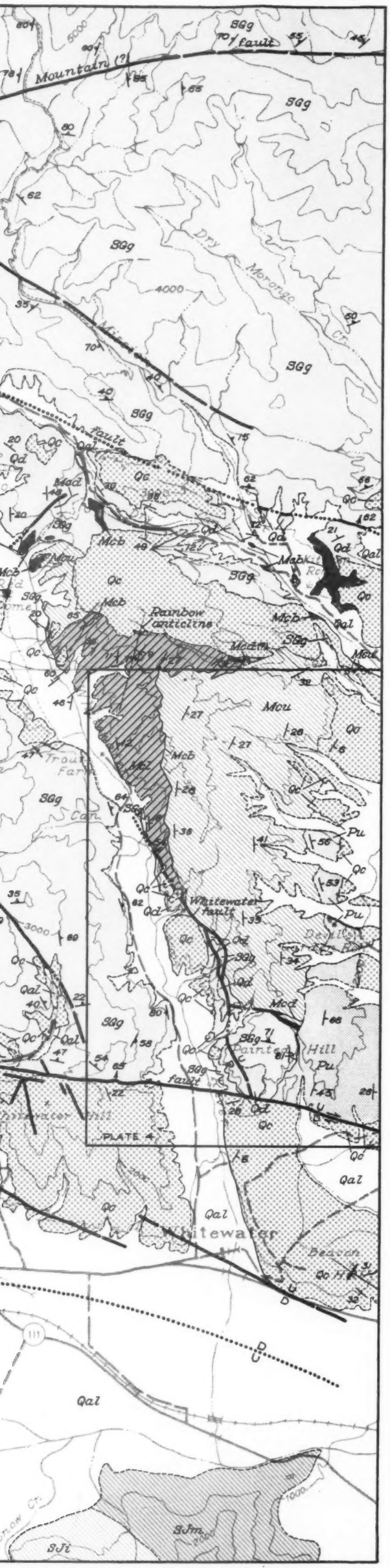

lo Pass by C. R. Allen, 1952-1954
io Pass adapted from D. M. Fraser (1931)

EXPLANATION

Qal — Alluvium

UNCONFORMITY

Qls — Landslide material

UNCONFORMITY

Qbc — Burnt Canyon breccia

UNCONFORMITY

Qt — Fanglomerates and terrace gravels of unknown correlation

UNCONFORMITY

Qh — Heights fanglomerate

UNCONFORMITY

Qc — Cabezon fanglomerate

UNCONFORMITY

Qd — Deformed gravels of Whitewater River

CONTACT NOT EXPOSED

Pu — Pliocene and Lower Pleistocene sedimentary and volcanic rocks, undifferentiated

UNCONFORMITY

Mcu / Mcl / Mcb / Mcd — Coachella fanglomerate

Upper member, Mcu; Lower member, Mcl; interlayered flows of olivine basalt, Mcb, and associated dikes of olivine basalt, Mcd.

UNCONFORMITY

SGf / SGp / SGg / SGqm / SGs / SGd — San Gorgonio igneous-metamorphic complex

Migmatitic gneiss, SGg, including flaser gneiss, SGf, piedmontite-bearing gneiss, SGp, and greenschist, SGs, pervasively intruded by Cactus (?) quartz monzonite, SGqm, with associated pegmatite dikes, SGd. All contacts are gradational.

CONTACT NOT EXPOSED

SJi / SJm — Crystalline rocks of the San Jacinto Mountains

Metamorphic rocks, SJm, and intrusive rocks, SJi

QUATERNARY

TERTIARY

Upper Miocene(?) Pliocene-Pleistocene

MESOZOIC AND OLDER

Contact
Dashed where approximately located

Fault, showing dip
Dashed where approximately located; dotted where concealed. U, upthrown side; D, downthrown side.

Thrust fault
Dashed where approximately located; dotted where concealed. T, overthrust plate.

Anticline, showing plunge
Dashed where approximately located; dotted where concealed

Syncline
Dashed where approximately located; dotted where concealed

Strike and dip of beds

Strike of vertical beds

Strike and dip of overturned beds

Strike and dip of foliation

A

BULLETIN OF THE GEOLOGICAL SOCIETY OF AMERICA
VOL. 68, PP. 315-350, 3 FIGS., 6 PLS. MARCH 1957

SAN ANDREAS FAULT ZONE IN SAN GORGONIO PASS, SOUTHERN CALIFORNIA

BY CLARENCE R. ALLEN

ABSTRACT

Unusual features of the San Andreas fault in the San Gorgonio Pass area of Southern California are the absence of rift topography, absence of lateral stream offsets, an abrupt change in trend of the fault trace, seismic evidence for the predominance of thrusting over strike-slip faulting, and a lack of great earthquakes in historic time.

Rocks of the San Gorgonio igneous-metamorphic complex crop out over most of the map area and constitute a metamorphic terrane of intermediate to basic composition that has been intimately intruded and partially reconstituted by Mesozoic(?) quartz monzonite. Flaser gneiss, greenschist, and piedmontite-bearing gneiss are distinctive rock types in the otherwise rather uniform migmatitic gneisses. Most of the younger rocks of the pass area are sedimentary and reflect a history of recurrent deformation and deposition; they range in age from upper Miocene(?) to Quaternary, and nearly all are of alluvial-fan or flood-plain origin.

Quaternary alluvial fans that once buried a former rugged topography are now being dissected along the north side of the pass, leaving numerous surfaces of low relief and associated stream terraces. Warping of these surfaces suggests Quaternary arching of the mountain range along a north-south axis.

Within San Gorgonio Pass, the San Andreas fault curves abruptly southward from its normal southeast trend and butts into the eastward-trending Banning fault at 45°. The Banning fault is a major tectonic feature that delineates the north side of the pass and forms the southern limit of the Transverse Ranges in this region. Thrust and reverse movements of at least 5000 feet have taken place on this fault in Quaternary time, and, although there is little evidence of Recent lateral displacements, late Pliocene and Pleistocene right-hand strike-slip movements totaling at least 5 miles are suggested. The Mill Creek and Mission Creek faults are major branches of the San Andreas fault that diverge northward; both evince considerable late Cenozoic vertical displacement, but possible lateral movements are unknown.

This study neither proves nor disproves the existence of lateral displacements amounting to perhaps hundreds of miles along the San Andreas fault zone as a whole. But if large lateral displacements have taken place, they must have been followed by deformation and disruption of the fault traces then existent, because lateral movements of even 1 mile are difficult to reconcile with the complex surface geometry of faults within the pass area. Faults previously considered branches of the San Andreas, particularly the Mission Creek and San Jacinto faults, may have absorbed much of the lateral strain, and the Banning fault may represent an ancestral San Andreas fault—now deformed into a Transverse Range fault. The deformation and disruption of former breaks appear to represent a pattern that is typical of the entire eastern half of the Transverse Ranges, where elements of San Andreas and Transverse Range structure have been vying for control; evidently one set has alternated with the other in attaining temporary dominance. Southeast of San Gorgonio Pass it is not clear which, if any, fault trace deserves the name of San Andreas, and it is suggested that the entire area between the Elsinore fault on the west and the east side of the Salton depression on the east be termed the San Andreas fault zone.

CONTENTS

TEXT

	Page
Introduction	316
Background of investigation	316
Geographical setting	318
Acknowledgments	318
Crystalline rocks	318
Introduction	318
San Gorgonio igneous-metamorphic complex	318
Crystalline rocks of the San Jacinto Mountains	322

	Page
Stratigraphy of sedimentary rocks	323
Introduction	323
Coachella fanglomerate	323
Hathaway Formation	326
Imperial Formation	327
Painted Hill Formation	328
San Timoteo (?) Formation	329
Deformed gravels of Whitewater River	330
Cabezon fanglomerate	331
Heights fanglomerate	331
Burnt Canyon breccia	332
Alluvium	332
Geomorphology and ground water	332
Introduction	332
Surfaces of low relief	332
Closed depressions	335
Alluvial fans	335
Ground water	336
Geologic structure	336
San Andreas fault	336
Banning fault	339
Mission Creek fault	341
Pinto Mountain (?) fault	342
Mill Creek fault	343
Folding	344
Mechanics of the Banning-San Andreas fault system	344
The problem of large lateral displacement	346
Origin of San Gorgonio Pass	347
References cited	347

ILLUSTRATIONS

Figure	Page
1. Index map	317
2. Generalized correlation chart of sedimentary rocks of San Gorgonio Pass region	324
3. Principal stress relationships necessary to cause thrust and strike-slip faulting	345

Plate	Facing page
1. Reconnaissance geologic map of the San Gorgonio Pass area	315
2. Geologic map and structure sections of the foothills north of Banning	322
3. Geologic map and structure sections of the foothills between Millard and Cottonwood canyons	326
4. Geologic map and structure sections of the Painted Hill area	328
5. San Gorgonio Pass	344
6. Features of faulting	345

TABLES

Table	Page
1. Sequence and character of sedimentary rocks of San Gorgonio Pass	325

Introduction

Background of Investigation

The investigations here described were aimed at increasing the knowledge of a part of the San Andreas fault system of California. The many unanswered and significant tectonic problems relating to this fault have been summarized by Hill and Dibblee's (1953) study, which includes a bibliography of most earlier studies. These investigators have stimulated further field work by their suggestion that the total lateral displacement on the San Andreas fault zone may be as much as 350 miles, in sharp contrast to a previous suggestion of less than 1 mile (Taliaferro, 1943).

The San Gorgonio Pass area, 70 miles east of Los Angeles (Fig. 1), has held particular promise for studies of the San Andreas fault zone, because the rugged topography affords excellent exposures (Pl. 5) and because Tertiary marine beds crop out on both sides of the supposed trace of the fault. Several anomalous features give added interest to the San Gorgonio Pass area:

(1) Rift topography is absent along much of the supposed trace of the San Andreas fault. Potato Canyon (Pl. 5), northwest of San Gorgonio Pass, was recognized by Fairbanks (*in* Lawson *et al.*, 1908, p. 45) as "the last of the longitudinal depressions of any size marking the line of the rift." Fairbanks ascribed the lack of rift topography in the pass area to rapid erosion caused by "recent disturbances." Vaughan (1922), who first mapped the geology of this area, interpolated a segment of the fault between Pine Bench and the mouth of Stubby Canyon (Pls. 1, 5) despite the admitted absence of good physiographic and structural evidence for faulting between these two points.

(2) Lateral stream offsets, caused by strike-slip displacements, are among the most typical features of the San Andreas fault zone over most of its course, yet air photos reveal no undisputable stream offsets in the San Gorgonio Pass region nor are lateral stream offsets visible in the Indio Hills southeast of the pass. These observations are difficult to reconcile with historically known strike-slip movements and geodetic confirmation of the San Andreas type of strain both northwest and southeast of the pass.

(3) As mapped by Vaughan (1922), the San Andreas fault on the north side of San Gorgonio Pass makes an abrupt change of trend which amounts to 35° in 8 miles. Nowhere else along

the fault is such a sharp bend known. The only other major change in trend, at the south end of the San Joaquin Valley, is associated with marked structural complications, and analogous

Cabazon] are consistent with reverse or thrust movements.

(5) No great earthquakes are known from the pass area, and probably none has displaced

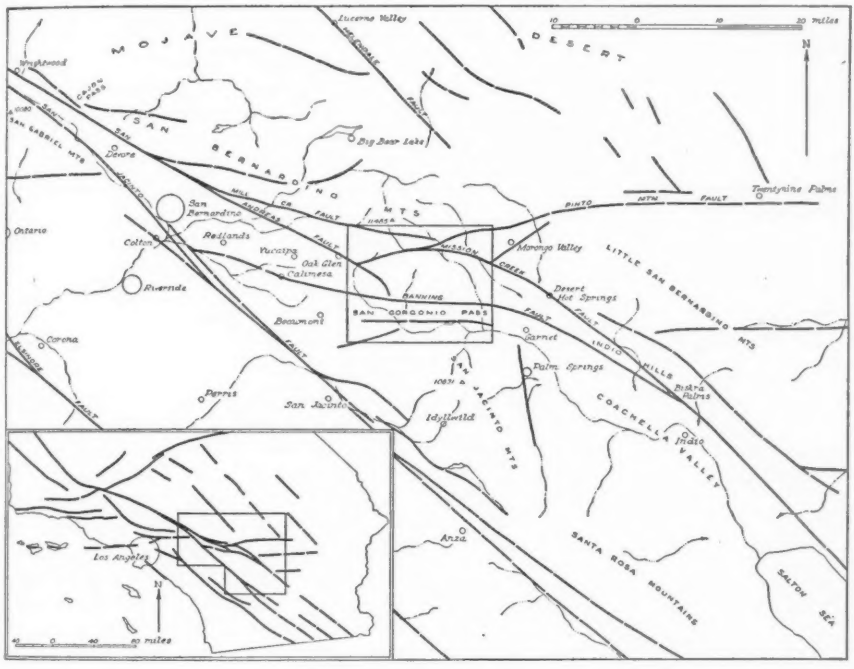

FIGURE 1.—INDEX MAP

Relation of faults in the San Gorgonio Pass area to those of adjacent regions. Area outlined by rectangle is shown on Plate 1. Inset shows location of index map relative to Los Angeles and larger features of Southern California.

features should be expected in the San Gorgonio Pass area.

(4) A recent study by Dehlinger (1952), in which fault displacements in Southern California are correlated with initial motions of transverse earthquake waves, indicates the predominance of thrusting over strike-slip faulting in the San Gorgonio Pass area near Cabazon. Dehlinger (1952, p. 171) states:

Along the San Andreas fault and northeast and southeast from Riverside, transcurrent displacements trending northwesterly occur. In addition, east-west trending reverse or thrust faults may exist east of Riverside. In this region, where the San Andreas fault strikes briefly east-west, displacements may have large vertical components instead of being primarily horizontal. Initial motions of a series of aftershocks from this region [north of

the surface in historic time. This is in contrast to seismic activity along most of the San Andreas zone. The near-by San Jacinto fault (Fig. 1) is characterized by frequent seismic shocks; the shocks of 1899 and 1918 were of intensity X on the Rossi Forel scale in San Jacinto and perhaps were associated with surface disruptions (Wood and Heck, 1951, p. 16, 22). The writer doubts the contention of Wood (1955, p. 60) that the 1857 earthquake fissure on the San Andreas fault extended through San Gorgonio Pass into the Colorado Desert.

Aside from Vaughan's pioneer geologic work in the San Bernardino Mountains, which was of a reconnaissance nature, no areal geologic studies of the north side of San Gorgonio Pass

have been published. Nor have comprehensive reports been published on any immediately adjacent areas, except for the San Jacinto quadrangle south of the pass (Fraser, 1931). On the other hand, numerous studies have been made on various specific aspects of the geology, paleontology, and physiography of this and near-by regions; references to these studies are made in the text of this paper.

Geographical Setting

In its setting between two of the highest and most rugged mountain peaks of Southern California, San Gorgonio Pass is a spectacular physiographic feature (Pl. 5). Despite its narrowness, the pass is the greatest break in the ring of mountains that surrounds the coastal valleys of Southern California.

San Gorgonio Pass is essentially a tectonic feature rather than a simple erosional divide as the term "pass" might imply. From the relatively high plains near Beaumont, it appears as a deep narrow notch that cuts through the mountains into the Colorado Desert below. Its unusual form is reflected in the fact that the name San Gorgonio Pass usually is applied to the narrow easterly part of the notch near Cabazon, where it is flanked by the high peaks, rather than to the gentle and indistinct summit of the pass at Beaumont 12 miles farther west (Fig. 1). This and other aspects of the regional geography have been discussed by Russell (1932).

The area covered in this report ranges in altitude from 1000 feet near Whitewater to 10,000 feet north of Raywood Flat (Pl. 1). Geographic contrasts consequently are great, not only because of the topographic differences but also because the mountain range north of the pass forms a meteorological barrier that separates the semiarid coastal valleys from the arid Colorado and Mojave deserts farther north and east.

The time and space distribution of rainfall in the pass area has particular geologic significance, inasmuch as stream erosion and deposition are almost wholly confined to periods of infrequent floods. The hydrology of this region is the subject of an exhaustive study by Troxell *et al.* (1954).

Acknowledgments

Successful completion of this study depended upon the co-operation of many individuals and organizations. The field work was facilitated by personnel of the United States Forest Service, the Morongo Indian Reservation, and local water companies.

This study was formulated and carried out under the supervision of R. H. Jahns, and his stimulating criticism is especially appreciated. Others who offered helpful criticism include J. P. Buwalda, A. E. J. Engel, S. S. Goldich, R. P. Sharp, and L. T. Silver. The manuscript was critically reviewed by Mason Hill and Peter Misch. The writer benefited from discussions of the regional geology with R. A. Bramkamp of the Arabian-American Oil Company, and with T. W. Dibblee, Jr., D. F. Hewett, and L. F. Noble, all of the United States Geological Survey. Vertebrate fossils were identified by J. F. Lance of the University of Arizona.

The investigations were made possible by generous grants from the California Institute of Technology, the D. F. Hewett Fellowship Fund, the University of Minnesota Graduate School, the National Science Foundation, and the Standard Oil Company of California.

Crystalline Rocks

Introduction

The crystalline rocks of the San Gorgonio Pass area can be grouped into two distinct categories: the rocks north of the pass, herein termed the San Gorgonio igneous-metamorphic complex, have been mapped in reconnaissance in this study; the distinctly different intrusive and metasedimentary rocks of the San Jacinto Mountains south of the pass have been investigated by Fraser (1931), Miller (1944), and Larsen (1948). Of primary interest in this study are the relationships of major rock units across the numerous faults of the area.

San Gorgonio Igneous-Metamorphic Complex

GENERAL FEATURES: In his mapping of the crystalline rocks north of San Gorgonio Pass, Vaughan (1922) distinguished only "hetero-

geneous plutonic rocks" and "undifferentiated schists" in the south part of the range. Vaughan was more realistic in this seemingly oversimplified classification than might be imagined. Most of the crystalline rocks of the south and east flanks of San Gorgonio Mountain are hybrid types of varying composition and transitional boundaries. In general, a metamorphic complex of intermediate or basic composition has been intimately intruded by, and in large part reconstituted by, plutonic rocks of quartz monzonitic composition. In the foothills north of the pass, the intrusive rocks are represented by numerous pegmatite dikes and *lit-par-lit* injections. Northward in the range, more pervasive introduction of granitic material has given rise to contorted migmatitic rocks. Farther north, the predominant rock is plutonic quartz monzonite with included fragments of metamorphic rock in all degrees of assimilation. Several east-west faults that cross the south flank of San Gorgonio Mountain make it difficult to determine whether an actual lateral transition is exposed, or whether rocks from different depth zones have been brought into juxtaposition by vertical movements on the faults.

The most appropriate name that can be applied to the diverse gneissic rocks of the igneous-metamorphic complex is migmatitic gneiss. Important varietal types, differentiated on Plate 1, are flaser gneiss, greenschist, and piedmontite-bearing gneiss. In three places intrusive quartz monzonite units are large enough to be shown on the map.

MIGMATITIC GNEISS: Biotite-hornblende-quartz-andesine gneiss[1] with varying amounts of potassium feldspar is the most widespread crystalline rock on the north side of San Gorgonio Pass. Although gneiss predominates, both schist and foliated quartz diorite are locally important gradational textural types. Foliation is pronounced in most of these rocks, but it is so contorted and variously oriented that efforts to define major faults by means of discontinuities in trend of foliation proved disappointing. Only in the southeastern part of the map area do the rocks have a consistent regional trend; foliation in the biotite-hornblende-microcline-andesine schist of this area strikes north and dips steeply east.

Although interlayered pegmatitic material is abundant even in the most uniform gneisses, a typical specimen has the composition of a quartz diorite (40 per cent andesine, 30 per cent quartz, 15 per cent biotite, and 15 per cent blue-green hornblende). Common accessory minerals are apatite, clinozoisite, and sphene. A near-by rock has 45 per cent orthoclase and 2 per cent andesine; such wide variation in the proportions of light minerals is compatible with field observations, which suggest pervasive permeation of the older rocks by granitic material. Potassium feldspar is represented by both microcline and orthoclase; the latter commonly occurs as augen in the somewhat sheared rocks. Albite is locally abundant in retrograde cataclasites from north of the San Andreas fault in the Burro Flat area. The albite commonly occurs as altered white porphyroblasts that give the rock a knotty appearance, and it is accompanied by increased proportions of epidote and chlorite.

Rocks in the southeast part of the range show extensive hydrothermal alteration. Near Red Dome, the crystalline rocks include a distinctive biotite-quartz-oligoclase-orthoclase gneiss in which saussuritization of the plagioclase gives the rock a dark-green color, despite the presence of large flesh-colored porphyroblasts of orthoclase. The prominent rock of Painted Hill is a tourmaline-bearing hematite-muscovite-plagioclase-microcline-quartz schist.

Pegmatite dikes north of the mouth of Cottonwood Canyon and along the west wall of Whitewater Canyon are strikingly rich in ilmenite, some of which occurs as masses more than an inch across. Gneisses as far west as Millard Canyon also contain abnormal concentrations of ilmenite, apparently as a result of permeation by titanium-rich solutions. North of the Mission Creek fault in this same region, sphene is abundant in areas of pegmatite intrusion and locally constitutes as much as 10 per cent of the amphibolitic gneisses. Many of these titaniferous rocks from north of the Mission Creek fault have a spotted appearance because of quartz-feldspar aggregates that contrast with a darker matrix.

[1] In this report, rock names include minerals that constitute more than 5 per cent of the rock; last-named minerals are most abundant.

The amphibolitic layers, the biotite-rich schist inclusions, and the hornblendite fragments within the partially reconstituted gneisses suggest a parent rock of intermediate to basic composition. The complex history of injection and metamorphism precludes the detailed determination of original rock types, but the parent probably was a tuffaceous, volcanic, or graywacke terrane of dioritic to gabbroic composition.

The widespread association of quartz, microcline, biotite, blue-green hornblende, and andesine is characteristic of Turner's staurolite-kyanite subfacies (1948, p. 81). The retrograde chlorite-hornblende-quartz-albite cataclasites on the borders of the greenschist area of San Gorgonio Canyon represent the intermediate albite-epidote-amphibolite facies, as do many other epidote-rich rocks of the area.

Correlation of the migmatitic gneisses of the San Gorgonio igneous-metamorphic complex with other rocks of Southern California is uncertain, owing to the lack of geologic mapping in areas adjacent to that of this study and to the fact that rocks of this general composition and degree of metamorphism are widespread throughout the region. The Baldwin gneiss on the north side of the San Bernardino Mountains, named and described by Guillou (1953, p. 6), has many features in common with the gneiss 20 miles to the south, and the two units probably are correlative. Miller's Pinto gneiss (1938, p. 424–428), presumably a part of his more extensive Chuckwalla complex, is strikingly similar to the San Gorgonio gneisses. The San Gabriel Formation (Miller, 1934, p. 49–56), a widespread igneous-metamorphic complex of the San Gabriel Mountains, has many features in common with the San Gorgonio gneisses. Most of the metamorphic rocks south of San Gorgonio Pass are metasedimentary types.

FLASER GNEISS: In the foothills north of the Banning fault, many of the gneisses show distinctive structures developed by deep-seated cataclastic metamorphism. These rocks range from slightly sheared augen gneisses to mylonitized and lenticularly layered rocks, and these types grade into one another. Foliation generally strikes east.

A thin section of one of the highly sheared rocks shows distinct fluxion structure. Eye-shaped porphyroclasts, white in hand specimen, constitute about 50 per cent of the rock and consist of (1) fine-grained aggregates of quartz and orthoclase, (2) altered plagioclase, probably andesine, or (3) orthoclase. The orthoclase porphyroclasts, though least common, have the most striking appearance in hand specimen; Carlsbad-twinned crystals 2 inches long have been observed. The generally idioblastic outlines of many of the sheared crystals suggest that the orthoclase is of porphyroblastic origin. The remaining comminuted portion of the gneiss is holocrystalline and consists of fine-grained recrystallized quartz, with minor biotite and orthoclase(?). Biotite, though a minor constituent, gives the matrix a gray to black color in hand specimen. This rock is termed a flaser gneiss, rather than a mylonite, on the basis of the abundant porphyroblasts and the almost complete recrystallization of the comminuted paste.

That the flaser gneisses cannot be an expression of present-day faulting is indicated not only by textural characteristics of deep-seated origin but also by their intense folding and contortion and by field evidence of contemporaneous and post-shearing injection by granitic material. The Banning fault more nearly parallels the zone of cataclastic rocks than does the San Andreas fault. It seems reasonable, therefore, that either (1) the Banning fault is very old, so that its early "roots" are now exposed, or (2) the course of the Banning fault has been determined by the zone of east-west weakness that is defined by the location and predominant foliation of the much older sheared rocks.

GREENSCHIST: A distinctive and localized body of quartz-actinolite-albite-epidote schist is exposed on the north side of San Gorgonio Canyon for 3 miles above the San Andreas fault, which cuts off the unit on the southwest (Pl. 1). Faults also border this rock unit on the northwest and southeast. But to the northeast, near the junction of Black and Mill canyons, the greenschist appears to be transitional with the migmatitic gneisses. The greenschist is structurally significant not only because of its anomalous position among rocks of a seemingly different type but also because it has contributed distinctive fragments to Cenozoic

sedimentary rocks that lie south of the San Andreas fault.

In hand specimen, the greenschist is dark blue green, has well-developed foliation, and contains many porphyroblasts of white albite that give the rock a distinctive knotty appearance. In thin section, the most typical greenschist shows fluxion structure, with eye-shaped, sheared porphyroblasts of both albite and epidote in a matrix of aligned actinolite needles. The mineralogy suggests origin as a rock of gabbroic composition.

Although the greenschist has been partly faulted to its present position, transitional rock types occur both eastward and across the Mission Creek fault to the south. On the ridge south of the Mission Creek fault near Burro Flat, "spotted" retrograde cataclasites—grouped together with the migmatitic gneisses in mapping—contain porphyroclasts of white albite-oligoclase, and hornblende that is partly altered to chlorite and tremolite-actinolite. The seemingly transitional boundary suggests either that (1) the greenschist represents the parent rock of the migmatitic gneisses, which perhaps have been upgraded during migmatitization, or (2) the greenschist represents a locally degraded and little-injected phase of the more widespread amphibolites. Certainly the environment close to the San Andreas and Mission Creek faults is one of high shear stress and hydrothermal activity—both important factors in retrogressive metamorphism. Indeed, the localization of similar greenschists close to major faults throughout Southern California suggests that the intense shearing and hydrothermal activity may have been important factors in the origin of this distinctive rock type.

Rocks similar in texture and composition to the greenschists of San Gorgonio Canyon occur in the Pelona schist of the San Gabriel Mountains and in schist of the Orocopia Mountains north of the Salton Sea (Fig. 1). These rocks were discussed in detail by H. S. Hill (1939, M. S. thesis, Claremont College), and Hill and Dibblee (1953, p. 450) believed that they might be parts of a formerly continuous rock body that has been offset 160 miles along the San Andreas fault. Thus it might be argued that the San Gorgonio greenschists and associated rocks represent a large fault sliver that was left behind midway between the two larger outcrops. Present knowledge of the "basement" rocks of Southern California does not permit a comprehensive statement of the regional significance of rock with Pelona schist lithology. Assuredly this is a problem worthy of further study.

PIEDMONTITE-BEARING GNEISS: One mile west of the mouth of Stubby Canyon is a localized mass of piedmontite-bearing gneiss that is a distinctive rock type within the otherwise normal migmatitic gneisses of the foothills area. Particular significance is attached to this unusual rock because it has contributed fragments to sedimentary rocks south of the Banning fault. The distribution of these clasts, compared with the distribution of the source rocks, provides evidence of the amount of subsequent displacement along this fault.

The piedmontite-bearing gneiss is associated with pegmatite intrusions in the older metamorphic rocks; the largest piedmontite crystals occur within and near the borders of the pegmatite dikes. The average gneissic rock is a piedmontite-ilmenite-quartz-microcline gneiss with accessory biotite, apatite, sphene, garnet, amphibole, and pyroxene. Altered oligoclase-andesine is present in widely varying amounts. The piedmontite occurs as euhedral crystals as much as three-fourths of an inch long and constitutes as much as 5 per cent of the rock. Many of these minerals have peculiar optical properties, and a detailed mineralogical study of this occurrence should prove fruitful.

A second occurrence of piedmontite-bearing gneiss is on the west wall of Whitewater Canyon, between the trout farm and Red Dome (Pl. 1). This rock is similar to the exposure at Stubby Canyon except for the local abundance of yellow-green epidote and the presence of a light-pink mica that probably is alurgite. Similar pink mica occurs in clasts of the San Timoteo(?) Formation north of Banning and undoubtedly was derived from the eastern end of the range. Examination of stream gravels from all canyons draining the north side of San Gorgonio Pass failed to reveal evidence of any major outcrops of piedmontite-bearing gneiss other than those at Stubby and Whitewater canyons.

Piedmontite has been described from numer-

ous localities in Southern California (Murdoch and Webb, 1948, p. 230–231), although the only previous report of this mineral from the San Bernardino Mountains concerned piedmontite-bearing fragments from sedimentary rocks near Painted Hill. H. S. Hill (1939, M. S. thesis, Claremont College, p. 93–96) describes several occurrences of piedmontite in the Pelona schist; this is significant because the schist crops out on the south side of the San Andreas fault 50–60 miles northwest of the San Gorgonio Pass locality. According to Hill (1939, M. S. thesis, Claremont College, p. 109), however, the associated rocks in the two regions are very different.

CACTUS(?) QUARTZ MONZONITE: Three masses of quartz monzonite, each sufficiently large to be separated in mapping from the transitional migmatitic gneisses, occur (1) in the foothills 4 miles northwest of Banning, (2) on Yucaipa Ridge between Pine Bench and Mill Creek, and (3) on the southwest slope of San Gorgonio Mountain, near the headwaters of Vivian Creek (Pl. 1). These three exposures of almost identical rock are separated by two of the largest faults of the region—the San Andreas and Mill Creek faults.

Specimens from the three masses of quartz monzonite contain 30–45 per cent microcline, 25–40 per cent altered albite-oligoclase, 25–30 per cent quartz, and 5–10 per cent green biotite. The texture is equigranular with grain size averaging 2 mm; sutured contacts between grains are common. Vaughan (1922, p. 363–374) included these rocks in his "heterogeneous plutonic rocks." Subsequent studies by Woodford and Harriss (1928, p. 271–274) and by Guillou (1953, p. 12–13) indicate that many of these plutonic rock types, only one of which appears to crop out in the area of Plate 1, probably are variants of a single major intrusion—Vaughan's Cactus granite. The name recently has been modified by Guillou (1953, p. 12) to Cactus quartz monzonite. On the basis of these observed variant Cactus types, the quartz monzonite of the south part of the range is herein tentatively assigned to the Cactus quartz monzonite. These rocks, however, are uniformly finer-grained than those at the type area near Cactus Flat, and further work may modify this correlation.

Studies by Hewett and Glass (1953, p. 1049) of uranium-lead ratios of euxenite in pegmatite dikes in the Cactus quartz monzonite suggest a Middle Jurassic age (about 150 million years). The isotopic composition of the lead was not determined, however, so that the actual age is probably somewhat less. These rocks might be as young as the Southern California batholith, which is Cretaceous.

DIKE ROCKS: Leucocratic dike rocks other than pegmatite crop out in scattered parts of the area. Dikes of quartz latite porphyry north of Burro Flat transect the foliation of the migmatitic gneiss and are of problematical origin. If the dikes were derived from the Cactus quartz monzonite, it is difficult to explain the pegmatite of apparently similar origin which permeates the gneiss; if the dikes represent younger intrusives, their parent material is not recognized anywhere in this area.

Crystalline Rocks of the San Jacinto Mountains

METAMORPHIC ROCKS: Scattered remnants of an old metamorphic series occur as inclusions and roof pendants in the intrusive rocks of the San Jacinto Mountains. According to Fraser (1931, p. 534), the principal metamorphic types are quartzo-feldspathic gneisses and schists, hornblende schist, phyllite, crystalline limestone, and quartzite. Recrystallized limestones are particularly well exposed on the outlying spurs of San Jacinto Peak 2 miles south of Whitewater. These rocks were included in the Palm canyon complex by Miller (1944, p. 21–25), who recovered from points near Cathedral City possible fossil material that suggests a Paleozoic age for these rocks.

Seemingly correlative rocks have been mapped west of the San Jacinto Mountains by Larsen (1948, p. 16–18, Pl. 1), who also assigns a Paleozoic age to them on the basis of supposedly Carboniferous fossils described by Webb (1939). These rocks have been extensively intruded, and numerous layered gneisses and schists have been formed by *lit-par-lit* injection of igneous material. In this respect, they are much like the migmatitic gneisses of San Gorgonio Mountain. All investigators agree, however, that the San Jacinto metamorphic rocks are largely of sedimentary origin.

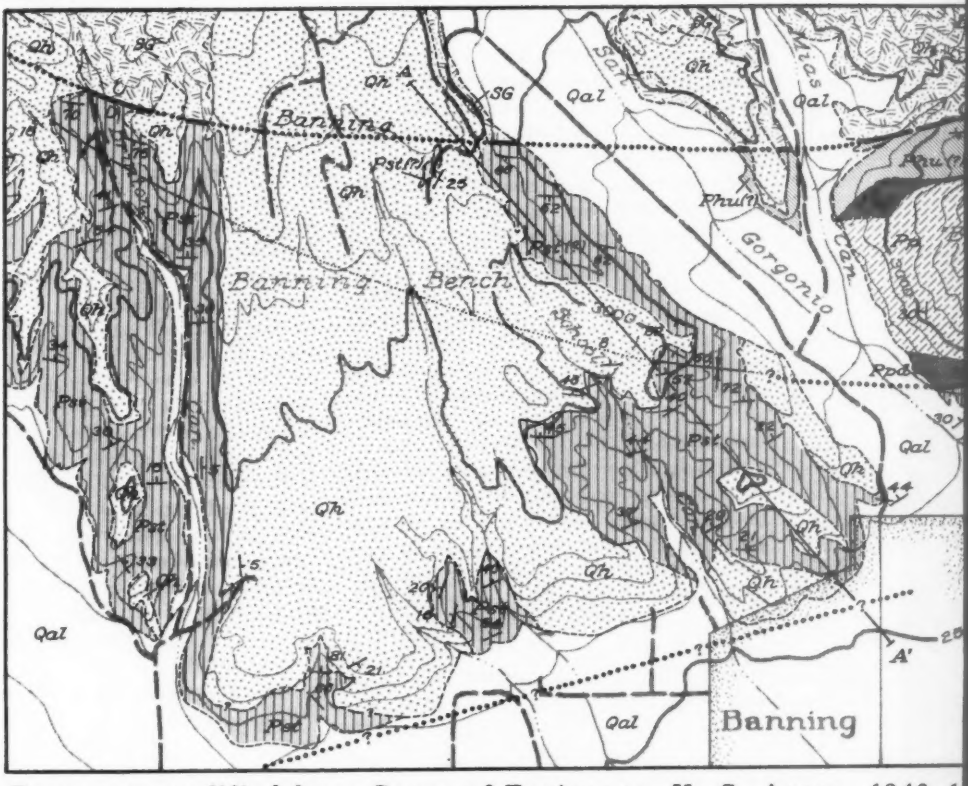

Base map modified from Corps of Engineers, U. S. Army, 1943-1

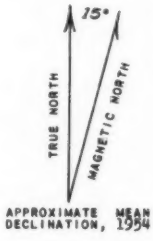

Contour

GEOLOGIC MAP AND STRUCTURE SECT

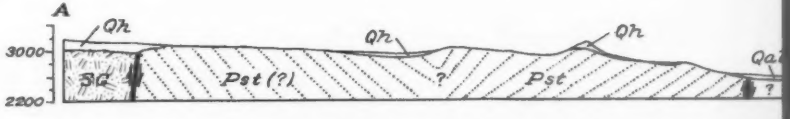

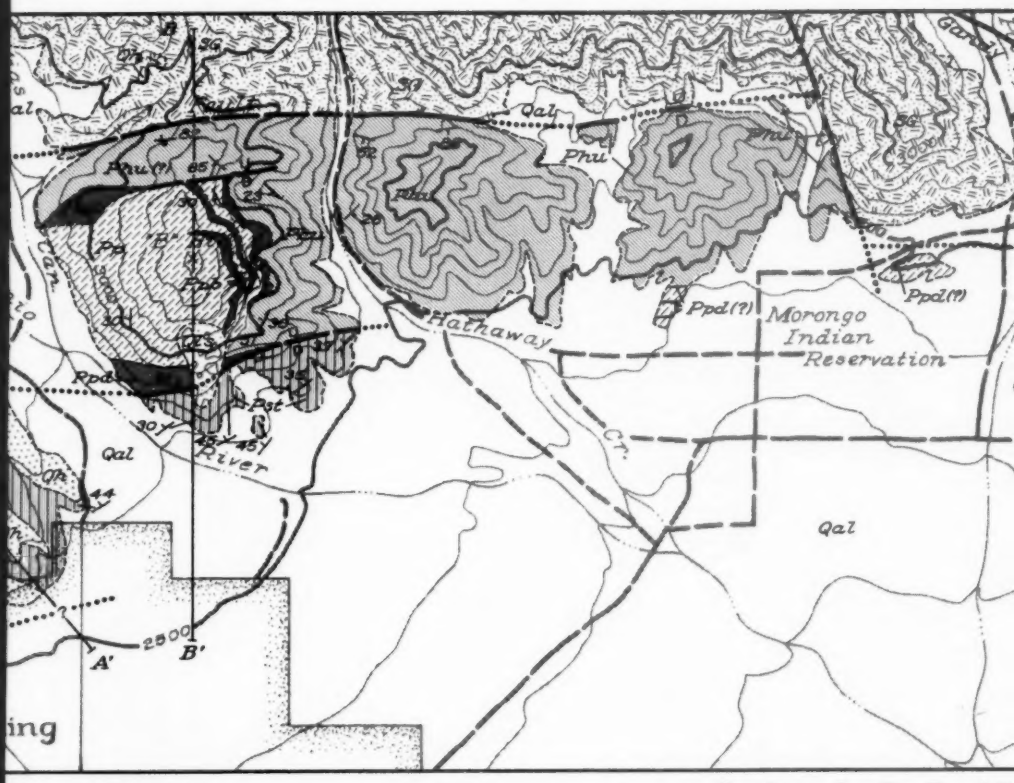

my, 1943-1944 Geology by C. R. All

0 1 2 Miles

Contour interval 100 feet

RE SECTIONS OF THE FOOTHILLS NORTH OF BANNI

R. Allen, 1952-1954

BANNING

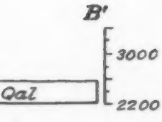

EXPLANATION

Qal
Alluvium

UNCONFORMITY

Qls
Landslide material

UNCONFORMITY

Qh
Heights fanglomerate

UNCONFORMITY

Pot
San Timoteo(?) formation

CONTACT NOT EXPOSED

Ppc
Pp
Ppb
Ppd
Painted Hill formation
Resistant conglomerate bed, Ppc; interlayered flows of olivine basalt, Ppb, and associated dikes of olivine basalt, Ppd.

Phu
Phl
Hathaway formation
Upper member, Phu; Lower member, Phl

CONTACT NOT EXPOSED

SG
San Gorgonio igneous-metamorphic complex

Pliocene-Pleistocene
Lower Pliocene(?)

QUATERNARY
TERTIARY
MESOZOIC AND OLDER

Contact
Dashed where approximately located

25
Fault, showing dip
Dashed where approximately located; dotted where concealed. U, upthrown side; D, downthrown side

Syncline
Dashed where approximately located; dotted where concealed

67
Strike and dip of beds

78
Strike and dip of overturned beds

INTRUSIVE ROCKS: Rocks of the Southern California batholith of Cretaceous age underlie most of the San Jacinto Mountains. This area has been studied in reconnaissance by Fraser (1931, p. 525–533), Larsen (1948, p. 67–69), and Miller (1944, p. 52–59), and the following comments are based on observations of these investigators.

Coarse-grained homogeneous well-jointed rocks predominate in this area, and the steep boulder-covered slopes contrast with the more gentle and diverse slopes underlain by gneiss on the north side of the pass. The rocks have an average composition near that of a basic granodiorite. Light-gray tonalite forms the hills for a few miles south of Banning, and it is bordered on the south by a coarse-grained granodiorite that also occurs in much of the Snow Creek drainage to the east. Tonalite underlies much of the southern part of the range. The gneissoid rock that forms the flatirons west of Palm Springs is a highly sheared and foliated granodiorite, whose relation to the more widespread plutonic rocks bordering it on the west has not been definitely established.

Stratigraphy of Sedimentary Rocks

Introduction

The sedimentary rocks of San Gorgonio Pass are of continental origin except for the Imperial Formation, which represents northward incursion of marine waters into the Salton depression from the Gulf of California. All are of late Tertiary and Quaternary age. Correlation is complicated by Recent faulting and folding, interrupted exposures, scarcity of vertebrate fossils, marked lateral variations, and other stratigraphic complexities that reflect a history of simultaneous deposition and deformation. Only because of the distinctive Imperial Formation is it possible to place the overlying and underlying continental strata at reasonably definite positions in the stratigraphic column.

Regional correlations with previously studied sedimentary rocks in areas east and west of San Gorgonio Pass are shown in Figure 2. Table 1 is a summary of the stratigraphy within the pass.

Coachella Fanglomerate

GENERAL RELATIONS: The oldest sedimentary unit in the pass area is the Coachella fanglomerate, which was named and first described by Vaughan (1922, p. 386). As was pointed out by Bramkamp (1934, Ph.D. thesis, Univ. Calif., Berkeley, p. 18), some of the rocks mapped by Vaughan as Coachella fanglomerate belong to younger units in the section, but the formational name is herein retained for the prominent cliff-forming beds exposed along the east wall of Whitewater Canyon near the trout farm (Pl. 4). Coachella rocks crop out over an area of about 6 square miles north of Painted Hill and east of Whitewater River; no other rocks correlative with this unit are known.

LITHOLOGIC FEATURES: The Coachella fanglomerate shows marked lateral variations in composition, which reflect localized provenance. Probably the most typical section is exposed along an east-west line half a mile south of the trout farm (Pl. 4, Section I–I′). On the canyon wall here, eastward-dipping Coachella beds lie with depositional contact on the crystalline complex, and 1½ miles to the east the formation is unconformably overlain by the Painted Hill Formation. The total thickness of beds along this line is 4600 feet and probably is near maximum for the formation.

Near the trout farm, the basal beds consist of massive breccia of locally derived fragments of gray schist as much as 6 feet in diameter. Within a few hundred feet upward in the Coachella section, clasts of olivine basalt become the principal constituents of the rock and are responsible for the reddish-brown color of the cliffs along Whitewater Canyon. Interlayered with these beds 850 feet above the base of the section is a pale-red-purple basalt flow that separates the upper and lower members of the Coachella fanglomerate. The maximum thickness of this flow is about 50 feet, and it wedges out to the southeast; northward, it is apparently correlative with the prominent flow on the north flank of the Rainbow anticline (Pl. 1). The flow probably originated in the Mission Creek fault zone.

The varicolored flows exposed near the mouth of Mission Creek probably were formed during the period of deposition of the Coachella beds;

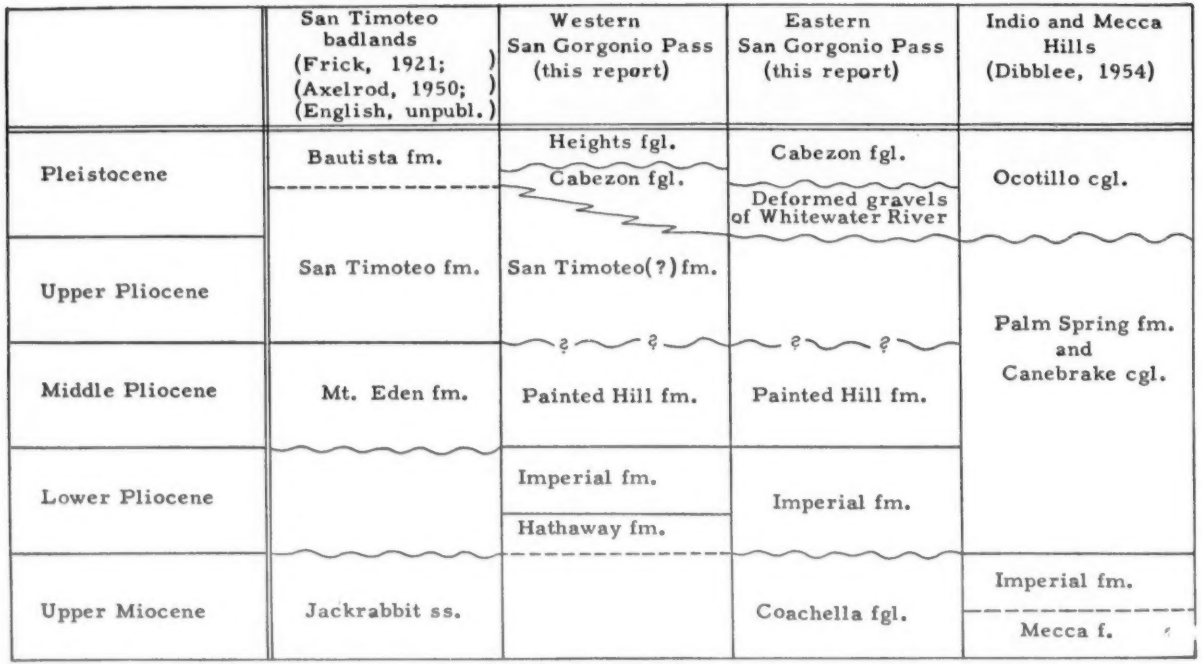

FIGURE 2.—GENERALIZED CORRELATION CHART OF SEDIMENTARY ROCKS OF SAN GORGONIO PASS REGION

All contacts are of doubtful age. Wavy lines indicate angular unconformities; solid lines indicate conformable contacts; dashed lines indicate contacts not exposed.

TABLE 1.—SEQUENCE AND CHARACTER OF THE SEDIMENTARY ROCKS OF SAN GORGONIO PASS

Formation	Map symbol	Age	Maximum thickness (feet)	Lithology
Alluvium	Qal	Recent		Unconsolidated stream gravels and low stream terrace gravels
----------UNCONFORMITY----------				
Landslide deposits	Qls	Recent		
----------UNCONFORMITY----------				
Undifferentiated terrace gravels	Qt	Quaternary		Terrace gravels and canyon-fill material of doubtful correlation
----------UNCONFORMITY----------				
Burnt Canyon breccia	Qbc	Quaternary	100+	Dissected landslide deposit
-------UNCONFORMITY----------				
Heights fanglomerate	Qh	Quaternary	500	Tan to dark-brown, ill-sorted conglomerate, dominantly dark clasts of gneissic rock
----------UNCONFORMITY--------				
Cabezon fanglomerate	Qc	Quaternary	1500+	Gray to tan ill-sorted conglomerate, rich in clasts of pegmatitic and granitic rocks
----------UNCONFORMITY----------				
Deformed gravels of Whitewater River	Qd	Quaternary(?)		Gray to tan, ill-sorted conglomerate, rich in clasts of pegmatitic and granitic rocks
-------CONTACT NOT EXPOSED-------				
San Timoteo (?) Formation	Pst	Pliocene-Pleistocene	1800+	Tan to gray sandstone, siltstone, and conglomerate, rich in light-colored clasts of granitic rocks; interbedded fresh-water limestone
-------CONTACT NOT EXPOSED-------				
Painted Hill Formation	Pp Ppc Ppb Ppd	Middle Pliocene (?)	3400+	Light-gray sandstone and conglomerate, rich in clasts of granitic and volcanic rocks; Ppc, resistant conglomerate bed; Ppb, interlayered flows of olivine basalt; Ppd, associated dikes
Imperial Formation	Pi	Lower Pliocene (?)	300	Tan to yellow marine sandstone, siltstone, and shale; gypsiferous; fossiliferous
Hathaway Formation				
Upper member	Phu	Lower Pliocene (?)	650	Gray, massive, ill-sorted conglomerate and breccia, rich in clasts of augen and flaser gneiss
Lower member	Phl	Lower Pliocene (?)	1100+	Light-gray sandstone, siltstone, conglomerate, and fresh-water limestone
-------CONTACT NOT EXPOSED-------				
Coachella fanglomerate				
Upper member	Mcu Mcb Mcd Mcm	Upper Miocene (?)	3750+	Massive conglomerate, locally rich in clasts of basalt and dark-green saussuritized gneiss; Mcb, interlayered flows of olivine basalt; Mcd, associated dikes; Mcm, marker horizon containing distinctive clasts
Lower member	Mcl	Upper Miocene (?)	850	Well-indurated massive conglomerate, locally rich in clasts of olivine basalt; basal breccia of gray schist fragments

they are fine-grained to aphanitic basalts with phenocrysts of olivine and labradorite. A basalt dike of similar composition has been intruded along a fault between the crystalline complex and Coachella fanglomerate north of Painted Hill but is truncated by the Imperial Formation. It must be immediately post-Coachella in age or perhaps contemporaneous with uppermost Coachella beds that have been removed by erosion along the Coachella-Imperial unconformity. This dike is mapped with the other Coachella basalts.

Northward from the trout farm in Whitewater Canyon, successively younger Coachella beds rest with depositional contact on the crystalline complex, and the basalt flow that is 850 feet above the base of the section at the trout farm lies directly on the crystalline rocks opposite Red Dome. Farther north, fanglomerate beds of the upper member are depositional on the crystalline rocks. These stratigraphic relations reflect major topographic relief at the time of Coachella deposition.

Clasts of volcanic rocks become less abundant toward the top of the upper member, and the beds become lighter gray, owing to increased proportions of well-rounded granitic[2] and pegmatitic clasts. To the north, however, a dark-green saussuritized gneiss, which forms the bedrock opposite Red Dome, locally has contributed debris to upper Coachella beds. Stringers of dark-gray conglomerate, in which clasts of this gneiss are abundant, permit mapping of discontinuous marker horizons throughout the badlands north of Painted Hill, but they pinch out southeastward. Except for such beds and widely separated layers rich in clasts of volcanic rocks, the upper member of the Coachella fanglomerate is a uniform series of beds that become less consolidated upward in the section.

AGE: No fossils have been found in the Coachella fanglomerate, but its unconformable position beneath the early Pliocene(?) Imperial Formation and its high degree of induration and well-developed jointing suggest an age at least as old as late Miocene.

[2] In this section, the term granitic is applied to rocks that range in composition from granodiorite to granite. Quartz monzonite predominates.

Hathaway Formation

GENERAL FEATURES: In the Lion Canyon area north of Cabazon (Pls. 3, 5) is exposed 1750 feet of highly deformed continental sandstones, siltstones, and conglomerates that was included in the Hathaway Formation by Vaughan (1922, p. 377) and Bramkamp (1934, Ph.D. thesis, Univ. Calif., Berkeley, p. 10). Vaughan also included in this formation similar sedimentary rocks north of Banning, but fossil evidence now suggests that these rocks are much younger than the beds in Lion Canyon, and they are herein assigned tentatively to the San Timoteo Formation instead. The type section of the redefined Hathaway Formation is in the Main Branch of Lion Canyon, where the formation consists of two members.

LOWER MEMBER: The lower member of the Hathaway Formation consists of 1100 feet of tan to light-gray arkosic sandstone with subordinate siltstone and lenticular beds of conglomerate. Most clasts are light-colored granitic rocks and flaser and augen gneisses; no fragments of volcanic rocks were noted. In the West Branch of Lion Canyon, two vertical beds of white fresh-water limestone crop out plainly on the west wall of the canyon. The localized and lenticular nature of the limestone, together with its structure and the lack of calcareous material in adjacent rocks, suggest that it was deposited from hot-spring waters. The base of the lower member is not exposed.

UPPER MEMBER: Conformably overlying the lower member of the Hathaway Formation is a 650-foot unit of massive conglomerate and breccia that is distinguished by a high proportion of flaser gneiss boulders as much as 3 feet in diameter. Sparse fragments of gray silicified limestone also are present. This upper member of the Hathaway Formation is best exposed on the south flank of the Lion anticline, where it is cut by Lion Canyon. At the head of First Canyon, half a mile to the northeast, this unit lies conformably beneath the Imperial Formation. It is not exposed farther east.

The clasts of flaser gneiss within the upper member suggest local provenance, because crystalline rocks of this type are limited in present outcrop to the ground north of the Banning fault between Cottonwood and San

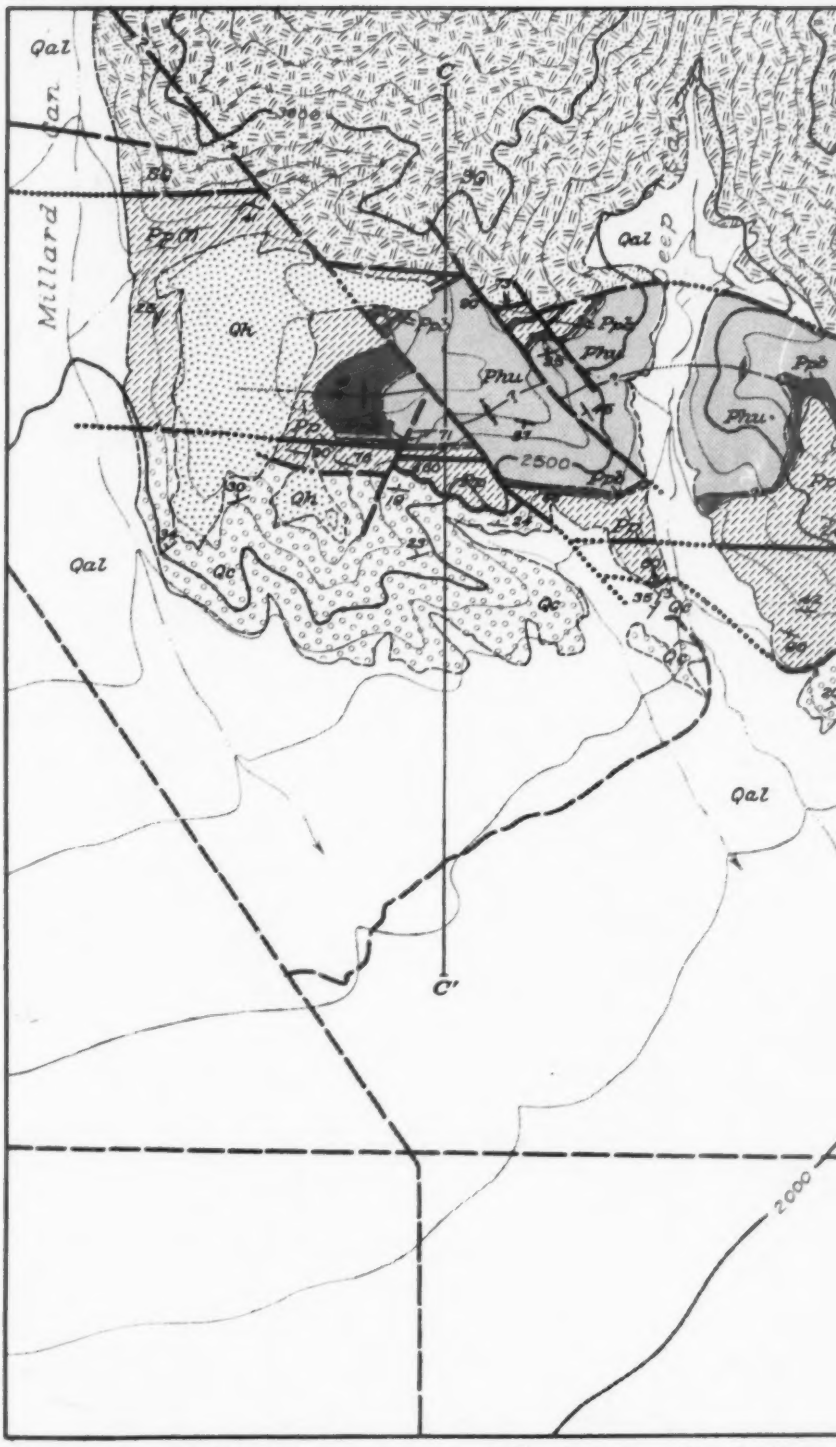

Base map modified from Corps of Engineers, U. S. Arm

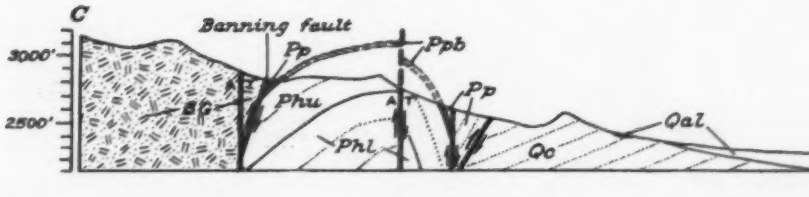

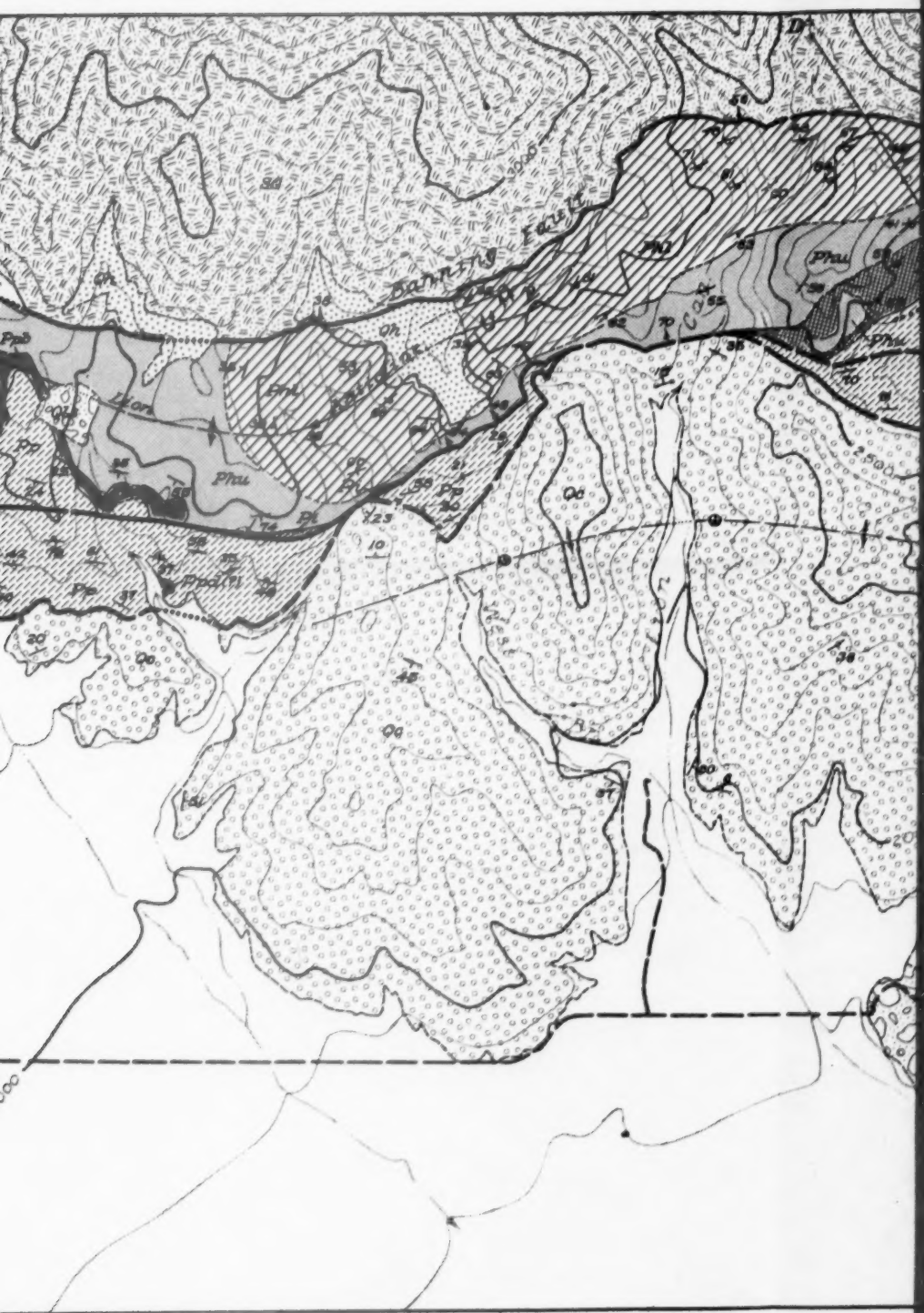

rmy, 1943-1944

1 0.5

GEOLOGIC MAP AND STRUCTURE SECT

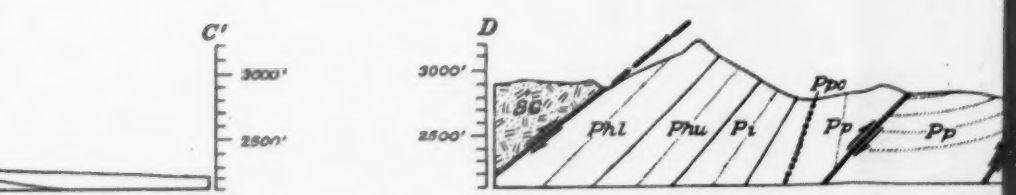

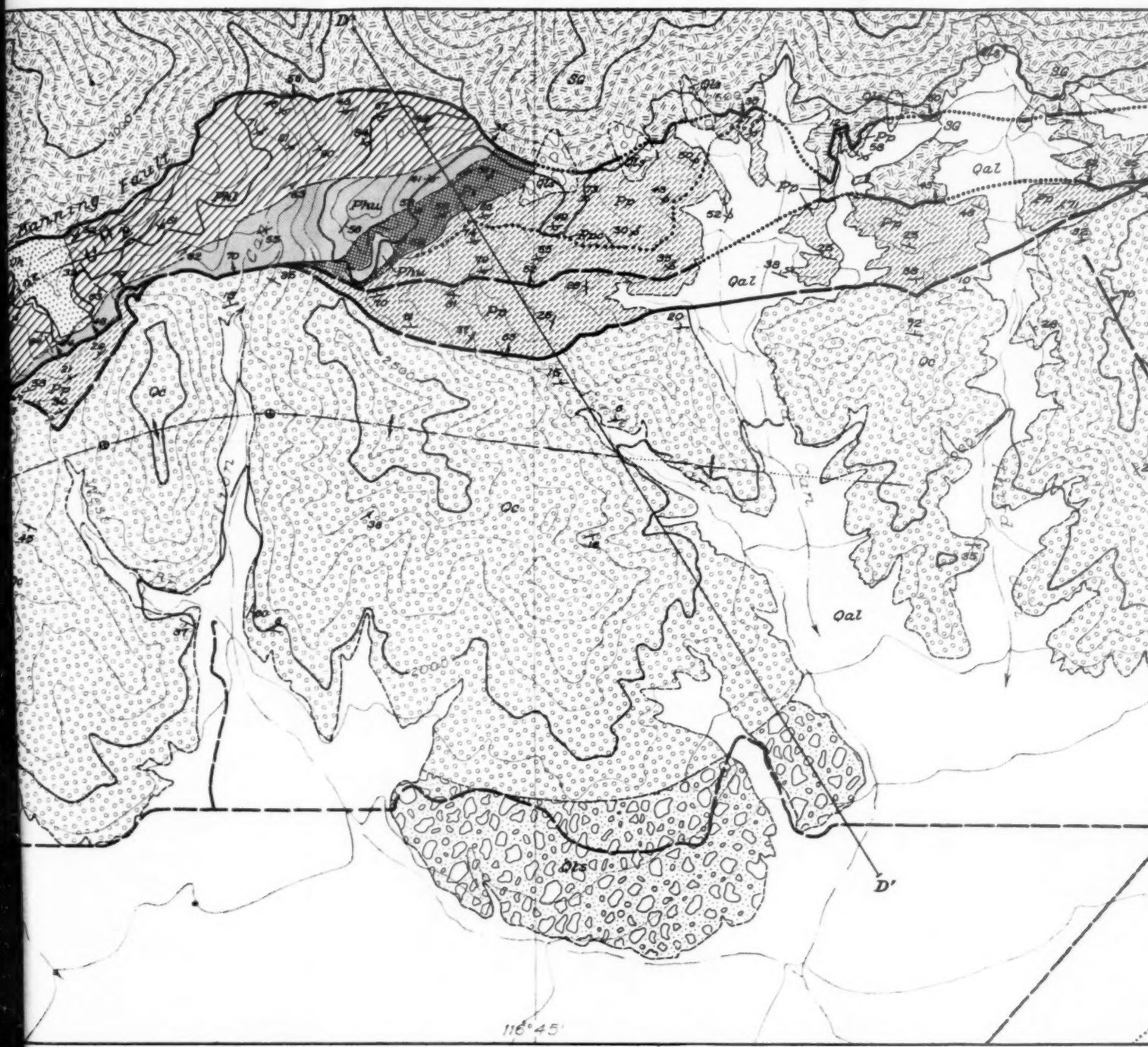

Contour interval 100 feet

MAP AND STRUCTURE SECTIONS OF THE FOOTHILLS BETWEEN MILLARD AND

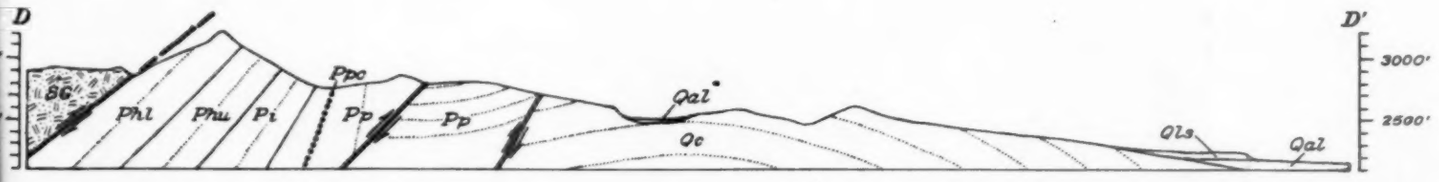

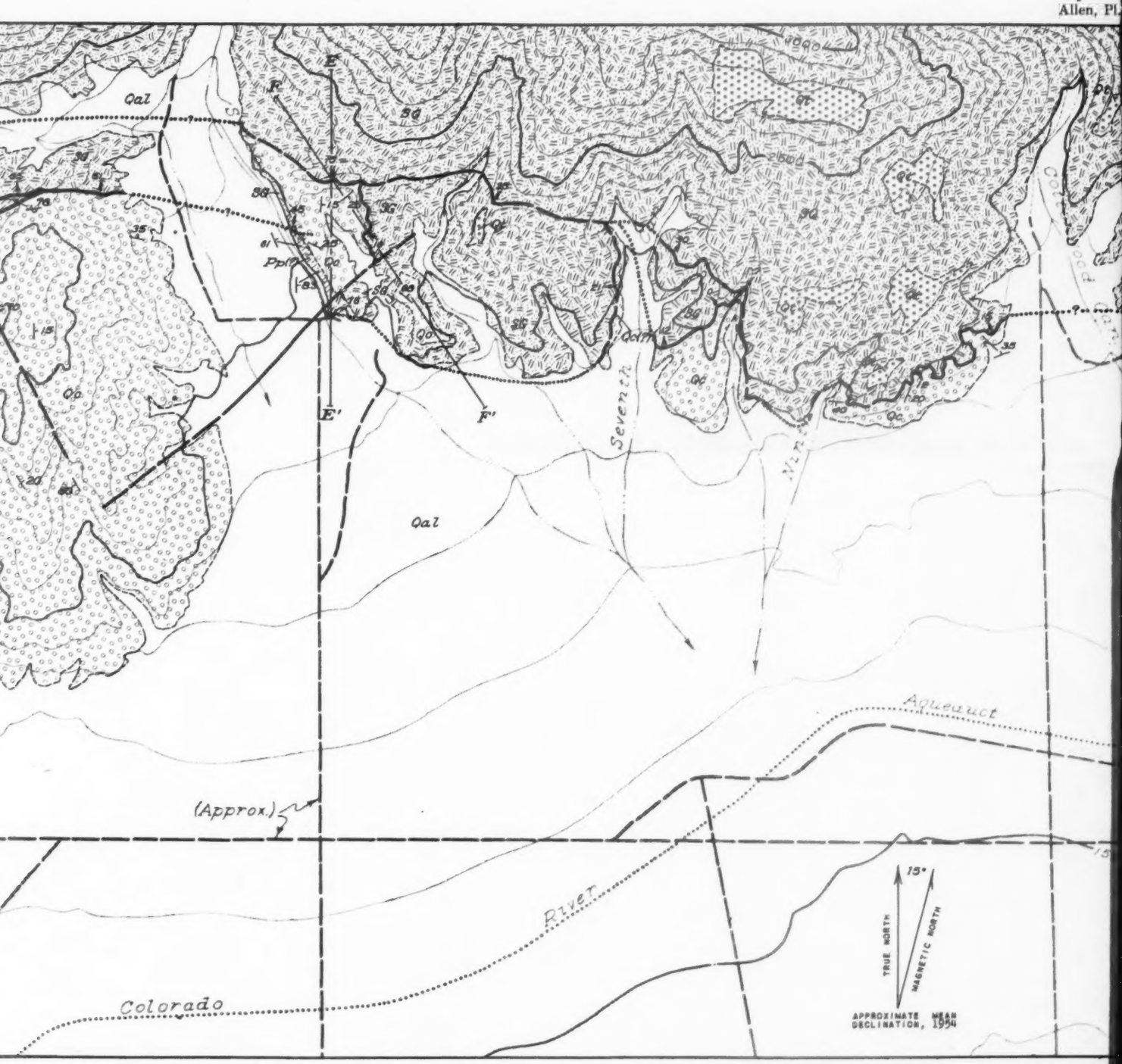

Geology by C. R. Allen, 1952-195

2 Miles

ND COTTONWOOD CANYONS

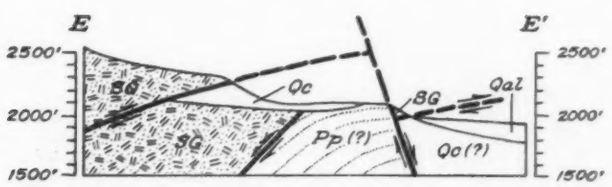

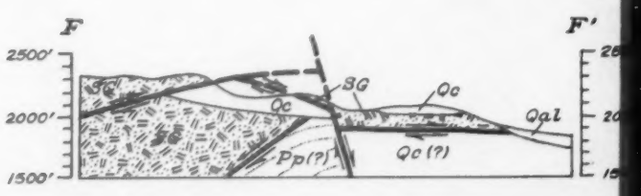

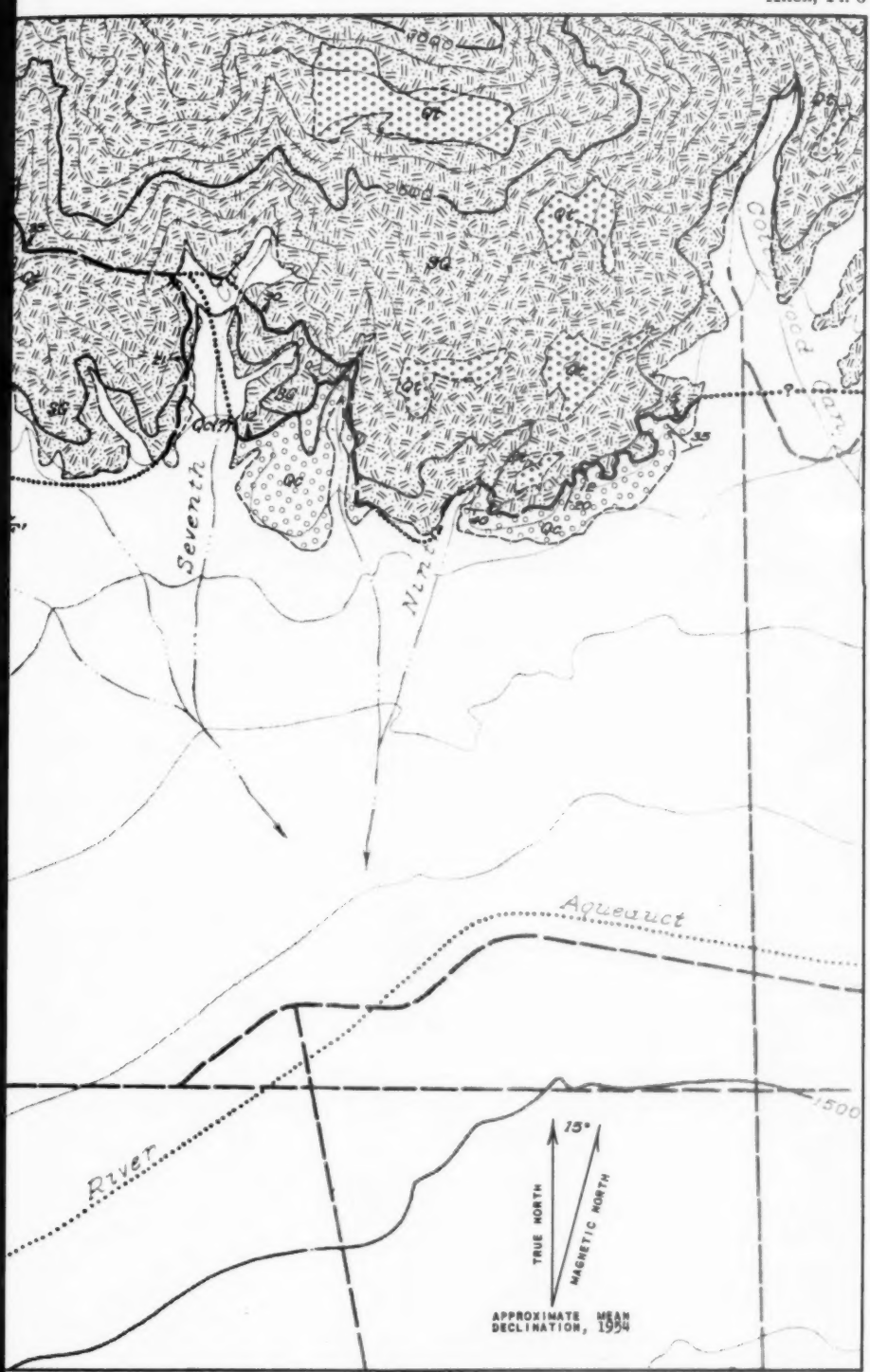

Geology by C. R. Allen, 1952-1954

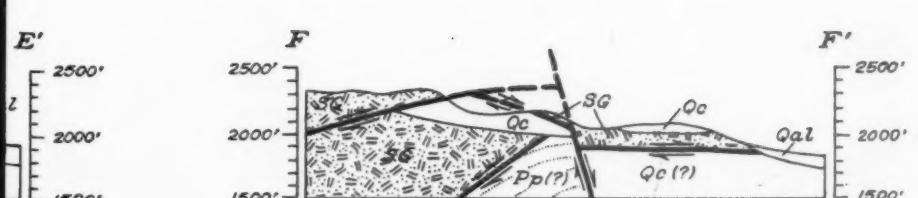

EXPLANATION

Alluvium

UNCONFORMITY

Landslide material

UNCONFORMITY

Conglomerates and terrace gravels of unknown correlation

UNCONFORMITY

Heights conglomerate

UNCONFORMITY

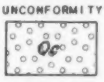

Cabezon conglomerate

QUATERNARY

UNCONFORMITY

Middle Pliocene(?)

Painted Hill formation

Resistant conglomerate bed, Ppc; interlayered flows of olivine basalt, Ppb, and associated dikes of olivine basalt, Ppd.

Lower Pliocene(?)

Imperial formation

Hathaway formation

Upper member, Phu; Lower member, Phl

TERTIARY

UNCONFORMITY

San Gorgonio igneous-metamorphic complex

MESOZOIC AND OLDER

Contact

Dashed where approximately located

Fault, showing dip

Dashed where approximately located; dotted where concealed. U, upthrown side; D, downthrown side.

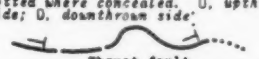

Thrust fault

Dashed where approximately located; dotted where concealed. T, overthrust plate.

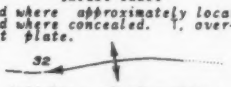

Anticline, showing plunge

Dashed where approximately located; dotted where concealed

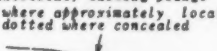

Syncline

Dashed where approximately located; dotted where concealed

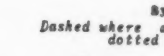

Overturned anticline

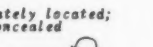

Overturned syncline

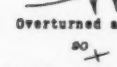

Strike of vertical beds

Strike and dip of beds

Strike and dip of overturned beds

Gorgonio canyons. The possible post-lower Pliocene lateral displacement on the north branch of the Banning fault is thus probably no more than 5 miles. This evidence is not definitive, inasmuch as similar crystalline rocks could conceivably be concealed beneath the alluvium of Coachella Valley farther east.

DEPOSITIONAL ENVIRONMENT: The similarity in texture and lithology between the Hathaway Formation and the overlying sedimentary beds of the pass area suggests that the same type of depositional environment prevailed throughout much of Pliocene and early Pleistocene time. Delicately bedded fine-grained deposits interfinger with massive bouldery beds as if they might have been laid down in a broad valley at the foot of steep mountain slopes. The sandstones and siltstones probably accumulated on an alluvial flood plain with some shallow-water lacustrine and paludal sedimentation. The near-by San Jacinto Valley seems to be a modern example of a somewhat similar depositional environment. Studies of plant fossils from the Mt. Eden Formation by Axelrod (1937; 1950) suggest growth in a low-lying basin within 1000 feet of sea level, characterized by a plains-savanna habitat and surrounded by forested uplands.

AGE: The conformable position of the Hathaway Formation beneath the Imperial Formation permits a tentative age assignment as early Pliocene. Inasmuch as the true age of the Imperial Formation is questionable, the Hathaway Formation must share in this uncertainty.

Imperial Formation

GENERAL FEATURES: Marine beds in the San Gorgonio Pass area were first recognized by Vaughan (1922, p. 375–376). He described them as the "Lion sandstone" of the Lion Canyon area but evidently overlooked the similar beds near Painted Hill. These northernmost exposures of the Imperial Formation have been the subject of a thorough study by Bramkamp (1934, Ph.D. thesis, Univ. Calif., Berkeley). Woodring (1932) briefly described these and other outcrops of the Salton trough, and numerous authors have studied the type Imperial section at Carrizo Mountain, 85 miles southeast of San Gorgonio Pass. A good bibliography of the more recent studies is given by Durham (1950, p. 3, 23).

LITHOLOGIC FEATURES: East of Painted Hill, a thin stringer of Imperial Formation, about 1 mile long, lies unconformably on both the Coachella fanglomerate and the much older crystalline complex (Pl. 4). At this locality, the Coachella fanglomerate is faulted against the red hematitic schist of Painted Hill, and the Imperial beds truncate a series of alternating fault-bounded slices of schist and fanglomerate. Also truncated, at nearly 90°, is a dike of olivine basalt that lies along one of the faults.

Imperial beds are overturned as much as 45° where they lie on the crystalline complex east of Painted Hill (Pl. 4, Section G–G′). Although minor faulting confuses some of the relations along the contact, the contact's depositional character is indicated by parallelism of bedding with the contact, by channeling of the "underlying" bedrock, and by a basal conglomerate of locally derived fragments of hematite-bearing schist and gneiss. The Imperial Formation here comprises deep yellowish to brownish sandstone, siltstone, and shale, with a thickness ranging from 6 inches to 100 feet. Fossils locally are so abundant that they give the rock a coquinalike appearance. The section has been thoroughly studied by Bramkamp (1934, Ph.D. thesis, Univ. Calif., Berkeley, p. 18–23). The contact with the overlying Painted Hill Formation is arbitrarily placed above the uppermost marine bed, and the conformable and transitional nature of this contact is demonstrated by stringers of fossiliferous yellow siltstone that occur as much as 50 feet up in the otherwise continental-appearing gray conglomerates.

North of Cabazon, the Imperial Formation crops out in two separate small exposures on the south flank of the overturned Lion anticline (Pl. 3). About 300 feet of Imperial strata is exposed in the easternmost outcrop and represents the greatest known thickness of this formation in the pass area. Thin interbeds of gypsum are common. Although the section is overturned, conformability of the Imperial strata with the "underlying" Hathaway Formation is indicated by parallelism of bedding and by large-scale interfingering of the two formations. Fragments of Hathaway sandstone occur as clasts in the basal conglomerate of the Imperial Formation.

Conformity of the Imperial beds with the "overlying" Painted Hill Formation is suggested by parallelism of bedding, although no actual interfingering of strata is evident.

One mile farther west, an incomplete section of the Imperial Formation is exposed on the wall of the West Branch of Lion Canyon and on two ridges between there and Deep Canyon. These beds also appear to overlie the Hathaway Formation on the south flank of the Lion anticline. Farther west, on the west wall of Deep Canyon, Imperial strata do not crop out along the presumed Hathaway-Painted Hill contact, and the Imperial Formation probably pinches out between Lion and Deep canyons. This conclusion is further supported by the coarseness of Imperial strata where last exposed. No exposures of Imperial Formation occur farther west in San Gorgonio Pass, and it seems unlikely that Imperial seas extended much beyond the Cabazon area.

DEPOSITIONAL ENVIRONMENT: The Imperial Formation of San Gorgonio Pass was deposited in a littoral or shallow neritic environment, as is indicated by the fauna (Bramkamp, 1934, Ph.D. thesis, Univ. Calif., Berkeley, p. 44; Durham, 1950, p. 24) and also by the wide variation in grain size and the concentrations of broken fossils. The waters evidently were of normal salinity and represent a single incursion of the sea from the southeast. Variations in thickness and lithology of the basal Imperial beds east of Painted Hill suggest a rocky shore line with moderate relief.

AGE: There has been much disagreement among paleontologists concerning the age of the Imperial Formation, inasmuch as the fauna is of tropical affinity and has little in common with the better-known Coast Range Tertiary faunas. Age estimates have ranged from Cretaceous to late Pliocene. The most recent studies by Wilson (1948, p. 1779–1780) and Durham (1950) suggest an early Pliocene age, and the Imperial Formation is therefore considered to be of early Pliocene(?) age in this report.

Painted Hill Formation

GENERAL FEATURES: The name Painted Hill Formation (a new name) is herein applied to the continental beds that conformably overlie the Imperial Formation east of Painted Hill. Bramkamp (1934, Ph.D. thesis, Univ. Calif., Berkeley, p. 15) termed this unit the Indio Formation because its stratigraphic position is similar to that of the Indio Formation in the Indio Hills (Buwalda and Stanton, 1930). As pointed out by Woodring (1932, p. 10), however, the name Indio Formation is preoccupied, and Dibblee (1954) recently has included in the Palm Spring Formation those beds of the Indio Hills that are immediately post-Imperial in age. There is no assurance that the post-Imperial rocks at Painted Hill and those in the Indio Hills are actually parts of the same formational unit.

LITHOLOGIC FEATURES: Along a line extending eastward from the top of Painted Hill (Pl. 4, Section G–G′), the Painted Hill Formation comprises 3400 feet of pale-brown to light-gray conglomerate and conglomeratic sandstone with subrounded to well rounded clasts as much as 2 feet in diameter. Fragments of basalt constitute 50 per cent of the clasts near the bottom of the section but give way upward to increased proportions of clasts of gray gneiss, pegmatite, and granite. The rock generally is poorly consolidated, but two resistant ridge-making conglomerate beds are present in the interval between 300 and 500 feet above the base of the section.

North of the point where Imperial beds pinch out, the Painted Hill Formation lies directly on the Coachella fanglomerate with marked angular unconformity. The two units are similar in general appearance, and the contact between them cannot be placed accurately; it is located on the basis of changes in dip along the unconformity.

The Painted Hill Formation also conformably overlies the Imperial Formation northeast of Cabazon (Pl. 3), where flows of grayish-red amygdaloidal olivine basalt are interlayered with Painted Hill beds. Only one flow is present on the south flank of Lion anticline, whereas two flows are exposed on the north flank of this fold west of Deep Canyon, and three flows crop out west of Hathaway Canyon on "B" Hill (Pl. 2). West of Lion Canyon, where the Imperial Formation pinches out, the contact between the Hathaway and Painted Hill formations is arbitrarily placed at the base of the

lowermost basalt flow. Feeder dikes, presumably contributory to these flows, occupy fault zones in "B" Hill, and basalt possibly representing one or more dikes is exposed on several spurs between Banning and Millard canyons. These latter rocks are included in the Painted Hill Formation, although their structural relation to the adjacent foothills is obscure.

PROVENANCE AND STRUCTURAL IMPLICATIONS: The high proportion of well-rounded clasts of granitic rocks in the Painted Hill Formation suggests that much of the source area lay beyond the area of predominantly metamorphic rocks that now contributes detritus to streams on the north side of San Gorgonio Pass. A large area of granitic rocks is exposed north of the Mission Creek and Mill Creek faults, and the streams that deposited the Painted Hill Formation probably had their headwaters in this area (as does Whitewater River now) and flowed southward across a metamorphic terrane of subdued topography. Subsequent uplift of this block of predominantly metamorphic rocks between the Banning and Mission Creek faults has given rise to the coarser and more angular fragments of metamorphic rock that make up a large proportion of the late Quaternary fanglomerates and Recent alluvium.

The Imperial and Painted Hill beds north of the Banning fault are strikingly similar to those south of the fault, and possibly these units were once contiguous and have since been offset 7 miles along the Banning fault. The Imperial Formation, however, lies on crystalline rocks north of the fault and on Hathaway beds south of the fault, so that former contiguity of the outcrops would make it difficult to explain the transitional Hathaway-Imperial contact. Right-lateral displacement greater than 7 miles must be regarded as a possibility. The only definitive statement concerning fault displacement that can be founded on evidence based on present relative positions of Imperial and Painted Hill strata north and south of the fault is that post-early Pliocene displacement of over a few tens of miles is out of the question.

Painted Hill beds north and south of the Banning fault contain sparse but distinctive fragments of piedmontite-bearing gneiss and ilmenite-bearing pegmatite which were probably derived from the Stubby Canyon-Whitewater area. Clasts of these rocks as much as 7 inches in diameter occur in Painted Hill beds at the head of Second Canyon. This evidence suggests post-early Pliocene strike-slip displacement on the Banning fault of no more than 10 miles and does not require any displacement.

AGE: The Painted Hill beds lie conformably upon the Imperial Formation and hence are probably of early or middle Pliocene age. Camel remains, undiagnostic as to epoch, were found in Painted Hill beds in the first canyon east of Deep Canyon, but no other fossils are known to have been recovered from this formation.

San Timoteo(?) Formation

GENERAL RELATIONS: The San Timoteo Formation was named and first described by Frick (1921), who recovered a large vertebrate fauna of late Pliocene age from the San Timoteo badlands west of Beaumont (Fig. 1). Inasmuch as all the fossil localities lie at or near the base of the section, Eckis (1934, p. 51) and English (1953, M.S. thesis, Claremont College, p. 66) suggest that deposition of the formation probably continued into Pleistocene time. The entire unit is considered herein to be Pliocene-Pleistocene in age. In the vicinity of Eden Hot Springs, San Timoteo beds overlie the middle Pliocene Mt. Eden Formation, and older rocks, perhaps of Miocene age, are reported by English (1953, M.S. thesis, Claremont College, p. 33–36) to lie unconformably beneath the Mt. Eden Formation.

The correlation of the San Timoteo Formation with the sedimentary rocks beneath the Heights fanglomerate north of Banning (Pl. 2) is based on similar lithologies and structural relations to the adjacent rocks and on fossil evidence. Fragments of horse teeth were found in sandstone beds on the west wall of School Canyon. Dr. John F. Lance of the University of Arizona stated (Personal communication) that the material definitely represents the genus *Equus* and hence is no older than Blancan. It is probably Pleistocene. Correlation with the uppermost beds of the San Timoteo Formation is therefore not unreasonable, although there is also a possibility of correlation with the Pleistocene Bautista beds of San Jacinto Valley.

Additional fossil material and further interpretive work are needed before a definite as-

signment of age and formation can be given to these rocks north of Banning. Vaughan (1922, p. 376) included these rocks in the Pliocene Hathaway Formation, but the Hathaway Formation is herein restricted to the pre-Imperial rocks of the Lion Canyon area. The rocks from these two areas have striking similarities in lithology, structural position, and general appearance.

LITHOLOGIC FEATURES: Exposed in School Canyon are 1800 feet of northward-dipping San Timoteo(?) beds, and correlative with these are the near-by strata exposed in Brinton Canyon and on the south flank of "B" Hill (Pl. 2). The rock in School Canyon comprises tan to gray arkosic sandstone and siltstone interbedded with conglomerate containing subrounded clasts of granitic, pegmatitic, and minor metamorphic rocks. In contrast to the Painted Hill Formation, clasts of volcanic rock are rare. The proportion of fine-grained material increases downward in the section, and gray to green siltstone predominates at the mouth of School Canyon. Several thin beds of fresh-water limestone crop out within the San Timoteo(?) Formation at the upper ends of School and Brinton canyons; these beds appear similar to those in the lower member of the Hathaway Formation in Lion Canyon.

Eastward, the San Timoteo(?) Formation becomes somewhat coarser and richer in pegmatite clasts. It thus seems likely that the uppermost San Timoteo(?) beds are correlative with the Cabezon fanglomerate exposed farther east, although exposures are lacking in the critical area between Hathaway and Millard canyons. The eastward coarsening suggests deposition of the San Timoteo(?) beds from the east and northeast. As in the Painted Hill Formation, many of the clasts of granite may have been derived from areas north of the Mission Creek fault.

On the south flank of "B" Hill, the San Timoteo(?) beds contain sparse fragments of piedmontite-bearing gneiss that are as much as 3 inches in diameter, gray-green epidote schist, and ilmenite-bearing pegmatite. There can be little doubt that these distinctive clasts were derived from the eastern end of the range near Stubby and Whitewater canyons, 8–12 miles from their present positions. Although transport of such material over distances of 12 miles is possible, the relatively high concentration of these clasts at "B" Hill is difficult to explain in terms of a source area that far away. Post-San Timoteo(?) right-lateral displacement on the Banning fault provides the most reasonable explanation for the present position of these clasts. To assume that the rocks have been displaced the full 8–12 miles is not necessary, because much larger clasts of piedmontite-bearing gneiss occur in the Cabezon fanglomerate near Lion Canyon, which is 5½ miles closer than "B" Hill to the presumed source area. If the Cabezon and San Timoteo(?) beds are truly correlative, a post San Timoteo(?) displacement of about 5 miles would best explain the present distribution of the distinctive clasts, but reasonable arguments could be made for still greater lateral displacement, or for none at all.

Deformed Gravels of Whitewater River

Along the east flank of the San Bernardino Mountains, Whitewater River and Mission Creek are dissecting a thick series of gravels whose structure, compared to that of the more severely deformed older sedimentary rocks, suggests a Quaternary age. A marked angular unconformity within the section is well exposed 1 mile northeast of Red Dome and near Kitchen Ranch (Pl. 1) and is sufficiently continuous in this area to serve as a means of distinguishing between two formations in the otherwise uniform-appearing gravels. The tilted beds beneath the unconformity are herein termed the deformed gravels of Whitewater River; the relatively undeformed beds above the unconformity appear to be continuous with the Cabezon fanglomerate farther south. The most widespread exposures of the deformed gravels are between Red Dome and the Mission Creek fault, where the formation consists of gray to light-tan sandstone and conglomerate with well-rounded clasts of granitic rocks that are as much as 2 feet in diameter.

Numerous outcrops of gravel are well exposed on the steep banks of Whitewater River where it is re-excavating its old channel south of Red Dome. Although stratigraphic relations here are not so clear cut as farther north, the gravels again appear to consist of two map-

pable units. Evidently deformation has been contemporaneous with deposition in this area (as it must be now), and any formational division must be somewhat arbitrary.

The deformed gravels of Whitewater River have not been recognized south of the Banning fault, although the lower part of the Cabezon fanglomerate or the upper part of the Painted Hill Formation probably includes beds contemporaneous with the deformed gravels.

Cabezon Fanglomerate

GENERAL FEATURES: Vaughan (1922, p. 387) included in the Cabezon[3] fanglomerate numerous bodies of dissected gravels that are exposed between San Gorgonio Pass and the Mojave Desert. All presumably are of Quaternary age. The type area apparently is in the foothills north of Cabazon, and the formational name is therefore retained for the extensive body of fanglomerate that appears to be continuous from Millard Canyon east to Whitewater and thence northward around the flank of the range. More than 1000 feet of Cabezon beds crops out at Whitewater Hill, and the base of the section is not exposed. Whether or not basal Cabezon beds are exposed anywhere south of the Banning fault is problematical; the angular unconformity on the west wall of Stubby Canyon (Pl. 3) is tentatively regarded as the contact between the Cabezon and Painted Hill formations, although it may be merely a local angular unconformity within the Cabezon section.

LITHOLOGIC AND STRUCTURAL FEATURES: Along the north side of San Gorgonio Pass east of Millard Canyon, Cabezon fanglomerate forms most of the rugged foothills in front of the main mountain scarp (Pl. 5). Deformation contemporaneous with deposition is indicated not only by the coarse and heterogeneous lithology of the Cabezon fanglomerate but also by structural relationships east of Stubby Canyon, where Cabezon fanglomerate is exposed beneath a thrust plate of crystalline rocks that in turn is overlain by still younger deformed Cabezon beds (Section F–F′, Pl. 3).

In the eastern part of the area, rocks north of the Banning fault are correlated with the Cabezon fanglomerate on the basis of similar composition, texture, and degree of deformation. In addition, a deformed layer of red soil, semiconcordant with the underlying Cabezon beds and therefore considered part of the formation, can be traced from Beacon Hill northward to the mouth of Mission Creek. In upper Whitewater Canyon, Cabezon(?) gravels lie in the old river channel and in the adjacent areas of formerly gentle topography.

On the east side of the mouth of Millard Canyon, northward-dipping Cabezon fanglomerate is well exposed beneath horizontal Heights fanglomerate. Here, Cabezon beds contain nearly equal proportions of clasts of pegmatite and metamorphic rock in a grayish-brown sandy matrix. Eastward, clasts of pegmatite become scarcer, and their place is taken by fragments of granitic, basaltic, and light-colored metamorphic rocks. Clasts of granitic rock form most of the fanglomerate at the mouth of Mission Creek and at Raywood Flat.

The lithology of the Cabezon fanglomerate suggests local derivation from streams similar to those of today; indeed, much of the fanglomerate north of the Banning fault lies within the valley of the present Whitewater River and must have been deposited by the "ancestral" Whitewater River before re-excavation of the valley. As in the Painted Hill Formation, many clasts of granitic rock were derived from sources north of the Mission Creek fault. Interbedded with the Cabezon fanglomerate at Beacon Hill is a 30-foot-thick lens of light-gray limestone breccia that was probably derived from one of the numerous areas of limestone in the San Jacinto block. This breccia is the only sedimentary rock on the north side of San Gorgonio Pass that appears to contain a significant amount of material derived from the San Jacinto block.

AGE: A Quaternary age for the Cabezon fanglomerate is suggested by its lack of intense deformation compared to that of the late Tertiary rocks and by its similarity to the uppermost San Timoteo(?) beds to the west.

Heights Fanglomerate

North of Banning and Beaumont is an extensive area of deeply dissected but relatively

[3] Although the post office name is now spelled Cabazon, the former (Indian) spelling of Cabezon was used by Vaughan, and is retained herein for the formational name.

undeformed gravels, named the Heights fanglomerate by Vaughan (1922, p. 392). Its Quaternary age is indicated by its unconformable position above the Cabezon fanglomerate, a relationship which is well illustrated at the mouth of Millard Canyon. The best exposures of Heights fanglomerate are on the west wall of the San Gorgonio Canyon, where the rock surface underlying the fanglomerate is one of considerable relief. The maximum thickness here is greater than 240 feet.

The Heights fanglomerate is distinctive, compared with the other Quaternary fanglomerates, in its content of clasts of predominantly metamorphic rocks; extremely weathered boulders of gray migmatitic gneiss compose most of the rock. These clasts are so thoroughly decomposed that boulders are cleanly truncated by erosion on stream banks. Distinctive fragments of greenschist in the exposures north of Banning indicate a local provenance in the mountain area across the San Andreas fault to the north. Post-Heights lateral movements on the San Andreas fault probably have displaced these gravels no more than 1 mile relative to the source area.

Burnt Canyon Breccia

A coarse breccia deposit that underlies much of Burro Flat causes this area to be one of grassy rolling hills which is anomalous in the otherwise rugged and brush-covered terrain of the pass area. Origin of this deposit as a landslide mass is indicated by: (1) angularity, freshness, and lack of sorting of the clasts; (2) absence of matrix material; (3) steep bordering scarps and bulbous outline of the rock mass; (4) longitudinal streaks of coarser rock fragments on the surface of the slide; (5) lack of surficial soil, with a consequent grass (rather than brush) cover.

The landslide mass rests partly on the crystalline complex and partly on the flat surface of the Heights fanglomerate and therefore must be younger than the fanglomerate. Recent movements on the San Andreas fault have left prominent scarps in the Burnt Canyon breccia, and the scarps have survived better in this porous material than in the weathered crystalline rock of adjacent areas. The wide flat debris-covered floors of Wood Canyon and its tributary, Burnt Canyon, suggest that much of the slide material had its source in the rugged scarp at the head of these canyons. The crystalline rock types here and in the other small canyons north of the slide are identical with those found as fragments in the Burnt Canyon breccia.

Alluvium

Extensive alluvial fans, the gravels of which are similar to the older dissected fanglomerates, are being built on the floor of San Gorgonio Pass, and the heads of these fans extend up many of the wider stream canyons. Gravels of low stream terraces, discussed in detail by Russell (1932), are grouped together with the Recent alluvium.

Geomorphology and Ground Water

Introduction

In this section only those aspects of geomorphology and ground water that pertain directly to the structural geology are considered. These include surfaces of low relief, closed depressions, alluvial fans, and location of springs; all these aid in the interpretation of Recent deformation in this area. Other authors have discussed many of the remaining aspects.

Surfaces of Low Relief

GENERAL FEATURES: Within the hills along the north side of San Gorgonio Pass, the present regimen is one of re-excavation following widespread burial of the former terrain by Quaternary alluvial fans. Present streams are incised into thick and extensive fanglomerate deposits which rest on a surface of considerable relief cut across the crystalline complex and Tertiary sedimentary rocks. Many of the deeply incised streams are guided by former canyons that were cut into the older rocks before the period of gravel filling. Within the mountains, Quaternary gravels extend up to altitudes above 8000 feet, and surrounding these gravel-covered areas are surfaces of low relief and thick residual soils on the old crystalline rocks. Such areas of gentle relief are especially widespread farther north in the San

Bernardino Mountains (Vaughan, 1922, p. 321–334) and probably indicate a Recent history different from that of adjacent mountain masses.

Interruptions in the dissection of the Quaternary fanglomerates by streams draining the north side of the pass have led to the development of numerous terraces and benches. The principal surfaces at the west end of the pass are Beaumont plain, Banning Bench, and Pine Bench; at the east end of the pass are the Cabezon surface and Whitewater River terrace.

BEAUMONT PLAIN: West of the area of Plate 1, tributaries of San Timoteo and Potrero creeks are dissecting the Beaumont plain; Russell (1932, p. 72–73) described these features in detail. The Beaumont plain probably is correlative with the extensive bench of the Yucaipa-Calimesa area and Redlands Heights (Fig. 1). It increases in height above the present stream level in a downstream direction; the cause of rejuvenation is not known.

BANNING BENCH: A surface of erosion distinctly higher than the Beaumont plain truncates much of the foothills area between the floor of the pass and the steep mountain front several miles north (Pl. 5). The Banning Bench surface possibly represents a portion of the Beaumont plain that has been raised by faulting, but further field work west of the area of Plate 1 will be necessary before the relationship between these two surfaces can be established. The easternmost exposures of the Banning Bench surface are near the mouth of Millard Canyon (Pl. 1), although scattered remnants of gravel and areas of low relief within the mountains farther east may also be correlative with this surface. In the mountains to the north, well-defined terraces represent the Banning Bench surface in many of the canyons.

That the surface of Banning Bench is a degradational surface and not the uppermost surface of Heights deposition is indicated by higher surfaces on Heights fanglomerate at the north and south ends of the bench, as well as by greater thicknesses of Heights gravels near the mouth of Smith Creek. The red soil-covered surface near upper Hathaway Creek, which probably is correlative with the Banning Bench surface, is also surrounded by hills representing greater thicknesses of the same fanglomerate that underlies the surface.

Banning Bench shows little evidence of local deformation except for one Recent fault scarp south of the ranger station (Pl. 1). Warping of beds along the south edge of the bench near Banning probably is ascribable to movements on a bordering fault.

One significant structural feature of the Banning Bench surface is its upstream divergence from the present stream levels. At the mouth of San Gorgonio Canyon the bench surface is about 160 feet above the stream, whereas 5 miles north (upstream) the difference in levels is 500 feet. Similar relations hold north of Beaumont, where the divergence has been attributed by Dennis and Melin (1942, Unpub. Rept., U. S. Geol. Survey, p. 5) to regional southward tilting. On the other hand, streams that constantly reduce gradient might leave remnants of former steeper channels and fans if the dissection were sufficiently rapid. Eckis (1928, p. 237–243) pointed out that such "fanhead trenches" are almost universal in Southern California and are the result of normal continuous degradation rather than a result of tilting or faulting. Certainly, normal reduction of the gradients of streams crossing Banning Bench has contributed in some degree to the upstream divergence of bench and stream levels. But several lines of evidence suggest that tilting also has taken place:

(1) It is unlikely that such an extensive deeply weathered soil-covered surface of low relief could have developed on slopes of 4°–5°, which now characterize the upper parts of these benches.

(2) The sizes of fragments within the gravels on the surface of Banning Bench are not significantly different from those in near-by present stream channels. Fans of the pass area with slopes of 4°–5° generally have much larger fragments, although this varies widely with rock type and drainage area.

(3) If upstream divergence of terrace and present stream levels is attributed solely to normal degradation, it is strange that the adjacent Beaumont plain is incised by streams whose levels diverge from the plain in a down-

stream direction. It seems more likely that tilting has increased toward the mountains.

PINE BENCH: The highest fanglomerate deposits in the foothills north of Banning and Beaumont are at Pine Bench (Pl. 5). This small area, at an altitude of 5500 feet, is surrounded by steep scarps sloping down to the surface of Banning Bench. Gravels similar to those at Pine Bench are exposed on at least one ridge farther west.

At the extreme north and south ends of Banning Bench are small remnants of surfaces on Heights fanglomerate at altitudes intermediate between those of the Banning Bench and Pine Bench surfaces. The terrace remnant north of the San Andreas fault between San Gorgonio Canyon and Burro Flat may be correlative with this intermediate level, although it also may be a remnant of the Banning Bench surface that has been raised along the fault.

CABEZON SURFACE: Heights fanglomerate, capped by a distinct undeformed layer of soil, overlies Cabezon fanglomerate at the mouth of Millard Canyon. Nine miles east, at the mouth of Whitewater Canyon, the Cabezon fanglomerate is itself capped by a reddish soil layer that is semiconcordant with the underlying fanglomerate. This surface is herein termed the Cabezon surface. Although it is similar in appearance to the Banning Bench surface, its greater age is indicated by its greater degree of dissection and marked deformation. At Beacon Hill (Pl. 1), both Cabezon beds and the soil that caps them show quaquaversal dips of as much as 30°, and the soil layer plunges beneath Recent alluvium around the periphery of the domical structure.

The Cabezon surface can be projected across Whitewater Canyon between Beacon and Whitewater hills, but farther west the increased deformation of the Cabezon fanglomerate and its greater degree of dissection preclude tracing of the surface. The Banning fault displaces the Cabezon surface near Whitewater, and northeast of Painted Hill the gently eastward-dipping soil layer marking the Cabezon surface is being buried beneath Recent alluvium.

At the mouth of Mission Creek, the Cabezon surface probably is an old fan surface, but it now dips 6° southeast and plunges beneath Recent alluvium 2 miles southeast of Kitchen Ranch (Pl. 1). This surface is transected by Mission Creek and is incised by Whitewater River farther west near Red Dome. Mission Creek and Whitewater River at one time perhaps joined on this fan surface; subsequent incision has superposed these two streams on rocks of differing hardness and structure, with a resulting divergence of stream paths. Local eastward tilting of this old fan surface is suggested by four lines of evidence:

(1) Tentatively correlated remnants of this surface near the mouth of Mission Creek have gradients that increase southeastward toward the valley. Such convexity is difficult to explain except by warping.

(2) The Cabezon surface intersects the Recent alluvium with an abrupt change in slope. None of Eckis' "fanhead trenches" (1928, p. 237–243), which presumably are the result of normal degradation, is associated with such an abrupt change in slope.

(3) If the slope of the Cabezon surface is projected upstream (northwest), it clears the ridge tops for more than 6 miles. If all this intervening material was removed after development of the fan, the more easily erosible fan deposits should be completely dissected.

(4) A broad surface of low relief at altitudes ranging from 6500 to 8000 feet is associated with thick Cabezon(?) gravels at Raywood Flat. This area is presently undergoing spectacular dissection by Mill Creek and Whitewater rivers. The presence of this surface and the underlying gravels suggests either upwarping or faulting, inasmuch as the steep stream gradients between Raywood Flat and the borders of the range make any other explanation difficult. Reconnaissance of the upper Whitewater River area suggests that no major Recent faulting is present in this river system; tentatively correlated terrace remnants can be followed for most of the distance between Whitewater and Raywood Flat. The eastward-tilted Cabezon surface at the mouth of Mission Creek is probably the mountain-border equivalent of the surface at Raywood Flat. It is thus likely that Raywood Flat represents a broad upwarping of the San Bernardino Mountains in this area, perhaps along a north-south axis. Such arching would also help explain the San Jacinto Mountains and the present altitude of Pliocene marine beds in San Gorgonio Pass near Cabazon. Upwarping of a similar nature

has been postulated from regional evidence by Sharp (1954, p. 8).

WHITEWATER RIVER TERRACE: In removing the Cabezon fanglomerate that once filled its former channel, Whitewater River has cut a prominent terrace that can be followed discontinuously for 6 miles between the Banning fault and Island Mountain (Pl. 1). All these terraces are rock-defended, which explains their survival in the rapidly deepening canyon. Near Red Dome, it can be distinguished from the Cabezon surface by (1) its set-in geometric relation to the river gorge, (2) its slightly lower altitude, (3) the lesser degree of its surface dissection, and (4) its capping of relatively fine-grained gravels.

The Whitewater River terrace rises progressively higher above stream level in the upstream direction. The farthest upstream remnant is on Island Mountain, at an elevation of 650 feet above the present stream. The terrace has not been recognized south of the Banning fault.

Closed Depressions

"Dry Lake," a closed basin on the ridge west of the mouth of Stubby Canyon (Pl. 5), probably owes its closure to northward tilting which has cut off the branch of Lion Canyon that formerly drained this area. No Recent fault scarps cross the basin, but the Banning fault is only half a mile south.

A large closed depression is located near the headwaters of Grapevine Canyon, about 7 miles west of Kitchen Ranch (Pl. 1); this area is locally called "The Sinks." The principal cause of closure appears to be large-scale slumping, rather than faulting. Numerous smaller slump basins occur near the tops of ridges throughout the rugged mountain area.

Small basins and sag ponds caused by Recent faulting are characteristic features along the San Andreas fault and are especially well developed at Burro Flat (Pl. 5). Closed depressions are associated with glacial topography in the higher mountains (Fairbanks and Carey, 1910), but no glaciers extended into the area of Plate 1.

Alluvial Fans

Alluvial fans derived from the San Bernardino Mountains cover the floor of San Gorgonio Pass and cause the southward gradient across the pass to be greater than the eastward gradient down the pass (Pl. 5). Vaughan (1922, p. 340–342) and Russell (1932, p. 32–34) commented on the fact that these south-sloping alluvial fans dominate the fans that have been built out from the much steeper San Jacinto scarp on the south, so that San Gorgonio River washes against the south wall of the pass over almost its entire course in this area. Vaughan attributed this unequal fan development to the greater stream flow resulting from larger drainage areas on the north, assisted by possible raising of the San Gorgonio block by Recent faulting on the north side of the pass. Russell discounted the effects of differences in drainage area and amount of precipitation and emphasized the contrast in rock types of the San Jacinto and San Gorgonio blocks.

The writer favors two principal explanations for the predominance of fans derived from the north:

(1) Alluvial fans are built only during floods, and comparison of precipitation figures for the two sides of the pass indicates a greater "flood potential" of streams that drain the San Gorgonio block. Southward- and southwestward-facing slopes of the coastal mountains of Southern California receive most of the heavy storm rainfall (Troxell *et al.*, 1942, p. 49–54; Hamilton, 1944). The north side of San Gorgonio Pass is therefore in an especially vulnerable position; 24-hour precipitation of 5 inches was equalled or exceeded at Raywood Flat 26 times between 1921 and 1945. Furthermore, the steep barren slopes carved in the Mill Creek fault zone along Mill Creek and Whitewater River contribute to the unusually high runoffs from these two drainage areas (Troxell *et al.*, 1942, p. 315). Flood runoff from the north side of the pass is also greater, because the drainage area is larger than in the San Jacinto block to the south.

(2) The difference in rock types on the two sides of the pass is an important factor. However, the writer disagrees with Russell (1932, p. 34) that a considerable part of this difference is caused by the thin strip of easily erosible Tertiary sedimentary rocks along the north side of the pass and that this strip furnishes "a very large amount of material for the active

fans of today." The writer believes that the San Gorgonio igneous-metamorphic complex is more easily eroded because of its heterogeneity and thoroughly fractured structure, in addition to several great zones of crushed rock along major faults within it. In contrast, the homogeneous rocks of the San Jacinto Mountains tend to break off into such large boulders that only exceptional floods can move great quantities of such material. The granular material (grus) resulting from disintegration of the boulders perhaps is carried off by minor annual floods and hence does not accumulate close to the mountain to form a large fan. The steep "boulder-controlled" slopes of San Jacinto Peak may be more stable under existing climatic conditions than the gentler slopes across the pass to the north.

Ground Water

Springs in San Gorgonio Pass delineate many structural features. The writer has divided the springs into three groups, according to whether they are caused by (1) fault damming, (2) exposure of unconformities, or (3) canyon constriction.

FAULT DAMMING: Much water rises along the San Andreas fault and is tapped by local water companies. The most important springs of this type are at Camp Comfort, in San Gorgonio Canyon, and in Burro Flat at Thompson and Peat Cienegas. There is little evidence that great quantities of water are carried by the crushed rock in the fault zone itself.

The western portion of the Banning fault does not appear to affect the distribution of ground water, but the cienega in Whitewater Canyon is evidence of Recent displacement in the fault's eastern portion. Farther east in Coachella Valley, the Banning fault can be traced only by subtle changes in vegetation resulting from differences in ground-water levels on the two sides of the fault.

Recent displacements characterize the east end of the Gandy Ranch fault, and prominent springs mark the crossings of Millard, Potrero, and Hathaway canyons (Pl. 1). In Hathaway Canyon, southern termination of the Heights fanglomerate may be an important factor contributory to the rising ground water. At the forks of Millard Canyon, 5 miles north of Cabazon, the prominent springs must be caused by faulting, although the break is not discernible far east and west of the canyon bottom.

EXPOSURE OF UNCONFORMITIES: The permeability and porosity of Quaternary fanglomerates of the pass area make them excellent aquifers, and the base of the fanglomerate deposits has been exposed by dissection in many areas, so that springs are common along this unconformity. The best examples are at the edge of Banning Bench, where water percolating southeastward forms springs at the Heights-San Timoteo(?) contact in many of the small canyons north of Banning. Springs in Smith Creek, 1 mile above Highland Springs Resort, are on the contact between Heights fanglomerate and the crystalline complex. The sporadic success of wells drilled on Banning Bench and evidence that the rock floor beneath the Heights fanglomerate is one of considerable relief suggest that ground water is guided by old stream channels in the buried topography.

In a situation similar to that at Banning Bench, springs occur in the South and East forks of Whitewater River at the base of the dissected Cabezon(?) fanglomerate of Raywood Flat. Water also rises at Perched Spring in Burro Flat at the base of the Burnt Canyon breccia, which is an aquifer even more permeable than the underlying Heights fanglomerate.

CANYON CONSTRICTION: Lessening of the cross-sectional area of stream gravels by constriction of the canyon walls can force ground water to the surface. Such constriction may be caused by differential rock types, old faulting, or stream superposition. Superposition probably is the explanation for the cienegas in San Gorgonio Canyon 5 miles north of Banning, and in Whitewater Canyon opposite the trout farm. The springs half a mile east of Kitchen Ranch apparently are caused by superposition of Mission Creek onto a ridge of relatively resistant Miocene(?) basalt.

GEOLOGIC STRUCTURE

San Andreas Fault

INTRODUCTION: The San Andreas fault is a major tectonic feature of western North America. Seismic activity suggests that faulting related to this great zone of weakness extends more than 700 miles from the Gulf of California

to the Pacific Ocean north of San Francisco. Noble (1926, p. 416–417) distinguished the San Andreas fault from the San Andreas fault zone; the fault itself is defined as the linear trace of recent activity—the "master break"—within the elongate area characterized by the "branching and interlacing, roughly parallel fractures" that make up the fault zone. The fault zone is as much as 6 miles wide in central California, and the present study suggests that it is even wider in parts of Southern California. Detailed descriptions of the fault features and summaries of the evolution of thought concerning the fault have been contributed by Lawson *et al.* (1908), Taliaferro (1943), Wallace (1949), Hill and Dibblee (1953), and Noble (1926; 1932; 1953; 1954a; 1954b).

From the type locality at San Andreas Valley near San Francisco (Willis, 1938, p. 806), the San Andreas fault forms an uninterrupted break for more than 350 miles southeast to the Cajon Pass area (Fig. 1). Beyond this point the fault splits into several great branches (Noble, 1932, p. 360), but the name San Andreas traditionally has been applied to the most nearly aligned and obvious prolongation—the fault that lies at the foot of the San Bernardino Mountains and continues into San Gorgonio Pass. Within the pass area, however, various structural complications make the continuity of the fault through this region doubtful.

TRACE OF THE FAULT THROUGH SAN GORGONIO PASS: The steep front of the San Bernardino Mountains clearly defines the trace of the San Andreas fault from Cajon Pass to Pine Bench, on the north side of San Gorgonio Pass (Pl. 5); southeastward into Burro Flat the trace is marked by numerous northward-facing scarplets, springs, sag ponds, and exposed zones of greenish pulverized rock. In the interval between Pine Bench and Burro Flat, however, the Recent scarps show a systematic change in trend of more than 30° in a distance of less than 6 miles; if the fault continued southeastward from Burro Flat with the trend that is indicated by the easternmost scarps, it would cross San Gorgonio Pass and extend almost through the top of San Jacinto Peak. That the fault does not continue in this direction is indicated not only by the absence of physiographic evidence of faulting but also by the continuity of rock types in the San Jacinto block. Southeast of Burro Flat, the so-called San Andreas therefore must (1) turn abruptly eastward, (2) be offset by another fault, (3) continue with a trend different from that indicated by the Recent scarps, (4) dive beneath a thrust plate, or (5) die out.

The southeasternmost scarps of the San Andreas fault at Burro Flat are only 2 miles north of the trace of the eastward-trending Banning fault, yet the over-all continuity of the Banning fault indicates that it is not offset by a fault of major displacement. For the San Andreas fault to turn abruptly and join the Banning fault would require a change in trend of more than 45° in this 2-mile interval. The Banning fault, despite its over-all continuity, is broken in three places by minor faults that trend parallel to the San Andreas fault at Burro Flat (Pls. 2, 3). Although none of these small faults is directly in line with the southeasternmost scarps at Burro Flat, they indicate that Recent strain, however small, has continued in this southeasterly trend.

Offset of the San Andreas fault by another fault is precluded by the absence of either the offset portion of the fault or evidence of a fault capable of such offsetting movement. The Banning fault, for instance, is offset by faults of San Andreas trend, rather than vice versa.

Previous workers (Lawson *et al.*, 1908; Vaughan, 1922) have linked the trace of the San Andreas fault as a smooth curve between Pine Bench and Whitewater, but they either have not observed the trend of Recent scarps in Burro Flat or have discounted them. The Recent scarps may not reflect the trend of the major fault line, and minor irregular divergences of scarps within the fault zone are known to be characteristic features elsewhere along its trace (Wallace, 1949, p. 804; Hill and Dibblee, 1953, p. 445). The changes in trend of scarps in the Burro Flat area, however, are neither irregular nor minor. Further proof that the main fault does not continue in a more easterly direction from Burro Flat is provided by the following two lines of evidence:

(1) Inasmuch as the topographic "groove," or rift, seems to be even more characteristic of the San Andreas fault than Recent scarps (Wallace, 1949, p. 804), at least some longitudinal valleys should mark the fault trace. Except for the locally trough-shaped valley of the

West Branch of Millard Canyon, such rift topography is definitely absent from the area through which the fault presumably would pass. The suggestion by Fairbanks (*in* Lawson *et al.*, 1908, p. 45) that the lack of rift topography in this area is caused by Recent uplift and dissection of the range is not tenable. The existence of rift valleys along the San Andreas fault in Southern California is caused primarily by erosion of the pulverized rocks from within the fault zone (Crowell, 1952, p. 22), especially in areas of Recent uplift, and increased erosional efficacy should accentuate, not conceal, the rift topography.

(2) Although the crystalline rocks in the area between Burro Flat and Whitewater are extremely shattered and contorted, presumably because of their proximity to the Banning fault, no evidence of a throughgoing break north of the Banning fault is present within these rocks: the rock types across this zone are similar, and there exist no one aligned discontinuity in attitudes of foliation, no throughgoing zone of pulverized rock, and no springs in the canyons at points where they would cross the hypothetical fault.

Inasmuch as the Banning fault is a flat thrust across much of the area in which the continuity of the San Andreas fault is questioned, it might be argued that the San Andreas fault merely is concealed beneath this thrust plate. However, most of the change in trend of Recent scarps along the San Andreas fault takes place west of the point where the fault presumably would dive beneath the thrust plate, so that this hypothesis still must explain the markedly nonlinear trend of the fault in the pass. Furthermore, there is good evidence that the Banning fault gradually steepens at the west end of the thrust zone and does not trend north to overlap the San Andreas fault.

According to a related hypothesis, thrusting in the Millard Canyon-Whitewater area represents Recent deformation of the San Andreas fault plane itself, so that at depth the thrust steepens and becomes part of a continuous, essentially planar, northwestward-trending fracture. Large strike-slip displacement presumably could have taken place on the San Andreas fault before it was thus deformed to yield its present complex near-surface configuration. This hypothesis, however, does not explain the westward continuity of the thrust zone with the Banning fault rather than the San Andreas fault. If there has been large prethrusting lateral movement, it has probably taken place on the Banning fault, rather than on the San Andreas fault.

There appears to be only one remaining explanation: the surface break that has been called the San Andreas fault is dying out in the vicinity of Burro Flat. This conclusion implies, of course, that displacement on the fault in this area has not been large.

DISPLACEMENT: Within San Gorgonio Pass, the various lines of evidence of displacement on the San Andreas fault are:

(1) Lateral stream offsets along the fault are absent. At least the deeply intrenched canyon of San Gorgonio River should show some evidence of offset if there had been appreciable Recent strike-slip movement on the fault.

(2) Recent scarps in this area consistently indicate upward movement of the south block, although not more than 50 feet of such movement is required to explain any of the scarps. The steep mountain front north of the fault suggests a Quaternary or late Tertiary vertical component of movement amounting to several thousand feet, with the north side relatively raised.

(3) All crystalline rocks within the area of Plate 1 and north of the Banning fault are of the same family—the San Gorgonio igneous-metamorphic complex. The similarity of rock types across these faults does not suggest large lateral movements, but possible displacements of tens or even hundreds of miles cannot be precluded on this basis alone. Similar rocks occur in parts of the San Gabriel Mountains and Little San Bernardino Mountains, and migmatitic amphibolites of this type are common at even greater distances along the fault zone.

(4) Distinctive clasts of greenschist in the Heights fanglomerate of Banning Bench must have been derived from the greenschist exposures in San Gorgonio Canyon north of the San Andreas fault (Pl. 1); no other possible source is known in this region. The present location of this fanglomerate relative to the source area indicates that less than 1 mile of post-Heights lateral displacement has taken

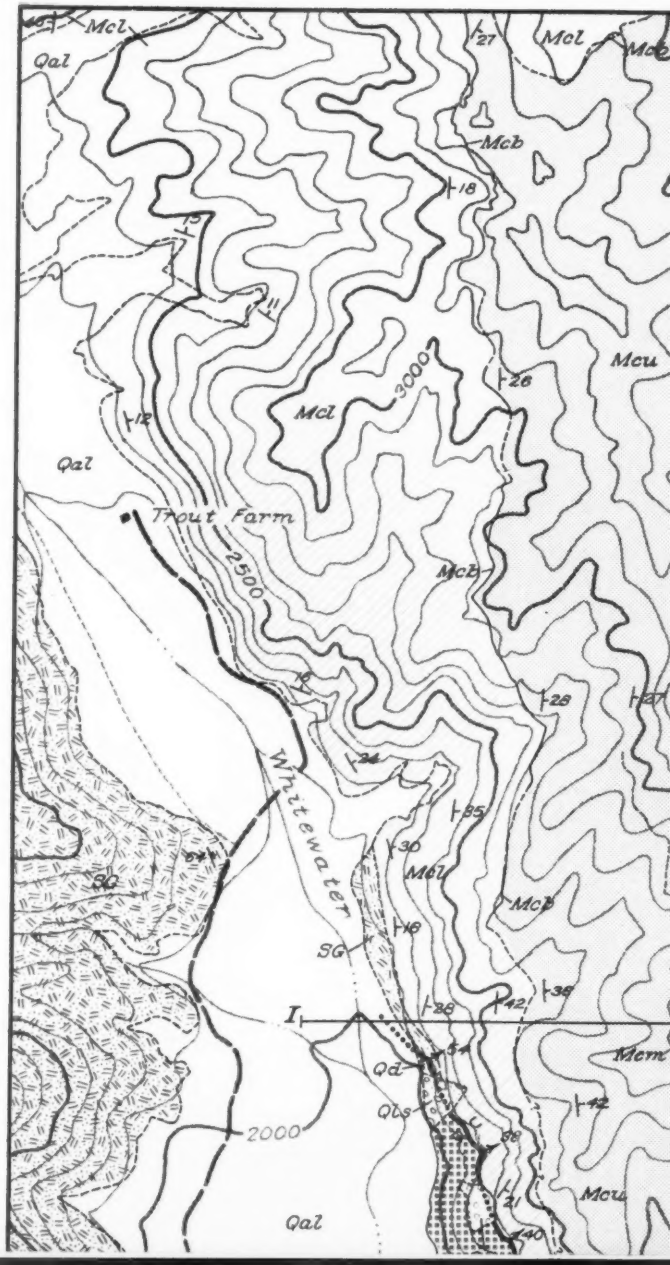
Mcl
Qal
27
Mcl
Mcb
18
Mcu
3000
26
Mcl
12
Qal
Trout Farm
2500
Mcb
28
27
24
Whitewater
35
30
Mcl
Mcb
SG
48
SG
I
38
42
39
Mcm
Qd
54
Qls
42
2000
68
21
Mcu
Qal
40

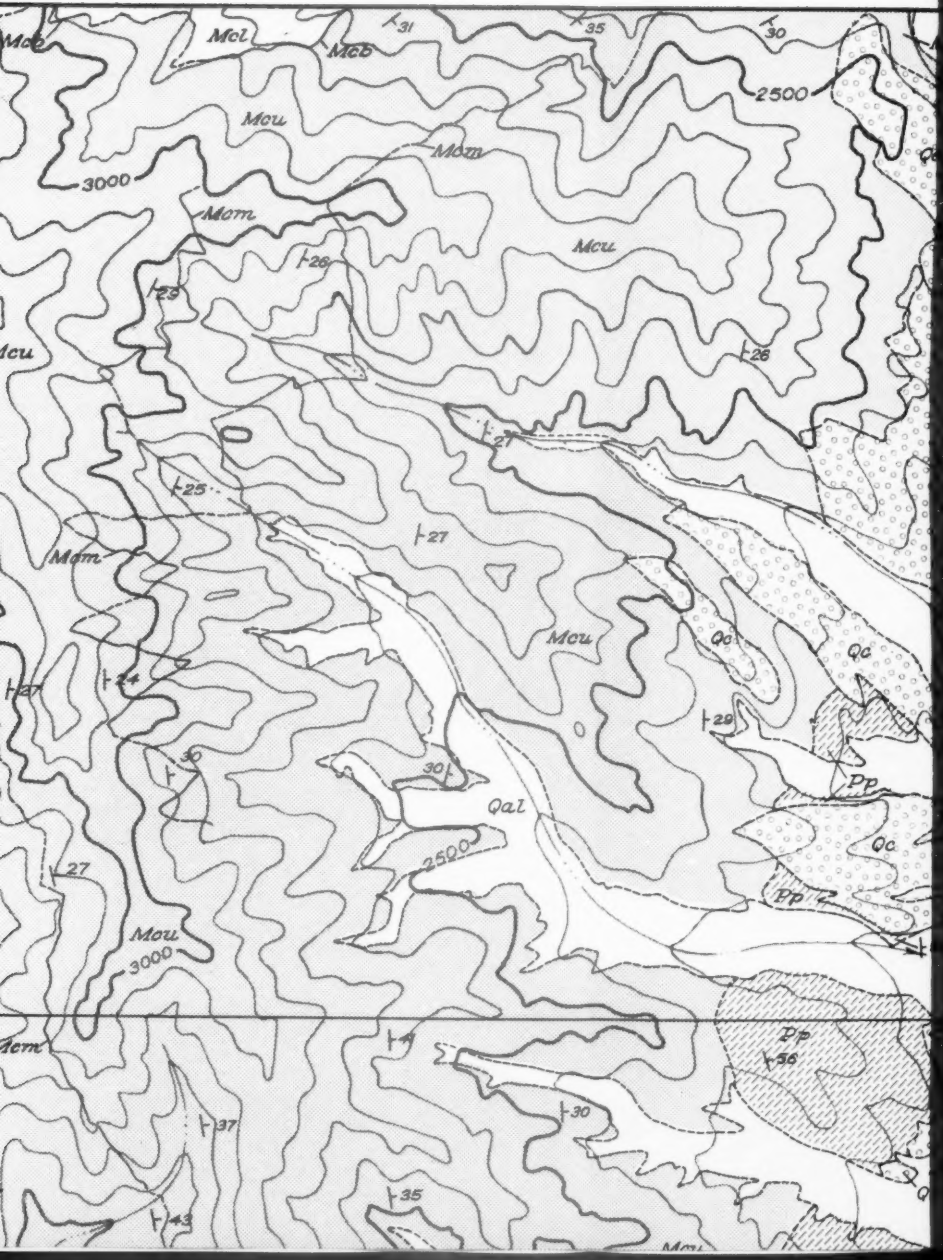
Mcl
Mcl
Mcl
Mcu
Mcu
Mcm
Mcm
Mcu
Mcu
Mcu
Mcu
Mcm
Mcm
Mcu
Mcu
Qal
Qc
Qc
Qc
Pp
Pp
Pp
Pp
3000
3000
2500
2500
3000
31
35
30
28
29
26
27
25
27
24
27
30
27
29
36
37
43
35
30
36

Allen, Pl. 4

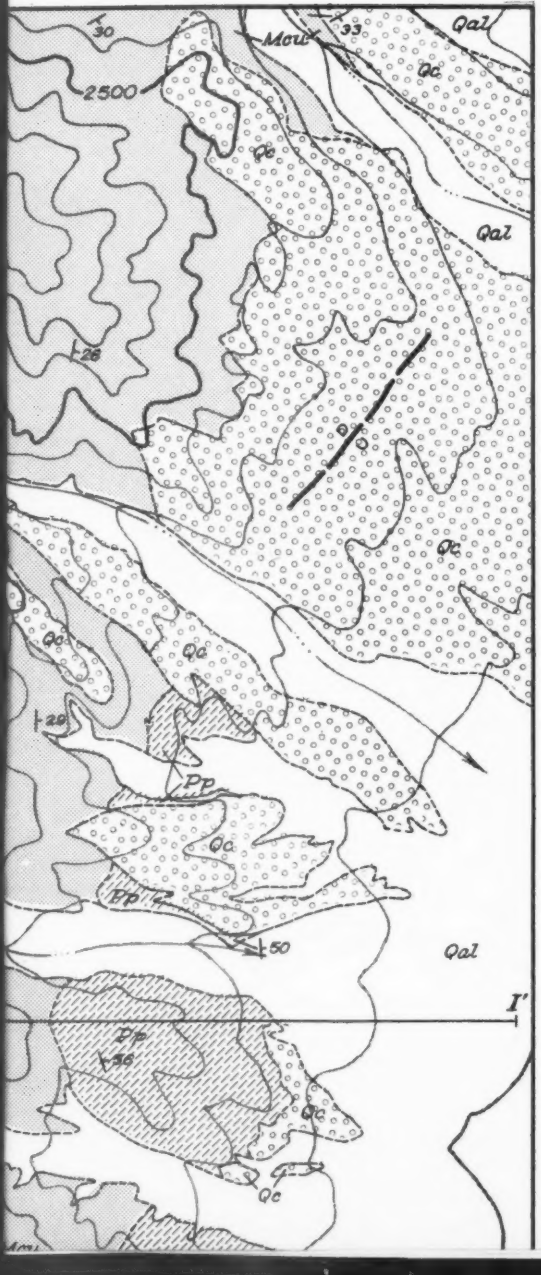

Upper Miocene(?) Lower Pliocene(?) Middle Pliocene(?)

Resistant c
olivine bas
basalt, Ppd

Upper memb
flows of o
olivine
tinctive c

Bas

EXPLANATION

Alluvium

UNCONFORMITY

Cabezon fanglomerate

UNCONFORMITY

Deformed gravels of Whitewater River

CONTACT NOT EXPOSED

Painted Hill formation

tant conglomerate bed, Ppc; interlayered flows of e basalt, Ppb, and associated dikes of olivine , Ppd.

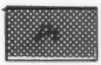

Imperial formation

UNCONFORMITY

Coachella fanglomerate

r member, Mcu; Lower member, Mcl; interlayered of olivine basalt, Mcb, and associated dikes of ne basalt, Mcd; marker horizon containing dis- tive clasts, Mcm.

UNCONFORMITY

San Gorgonio igneous-metamorphic complex

QUATERNARY

TERTIARY

MESOZOIC AND OLDER

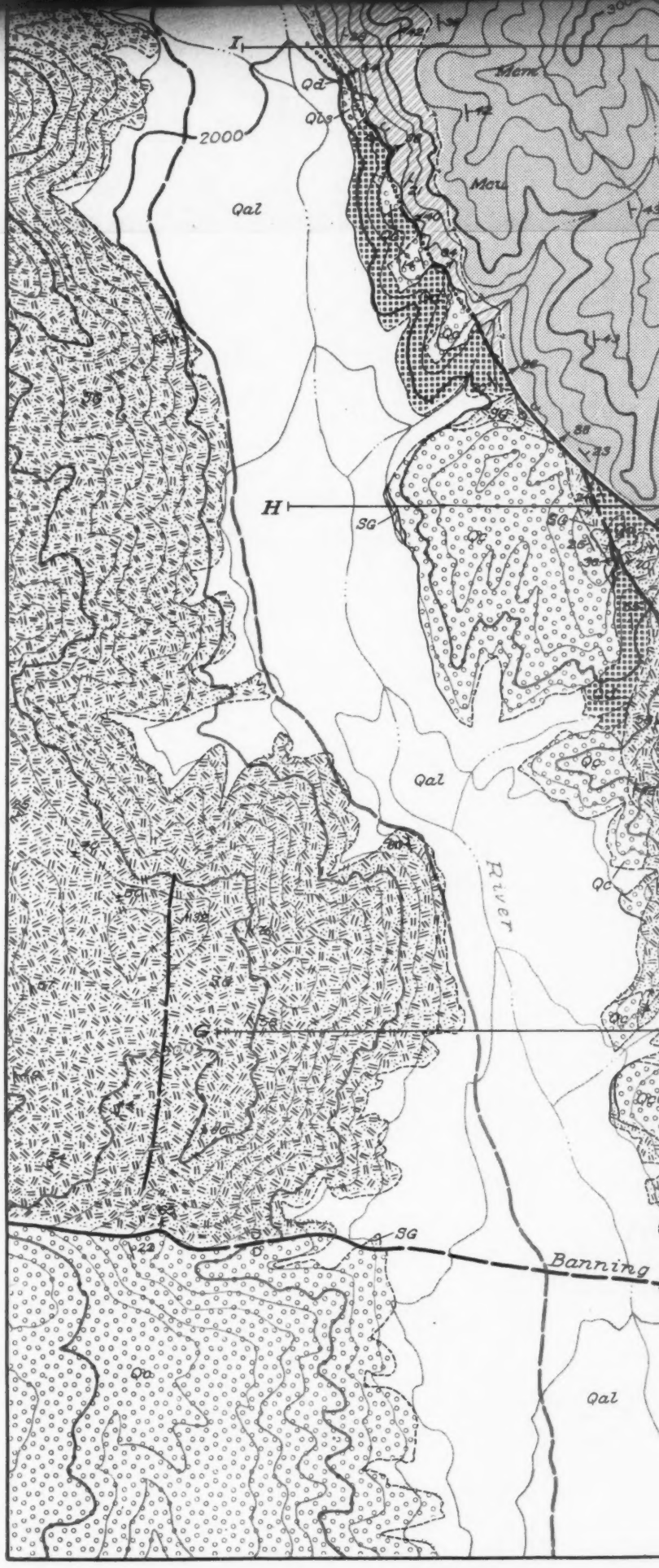

Base map modified from Corps of Engineers, U. S. Army, 1943-1944

1 0.5

Conto

GEOLOGIC MAP AND STRUCTUR

Mcu
Qal
Pp
Qc
Devil's Garden
Bandit
Mcu
Pi
Mcd
Qal
Pp
Qc
Qal
Qc
Qal
Qc
Qc
Qal
Qc
Qc
Qal
Qc
Qc
Qc

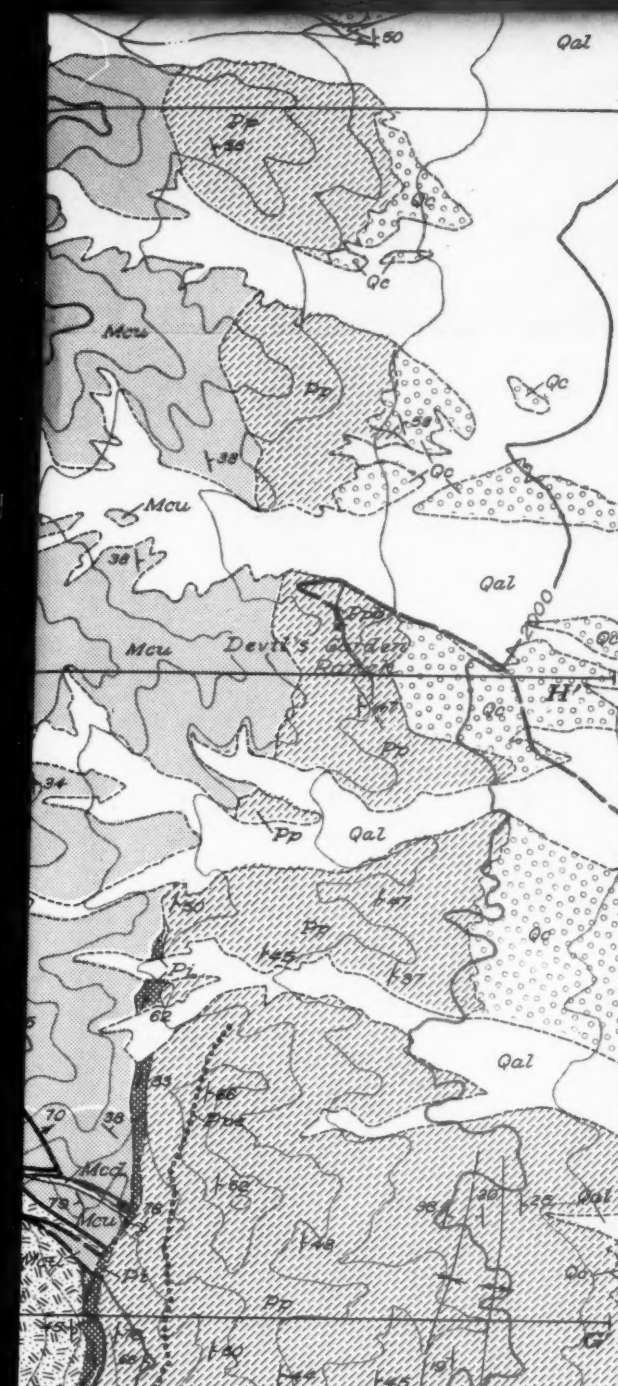

PAINTED HILL AREA

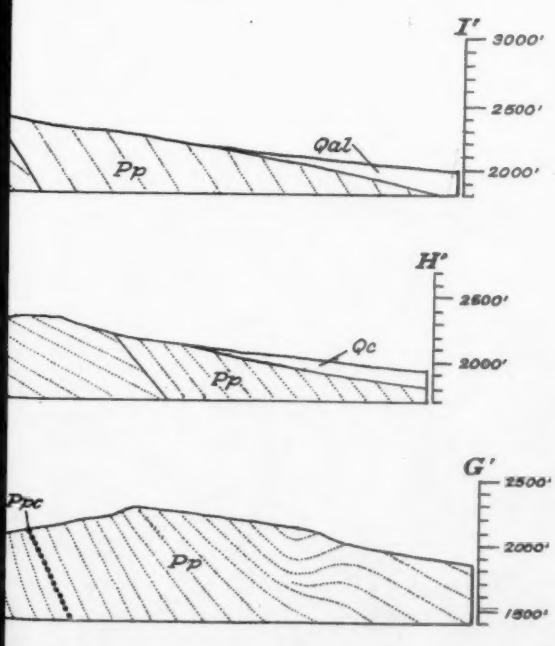

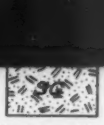

San Gorgonio igneous-metamorphic complex

MESOZOIC AND OL

Contact
Dashed where approximately located

25

Fault, showing dip
Dashed where approximately located; dotted where concealed. U, upthrown side; D, downthrown side

32

Anticline, showing plunge
Dashed where approximately located; dotted where concealed

Syncline
Dashed where approximately located; dotted where concealed

67

Strike and dip of beds

90

Strike of vertical beds

78

Strike and dip of overturned beds

19

Strike and dip of foliation

15°

TRUE NORTH

MAGNETIC NORTH

APPROXIMATE MEAN DECLINATION, 1954

pl
er

is
me
see
he

tre
pr
Fla
als

fau
lat

An
hav
1 r
mo
asr
of
spr
Ca
lat
thi

mil
the
Ca
mu
Go
eve
con
of t
is li
hav
pre
serv
con
of t

ma
Gor
roc
line
bet
it p
Jac

place on the fault here. The Heights fanglomerate is probably of late Pleistocene age.

(5) The greenschist of San Gorgonio Canyon is cut off on the south by the fault, but movements no greater than several thousand feet seem to be necessary to explain its presence here.

(6) An almost continuous zone of eastward-trending pegmatite dikes extends across the projected trace of the fault south of Burro Flat. Recent scarps of the Gandy Ranch fault also continue unbroken across this same area.

(7) Where the Banning fault is broken by faults of San Andreas trend, the maximum lateral component of displacement is 2000 feet.

SUMMARY: Recent displacements on the San Andreas fault in San Gorgonio Pass probably have been largely vertical with less than 1 mile of strike-slip component. Earlier lateral movements also may have been small, inasmuch as the crystalline rocks on the two sides of the fault are similar. Owing to the widespread occurrence of this rock type in Southern California, however, the possibility of large lateral displacement cannot be eliminated on this basis.

Noble (1954b) gave good evidence of 20–30 miles of late Tertiary lateral displacement along the San Andreas fault in the area northwest of Cajon Pass, and some of this lateral strain must have been transmitted into the San Gorgonio Pass area. But large movements, or even movements of 1 or 2 miles, are not compatible with the present surface geometry of the fault trace in San Gorgonio Pass. Thus it is likely that older lines of San Andreas faulting have been deformed and broken up, so that the present fault trace in this area may not deserve the parent name. Other faults, previously considered branches, may have absorbed most of the lateral strain.

Banning Fault

GENERAL FEATURES: The Banning fault, the major structural break on the north side of San Gorgonio Pass, brings Cenozoic sedimentary rocks into contact with the much older crystalline complex throughout the 25-mile interval between Whitewater and Yucaipa Valley, and it probably extends farther west to the San Jacinto fault zone. Vaughan (1922) mapped this fault only as far west as San Gorgonio River, whereas R. T. Hill (1928, p. 142) recognized its much greater westerly extent and gave it the name Banning fault.

West of Cabazon the Banning fault neither displaces Quaternary gravels nor appears to affect the distribution of ground water. Eastward in Coachella Valley, where it has usually been called the San Andreas fault, Recent scarps permit easy recognition of the Banning fault at least as far as Biskra Palms, near which it is joined by the Mission Creek fault (Fig. 1). The type locality is here designated as the area in which the fault crosses San Gorgonio River north of Banning. The most extensive exposures, however, occur between Millard and Cottonwood canyons (Pl. 1), where they show far greater structural complexity than those near Banning.

FEATURES OF THE FAULT TRACE: The westernmost exposure of the Banning fault is in the foothills between Beaumont and Calimesa (Fig. 1), where the light-colored crystalline rock north of the fault zone forms a prominent fault-line scarp. The break is here known as the White Hill fault (Dennis and Melin, 1942, Unpub. Rept., U. S. Geol. Survey), but its continuity with the Banning fault 4 miles farther east is demonstrated not only by similar trend and alignment but also by corresponding rock types and structural features that lie adjacent to the fault in the two areas. In this western area the break is a steep reverse fault that dips 70°–80° north (Shuler, 1953, M. S. thesis, Univ. Southern Calif., p. 59).

Still farther west, the fault is concealed beneath the unbroken alluvium and older Quaternary gravels of Yucaipa Valley and Redlands Heights, but the thick section of San Timoteo beds exposed 3 miles southeast of Redlands is almost assuredly faulted against the crystalline rocks that crop out less than 1 mile north. This suggests that the Banning fault may continue westward beneath Redlands to the San Jacinto fault zone. Recent work by English (1953, M. S. thesis, Claremont College), and Sprotte (1949), indicating as much as 11 miles of post-Pliocene right-lateral displacement on the San Jacinto fault, leads to the speculation that the Banning fault may be the offset segment of one of the prominent east-west faults of the San Gabriel Mountains.

North of Banning the Heights fanglomerate has not been displaced by the Banning fault, but the fault is exposed in rocks beneath the fanglomerate in several of the canyons (Pl. 2). The difference in thickness of the overlying fanglomerate north and south of the break suggests that a fault scarp existed at the time of fanglomerate deposition. The relatively straight course of the fault in this area is indicative of steep dip of the fault plane.

Two main breaks mark the trace of the Banning fault between Millard and Stubby canyons (Pl. 3). In general, crystalline rocks have been thrust over Tertiary sedimentary rocks along the northern break, and the Tertiary rocks in turn have been faulted against Quaternary Cabezon fanglomerate along the southern break. The greater degree of similarity in rock types across the southern branch suggests that most of the movement on the Banning fault took place on the northern break. The plane of the northern break, which is well exposed in most of the canyons that cross it, shows a general flattening eastward and locally becomes horizontal in the region of Stubby Canyon. The attitudes of the southern branch are grossly similar to those of the northern branch, but dips are steeper.

Abrupt variations in the attitude of the fault plane, which even dips south at the head of Second Canyon, suggest that it has been folded locally. Early movements on the fault may have taken place before it was deformed; possibly it was then vertical. That the Recent movements have been thrusts, however, is indicated not only by the seismic evidence (Dehlinger, 1952) but also by the displacement of horizontal Heights fanglomerate at the head of the West Branch of Lion Canyon by a thrust fault that dips 38° north. A normal fault displaces both Recent alluvium and one of the older thrusts at the mouth of Stubby Canyon, but this faulting appears to be a local adjustment that is not typical of the breaks along the mountain front.

East of Cottonwood Canyon an abrupt change in topographic expression is associated with the faulting. Not only is there no evidence of low-angle thrusting, but the fault trace is marked by a longitudinal valley suggestive of rift topography. Where next exposed, 1 mile west of Whitewater, the fault dips 65° north and appears to be a single break. Throughgoing Recent scarps, whose topographic expression indicates relatively steep dip of the fault plane, begin to appear not far east of Cottonwood Canyon. These same scarps do not extend westward into the thrust zone between Cottonwood and Stubby canyons, however, and it thus seems that the Banning fault changes from a flat thrust to a high-angle reverse fault within less than 3 miles.

East of Whitewater River, topographic expression of the Banning fault suggests that it is nearly vertical. From Painted Hill eastward into Seven Palms Valley and Coachella Valley, the fault is marked by subtle changes in vegetation that reflect differences in ground-water levels on the two sides of the fault (Pl. 6). Although it is nearly an east-west break at Whitewater, the Banning fault curves southward and trends S. 60°E. where it extends into the Indio Hills 15 miles to the southeast. This is the same trend as that of the San Andreas fault in the Transverse Ranges northwest of San Gorgonio Pass.

DISPLACEMENT: The various lines of evidence of displacement on the Banning fault are:

(1) The length and continuity of its trace suggest that the fault is a major tectonic feature of Southern California and possibly one of large displacement.

(2) Throughout the pass area, the fault is characterized by a zone of crushed rock thicker than similar zones along the San Andreas fault in the same general area. This zone, which is light green, reaches thicknesses of several thousand feet.

(3) The existence of San Gorgonio Pass suggests large vertical displacement on the Banning fault. Further evidence of a vertical component of movement is provided by records of a well drilled in 1926 less than 1 mile south of the probable trace of the fault in Yucaipa Valley; this well bottomed at 5358 feet while still in Tertiary(?) sedimentary rocks (Oakeshott *et al.*, 1952, p. 32), yet no Tertiary rocks crop out north of the fault in this area.

(4) Stream offsets indicative of Recent lateral displacement are absent along the trace of the fault in San Gorgonio Pass. Although most of the streams draining the north side of the pass debouch onto alluvial fans and therefore might not be expected to show lateral

offsets, the entrenched canyon of Whitewater River should be displaced if this type of Recent movement had been large. However, several lines of evidence point to an earlier history of strike-slip movement on the Banning fault: Tertiary beds south of Painted Hill have been dragged along the fault in a manner suggestive of right-lateral displacement; pebbles derived from the Painted Hill Formation have been dragged eastward along the fault plane between the heads of Second and Third canyons; the occurrence of piedmontite-bearing clasts within the San Timoteo Formation near Banning is most reasonably explained by approximately 5 miles of post-San Timoteo right-lateral displacement on the Banning fault, although logical arguments could be made for greater displacement or for none at all.

(5) The crystalline rocks north and south of the Banning fault, underlying San Gorgonio and San Jacinto peaks, respectively, appear to be of different types. Whereas this discontinuity might be explained by large pre-Pliocene lateral displacement on the Banning fault, there is no known locality where the "fit" across this east-west shear zone is any better than it is now. The discontinuity of rock types may have been caused by displacement on the fault, but it is also possible that the Banning fault is here because of a natural zone of weakness between two geologic units.

SUMMARY: The Banning fault is a major east-west tectonic feature of Southern California and forms the southern limit of the Transverse Ranges in the area of San Gorgonio Pass. Thrust and reverse movements of many thousands of feet have taken place in Quaternary time, although Recent (post-Heights) displacement is restricted to the portion of the fault that lies east of Millard Canyon. There is little evidence of Recent strike-slip movement in the San Gorgonio Pass area, but earlier lateral movements are strongly suggested; the geographic positions of clasts in the San Timoteo(?) Formation are best explained by a post-San Timoteo(?), pre-Heights right-lateral displacement of about 5 miles. Post-early Pliocene lateral displacement is probably no greater than 10 miles. Pre-Pliocene lateral displacement on the Banning fault may have been great, but it is not demanded by known geologic relations in this area.

Mission Creek Fault

NOMENCLATURE AND PREVIOUS WORK: The Mission Creek fault was named and first described by Vaughan (1922, p. 401–403) on the basis of exposures near the mouth of Mission Creek. Partly because of inadequate topographic base maps, it has been incorrectly assumed that this fault is continuous with the prominent fault that is marked by the straight canyons of Mill Creek and the North Fork of Whitewater River (Pl. 1). The present study indicates that the Mission Creek fault extends west from the mouth of Mission Creek along the South Fork of Whitewater River and thence veers southward to join the San Andreas fault in San Gorgonio Canyon north of Banning. The western part of this redefined Mission Creek fault corresponds to the Raywood fault of R. T. Hill (1928, p. 147, 162). The more northerly fault marked by the course of Mill Creek is herein renamed the Mill Creek fault.

FEATURES OF THE FAULT TRACE: The trace of the Mission Creek fault is delineated by the deeply dissected and linear branches of San Gorgonio and Whitewater canyons. The best exposures of the fault zone are in the gorge of the South Fork of Whitewater River, 1 mile east of Raywood Flat; here the fault zone dips 45° north and is characterized by a thickness of pulverized rock exceeding a quarter of a mile. One mile northeast of the junction of the North and South forks of Whitewater River, several distinct fault slices are present in the fractured zone. Sedimentary rocks, tentatively assigned to the deformed gravels of Whitewater River, form the northernmost wedge; the remaining rocks comprise dark crushed amphibolite, and Miocene(?) basalt intruded and subsequently crushed along the fault zone.

The prominent scarp along the fault north and west of Kitchen Ranch probably is in large part a fault-line scarp, inasmuch as a surface of low relief that truncates the crystalline rocks north of the fault seemingly is correlative with the dissected Cabezon surface at nearly the same altitude on the south. Southeast of Kitchen Ranch, beyond the area mapped in this study, the Mission Creek fault curves gradually southward and is marked by Recent scarps from Desert Hot Springs to its junction with the Banning fault near Biskra Palms

(Fig. 1) (Dibblee, 1954). This region has been the center of considerable seismic activity, and a 1948 earthquake of magnitude 6½ near Desert Hot Springs is of particular interest (Richter, Allen, and Nordquist, 1956). The main shock and most of the numerous aftershocks were concentrated in a zone 18 km long, parallel to the fault trace but 5 km north of it. Their distribution suggests that the north dip characteristic of the fault plane in the San Bernardino Mountains continues southeast. First motions at near-by seismograph stations indicated a combination of right-lateral and thrust displacement, which is compatible with the idea of stresses of the San Andreas type applied to a fault plane of this orientation.

DISPLACEMENT: The covering of unbroken Cabezon(?) fanglomerate at Raywood Flat indicates the absence of Recent movement here. Alluvial scarps near Desert Hot Springs, however, testify to increased Recent activity toward the east. The relatively gentle dip of the fault plane in the central part of the map area is not suggestive of contemporary strike-slip movement, nor is the abutment of this fault into the San Andreas fault. However, the fault may have had a different configuration at the time of earlier movements. The nature and distribution of crystalline rock types on opposite sides of the fault does not suggest large lateral displacement. But neither is such movement precluded, in view of the widespread occurrence of rocks of this type throughout Southern California.

AGE: Basalt flows are interlayered with the upper Miocene(?) Coachella fanglomerate near the mouth of Mission Creek. These flows increase in number and thickness toward the fault, and the basalt evidently was extruded along the fault zone. Crushed basalt dikes are present within the fault zone near Whitewater River. Thus the Mission Creek fault must have existed as a throughgoing break in late Miocene(?) time.

Pinto Mountain(?) Fault

NOMENCLATURE AND PREVIOUS WORK: Along the north side of the Little San Bernardino and Pinto mountains (Fig. 1), east of the area mapped in this study, is a prominent east-west lineament that probably marks a major fault. This break was first recognized by R. T. Hill (1928, p. 146), who named it the Pinto Mountain fault. Later investigators have termed it the Pinto fault (Miller, 1938, p. 419), the Warrens Well fault (Hill and Dibblee, 1953, p. 453), and the Base Line fault (Hewett, 1955), but R. T. Hill's original name is used herein.

FEATURES OF THE FAULT TRACE: As followed westward from its presumed type locality in the Twentynine Palms area (Pl. 6), the Pinto Mountain fault veers southward and probably extends into Morongo Valley at the summit of the highway grade between Morongo and Yucca valleys. Lack of geologic mapping in this critical area raises some question concerning use of the name farther west, but field reconnaissance and study of air photographs strongly suggest continuity of this fault along the northwest side of Morongo Valley into Big Morongo Canyon (Pl. 6). Most previous maps represent the fault as turning more abruptly southward and following the southeast side of Morongo Valley to join the Mission Creek fault at a high angle near Kitchen Ranch.

Near the mouth of Big Morongo Canyon, the Pinto Mountain(?) fault is marked by prominent scarps and springs, and ground water is dammed by the fault where the canyon turns abruptly north 2 miles from its mouth. Within the area of Plate 1, the fault is marked primarily by aligned stream courses that reflect erosion in the crushed rocks along the fault trace. The greenish crushed rocks are exposed near the points where the fault is crossed by Mission Creek and the North Fork of Whitewater River. Near the junction of the North and South forks of Whitewater River, the Pinto Mountain(?) fault merges with the Mission Creek fault at a low angle. Nowhere is the attitude of the fault plane discernible, although the relatively straight course of its trace across rugged topography suggests a steep dip.

DISPLACEMENT: Within the map area, Recent movements have been minor; ground water is not affected by the fault in either Mission Creek or Whitewater River. Just east of the map area, however, Recent scarps indicate upward movement of the south block. There is no direct evidence for lateral displacement along the fault, but this type of movement is made plausible by evidence of a varying vertical component of movement, and by the exceptionally uniform trend of the fault trace.

The crystalline rocks north and south of the fault are similar migmatitic types, which does not suggest large lateral displacement.

TECTONIC SIGNIFICANCE: It is noteworthy that the Pinto Mountain(?) and associated faults have a pattern remarkably similar to that of the Garlock-San Andreas system, as has been pointed out by Hill and Dibblee (1953, p. 453), and conclusions concerning that better-known system may prove applicable to the Pinto Mountain(?)-Mission Creek-San Andreas fault system as well. Both systems are associated with major changes in trend of the San Andreas fault zone.

Of particular regional tectonic significance is the fact that the eastern part of the Pinto Mountain fault marks the southward termination of the northwestward trending faults of the Mojave Desert (Fig. 1) (Hewett, 1955). As was pointed out by R. T. Hill (1928), this east-west lineament and at least two similar fault lines south of it may represent a continuation of Transverse Range structure eastward from the San Gabriel and San Bernardino mountains. This zone now appears to be breaking up along northwestward-trending faults of the San Andreas system, and the entire east-west zone possibly has been offset somewhat by right-lateral movements on these younger faults.

Mill Creek Fault

NOMENCLATURE AND PREVIOUS WORK: The name Mill Creek fault is applied herein to the prominent fault that has determined the courses of Mill Creek and the eastward-trending segment of the North Fork of Whitewater River (Pls. 1, 6). The name originally was used by R. T. Hill (1928, p. 162–163), who applied it to the break that previously had been described by Vaughan (1922, p. 401–403) as the Mission Creek fault. The present study indicates that both investigators were mistaken in their conception of a single fracture linking Mill Creek with the mouth of Mission Creek.

FEATURES OF THE FAULT TRACE: Near the mouth of Waterman Canyon north of San Bernardino, the Mill Creek fault diverges from the San Andreas fault at a low angle, and its trace is marked by Recent scarps as far east as City Creek. Physiographic features testify to continuity of the fault to Mill Creek, where it forms the northern boundary of the Potato sandstone fault block. For 10 miles farther east the straight incised valley of Mill Creek has been determined by the fault, and rapid erosion of the main canyon has left the valleys of Falls, Vivian, and High creeks hanging 1000 feet above the floor of the main canyon. A cross section of the fault zone is well exposed at the head of Mill Creek, 3 miles east of Fallsvale, where the zone of greenish and purplish crushed rock is several hundred feet thick and dips 60° south.

Rapidly progressing excavation by the headwaters of Mill Creek and a tributary of Whitewater River has carved giant amphitheaters into the relatively flat and gravel-covered area north of Raywood Flat. These spectacular features locally have been termed jump-offs because of the great topographic contrast at their rims (Pl. 6).

The eastward-trending segment of the canyon of the North Fork of Whitewater River is analogous to the valley of Mill Creek; rapid erosion of the main canyon has caused development of spectacular falls where it is joined by Hell-for-sure Creek and the headwaters of the North Fork. During normal stream flow, practically all the water contributory to the North Fork comes over the falls from the high country to the north; during floods, most of the water must come down the normally drier canyon from Whitewater Jump-off.

Near the junction of Hell-for-sure Canyon and the North Fork of Whitewater River, the Mill Creek fault appears to fray out and end. It is possible that the fault extends eastward to the Pinto fault and has been offset by it. If this is true, this easternmost segment is not characterized by the thick zone of greenish crushed rock typical of exposures farther west.

DISPLACEMENT: Both pure strike-slip and pure dip-slip movement are indicated by two sets of slickensides at Mill Creek Jump-off, but the time relationship of the two movements is not determinable. If this fault dies out to the east, strike-slip movement cannot have exceeded a few miles. The consistently greater height of the San Bernardino Mountains north of the Mill Creek fault suggests gross uplift of the north block.

Folding

Pliocene sedimentary rocks on the floor of San Gorgonio Pass show intense folding, whereas the early Quaternary rocks are only gently folded, and the youngest dissected Quaternary fanglomerates are virtually undeformed. Near the Banning fault, fold axes trend eastward and reflect north-south compression. The most intense folds are in the areas of low-angle thrusting, and these folds probably are drag features resulting directly from vertical movements on the Banning fault. The configuration of the Cabezon surface gives abundant evidence of large-scale Quaternary warping. The anomalous radial drainage pattern of Beacon Hill (Pl. 1), together with the quaquaversal dips of both the underlying fanglomerate and the semi-concordant capping of weathered material, indicate that folding probably is taking place here at the present time.

Mechanics of the Banning-San Andreas Fault System

Right-lateral displacement has taken place on faults both northwest and southeast of San Gorgonio Pass, as established not only from geodetic observations (Meade, 1948; Whitten, 1948) but also from study of the earthquake displacements of 1857 in Tejon Pass (Wood, 1955) and 1940 in Imperial Valley (Ulrich 1941). Some component of this strike-slip strain probably continues into San Gorgonio Pass along the San Andreas fault from the northwest and along the Banning fault from the southeast. What, then, is the structural significance of an eastward-trending thrust fault within the pass?

A possible answer is found in the structural analysis elucidated by Anderson (1951, p. 7–21). Utilizing Mohr's theory of failure, Anderson relates normal, thrust, and wrench (strike-slip) faults to the three possible orientations of the maximum and minimum principal stresses, assuming that one of the principal stresses is vertical. Of particular interest is the situation in which the intermediate and maximum principal stresses are nearly equal. If, for example, the intermediate stress should locally exceed the maximum stress and become the new maximum stress, a different type of faulting would result despite the fact that the over-all stress system had changed only slightly. Anderson (1951, p. 20) used this type of analysis to demonstrate the possible close relationship of thrust and strike-slip faulting, and the fault pattern of San Gorgonio Pass may be an example of such a situation. If the maximum principal stress were in a generally north-south direction and the minimum stress oriented east-west, strike-slip faulting of the San Andreas type would result when the stress differential became sufficiently large (Fig. 3). If the east-west least stress were of almost the same magnitude as the vertical intermediate stress, a slight local increase in the east-west compression could cause a sudden change from northwestward-trending strike-slip faulting to thrusting along east-west faults.

The above argument assumes perfect homogeneity of the rocks, but possibly recently established lines of faulting in San Gorgonio Pass are controlled as much by previously existing zones of weakness as by variations in the regional stress pattern. It seems likely that the northwestward-trending faults are relatively recent features transecting a zone of much older east-west breaks and that within the pass the recent movement has been "deflected" along the older east-west Banning fault, somewhat as Seigel (1950, p. 615–618) postulated. The limiting of Recent activity to the eastern portion of the Banning fault tends to support this hypothesis. An old, deep-seated, east-west shear zone, well defined by cataclastic metamorphism of the crystalline

PLATE 5.—SAN GORGONIO PASS

FIGURE 1.—San Gorgonio Pass and San Gorgonio Mountain. View north across San Gorgonio Pass from 7500-foot level on San Jacinto Peak. Most of this area is shown on the reconnaissance geologic map (Pl. 1).

FIGURE 2.—San Gorgonio Pass and San Jacinto Peak. Aerial view southeast from near Yucaipa. Banning and Cabazon lie on the floor of the pass, the summit of which is to the right off the photograph. The San Andreas fault enters the pass area through Potato Canyon (center foreground). Photograph by Fairchild Aerial Surveys, Inc.; diagramming by author.

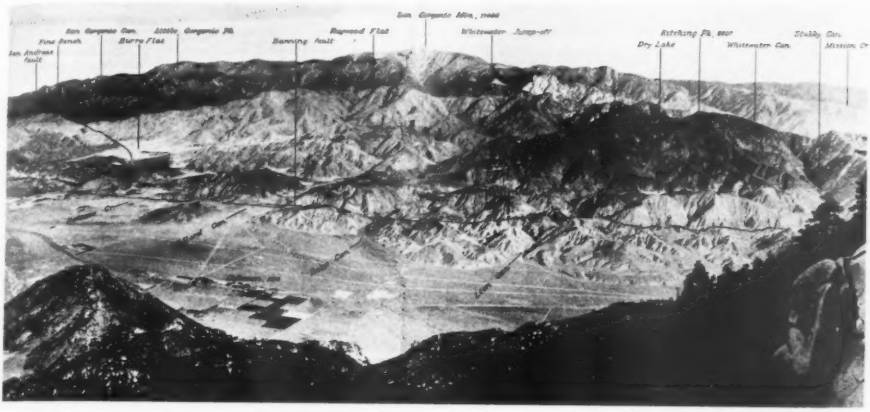

FIGURE 1

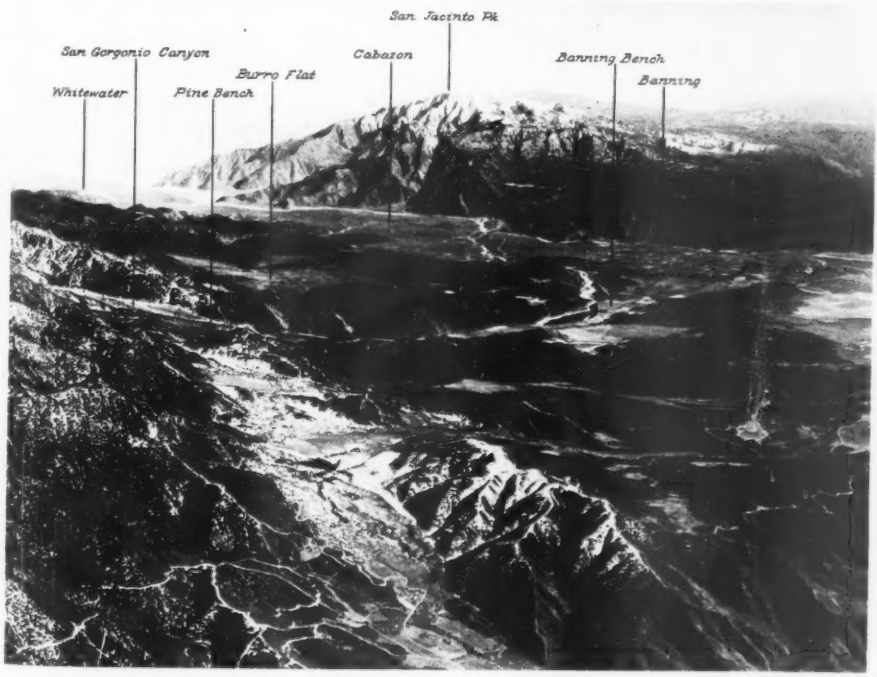

FIGURE 2

SAN GORGONIO PASS

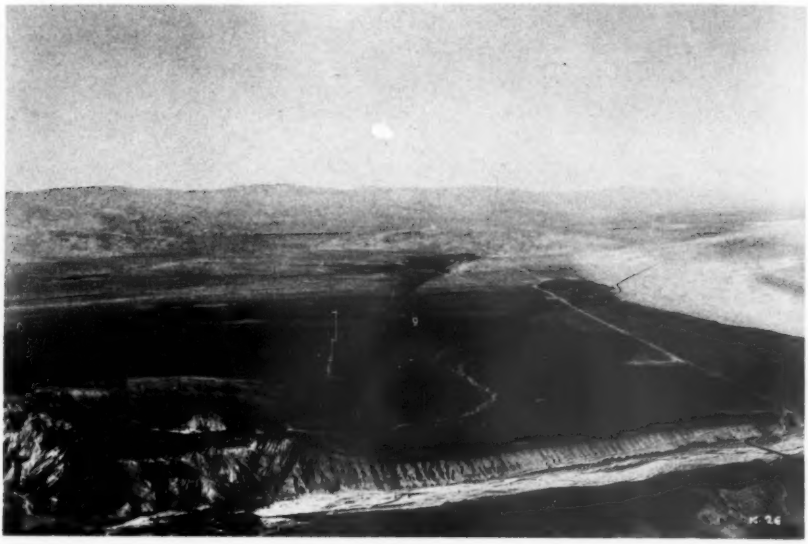

FIGURE 1

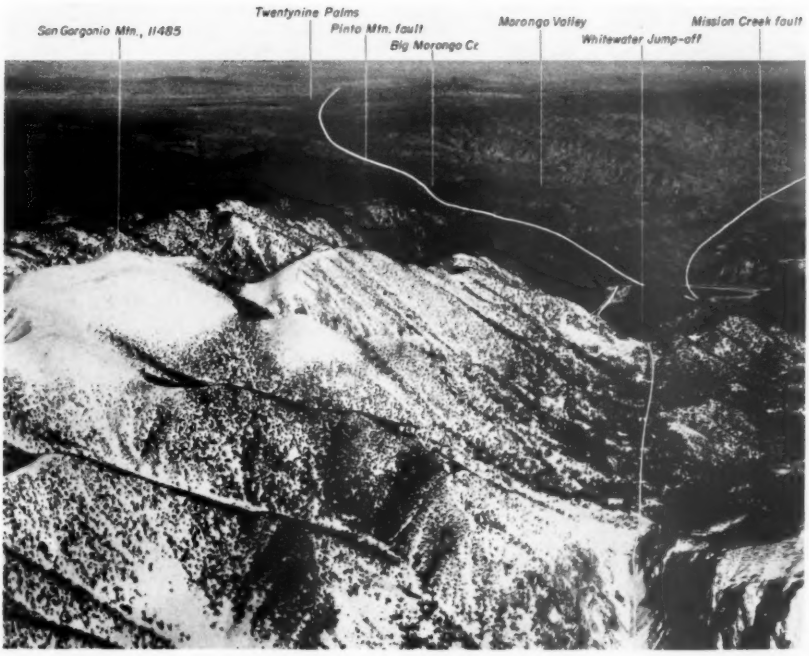

FIGURE 2

FEATURES OF FAULTING

complex, exists in the foothills along the north side of the pass. Such an east-west zone of weakness would seem to favor eastward-trending thrust faults over northwestward-trending lateral faults. In a manner analogous to variations in the principal stresses, a very small difference in rock strength could cause an abrupt change in the type of faulting, as is observed in the pass area.

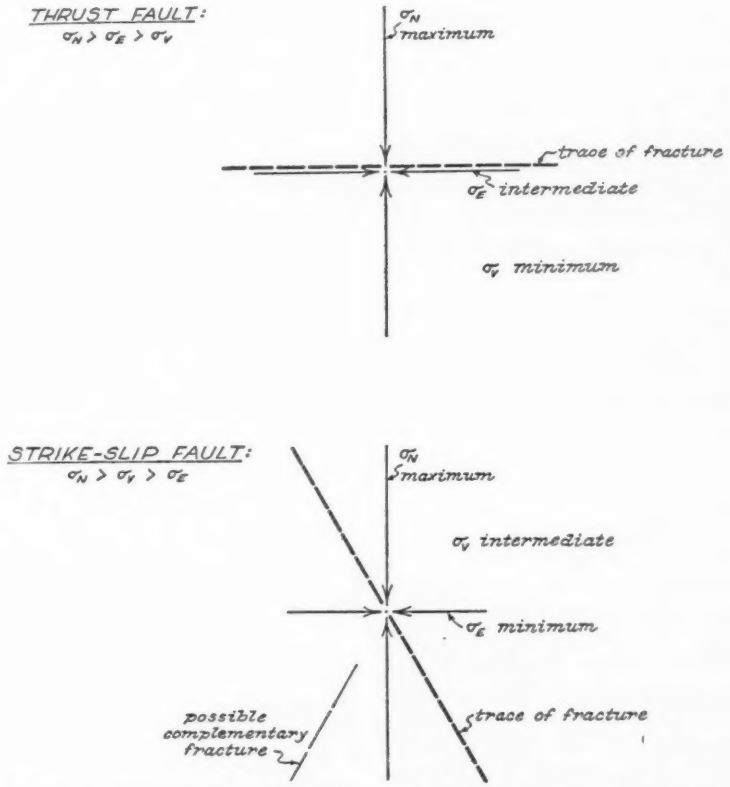

FIGURE 3.—PRINCIPAL STRESS RELATIONSHIPS NECESSARY TO CAUSE THRUST AND STRIKE-SLIP FAULTING

If the east-west and vertical stresses (σ_E and σ_V) are nearly equal, a very slight relative change in these stresses could cause a reversion from strike-slip to thrust faulting and vice versa.

In summary, Recent movements on both the Banning and San Andreas faults probably have been caused by an over-all stress system in-

PLATE 6.—FEATURES OF FAULTING

FIGURE 1.—Banning fault. Aerial view east from near Whitewater. Ground water is dammed by the fault where it is crossed by Whitewater River (lower left). Similarly, in Seven Palms Valley (center of photo) the fault trace is marked by changes in vegetation that reflect differences in ground-water levels on the two sides of the fault.

FIGURE 2.—Mill Creek, Mission Creek, and Pinto Mountain faults. Aerial view east from near the summit of San Gorgonio Mountain. Mill Creek Jump-off and the trace of the Mill Creek fault are shown at lower right. Photograph by Fairchild Aerial Surveys, Inc.; diagramming by author.

volving a general north-south maximum stress with an east-west stress only slightly less than the vertical stress. In the vicinity of the pass, the older east-west line of weakness has caused the east-west stress effectively to become the intermediate stress, and thrust faulting along eastward-trending fault lines hence has predominated over a strike-slip faulting in this one local area. Where the San Andreas fault cuts across all previous structure elsewhere, the east-west principal stress either has been much less than the vertical stress, or the zones of weakness in the older adjoining rocks have been of insufficient continuity to modify the regional stress pattern.

The Problem of Large Lateral Displacement

Hill and Dibblee (1953) recently suggested that right-lateral displacement on the San Andreas fault zone perhaps has totaled 65 miles since upper Miocene time, 225 miles since Eocene time, and more than 350 miles since Jurassic time. Are such lateral displacements compatible with structural relations within San Gorgonio Pass?

The results of the present study neither prove nor disprove the existence of large lateral displacement along the San Andreas fault zone as a whole. They do suggest that certain faults within the zone are more likely to have had large movements than others, and they emphasize that if large lateral movements have taken place, they must have been followed by deformation and disruption of the fault traces then existent. Even lateral movements of 1 or 2 miles are difficult to reconcile with the complex surface geometry of faults within the pass area; the San Andreas fault appears to butt into the Banning fault and die out, the Mission Creek fault does not form a smooth curve with the San Andreas fault, and the Mill Creek fault probably dies out eastward. Thus, lateral strain—large or small—has been transmitted through this region by three principal mechanisms:

(1) During periods of pre-Quaternary movements, the surface geometry of faults in the pass area probably differed from that of the present time, so that, for instance, the Mission Creek fault may then have been aligned with the San Andreas fault to absorb more easily the lateral strain.

(2) Much of the shear strain along the San Andreas fault has been relieved by fraying out into major branches, at least four of which diverge eastward from the northern side of the fault between Cajon Pass and San Gorgonio Pass (Bailey and Jahns, 1954, Pl. 4). On the south side, the San Jacinto fault may have absorbed much of the regional strain; it is straighter, more continuous, and shows greater seismic activity than any faults of the San Gorgonio Pass area.

(3) Lateral strain has been relieved to some extent by thrusting on east-west faults in the San Gorgonio Pass area.

The Banning fault is different from other faults in the pass area, in that it separates very different crystalline rock types. Although Recent movements on this fault have been small and mainly vertical, pre-Pliocene lateral displacements may have been large. In this area, the Banning fault may represent the "ancestral" San Andreas fault which is now deformed into a Transverse Range fault. No evidence within San Gorgonio Pass, however, demands large pre-Pliocene displacement on the Banning fault.

The deformation and disruption of former breaks appear to represent a tectonic pattern that is typical of the entire eastern half of the Transverse Range Province, where elements of San Andreas and Transverse Range structure in effect have been vying for control; evidently one set has alternated with the other in attaining temporary dominance. To reconstruct the history of San Andreas movement through this region remains a large and challenging project, and possibly the present study has contributed more to pointing up the problem than to supplying satisfactory answers.

In view of the increasing evidence of complexity of strike-slip faulting within and south of the Transverse Ranges of Southern California, the writer feels that the entire zone between the Elsinore fault and the eastern side of the Salton depression properly could be regarded as the San Andreas fault zone. No convincing evidence yet exists that any particular fault within the 50-mile-wide zone deserves the parent name.

Origin of San Gorgonio Pass

There can be little doubt that faulting is the ultimate cause of the feature known as San Gorgonio Pass, but fundamental questions remain. To what degree is the present configuration of the pass attributable to erosion in the fault zone rather than to actual fault movement, and why should such a deep gash occur between two of the highest mountains in Southern California?

The Banning fault is the logical northern boundary of the pass. The slopes of San Jacinto Peak form the south wall (Pl. 5), but except for this precipitous scarp itself there is no surficial evidence of Recent faulting south of the Banning fault. One might argue, therefore, that the pass is caused primarily by erosion in a wide zone of crushed rock and is not the direct result of movement along bounding faults. Certainly the many dissected benches and terraces on both sides of San Gorgonio Pass testify to the removal of great amounts of material in Recent time, and upwarping probably has caused removal of material from the floor of the pass. On the other hand, it is difficult to explain the presence of fine-grained Pliocene marine beds in the deepest and most rugged part of the pass if a predominantly erosional origin is postulated; these beds must be preserved in a relatively depressed fault block. Their present maximum elevation of 2500 feet reflects post-early Pliocene uplift, perhaps by gentle arching along north-south axis through the mountains in a manner suggested by Sharp (1954, p. 8). But still greater uplift along bounding faults must have taken place in the adjacent crystalline rocks.

A major break parallel to the Banning fault must lie beneath the alluvium at the base of the San Jacinto scarp near Cabazon. This fault must have displacement of the hinge type dying out westward, as indicated not only by the physiography of the mountains but also by the demonstrated absence of such a break farther west near Beaumont. San Gorgonio Pass appears, then, to be of composite origin, with faulting on the north and south predominant in its physiographic development.

The Banning fault is a reverse fault, and therefore its hypothetical analogue across the pass to the south also is probably a reverse fault. Thus San Gorgonio Pass probably is a graben bounded by reverse faults. Although this type of structure ordinarily has been considered unusual or questionable (Billings, 1954, p. 203), other Southern California valleys bordered by reverse or thrust faults are known within the Transverse Ranges (Reed and Hollister, 1936, p. 101–104; Bailey and Jahns, 1954). If the faults bordering San Gorgonio Pass are typical of others in the Transverse Ranges, the fault planes steepen with depth.

That such a deep gash as San Gorgonio Pass should separate two of the highest mountain peaks of Southern California is remarkable. It is more reasonable to assume that the mountains have reached their present heights because of faulting in the pass than that the pass is a down-faulted block transecting a formerly continuous high mountain range. The mechanics of the Banning-San Andreas fault system suggest that reverse and thrust faulting in the pass area have been caused by local "deflection" of the San Andreas type of strain along an older east-west line of weakness. Thus, local conversion of strike-slip strain into vertical displacements along the bounding faults of San Gorgonio Pass is a reasonable explanation of both the pass and the unusually high peaks adjacent to it.

References Cited

Anderson, E. M., 1951, The dynamics of faulting and dyke formation with applications to Britain, 2d ed.: London, Oliver and Boyd, 206 p.

Axelrod, D. I., 1937, A Pliocene flora from the Mt. Eden beds, Southern California: Carnegie Inst. Washington Pub. 476, p. 125–184

—— 1950, Further studies of the Mt. Eden flora, Southern California: Carnegie Inst. Washington Pub. 590, p. 73–118

Bailey, T. L., and Jahns, R. H., 1954, Geology of the Transverse Range province, Southern California, p. 83–106 (pt. 2) *in* Jahns, R. H., *Editor*, Geology of Southern California: Calif. Div. Mines Bull. 170, 878 p.

Billings, M. P., 1954, Structural geology, 2d ed.: N. Y., Prentice Hall, 514 p.

Buwalda, J. P., and Stanton, W. L., 1930, Geological events in the history of the Indio Hills and the Salton basin, Southern California: Science, new ser., v. 71, p. 104–106

Crowell, J. C., 1952, Geology of the Lebec quadrangle, California: Calif. Div. Mines Spec. Rept. 24, 23 p.

Dehlinger, Peter, 1952, Shear-wave vibrational directions and related fault movements in

Southern California earthquakes: Seismol. Soc. America Bull., v. 42, p. 155–173

Dibblee, T. W., Jr., 1954, Geology of the Imperial Valley region, California, p. 21–28 (pt. 2) *in* Jahns, R. H., *Editor*, Geology of Southern California: Calif. Div. Mines Bull. 170, 878 p.

Durham, J. W., 1950, Megascopic paleontology and marine stratigraphy, p. 1–216 (pt. II) *in* Anderson, C. A., *et al.*, 1940, E. W. Scripps cruise to the Gulf of California: Geol. Soc. America Mem. 43

Eckis, Rollin, 1928, Alluvial fans of the Cucamonga district, Southern California: Jour. Geology, v. 36, p. 224–247

—— 1934, South coastal-basin investigation; Geology and ground-water storage capacity of valley fill: Calif. Dept. Public Works, Water Res. Div. Bull. 45, 279 p.

Fairbanks, H. W., and Carey, E. P., 1910, Glaciation in the San Bernardino range, California: Science, new ser., v. 31, p. 32–33

Fraser, D. M., 1931, Geology of the San Jacinto quadrangle south of San Gorgonio Pass: Calif. Div. Mines 27th Rept. of State Mineralogist, p. 494–540

Frick, Childs, 1921, Extinct vertebrate faunas from the badlands of Bautista Creek and San Timoteo Canyon, Southern California: Calif. Univ. Dept. Geol. Sci. Bull., v. 12, p. 277–424

Guillou, R. B., 1953, Geology of the Johnston Grade area, San Bernardino County, California: Calif. Div. Mines Spec. Rept. 31, 18 p.

Hamilton, E. L., 1944, Rainfall-measurement as influenced by storm-characteristics in Southern California mountains: Am. Geophys. Union Trans., v. 25, p. 502–518

Hewett, D. F., 1955, Structural features of the Mojave Desert region, p. 377–390 *in* Poldervaart, Arie, *Editor*, Crust of the earth: Geol. Soc. America Spec. Paper 62, 762 p.

Hewett, D. F., and Glass, J. J., 1953, Two uranium-bearing pegmatite bodies in San Bernardino County, California: Am. Mineralogist, v. 38, p. 1040–1050

Hill, M. L., and Dibblee, T. W., Jr., 1953, San Andreas, Garlock, and Big Pine faults, California: Geol. Soc. America Bull., v. 64, p. 443–458

Hill, R. T., 1928, Southern California geology and Los Angeles earthquakes: Los Angeles, S. Calif. Acad. Sci., 232 p.

Larsen, E. S., Jr., 1948, Batholith and associated rocks of Corona, Elsinore, and San Luis Rey quadrangles, Southern California: Geol. Soc. America Mem. 29, 182 p.

Lawson, A. C., *et al.*, 1908, The California earthquake of April 18, 1906: Carnegie Inst. Washington Pub. 87, v. 1, 451 p.

Meade, B. K., 1948, Earthquake investigation in the vicinity of El Centro, California: Am. Geophys. Union Trans., v. 29, p. 27–31

Miller, W. J., 1934, Geology of the western San Gabriel Mountains of California: Calif. Univ. at Los Angeles Pub. Math. and Phys. Sci., v. 1, p. 1–114

—— 1938, Pre-Cambrian and associated rocks near Twenty-nine Palms, California: Geol. Soc. America Bull., v. 49, p. 417–446

—— 1944, Geology of Palm Springs-Blythe strip, Riverside County, California: Calif. Jour. Mines and Geology, v. 40, p. 11–72

Murdoch, Joseph, and Webb, R. W., 1948, Minerals of California: Calif. Div. Mines Bull. 136, 402 p.

Noble, L. F., 1926, The San Andreas rift and some other active faults in the desert region of southeastern California: Carnegie Inst. Washington Year Book 25, p. 415–428

—— 1932, The San Andreas rift in the desert region of southeastern California: Carnegie Inst. Washington Year Book 31, p. 355–363

—— 1953, Geology of the Pearland quadrangle, California: U. S. Geol. Survey quadrangle maps of the U. S., Map GQ 24

—— 1954a, Geology of the Valyermo quadrangle and vicinity, California: U. S. Geol. Survey quadrangle maps of the U. S., Map GQ 50

—— 1954b, The San Andreas fault zone from Soledad Pass to Cajon Pass, California, p. 37–48 (pt. 4) *in* Jahns, R. H., *Editor*, Geology of Southern California: Calif. Div. Mines Bull. 170, 878 p.

Oakeshott, G. B., *et al.*, 1952, Exploratory wells drilled outside of oil and gas fields in California to December 31, 1950: Calif. Div. Mines Spec. Rept. 23, 77 p.

Reed, R. D., and Hollister, J. S., 1936, Structural evolution of Southern California: Tulsa, Am. Assoc. Petroleum Geologists, 157 p.

Richter, C. F., Allen, C. R., and Nordquist, J. M., 1956, Desert Hot Springs earthquake of December 4, 1948, and its aftershocks (Abstract): Geol. Soc. America Bull., v. 67, p. 1780

Russell, R. J., 1932, Land forms of San Gorgonio Pass, Southern California: Calif. Univ. Pub. in Geography, v. 6, p. 23–121

Seigel, H. O., 1950, A theory of fracture of materials and its application to geology: Am. Geophys. Union Trans., v. 31, p. 611–619

Sharp, R. P., 1954, Some physiographic aspects of Southern California, p. 5–10 (pt. 5) *in* Jahns, R. H., *Editor*, Geology of Southern California; Calif. Div. Mines Bull. 170, 878 p.

Sprotte, E. C., 1949, The San Andreas and San Jacinto rift zones: Sigma Gamma Epsilon, The Compass, v. 26, p. 315–319

Taliaferro, N. L., 1943, Geologic history and structure of the central Coast Ranges of California: Calif. Div. Mines Bull. 118, p. 119–163

Troxell, H. C., *et al.*, 1942, Floods of March 1938 in Southern California: U. S. Geol. Survey Water-Supply Paper 844, 399 p.

—— 1954, Hydrology of the San Bernardino and eastern San Gabriel Mountains, California: U. S. Geol. Survey Hydrol. Inv., Atlas HA 1

Turner, F. J., 1948, Mineralogical and structural evolution of the metamorphic rocks: Geol. Soc. America Mem. 30, 342 p.

Ulrich, F. P., 1941, The Imperial Valley earthquakes of 1940: Seismol. Soc. America Bull., v. 31, p. 13–31

Vaughan, F. E., 1922, Geology of the San Bernardino Mountains north of San Gorgonio Pass: Calif. Univ. Dept. Geol. Sci. Bull., v. 13, p. 319–411

Wallace, R. E., 1949, Structure of a portion of the San Andreas rift in Southern California: Geol. Soc. America Bull., v. 60, p. 781–806

Webb, R. W., 1939, Evidence of the age of a crystalline limestone in Southern California: Jour. Geology, v. 47, p. 198–201

Whitten, C. A., 1948, Horizontal earth movement,

vicinity of San Francisco, California: Am. Geophys. Union Trans., v. 29, p. 318–323

Willis, Bailey, 1938, San Andreas rift, California: Jour. Geology, v. 46, p. 793–827

Wilson, I. F., 1948, Buried topography, initial structures, and sedimentation in Santa Rosalia area, Baja California, Mexico: Am. Assoc. Petroleum Geologists Bull., v. 32, p. 1762–1807

Wood, H. O., 1955, The 1857 earthquake in California: Seismol. Soc. America Bull., v. 45, p. 47–67

Wood, H. O., and Heck, N. H., 1951, Earthquake history of the United States: Part II, Stronger earthquakes of California and western Nevada: U. S. Coast Geod. Survey Serial 609, 35 p.

Woodford, A. O., and Harriss, T. F., 1928, Geology of Blackhawk Canyon, San Bernardino Mountains, California: Calif. Univ. Dept. Geol. Sci. Bull., v. 17, p. 265–304

Woodring, W. P., 1932, Distribution and age of the marine Tertiary deposits of the Colorado Desert: Carnegie Inst. Washington Pub. 418, p. 1–25

Division of the Geological Sciences, California Institute of Technology, Pasadena, California

Manuscript Received by the Secretary of the Society, August 9, 1956

Contribution No. 797, Division of the Geological Sciences, California Institute of Technology

BULLETIN OF THE GEOLOGICAL SOCIETY OF AMERICA
VOL. 68, PP. 351-358, 4 FIGS., 2 PLS. MARCH 1957

SOLUTION-SUBSIDENCE TROUGHS, CASTILE FORMATION OF GYPSUM PLAIN, TEXAS AND NEW MEXICO

BY WILDS W. OLIVE

ABSTRACT

Solution-subsidence troughs are straight narrow depressions ranging in width from a few hundred feet to 1 mile, and in length from about half a mile to 10 miles. The troughs are formed by subsidence of near-surface earth blocks to fill voids dissolved by underground waters moving along subjacent drainage channels parallel to the troughs. Numerous solution-subsidence troughs are developed in the Castile Formation (upper Permian) of the Gypsum Plain in west Texas and southeastern New Mexico where they characteristically have broad relatively flat bottoms, which occupy about two-thirds of the width of the trough. The bottoms are bounded by gentle slopes rising 15–20 feet to narrow straight divides, which stand 2 or 3 feet above the general level of the Gypsum Plain. The troughs trend roughly parallel to the direction of the regional dip, about 1°–2° eastward. Displacement and local folding in strata of the Castile formation in and near the troughs are not reflected in the Lamar limestone member of the Bell Canyon Formation (lower Permian), which conformably underlies the Castile. The trends of the underground channels are interpreted as the result of solution along eastward-trending joints parallel to the regional dip. Most of the water that causes the solution is believed to be derived by artesian flow from the mountainous area west of the Gypsum Plain.

CONTENTS

TEXT

	Page
Introduction	351
Acknowledgments	353
Stratigraphy of the Gypsum Plain	353
Structure of the Gypsum Plain	355
Origin of solution-subsidence troughs	356
Evolution of solution-subsidence troughs	356
Source of water which gives rise to solution-subsidence troughs	357
Anomalous areas of solution-subsidence trough development	358
References cited	358

ILLUSTRATIONS

Figure	Page
1. Block diagram showing an area of solution-subsidence development near the head of Castile Draw in west-central Gypsum Plain, Texas	352
2. Geographic and physiographic location of the Gypsum Plain and its position in the Delaware Basin	352
3. Map showing distribution of solution-subsidence troughs of the Gypsum Plain, Texas and New Mexico, and structural features in and near the Gypsum Plain	354
4. Cross section through Delaware Mountains, Gypsum Plain, and Rustler Hills, Texas	355

Plate	Facing page
1. Views of Gypsum Plain, Texas	356
2. Views of Gypsum Plain, Texas	357

INTRODUCTION

Solution-subsidence troughs (Fig. 1) are straight narrow shallow surface depressions formed by the collapse of rock into subterranean caverns. They resemble poljes in form (Cvijić, 1893) but differ in that they are not primarily tectonic in origin. The troughs are common in the Gypsum Plain (Fig. 2) of Culberson County, Texas, and Eddy County, New Mexico, where they are generally less than 20 feet deep, a few hundred feet to more than a mile wide, and a quarter of a mile to 10 miles long. Characteristically, they have relatively flat bottoms, which occupy about two-thirds of the

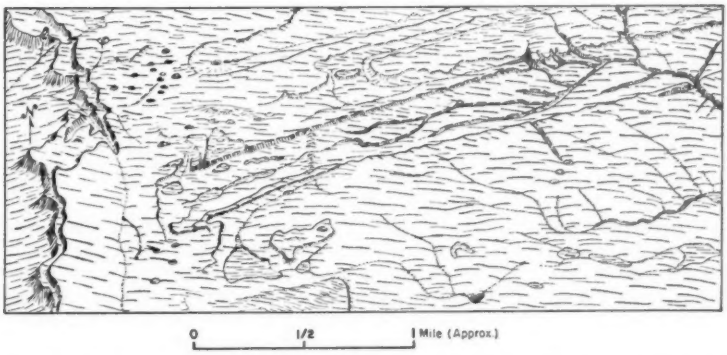

FIGURE 1.—BLOCK DIAGRAM SHOWING AN AREA OF SOLUTION-SUBSIDENCE DEVELOPMENT NEAR THE HEAD OF CASTILE DRAW IN WEST-CENTRAL GYPSUM PLAIN, TEXAS

Troughs are developed in the Castile Gypsum. Westward-facing scarp in left of view is developed on Bell Canyon formation. Sketched from a stereogram of aerial photographs. Photographs by courtesy of Edgar Tobin Aerial Survey.

FIGURE 2.—GEOGRAPHIC AND PHYSIOGRAPHIC LOCATION OF THE GYPSUM PLAIN AND ITS POSITION IN THE DELAWARE BASIN

width of the trough. The bottoms are bounded by moderate to gentle slopes (Fig. 1; Pl. 1, fig. 1; Pl. 2, fig. 1) that rise to narrow straight divides which stand 2 or 3 feet above levels adjacent to the trough. The low divides on either side of the trough are barriers which deflect much of the surface drainage away from the trough. Some solution-substance troughs are athwart streams which have incised narrow steep-walled valleys into the trough sides; a few contain streams whose drainage basins are within the area of trough development; others are sites where relatively large streams drain into open-bottomed sinks and thence into underground channels. Caverns, sinks (Fig. 1; Pl. 1, fig. 2), fissures, and small shallow undrained depressions, all of solution origin, are common in areas of trough development.

The Gypsum Plain in the western part of the Delaware Basin is an area of low relief about 7–25 miles wide and 55 miles long. It is bounded on the west by a gravel-surfaced plain at the foot of the reef escarpment and the Delaware Mountains and on the east by the Rustler Hills. It extends northward from the foot of the Apache Mountains to the vicinity of Carlsbad, New Mexico. The plain is crossed by shallow eastward-trending valleys and broad low divides. Scattered conical and circular hills rise 40–50 feet above the general surface level; open-bottomed sinks up to 30 feet deep, cracks, and shallow undrained depressions are common. The most striking features of the plain, however, are eastward- to northeastward-trending solution-subsidence troughs which are numerous in the west-central and northwestern parts (Fig. 3). They are absent in the southern part, except for a single trough about 8 miles north of the Apache Mountain front.

The region of which the Gypsum Plain is a part has a semiarid climate with an average annual precipitation of about 11–13 inches. However, the yearly rainfall varies widely from the average. According to a local inhabitant, no rain sufficient to cause runoff fell in the Gypsum Plain for about 4 years before April 1954. Numerous dead and dying junipers with trunks as much as 18 inches in diameter attested to the severity of the drought. However, during this prolonged drought water was observed in several sinks along the western margin of the plain.

Acknowledgments

The writer is grateful to the Gulf Oil Corporation for permission to publish this article. He also wishes to express his indebtedness to his colleagues, L. H. Lattman and B. A. Tator, who read and criticized the manuscript and gave valuable counsel and assistance.

Stratigraphy of the Gypsum Plain

The stratigraphy of the area of which the Gypsum Plain is a part is discussed by King (1942, p. 611–612), and the areal geology of the general area is shown on a map by King (1949). Figure 4 shows the stratigraphic sequence and general lithologies of rock units which crop out and underlie the western part of the Delaware Basin. The Gypsum Plain is developed along the outcrop of strata that are dominantly composed of gypsum or anhydrite. These rocks, which belong to the Castile Formation (Ochoa Series, upper Permian), are about 2000 feet thick near the eastern margin of the plain, but, because of post-Ochoan erosional truncation, they thin to the vanishing point at the western margin. The lower part of the formation is dominantly banded anhydrite which exhibits alternating light- and dull-gray bands a quarter of an inch to half an inch thick and contains several thin beds of petroliferous limestone which occur at widely spaced stratigraphic intervals. The upper half of the formation is almost exclusively massive banded anhydrite. Within the area of trough development the areal distribution of the section containing limestone coincides generally with the distribution of the troughs.

The Castile is conformably overlain by the Rustler limestone (Ochoan Series, upper Permian) which forms the cap rock of the Rustler Hills to the east and caps many of the circular hills which rise above the general level of the Gypsum Plain. Some hills are capped with massive Castile gypsum, and a few are capped with rubble composed of blocks of Rustler limestone and Cretaceous rocks. Strata of the Bell Canyon Formation (Guadalupe Series,

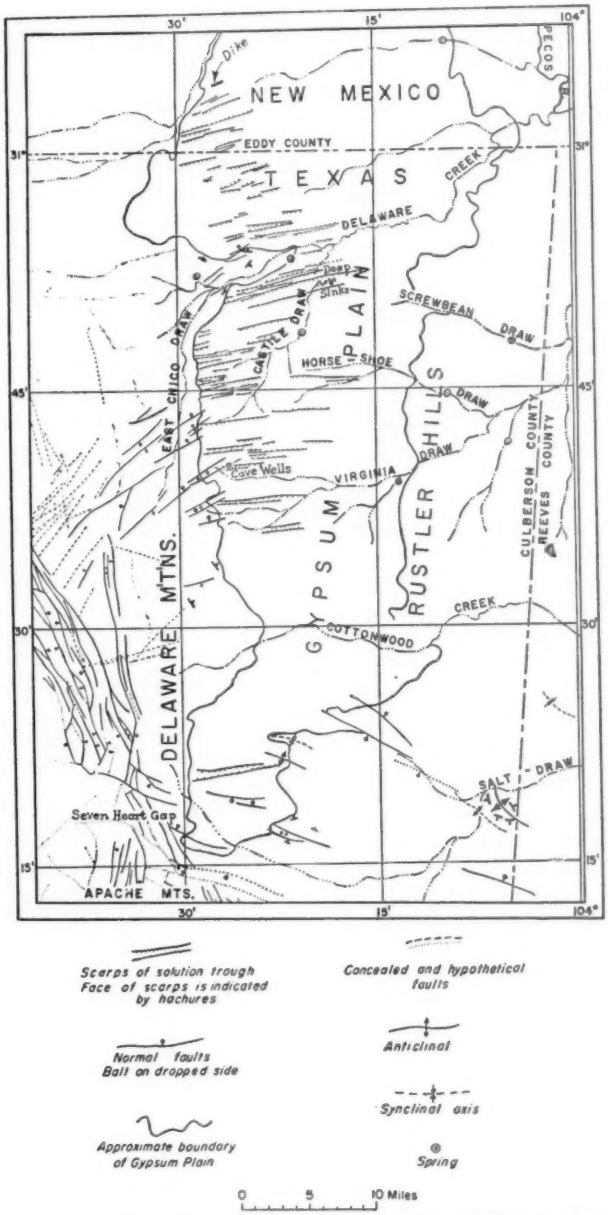

FIGURE 3.—MAP SHOWING DISTRIBUTION OF SOLUTION-SUBSIDENCE TROUGHS OF THE GYPSUM PLAIN, TEXAS AND NEW MEXICO, AND STRUCTURAL FEATURES IN AND NEAR THE GYPSUM PLAIN
After King (1949)

middle Permian) occur in normal stratigraphic sequence beneath the Castile formation and crop out in westward-facing scarps along the western margin of the Gypsum Plain. Rocks of the Bell Canyon constitute a section about 700 feet thick (King, 1942, p. 581) and are dominantly sandstone and minor amounts of limestone. The Lamar limestone, a widely used subsurface marker, caps the Bell Canyon Formation.

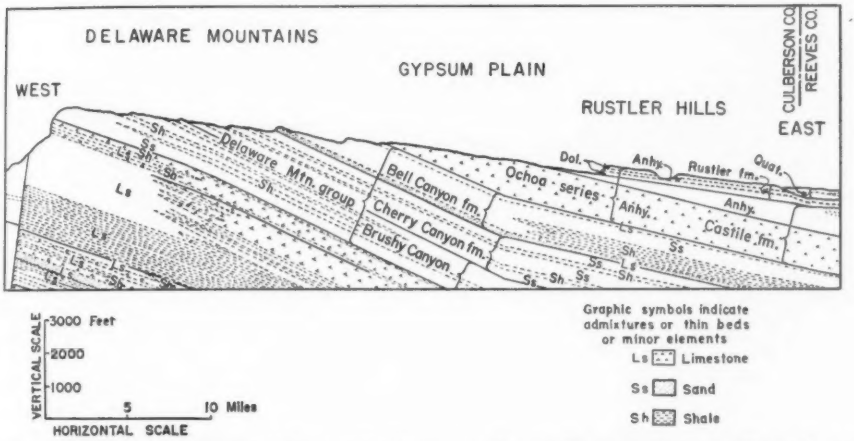

FIGURE 4.—CROSS SECTION THROUGH DELAWARE MOUNTAINS, GYPSUM PLAIN, AND RUSTLER HILLS, TEXAS
After West Texas Geological Society, Stratigraphic Problems Committee (1949).

STRUCTURE OF THE GYPSUM PLAIN

Because of the disoriented blocks and erratic dips in the Castile Formation, the structure of the Gypsum Plain can be interpreted from surface outcrops only in a general way. According to published structure maps (Haigh, 1951, Fig. 3; Stead, 1953, Fig. 2) contoured on top of the Lamar limestone, the strata beneath the Castile Formation dip rather uniformly 1°–2° eastward toward the axis of the Delaware Basin which is 50–60 miles east of the plain. The axis of a broad, eastward-plunging anticline, shown on the structure-contour maps, follows the eastward-trending course of the Delaware Creek in the northern part of the plain, and another follows the eastward-trending Cottonwood Creek in the southern part. A pronounced eastward-plunging synclinal downwarp occurs beneath the southern part of the plain at the foot of the Apache Mountains. King (1949) showed these broad features at the eastern and western margins of the plain by dip reversals and by curvatures in the outcrop patterns of formation contacts. King also plotted the positions of many normal faults along and near the western margin of the Gypsum Plain.

A well-developed joint system made up of northeastward- and northwestward-trending sets was observed at several localities along the outcrop of the Lamar limestone at the western margin of the Gypsum Plain, and at some of these localities a system of northward- and westward-trending sets was also found. King (1948, p. 90–91) described "superficial linear features" (scarps of solution-subsidence troughs) and stated that they "... probably resulted from differential erosion of cemented east-west fractures that have developed in the anhydrites of the Castile formation. The origin of the fractures is unknown, but they seem to be confined to the lower part of the Castile formation." King (1949) mapped the distribution of linear scarps (the sides of solution-subsidence troughs) and other linear features in the Gypsum Plain and referred to them in the map legend as "possible fracture zones".

Origin of Solution-Subsidence Troughs

The mode of origin of solution troughs was discovered from a photogeologic study of the Gypsum Plain and several days of field study. In an area of trough development in north-central Culberson County, Texas, about 1 mile south of the State line, an eastnortheastward-trending straight divide area, concave on top and bounded by outward-facing scarps (the sides of two adjacent troughs), is truncated at its western end by a northward-trending, westward-facing escarpment 40–50 feet high. The concave divide area is developed on a thin petroliferous limestone (Pl. 2, fig. 1), about 6 inches thick, in the lower part of the Castile Formation. The limestone dips inward at low angles toward the center of the concave divide area. The scarps and lower areas north and south of the divide are developed on anhydrite. The thin limestone, though not observed in the lower areas, probably is at shallow depth.

Numerous straight variously trending deep fissures, which are probably joints that have been widened by solution and subsidence, divide the outcropping rocks into a mosaic of blocks. These fissures, most of which are parallel to the concave divide area, are concealed in most places by an encrustation of secondarily deposited gypsum that forms low ridges 3–4 inches high. The depths of the fissures were not determined. At the foot of the northward-trending escarpment and directly beneath the concave divide area, a shallow eastnortheastward-trending depression about 50 yards long leads into a cavern (Pl. 2, fig. 2) which has a diameter of about 7 feet. The depression and the cavern have the same trend as the concave divide area above it. Tunnels, sinks, fissures, and undrained depressions, all formed by solution, occur at the foot of the westward-facing escarpment throughout its extent. These features mark sites where several eastward-flowing streams pass into underground drainage channels. (*See* Pl. 1, fig. 2.)

The writer concludes that the rock of the concave divide area is subsiding into the cavern beneath it, as indicated by the numerous deep fissures and the inward dips exhibited in the thin petroliferous limestone at the crest of the divide area. Tunnels, sinks, fissures, and undrained depressions at other localities along the base of the westward-facing escarpment indicate that solution is also active beneath the intermediate upland areas on either side of the divide. The lower elevations, with respect to the concave divide area, suggest that these areas have subsided more than the divide area. Further evidence that the troughs are the result of local subsidence is afforded by observations in the central part of the Gypsum Plain where several small outliers of Cretaceous (?) chert pebble conglomerate occur on the southward-facing scarp of a solution-subsidence trough. These outliers which are underlain by anhydrite of the Castile Formation are well below the rim of the trough and are probably preserved because they were lowered by solution subsidence to positions that protect them from erosion. One of these outliers is shown in Figure 1 of Plate 1.

Evolution of Solution-Subsidence Troughs

In the evolution of a trough the first step is the development along fractures (joints or faults) of straight underground drainage channels that closely parallel the dip direction.

Plate 1.—Views of Gypsum Plain, Texas

Figure 1.—View west along a southward-facing slope of the side of a solution-subsidence trough about 1 mile south of Horseshoe Draw, central Gypsum Plain, Texas. The slope rises gently from left to right. The low hill is composed of lower Cretaceous (?) chert-pebble conglomerate which rests on Castile gypsum (exposed in foreground).

Figure 2.—Aerial view of the gypsum Plain, Texas, near the Texas-New Mexico State line. Eastward-flowing streams drain into underground channels by way of sinks (dark circular areas) which are aligned at the foot of a north-northeastward-trending, westward-facing escarpment. The short dark band (indicated by arrow), upper right, is a narrow divide area between two solution-subsidence troughs. Ground views in this area are shown in Plate 2. The black line in lower right of view is approximately 2000 feet long. Photograph by courtesy of Edgar Tobin Aerial Survey.

FIGURE 1

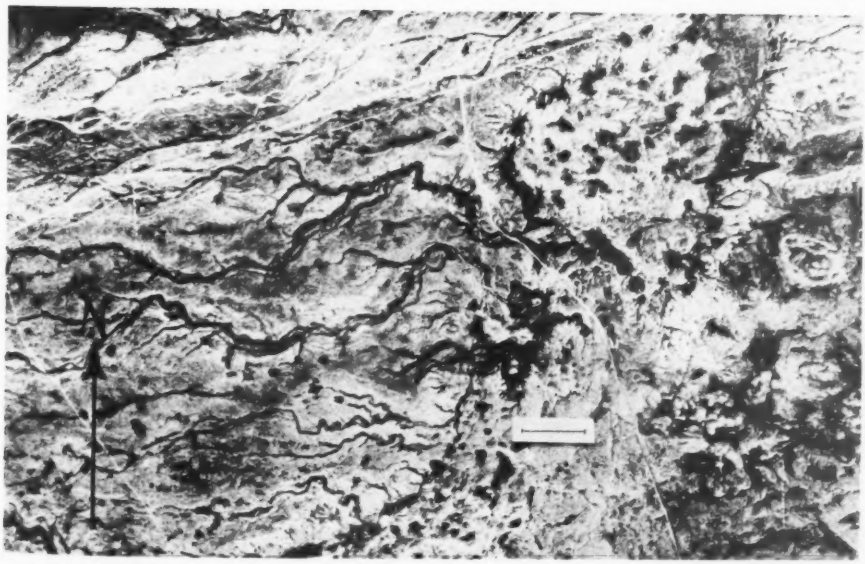

FIGURE 2

VIEWS OF GYPSUM PLAIN, TEXAS

FIGURE 1

FIGURE 2

VIEWS OF GYPSUM PLAIN, TEXAS

In the Gypsum Plain the controlling factors are eastward-trending joints of the poorly developed system. These joints determine positions of underground trunk streams, because they are parallel to the regional dip and afford the easiest avenues for underground movement. The solution effect of water moving along joints that parallel dip directions is discussed by Lattman and Olive (1955). Joints of other sets determine positions of underground tributaries.

When the channels cannot support their roofs collapse ensues. The collapse debris forms a barrier across the channels and causes the underground streams to seek passage elsewhere. The diverted underground drainage establishes new channels along near-by fractures, which also approximate the trend of the regional dip. Subsidence that gives rise to troughs probably is not the result of collapse of a single cavern but of several. Water rising from aquifers might find more than one level along which it could move laterally. The restriction of trough development to the outcrop area of the Castile section that contains petroliferous limestone suggests that the thin limestone beds may determine positions of such levels. Some newly formed troughs incorporate one wall of an older trough, and some are separated from the older trough by straight narrow divides.

Some old troughs are rejuvenated by removal of collapse debris and by increasing the width of old channels. In areas of trough development the process is continuous until the soluble roof rock has been removed. An entire area of trough development probably subsides gradually because of a "honeycomb" of caverns formed by solution. More rapid subsidence, which gives rise to solution-subsidence troughs, is due to greater solution caused by more rapid and abundant flow of water through trunk streams beneath troughs. Such a process accounts for the low narrow divides which bound the trough. If only the area within the trough subsided the surface adjacent to the trough would probably slope toward the trough bottom because of surface runoff which would be attracted by the low area. Once a trough is formed and drainage has been diverted into near-by underground channels, the area above the course begins to subside more rapidly, gives rise to a slightly depressed area, and produces slopes inclined away from the trough.

Source of Water Which Gives Rise to Solution-Subsidence Troughs

Most of the water that flows through the underground channels in the Castile Formation is probably derived from aquifers in the underlying Delaware Mountain group; only a minor amount is supplied by surface runoff. This concept is supported by several observations:

(1) Many troughs are athwart relatively large streams, so that their trend is not related to surface drainage trends.

(2) The low narrow divides which bound the troughs prevent much of the surface runoff from entering the troughs.

(3) Flowing springs occur throughout the area. Several of these springs contained water after a prolonged (4-year) period of drought.

(4) Several northwestward-trending faults occur in areas up-dip from the northwestern and west-central parts of the Gypsum Plain where solution-subsidence troughs are numerous. However, a northward-trending fault zone occurs 5–10 miles west of the southern part of the plain where there is only one trough 5 miles east of the southern end of the fault zone. These relationships strongly suggest that the water that produces the troughs is derived from aquifers fed from sources in the Delaware

---

Plate 2.—VIEWS OF GYPSUM PLAIN, TEXAS

Figure 1.—View west along the southern edge of an inter-trough divide area in northern Culberson County, Texas. The divide area is capped by a thin closely jointed petroliferous limestone of the Castile Formation. The limestone dips from the margins toward the center of the divide area. An aerial view of this general area is shown in Figure 2 of Plate 1.

Figure 2.—Eastward-trending drainage depression which leads to a cavern at the base of a westward-facing escarpment in the Gypsum Plain of northern Culberson County, Texas. Aerial view of this general area is shown in Figure 2 of Plate 1.

Mountains and the reef escarpment. Water moving through aquifers from the reef escarpment and northern Delaware Mountains flows parallel to the dip into the northwestern and west-central parts of the Gypsum Plain, where much of it rises along fractures to form the numerous troughs. (*See* Fig. 3.) Movement of underground water in this general area is obstructed only by the several northeastward-trending faults, which merely deflect the underground flow. Water that migrates downdip from the southern part of Delaware Mountains moves parallel to the dip toward the Gypsum Plain but encounters the northward-trending fault zone and is deflected southward along this zone to the vicinity of Seven-Heart Gap, where it drains eastward, passes along an eastward-trending fault into an eastward-plunging syncline at the foot of the Apache Mountains, and continues into areas east of the Gypsum Plain. Hence, no troughs are developed in the area east of the fault zone, because underground flow is diverted around it. The single trough east of the southern end of the fault zone is probably caused by flow along an east-southeastward-trending fault which intersects the zone.

Anomalous Areas of Solution-Subsidence Trough Development

Trough development in some areas of the Gypsum Plain is not entirely in accord with the mode of origin here advanced. The area in which solution-subsidence troughs are best developed is above the eastward-trending anticline that follows Delaware Creek across the northern part of the area. If underground drainage channels select the joints that most closely parallel the dip, the troughs should develop along northwestward- and southeastward-trending joints that parallel dip directions on the flanks of the anticline. However, some eastward- trending tension joints parallel to the axis of this anticline probably provide easier passage for water than more tightly closed joints of other sets.

Moneymaker (1948, p. 95) notes that "... bedrock solution [in limestones of the Tennessee Valley] is controlled rigidly by the geologic structure" and that "... solution is initiated along joints, bedding planes, unconformities, faults, and crests of anticlines." At several places along the southwestern edge of the Gypsum Plain northeastward-trending normal faults with small displacements intersect eastward-trending solution-subsidence troughs. The trends of the troughs are not influenced by the fault at any of these places, and no explanation of this seemingly abnormal circumstance is evident. The absence of troughs in the upper part of the Castile Formation may be due, at least in part, to the absence of near-surface impervious horizons, which would afford levels at which subterranean channels could develop. The process of solution and subsidence in areas where these rocks form the surface may be active at depth, but the effect of subsidence diminishes upward and is not expressed as solution-subsidence troughs.

References Cited

Cvijić, J., 1893, Das Karstphänomen: Penck's Geog. Abh. v. 5, p. 49–330

Haigh, B. R., 1951, Geology of Delaware Basin: Oil and Gas Jour., v. 49, no. 42, p. 149–151, 154, 156, 158

King, P. B., 1942, Permian of west Texas and southeastern New Mexico: Am. Assoc. Petroleum Geologists Bull., v. 26, p. 535–763

——1948, Geology of the Southern Guadalupe Mountains, Texas: U. S. Geol. Survey Prof. Paper 215, 183 p.

——1949, Regional geologic map of parts of Hudspeth and Culberson counties, Texas: U. S. Geol. Survey Oil and Gas Inv. Prelim. Map 90

Lattman, L. H., and Olive, W. W., 1955, Solution-widened joints in Trans-Pecos Texas: Am. Assoc. Petroleum Geologists Bull., v. 39, p. 2084–2087

Moneymaker, B. C., 1948, Some broad aspects of limestone solution in the Tennessee Valley: Am. Geophys. Union Trans., v. 29, p. 93–96

Stead, F. L., 1953, Delaware Basin may be next major oil province: World Oil, v. 137, p. 142–144, 149, 150, 152

West Texas Geological Society, Stratigraphic Problems Committee, 1949, East-west cross section through southern Permian Basin of West Texas: 34 p.

U. S. Geological Survey, American Embassy, Lima, Peru

Manuscript Received by the Secretary of the Society, April 13, 1956

BULLETIN OF THE GEOLOGICAL SOCIETY OF AMERICA
VOL. 68, PP. 359-378, 5 FIGS, 1 PL. MARCH 1957

GEOPHYSICAL INVESTIGATIONS IN THE EASTERN CARIBBEAN: VENEZUELAN BASIN, ANTILLES ISLAND ARC, AND PUERTO RICO TRENCH

BY C. B. OFFICER, J. I. EWING, R. S. EDWARDS, AND H. R. JOHNSON

ABSTRACT

The purpose of this investigation was to determine seismically the structure of an island-arc–deep-sea trench sequence and its associated interior basin. A series of seismic-refraction profiles were taken in the Eastern Caribbean and were designed to measure the crustal structure of the broad Venezuelan basin of the Caribbean sea, the island arcs of the Lesser Antilles and Greater Antilles, and the Puerto Rico trench. Results showed that the Caribbean basin, although similar in many respects, is significantly different from the standard ocean-basin structure. Material below the major seismic discontinuity has an average velocity of 7.4 km/sec., considerably different from the 8.0 km/sec. generally observed beneath the corresponding discontinuity in the Atlantic basin. Above this discontinuity the crustal velocities are lower than for the corresponding ocean-basin structure, which indicates a somewhat more acidic composition. Both the crustal and overlying sedimentary and igneous materials are thicker in the Caribbean. The seismic structure for the northern part of the Puerto Rico trench is the same as that for the Atlantic, except for a slight thickening of the crust. In general, the structure along the island arc is more complex than elsewhere but shows crustal velocities nearer the surface than in the Caribbean or Atlantic. From these results and their correlation with the known geology of the area and from other geophysical measurements the writers conclude that the entire Caribbean area has been extensively intruded by large bodies of basic magma which have differentiated deep in the mantle and migrated upward. The writers consider that the introduction of this material has been the primary cause of the tectonic effects observed in the area; in particular the island arcs and deep-sea trenches have been formed by horizontal compression along the border of the altered Caribbean and normal Atlantic basin.

CONTENTS

TEXT

	Page
Introduction	360
Acknowledgments	364
Geophysical results	365
Atlantic basin	365
Caribbean basin—Venezuelan basin, Aves swell, Grenada trough	365
Puerto Rico trench and adjacent area	366
Island arc	367
Interpretation of gravity measurements in terms of the seismic results	368
Geological and geophysical identification of Atlantic and Caribbean crust	369
Structure cross sections	371
Origin of the Venezuelan basin	372
Origin and development of an island-arc–deep-sea-trench sequence	374
Later developments	376
References cited	377

ILLUSTRATIONS

Figure	Page
1. Geographic location of seismic-refraction stations in the Eastern Caribbean	360
2. Average seismic sections for the Atlantic and Venezuelan basins with inferred geologic identifications	370
3. Density distribution for the Atlantic and Caribbean basins inferred from the seismic velocities	374
4. Resultant island-arc–trench structure	375
5. Later developments of island-arc–trench structure into an addition to the continents	376

Plate	Facing page
1. Seismic sections and structure cross sections	378

TABLES

Table	Page
1. Venezuelan basin and vicinity	361
2. Puerto Rico trench and vicinity	362
3. Island arc	363

Introduction

During the past few years crustal structure beneath oceanic areas has been examined extensively by seismic-refraction techniques. The results have increased knowledge of the crust under the ocean basins and in the vicinity of oceanic islands and knowledge of the changes that occur from ocean basins to continents. A next logical step was an intensive examination of an interior-basin, island-arc, deep-sea trench, exterior-basin sequence, because of its importance in large-scale geologic processes. The area studied includes the interior Venezuelan basin, island arc of the Lesser Antilles and Puerto Rico, Puerto Rico trench, Barbados ridge, and Atlantic basin. This paper covers the Venezuelan basin, the more northerly portion of the arc, and the Puerto Rico trench; a paper by Ewing *et al.* (in press) covers the more southerly portions including the Barbados ridge and the Trinidad shelf. There have been three

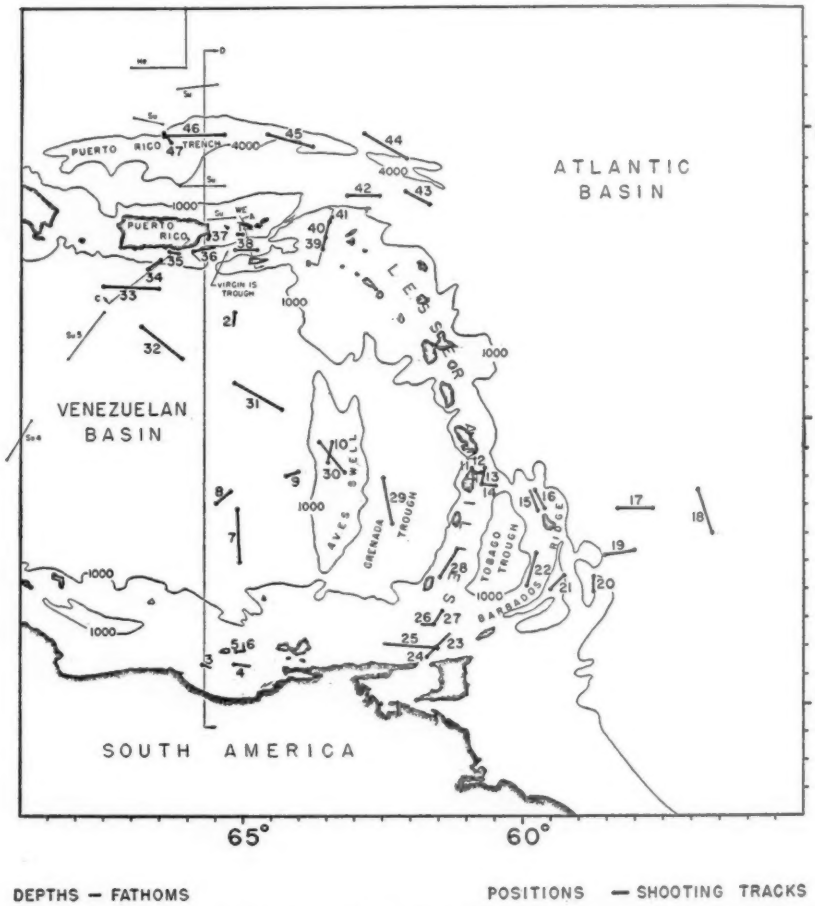

FIGURE 1.—GEOGRAPHIC LOCATION OF SEISMIC-REFRACTION STATIONS IN THE EASTERN CARIBBEAN

The 1000- and 4000-fathom depth contours taken from H. O. Chart 5487 have been included for reference. Profiles from this investigation are shown by heavy lines. Profiles from other investigations referred to in the text are shown by thin lines: those from G. H. Sutton (*in* Ewing and Worzel, 1954) are labelled Su, those from Hersey *et al.* (1952) by He, those from Worzel and Ewing (1948) by WE.

TABLE 1.—VENEZUELAN BASIN AND VICINITY

Layer \ Profile	2		7				8				9				10		29			
	T	V	Ts	Vs	Vn	Tn	Tw	Vw	Ve	Te	Tw	Vw	Ve	Te	T	V	Ts	Vs	Vn	Tn
Ocean	4.21		4.22			3.50	3.67			3.98	3.21			3.06	1.28		2.93			2.93
A	1.69	(2.14)	2.74		1.97	2.48	1.76		1.75	1.44	.46		1.78	.32	1.02		1.37		2.00	.66
B											.96		2.81	1.82						
C											2.67		3.71	2.40			2.88		3.82	2.05
D	2.56	(5.08)					2.39		4.57	2.74					1.37	(5.17)	2.69		5.29	1.94
E1		(6.16)	5.49		6.27	4.45			6.82				6.28			(6.32)	8.70		6.34	5.64
E2																				
F					7.27														7.47	
			12.45			10.43											18.57			13.33

Layer \ Profile	30				31				32				33				34			
	Ts	Vs	Vn	Tn	Ts	Vs	Vn	Tn	Ts	Vs	Vn	Tn	Tw	Vw	Ve	Te	Tw	Vw	Ve	Te
Ocean	1.30			1.68	3.44			4.28	4.45			4.45	4.50			5.01	3.28			1.59
A	.60			.36	.86		1.86	1.72	.45			.83	.38		2.03	1.52	.94		2.00	.80
B					1.08		(2.81)						2.31		(3.04)					
C	1.45		3.76	1.49					1.90		3.64	1.80					5.56		3.80	.67
D	2.78		4.33	3.89	3.22		4.47	1.57					2.41		5.00	2.98			5.11	
E1	4.07		6.02	1.50	3.05		(5.96)		6.73		6.60	4.94	4.83		6.62	1.23				
E2			6.63		7.83		6.58	2.79												
F							7.36				7.54				7.26					
					19.48			10.36	13.53			12.02	14.43			10.74				

A—unconsolidated sediment, velocity range 1.6–2.0 km/sec.
B—partially lithified to lithified sediment, velocity range 2.2–3.0 km/sec.
C—sedimentary or volcanic rock, velocity range 3.2–4.2 km/sec.
D—Sedimentary, igneous, or metamorphic rock.
E—crustal velocities, E1 and E2 where two are measured on same profile.
F—velocity beneath major discontinuity.

Numbers are given in km and km/sec. To convert to ft. and ft./sec. multiply by 3280. T and V columns are thickness and velocity respectively. n, s, e, w refer to the relative position of one receiving station on a given profile with respect to the other. Unreversed velocities are in parentheses. On some of the reversed profiles a layer measured at one end of the profile was not measured at the other, as shown by values for the thicknesses and velocities. Where a thickness for layers A through E with no associated velocity is given for a particular layer, the velocity has been assumed from a near-by profile. The number below row F in the thickness columns where given is the total depth from sea level to the major discontinuity. Each seismic layer in a refraction profile is measured over a limited range interval from the receiving station; thicknesses quoted above have been extrapolated back from the range interval of measurement by straight lines to beneath the receiving station.

TABLE 2.—PUERTO RICO TRENCH AND VICINITY

Layer \ Profile	42				43				44			
	Tw	Vw	Ve	Te	Tw	Vw	Ve	Te	Tw	Vw	Ve	Te
Ocean	5.94			5.94	6.31			5.94	6.30			6.34
A	1.13			1.24	.89			1.08	.13		1.70	.13
B												
C					.20		4.10	1.76	1.62		3.78	.70
D			5.49				5.47					
E									3.41		6.33	5.42
F											8.00	
									11.46			13.09

Layer \ Profile	45				46				47			
	Tw	Vw	Ve	Te	Tw	Vw	Ve	Te	Ts	Vs	Vn	Tn
Ocean	7.51			6.72	7.92			7.89	8.28			8.28
A	.17			1.60								1.13
B												
C			(4.33)	1.93	2.11		3.23	.63			4.14	3.78
D							(4.71)	1.23				
E	2.19		6.24	10.25	6.76		6.32	8.45			5.95	
F			7.90				7.95					
	9.87			18.26	16.79			19.43				

See Table 1 for identities of A, B, C, D, E.
F—velocity beneath major discontinuity, in this case identified by its velocity with the Mohorovicic discontinuity beneath continental areas.

TABLE 3.—ISLAND ARC

Layer \ Profile	Puerto Rico and Vicinity																											
	1				35				36		37				38				39				40				41			
	Tw	Vw	Ve	Te	Tw	Vw	Ve	Te	T	V	Tw	Vw	Ve	Te	Tw	Vw	Ve	Te	Ts	Vs	Vn	Tn	Ts	Vs	Vn	Tn	Ts	Vs	Vn	Tn
Ocean	.03			.03	.02			.02	1.88		.01			.01	4.34				1.35			1.04	1.09			.82	.82			.71
A	.04	1.97		.41	.75	1.95		.37	.96	(2.01)	.25	1.96		.09	.62				.91	1.92		.48	.34			.46	.46			.52
B		2.56													1.47	3.14			1.86	2.95		.97	1.37	2.92		.60	.60	2.34		.63
C																														
D						5.23			1.41	(4.98)		5.00			.92	4.72				5.37				5.70				5.24		
E										(5.83)					2.12	5.67														
																7.01														

Layer \ Profile	Lesser Antilles										South American Shelf									
	11				12				28		3		4		5				6	
	Ts	Vs	Vn	Tn	Tw	Vw	Ve	Te	T	V	T	V	T	V	Tw	Vw	Ve	Te	T	V
Ocean	.08			.08	.09			.95	.04		1.36		.95		.08			.08	.08	
A	.13	1.76		.05	.11	1.71		.61	.06						.07	1.67		.36	.46	(1.84)
B	1.66	2.68		1.37	1.52	2.39		1.43	1.34	(2.33)	1.37	(2.32)	3.13	(2.32)	1.03	2.17		1.52	1.09	(2.19)
C	2.49	3.44 + 4.41		.62	2.56	3.25 + 4.29		1.51	3.05	(4.00)		(4.48)		(5.27)		5.72				(5.96)
D		6.31				5.97				(6.40)										
E																				

See Table 1 for identities of A, B, C, D.

E—higher-velocity layers, in some cases grading to crustal velocities of Tables 1 and 2.

previous crustal seismic investigations over island-arc structures: a single profile by J. B. Hersey in 1949 in the Puerto Rico trench and a series of eight profiles in 1951 across the Eastern Caribbean, interpreted by G. H. Sutton, both reported in Ewing and Worzel (1954) and Ewing and Heezen (1955); a series of three profiles by Raitt *et al.* (1955) across the Tonga island arc. Excellent discussions of the correlation of the geologic sequences and history of the Caribbean islands have been given by Schuchert (1935), Trechman (1935), Maxwell (1948), and Woodring (1954).

The present investigation consisted of taking 47 seismic-refraction profiles during a cruise of the research vessels ATLANTIS and CARYN of the Woods Hole Oceanographic Institution from January to March 1955. The seismic equipment and procedures were similar to those used on other cruises (Officer *et al.*, 1952), with some improvements. A large number of shots was fired to determine the refraction lines on each profile, so that possible vagaries in the interpretations of the geophysical data would be reduced to a minimum. Nearly 2000 seismic shots, using about 23 tons of TNT, were fired during the cruise. The longer profiles, such as 29, 30, 31, had about 80 shots per profile. The profiles were shot to give a seismic-reflection profile, not reported here, at the shorter ranges and a seismic-refraction profile at the longer ranges. Profile locations are given in Figure 1. A receiving station at each end of a profile indicates a reversed profile; a receiving station at only one end indicates an unreversed profile.

The data taken from the seismic-refraction records and the travel-time curves are not included here. They will be given in a data report from the Woods Hole Oceanographic Institution. For those profiles where resultant velocities or thicknesses are questionable, as on many unreversed profiles, the various possibilities are discussed. The resultant seismic velocities and thicknesses are given in Tables 1, 2, and 3 and presented in Plate 1.

The presentation and discussion of the geophysical results are divided into four parts: the exterior Atlantic basin; the interior Venezuelan basin including the Aves swell and the Grenada trough; the Puerto Rico trench and the area adjacent to it; the island arc of the Lesser Antilles and Puerto Rico. The latter two are the border region between the first two.

In Plate 1, the lower velocity layers have been grouped into three velocity ranges. The groupings were sensible from the distribution of measured velocities and layering in the tables. The first group from 1.6–2.0 km/sec. are unconsolidated sediments. The second group from 2.2–3.0 km/sec. are more consolidated sediments, which grade to lithified sedimentary rock. The third group from 3.2–4.2 km/sec. are more difficult to identify; the velocities are valid for either sedimentary or volcanic rock. Higher-velocity layers are labelled with their measured seismic velocities.

ACKNOWLEDGMENTS

This investigation was supported through contact NObsr 43270 with the Bureau of Ships, U. S. Navy, contract Nonr-1367(00) with the Office of Navel Research, U. S. Navy, and the Associates fund of the Woods Hole Oceanographic Institution. The explosives were supplied through the U. S. Navy. The assistance in many ways of the U. S. Naval stations at Hamilton, Bermuda, Port of Spain, Trinidad, and Roosevelt Roads, Puerto Rico, were important to the success of the expedition.

Mr. G. R. Hamilton and the staff of the Columbia University Geophysical Field Station at St. Davids, Bermuda, provided their usual excellent co-operation in making the facilities of the station available.

It is a pleasure to acknowledge the support and co-operation of the captains, S. Bray and A. Karlson, and the crews of the research vessels, ATLANTIS and CARYN. The other scientists involved in one or more phases of the geophysical program were Messrs. A. Bradshaw, W. Dunkle, G. Duys, J. Hahn, W. Moss, D. Owen, M. Rutstein, and R. Vaccaro, Drs. F. Richards and J. Ryther of the Woods Hole Oceanographic Institution, Mr. W. Hudson of the Western Electric Company, and Mr. S. Wardani of the Scripps Institution of Oceanography. The geophysical equipment for the ATLANTIS and the echo-sounding equipment for both ships were supplied by the Woods Hole Oceanographic Institution; the geophysical equipment for the CARYN was supplied by

the Lamont Geological Observatory, Columbia University. Drs. J. B. Hersey and C. O'D. Iselin of the Woods Hole Oceanographic Institution and Prof. M. Ewing of Lamont Geological Observatory were helpful in making this expedition possible. In addition the authors wish to acknowledge the helpful criticisms and suggestions given by Prof. D. T. Griggs, H. H. Hess, and J. C. Maxwell who reviewed the paper before publication.

All four authors took part in the expedition and the preliminary analysis of the data. The final analysis, interpretations, and conclusions are those of the first two authors.

Geophysical Results

Atlantic Basin

The Atlantic basin profiles are presented in Plate 1. Profiles 16, 17, and 18 from Ewing *et al.* (1954) are north of the Puerto Rico trench on a line toward Bermuda; the profile from Hersey *et al.* (1952) is also north of the Puerto Rico trench at latitude 21°N.; the final two profiles, 17 and 18, are from this cruise and are discussed by Ewing *et al.* (in press). The first four profiles are in the Atlantic basin proper; the last two are in the border region from the Barbados ridge to the Atlantic. The last two show a shoaler depth of water and a greater thickness of sedimentary material; but the deeper crustal structure is the same for all the profiles.

The uniformity of crustal structure of the Atlantic sections in regions which have not been disturbed is one of their outstanding features. The depth to the major seismic discontinuity is about 10 km under the basin and deepens with approach to the continents. The velocity beneath this discontinuity is 8.0 km/sec. with small variation. The material above has an average thickness of 4–5 km and velocity 6.5 km/sec. Above this, under the basins, is a kilometer or less of primarily sedimentary material.

This major discontinuity beneath the ocean basins is identified as the *Mohorovicic discontinuity*, found 30–40 km beneath the continents, because (1) it is the major discontinuity, and (2) it is a velocity contrast to a value of 8.0 km/sec. The velocity beneath the Mohorovicic discontinuity is surprisingly similar under the ocean basin and continental areas; the average value under the continents is about 8.1 km/sec., but the average deviation from a value of 8.0–8.1 km/sec. for the earth is certainly not greater than .1 km/sec. Corresponding with the terminology used for the continents the material above the Mohorovicic discontinuity is called the *crust*. For the ocean basins this is the 4–5 km of 6.5 km/sec. material. The material above the crust of sedimentary or volcanic origin is identified where possible from its velocity, stratigraphy, and correlation with known geology.

Caribbean Basin—Venezuelan Basin, Aves Swell, Grenada Trough

The profiles from the interior basin are presented in Plate 1. Profile 29 is over the Grenada trough, profile 30 over the Aves swell, and profiles 31, 7, 32, and 33 over the Venezuelan basin. The locations are indicated in Figure 1. Only the longer profiles have been included; the data from the shorter profiles, 2, 8, 9, and 10, are given in Table 1 and are in agreement with the results presented in Plate 1 but do not measure the entire crustal section. Profiles 5 and 4 from G. H. Sutton's investigation (*in* Ewing and Worzel, 1954) have been included. They were also in the Venezuelan basin on a line from Aruba Island to Mona Island, near the left border of Figure 1. None of these profiles covers the central portion of the basin.

The similarities and differences of these sections compared with those in the Atlantic are immediately apparent. In general, the Caribbean sections resemble the Atlantic; the Caribbean is not a drowned continental area, but there are striking differences of crustal structure. (1) There is a major seismic discontinuity in the Caribbean, but the velocity beneath the discontinuity is significantly less than that in the Atlantic. This difference is apparent from a comparison of the Atlantic and Caribbean sections (Pl. 1); the Caribbean has an average value of 7.4 km/sec. beneath the discontinuity. Its depth is also somewhat greater—13 km, compared with 10 km. Because the velocity change is not to a value of 8.0–

8.1 km/sec., it shall not be referred to as the Mohorovicic discontinuity; that term is reserved for the universal velocity change beneath the continents and the ocean basins. It is the authors' opinion that the Caribbean is an altered oceanic section in the process of becoming an addition to the continent and that the Caribbean structure is temporary; it may be considered permanent only in the sense of permanency of an orogenic region. (2) The crustal velocities have a wider range in values on the low side than is found in the Atlantic. The velocities vary from about 6.0 km/sec. up to 6.6 km/sec. There is more variability in crustal structure and thickness than in the Atlantic; the average thickness of 5½ km is greater. Some profiles show a single velocity crust with variations from 7 km of 5.9 km/sec. on profile 5, 3 of 6.2 on 4, 5 of 6.3 on 7, 7 of 6.3 on 29, 3 of 6.6 on 33, to 6 of 6.6 on 31; others show two velocities such as 30 and 31 having 6.0 and 6.6 km/sec. (3) Above the crust and intimately associated with it in some cases is a greater thickness of material, averaging 4 km. The increase is due primarily to the addition of higher-velocity material, which is indicative of lithified sediments or igneous rocks or both.

The Caribbean, and presumably other interior basins associated with other orogenic regions of island arcs and deep-sea trenches, is not continental; nor is it oceanic, although it is more like the ocean-basin structure. One might expect that there should be a difference between the structure of the Atlantic and Caribbean; otherwise it would be difficult to understand how an island arc and deep-sea trench might develop between them. Also, from a consideration of the strength and thickness of material down to the depth of compensation it is difficult to imagine how an area as large as the Caribbean could be a drowned continent. With an understanding of this difference in structure lies one of the clues for the origin of such orogenic regions and the mechanisms involved in the formation of island arcs and deep-sea trenches.

Puerto Rico Trench and Adjacent Area

The island arc of the Lesser Antilles and Puerto Rico, with the associated Puerto Rico trench in the northern portion and Barbados ridge in the southern, form the border region between the Atlantic and Caribbean. The Puerto Rico trench and the Barbados ridge are not continuous features; the topographic extension of the axis of the ridge is inside that of the trench, *i.e.*, between the axis of the trench and the axis of the Lesser Antilles. The Puerto Rico trench has a maximum depth of about 4400 fathoms north of Puerto Rico, follows the trend of the island arc to the southeast at diminishing depth, and gradually disappears. The results of the profiles in the trench and adjacent to it are given in Plate 1. Profile 46 is in the deeper portion of the trench near its northern boundary. Profiles 45 and 44 are also in the trench, farther east. Profiles 42 and 43 are in the region south of the trench but still in deep water north of the submarine slope from the island arc.

The crustal structure of the trench profiles is similar to that for the Atlantic. The major seismic discontinuity shows a change to a velocity of 8.0 km/sec. The crustal velocity is 6.3 km/sec., a little lower than the average of 6.5 km/sec. for the Atlantic, but from this sample not significantly lower. There is a thickening of the crust, proceeding into the deeper part of the trench, from 4 km to 7 km.

The thickness of sedimentary and igneous rocks is about 2 km, and on profiles 44 and 46 there is no measurable thickness of unconsolidated sediment. However, profile 47 across the deeper portion of the trench shows the higher-velocity horizons dropping down from the north toward the center of the trench by what appear to be, from the seismic results, a series of normal faults. The ocean bottom remains nearly flat along this profile. The sediment thickens to 1 km, and the sedimentary and igneous rock layers thicken to 3½ km at the southern end of profile 47.

The adjacent profiles to the south, 43 and 42, show a different structure. Profile 42 unfortunately was shot over a ridge with observed structural complications; a lower horizon of 5.5 km/sec. was observed. Profile 43 was a long profile and showed no break from the 5.5 km/sec. line on either leg of the reversed profile. A minimum thickness calculation gives 8 km of 5.5 km/sec. material, as indicated in the Puerto Rico trench section (Pl. 1). Such mini-

mum thickness calculations should always be held in doubt; for although the size of explosives and receiving techniques used measured seismic discontinuities at this depth in adjacent deep-water locations, there may be complications beneath this section which do not allow a detectable signal to be returned.

Island Arc

All the island-arc profiles are included in Plate 1. Many are too short to measure a complete crustal section, and of the five longer profiles four are not reversed, and three have possible structural complications. The resultant picture is not complete, but several features stand out. Profiles 35 and 37 are south and east of Puerto Rico. Profile 36 is in an extension of the Virgin Islands trough at a depth of 1000 fathoms, and profile 38 is in the deeper central portion of the trough at about 2000 fathoms. Profiles 39, 40, and 41 are short profiles, because of the structural changes between Saba and Sombrero islands. Profiles 11 and 12 are short profiles off the island of St. Lucia. Profile 28 is a long unreversed profile along the trend of the Grenadine Islands. Also included are profile 25 from Ewing *et al.* (in press), a long unreversed profile on the Trinidad shelf, and profile 13, from G. H. Sutton (*in* Ewing and Worzel, 1954) a long unreversed profile in shallow water northeast of Puerto Rico.

Consider these seismic sections from the top of the column to the bottom. First, there is a variable amount of unconsolidated to consolidated sediments, velocities 1.6 to 3.0 km/sec. For those profiles in the vicinity of the Virgin Islands trough the thickness increases regularly with depth from profiles 35 and 37 to 39, 40, 41 and 36 to 38; the deeper profiles have the thicker sediments, as might be expected for transportation eventually toward the deeper basins. The source area is the nearby islands. On profile Su 13 an additional thickness of 1.8 km of 3.8 km/sec. material, shown by double crosshatching on Plate 1, is measured. This entire sequence is correlated from the land geology on Puerto Rico (Meyerhoff, 1933) with the Tertiary to recent coastal-plain development of limestones and shales with interspersed bioherms built out north and south from the Cretaceous platform of Puerto Rico. The development of this coastal plain out from Puerto Rico, which is indicated by the results of Su 13, is better seen on the profiles off the south coast and slope of Puerto Rico shown in Plate 1. For the profiles along the Lesser Antilles arc—39, 40, 41, 11, 12, and 28—the upper layers of 1.6 to 3.0 km/sec. are considered a combination of volcanic debris, material eroded from the near-by volcanoes and perhaps some recent pyroclastics, and reef material built out from the volcanic platform.

Below this is a large thickness of higher-velocity material. The velocities have been divided into two groups, one shown by crosshatching with velocities from 3.2 to 4.2 km/sec. and the other of higher velocities from 4.7 to 5.8 km/sec. These velocities are characteristic of many types of rocks; the only general statement that can be made is that they are too high for loose sediments and too low for the material generally associated with an oceanic crust. Velocities from 3.2 to 4.2 km/sec. would be appropriate for extrusive igneous or sedimentary rocks, and velocities from 4.7 to 5.8 km/sec. for hard limestones, intrusive igneous, or metamorphosed rocks. For the profiles along the Lesser Antilles the writers interpret this material as the igneous platform there. For those profiles off St. Lucia, 11 and 12, and the Grenadine Islands, 28, along the southern portion of the Lesser Antilles, the material, with velocities of 3.9, 4.1, and 4.0 km/sec., indicates primarily extrusive igneous rock. For those profiles along the northern and older portion of the Lesser Antilles, 39, 40, and 41, the velocity of material immediately beneath the sediments has an appreciably higher value —5.1, 5.6, 5.7, and 5.2 km/sec.—and indicates that the igneous platform there has been appreciably intruded during a later stage of development following the initial eruptive stage.

For the profiles near Puerto Rico and the Virgin Islands—35, 37, Su 13, 36, and 38—the material beneath the sediments has a range of velocity from 4.7 to 5.8 km/sec. From the land geology of Puerto Rico (Meyerhoff, 1933), this material is interpreted as the Cretaceous basement of folded shales, tuffs, and agglomerates, all of which have been severely intruded. The higher velocities in this area

approach that associated with crustal material, and the distinction between the crust and the overlying material is not as pronounced here as it is in the rest of the Eastern Caribbean. The writers interpret this as the eastward development of the Greater Antilles orogenic belt and believe that through the processes associated with that development, particularly metamorphism and extensive igneous intrusion, the clear-cut distinction between crustal and overlying material observed elsewhere in the Eastern Caribbean has been diminished. Although a distinction can be made from land geology between the Puerto Rico-Virgin Islands area of the Greater Antilles and the volcanic islands of the Lesser Antilles, this distinction is not evident in the deeper structure of the northwestern portion of the Lesser Antilles, as evidenced by the results of profiles 39, 40, and 41.

Crustal velocities are measured only on profile 38 in the deeper portion of the Virgin Islands trough, profile 25 north of Trinidad, and profiles 11, 12, and 28 of the Lesser Antilles. Crustal velocities are reached at a moderately shallow depth of about 4 km on profiles 11, 12, and 28, compared with 6½ km for the Atlantic basin, 7½ km for the Venezuelan basin, and 9 km for the Puerto Rico trench. The volcanics rest on material of crustal velocity which is above the depth at which it is normally found in an oceanic section. This material has been raised at least partially by the activity associated with the vulcanism and perhaps also by deformation contemporaneous with or prior to the vulcanism.

Under the Aves swell the seismic structure is similar to that described here for the Lesser Antilles, although the development has been less vertical and more horizontal. Material of crustal velocity has been raised above its normal depth and is overlain by material whose velocity is characteristic of extrusive igneous rocks; the topographic ridge is formed by a combination of the volcanics and raised crust. A structure cross section over the Aves swell is shown by Ewing *et al.* (in press).

This set of island-arc and trench profiles shows that the crust is raised under the island arc and depressed beneath the trench. The crust tends to follow the topography. This conclusion is strictly true only for those features in the first stage of development, such as the Lesser Antilles and the Puerto Rico trench. The Lesser Antilles development has been affected appreciably by igneous activity and probably by deformation producing uplift of the arc and depression of the trench. The Puerto Rico area of the Greater Antilles arc has been through one period of orogenesis and is in what might be called a second stage of development; the resultant structure is more complicated and in general thicker. The distinction between the crust and overlying material here is not as pronounced as it is in the younger islands of the Lesser Antilles.

Interpretation of Gravity Measurements in Terms of Seismic Results

As is well known from the measurements of Vening Meinesz (1948), there is a large negative gravity anomaly associated with the deep-sea trenches and a positive anomaly associated with the adjacent island arcs. The axis of the negative anomaly is offset from the axis of the trench toward the island arc. Gravity measurements from various submarine cruises over the Caribbean are summarized by Vening Meinesz (1948), Hess (1938), and Ewing and Worzel (1954). Two simple structures have been hypothesized to explain these anomalies. One hypothesis, advanced by Vening Meinesz (1930; 1948), and Vening Meinesz *et al.* (1934), involves a plastic buckling of the crust which forms a large downbulge of lighter more sialic material into a heavier more simatic substratum. A presumed aftereffect is the generation of a convective overturn in the adjacent substratum caused by the higher radioactive heat generation of the downbuckled material; this overturn has such structural effects as the formation of deep interior basins. This hypothesis has been extended and ramified by Hess (1938) and Griggs (1939). The other hypothesis, advanced by Gunn (1936; 1937; 1947; 1949), involves through over-all compression a bending of the crust with movement along a major fracture zone, so that the lighter continental side moves up and the heavier oceanic side down. This sequence is presumed

to be altered in time through continued erosion of the raised portion to fill the lowered portion.

The seismic results do not agree in detail with either hypothesis, but in general they agree with the geometry of Gunn's hypothesis and logical ramifications of it. The crust is raised above its normal level under the volcanic island arc and lowered beneath its normal level under the trench. There is a slight increase in crustal thickness under the trench to a value of 7 to 8 km, compared with 3 to 4 km under the ridge north of the trench. It is important to state here, to avoid possible confusion, that the seismic results measure only a relatively thin section of the earth of the order of 10 to 20 km beneath the ocean bottom; they show that no large downbuckle is measured in the oceanic crust, which itself is relatively thin under the normal ocean basin. They do not preclude the Vening Meinesz hypothesis of convection cells at greater depths.

The writers conclude that Gunn's hypothesis is the primary explanation of gravity anomalies over the trenches and island arcs. Before these seismic investigations Ewing and Worzel (1954) had come to much the same conclusion from an interpretation of gravity data. They demonstrated that the gravity anomalies could be as well explained by a smaller thickness of lighter sedimentary material near the ocean bottom as by a large downbuckle of crustal material at greater depth. On profile 46, the deepest trench profile, near the northern edge of the trench, no unconsolidated sediment was measured. A small thickness of material whose velocity is characteristic of sedimentary and igneous rock was observed, but from profile 47 across the trench this material and an overlying sediment thicken appreciably toward the central and southern portion of the trench. The effect of the large thickness of 5.5 km/sec. material measured on profiles 42 and 43 between the trench and the arc is unknown but may contribute appreciably to the negative anomaly.

Geological and Geophysical Identification of Atlantic and Caribbean Crust

Certain conclusions can be reached concerning the composition of the crust under the exterior (Atlantic) and the interior (Caribbean) regions from an identification of the measured seismic velocities with types of crustal material. An average for the Atlantic and Caribbean seismic columns is given in Figure 2. The Atlantic has a small thickness of sediment, probably not entirely unconsolidated sediment as shown. This is underlain by a 4–5 km crust with a velocity of 6.5 km/sec. and the Mohorovicic discontinuity below which is a velocity of 8.0 km/sec. The 6.5 km/sec. velocity is characteristic of basaltic material and the 8.0 km/sec. of peridotitic material. This is in agreement with the conclusions drawn from the igneous petrology of oceanic islands (Hess, 1954; Turner and Verhoogen, 1951); there the evidence also points to a crust of basaltic material underlain by peridotitic material.

The Caribbean has a somewhat different seismic structure. It has an increased, 4 km, section of sediment and sedimentary and igneous rocks. It is underlain by a thicker crust with velocities varying from about 6.1 to 6.5 km/sec. and a major discontinuity below which is found a velocity of 7.4 km/sec. The 6.1 km/sec. velocity is intermediate between that for the more basic and the more acidic rocks and would be characteristic of andesitic material. This again is in agreement with the petrographic evidence. The igneous rocks of the island arcs are andesites and diorites (Turner and Verhoogen, 1951), not olivine basalts. This petrographic difference between the island arcs and the oceanic islands led to the concept of the andesite line (Marshall, 1912), which circumscribes the Pacific and divides areas characteristically of andesites on the interior from areas of olivine basalts on the exterior. The same difference is found for the Atlantic; the igneous rocks of the Lesser Antilles where exposed are generally diorites and andesites (Schuchert, 1935; Christman, 1953). The andesite line is still considered by some to be the dividing line between continents and oceans, but this is not the case. It is a dividing line between an exterior region of oceanic structure and an interior orogenic region of Caribbean structure; the Caribbean structure is neither continental nor oceanic but resembles more the oceanic type. This

conclusion could be expected from a consideration of gravitational equilibrium. Many of these interior regions, such as the Caribbean, are broad basins with depths of water only slightly less than that of the exterior ocean has an average velocity. (3) It is a peridotitic material in a different phase or crystalline state, which results in a lowered seismic velocity. (4) It is a partially serpentinized peridotitic material, which also results in a lowered

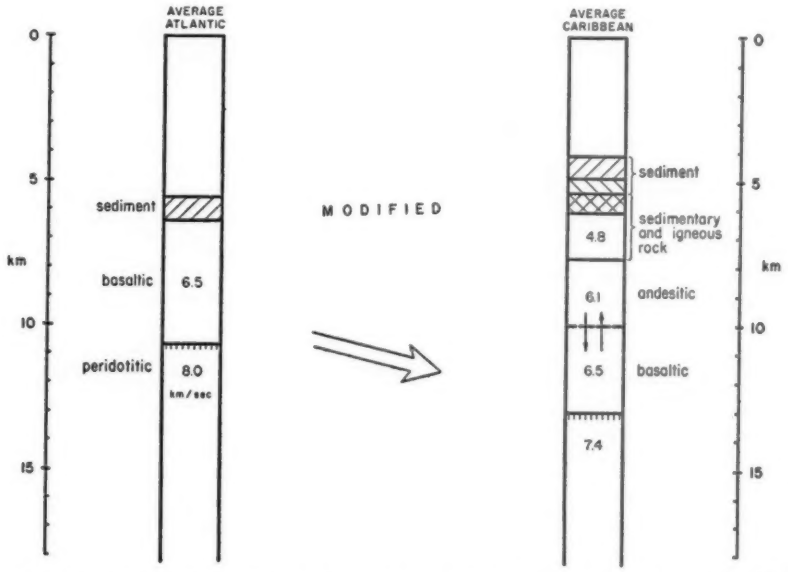

FIGURE 2.—AVERAGE SEISMIC SECTIONS FOR THE ATLANTIC AND VENEZUELAN BASINS WITH INFERRED GEOLOGIC IDENTIFICATIONS

basins. Such broad areas must be in gravitational equilibrium; they cannot be supported by the strength of the crust. Therefore, they cannot be drowned continental areas and must resemble oceanic areas at least to the degree that the total mass to the depth of compensation—*i.e.*, to the depth of superposition of equal density and pressure surfaces—is the same as that beneath an ocean basin.

The identification of the 7.4 km/sec. material is difficult. It is an uncommon velocity to observe in crustal refraction profiles, probably because of the petrologic fact that rocks between olivine basalts and peridotites are uncommon. Four possibilities are suggested: (1) It is a material whose chemical composition is intermediate between an olivine basalt and a peridotite. (2) It is a physical intermixture of 6.5 and 8.0 km/sec. material; each retains its individual identity more or less, but the whole velocity. There is a suggestion of a pattern for this lower-velocity media over the Caribbean which, if true, should help in its identification. Profiles toward the margins of the Venezuelan basin—7, 31, 33, and Su 4—have lower velocities (7.3, 7.4, 7.2, and 7.2 km/sec.) than the profiles toward the central portion (32 and Su 5 with 7.5 and 7.7 km/sec.).

Other more or less isolated instances of measurements of velocities around 7.4 km/sec. have occurred. J. I. Ewing (unpublished) obtained velocities like this for his deepest seismic layer in the Norwegian basin between Norway and Greenland. Bentley and Worzel (1956) found the same under the continental rise south of the Grand Banks off Newfoundland. Officer *et al.* (1952) reported a velocity of 7.2 km/sec. under the Bermuda rise south and southeast of Bermuda. Under the Bermuda rise, there seems to have been mixing of the

crustal and subcrustal material, probably through intrusive activity associated with the Bermuda volcanoes. Out from Bermuda 400–500 km, on the two lines of profiles made, the normal layering of a crust of 6.6 km/sec. overlying 8.0 km/sec. is obtained, but closer in on the Bermuda rise there is the single velocity of 7.2 km/sec.

More pertinent to this examination are the results that Raitt *et al.* (1955) obtained in the vicinity of the Tonga trench. On the Pacific side of the Tonga trench they measured a normal oceanic crust with a thickness of 4½ km and a velocity of 6.5 km/sec., underlain by the Mohorovicic discontinuity at a depth of 12 km with a subcrustal velocity of 8.2 km/sec. Under the trench the crust was 8 km thick with a velocity of 6.5 km/sec., underlian by the Mohorovicic discontinuity with a subcrustal velocity of 8.1 km/sec. Under the Tofua trough on the Tonga Islands side of the trench a crustal layer of 5 km thickness with a velocity of 7.0 km/sec., underlain by a major discontinuity at a depth of 12 km to a velocity of 7.6 km/sec., was measured. These results are remarkably similar to those presented here for the corresponding areas of the Atlantic basin, Puerto Rico trench, and Antilles arc and Venezuelan basin.

The boundary between the Atlantic and Caribbean types is drawn between the island arc and the trench. The seismic results for the Puerto Rico trench identify it with the exterior Atlantic basin; those for the island arc identify it with the interior Caribbean basin.

Structure Cross Sections

Plate 1 also shows a series of structure cross sections derived from the seismic-refraction profiles. The first three are across local features, and the fourth is a long north-south section from South America across the Venezuelan basin, Puerto Rico area, and Puerto Rico trench out to the Atlantic. The vertical exaggeration on all four is the same; the scale of the first three is double that of the fourth.

Section A is across the Virgin Islands trough separating St. Croix to the south from the Virgin Islands to the north. Profiles A, B, and C from Worzel and Ewing (1948) measured a moderately high-velocity basement at a moderate depth off the north and south shores of St. Thomas. This correlates with the intruded agglomerates and tuffs of the island. Farther seaward this horizon drops off in depth. Under profile 1 is an undetermined thickness of sediment. Profile 38 is in the Virgin Islands trough and gave a good determination of the trough structure. The higher-velocity horizons dip upward steeply on the slope up to St. Croix. From this data alone it is not possible to discern whether the Virgin Islands trough is a graben or simply a gap in the island-arc chain.

Section B is across the northern end of the Lesser Antilles. To the south of the section is Saba bank. Directly to the north-west of the northern end of the section is the island of Sombrero, which is part of the outer and older line of limestone-capped volcanoes. This line extends down from Sombrero to Anguilla, St. Martin, Barbuda, Antigua, Grande Terre, and Marie Galente (Schuchert, 1935; Davis, 1926). To the southeast of the central portion of the section are Saba and St. Kitts, part of the inner and younger line of volcanoes. This line extends down from Saba and St. Kitts to Montserrat, Basse Terre, Dominica, Martinique, St. Lucia, St. Vincent, the Grenadine Islands, and Grenada. The structure cross section shows the subsurface extension of the Saba-St. Kitts ridge. This extension is indicated in the surface topography but is more pronounced across the buried ridge itself.

Section C is along the line of profiles 33, 34, and 35 from the Muertos trench up the south slope of Puerto Rico. A rather large thickness of sedimentary rock above the high-velocity (5.1 km/sec.) basement is measured under the slope to deep water off Puerto Rico. This thick sediment correlates with the Miocene and Oligocene sediments of the south coast of Puerto Rico, and the 5.1 km/sec. basement correlates with the folded Cretaceous shales and igneous rocks of Puerto Rico (Meyerhoff, 1933). From this correlation and the known geologic history of Puerto Rico the writers conclude that this entire sequence of sediment is primarily Tertiary in age. Off the east coast of the United States a larger thickness of sediments of Atlantic Coastal Plain

age is found beneath the corresponding geographic location of the continental slope and continental rise (Officer and Ewing, 1954). This type of development probably exists for many other localities where the adjacent land mass has remained high for a sufficiently long time; it seems likely that this process is one of the more important ones in the continued outward growth of the continental land-mass areas.

Section D is a long north-south section across the Venezuelan basin and the border region of Puerto Rico and the Puerto Rico trench to the Atlantic. The differences between the Atlantic and Venezuelan structures are apparent. The crust and overlying sediments and volcanics in the Venezuelan basin are thicker, and their velocities are more variable than in the Atlantic; the velocity beneath the lowest horizon has an average value of 7.4 km/sec., compared with 8.0 km/sec. Both the upper and lower boundaries of the Atlantic basin crust can be observed at progressively lower depths from the Outer ridge into the Puerto Rico trench; the greatest decrease occurs under the slope on the northern side of the trench. Off the south of Puerto Rico is the Tertiary sedimentary development, and off the north a similar development is indicated, although it is not so well defined from the existing seismic profiles. Under Puerto Rico and the area north of it down to the trench, the deeper structure is not as well defined as elsewhere; only material of velocity between 5.3 and 5.8 km/sec. was observed.

Origin of the Venezuelan Basin

Up to this point this paper has been concerned primarily with the presentation of the geophysical data on the Venezuelan basin, the island arc, the Puerto Rico trench, and the Atlantic basin; the correlation of this data with other seismic and gravimetric information; and the geologic identification of the seismic results where possible. The remainder of this paper is speculative; it is a guess, primarily from this recent data, as to the possible origin and development of the island-arc, deep-sea trench, and interior basin areas of the Eastern Caribbean. It is realized that geologic speculations can often be a pitfall and ultimately of dubious value; however, the writers believe that the data point to some interesting deductions which are consistent within themselves and in accord with some of the ideas held by others on the origin and development of an area such as this.

From the several geophysical investigations of crustal structure two general types have been recognized: (1) the continental areas, which have a thickness of 30 to 40 km to the Mohorovicic discontinuity, generally thicker under mountain ranges, and a variable seismic-velocity structure to the Mohorovicic discontinuity; (2) the ocean-basin areas which have a crustal thickness of 5 km of rather uniform seismic-velocity composition and a depth to the Mohorovicic discontinuity of 10 km below sea level. The Venezuelan basin has a composition different from either of these. The crustal structure of the Venezuelan basin should not be considered as a general type in the sense of the first two. The Venezuelan basin is part of the active region of the Eastern Caribbean, and the writers believe that its present crustal structure was originally developed from one of the first two and is perhaps in the process of being altered from one to the other.

The Venezuelan basin probably did not develop from a continental area. For a former continental mass to be stable gravitationally at the depths of the Venezuelan basin, about 2600 fathoms, as such a large block would be, there must have been a large change in the mass-per-unit column down to the depth of compensation. This might have occurred through horizontal flow of material at depth or volume changes from chemical processes or through some other mechanism, but it does not seem possible for such a large change to take place without the occurrence of resultant observable subsidiary effects. This deduction is supported by the observation that throughout geologic time the trend has been toward growth of the continents, not diminution (Lawson, 1932; Wilson, 1949).

The alteration from an oceanic crust would not require an appreciable change in mass. Several mechanisms seem possible, each related for verification to the identification of the 7.4 km/sec. material. (1) There may be a rise in

the isotherms under the Venezuelan basin. This basin has a thick cover, 4 km, of sediment and sedimentary and igneous material which acts as a blanket over the crust and could produce a rise in the isotherms; in addition, the material of 4 km thickness may be more radioactive than the crust and give a further rise in the isotherms. This change in the isotherms might cause a shift in the equilibrium of the basaltic and peridotitic materials and create a continued alteration of these materials with perhaps some contamination from above. The result would be a crust of composition variable from the differentiate of andesitic material to the original basaltic material and of variable thickness; the Mohorovicic discontinuity would represent a different contrast in velocity and probably be shifted in depth. All these features are observed. However, it does not seem likely that the rise in isotherms, if it occurs at all, would be sufficient to cause the changes discussed above.

(2) There may have been mixing or intermixture of the 6.5 and 8.0 km/sec. material through igneous activity or physical forces. This would explain the development of a 7.4 km/sec. material, but such a process by itself could only reduce the thickness of the crust and would not explain the observed variability of crustal velocity and thickness.

(3) There may have been some sort of phase change of the submohorovicic material, as suggested by F. Press (personal communication). He mentioned the probable existence of a low-velocity section in the upper part of the mantle under the continents (Gutenberg, 1955) and stated that a comparison of the seismic-refraction results under the ocean basins with the earthquake surface wave results—the former measuring the material immediately below the Mohorovicic discontinuity and the latter a larger thickness of the mantle—shows slightly higher velocities for the refraction measurements; thus a similar low-velocity section may exist there. If there were a change in the conditions for existence of this low-velocity section, for example through a rise in the isotherms, the low velocity might occur immediately below the Mohorovicic discontinuity. This mechanism does not explain the variability within the crust, and it implies that the combination of increase of pressure and temperature with depth in the mantle beneath the continents, capable of causing a low-velocity section there, is such that a similar decrease under the ocean basins at different pressures and temperatures will produce a decrease there.

(4) Partial serpentinization of the submohorovicic and crustal material may have occurred. This suggestion has been advanced by Hess (1954; 1955) as a possible epeirogenic mechanism under the oceanic areas. Serpentinization would decrease the seismic velocity in agreement with the observations. The question is raised how this process by itself can explain all the apparent alterations observed for the crustal sections of the Venezuelan basin.

(5) The entire Caribbean area may have been extensively intruded by large bodies of primary basalt magma which differentiated deep in the mantle and migrated upward because of a density differential. This suggestion has been advanced by Ewing *et al.* (in press). This process may have contaminated the upper portion of the mantle with intrusives of material with crustal velocities and produced the observed decrease in velocity. It may also have caused crustal thickening and contamination of the upper portion of the crust with the more siliceous differentiates of the primary magma; this process explains the decrease of crustal velocities observed there. The continued ascent of the more volatile constituents of the magma could produce the extensive volcanic activity which has resulted in the widespread occurrence of material whose velocity is characteristic of extrusive igneous rocks.

Of the five possibilities the last seems to explain more of the features observed on the seismic-refraction profiles than the others. The emphasis here, however, has been on attempting to find a possible physical process which would explain the observed seismic results and not necessarily on discussing the probability of occurrence of the various possible processes.

An interesting demonstration can be given to show that the mass-per-unit column for the Atlantic, including the ocean, is approximately equal to that for the Venezuelan basin. This must be the case, for such broad areas as these can only have a small amount of their support from the strength of the crust and must be effectively in isostatic balance.

The density distributions for the two basins are derived empirically from the seismic velocities and the rock identifications. Usually the density increases with velocity, particularly through an orderly suite of related rocks

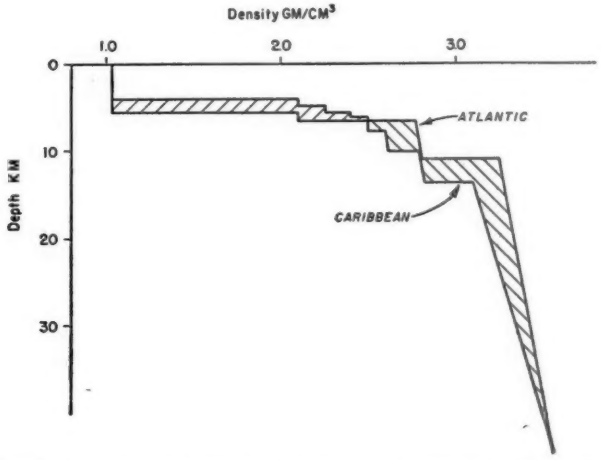

FIGURE 3.—DENSITY DISTRIBUTION FOR THE ATLANTIC AND CARIBBEAN BASINS INFERRED FROM THE SEISMIC VELOCITIES

(*see* Birch *et al.*, 1942); this is true because, although in the formula for velocity

$$v = \left(\frac{k + \frac{4}{3}\mu}{\rho}\right)^{1/2}$$

the density, ρ, is inversely proportional to velocity, the bulk modulus, k, and rigidity, μ, increase more rapidly than density, so that the resultant effect is an increase in velocity with increase in density. This relation holds in general, but exceptions can exist. In the present case if the difference between the 8.0 and 7.4 km/sec. material represented a phase change, the decrease in velocity would not necessarily imply a decrease in density.

The derived density distribution for the Venezuelan and Atlantic basins are sketched in Figure 3. The average depth of the Atlantic profiles is about 1½ km deeper than that of the Caribbean profiles. The Atlantic has 1 km of sediment whose density is taken to be around 2.1 gm/cm³ and is underlain by 4 km of basaltic material, density 2.8 to 2.9, which in turn is bounded by the Mohorovicic discontinuity and peridotitic material, density 3.2 to 3.3. The Caribbean has a thicker accumulation, 4 km, of sediment and sedimentary and igneous rocks. This is underlain by about 6 km of andesitic material, density 2.7 to 2.8, and basaltic material. The major discontinuity occurs at a lower depth and is a contrast to a lower velocity. A density of 3.1 to 3.2 is chosen for the 7.4 km/sec. material; gradually with depth this material is considered to approach the density of the submohorovicic material. The mass-per-unit column is the integral of density with respect to depth; thus, the difference in mass between the two is simply the difference between the two shaded areas and s approximately zero.

i

ORIGIN AND DEVELOPMENT OF AN ISLAND-ARC-DEEP-SEA-TRENCH SEQUENCE

The primary objective of this cruise was to determine the crustal structure of the Eastern Caribbean for the evidence it might give of the origin and development of such an orogenic region. The writers consider that there is a complementary relation between the origin of an island arc and deep-sea trench and the origin of the altered interior basin. An interior basin can be in various stages of development depending on its own past history and that of its associated island arcs and trenches. Simi-

larly, along any orogenic belt the various portions are not in the same stage of development or necessarily strictly continuous one with the other. The Caribbean is a good example. The Greater Antilles forms two orogenic belts, one synclinal proportions extending out from South America. All along this sequence different stages of development are seen.

Starting with adjoining Venezuelan and Atlantic basin structures, it is possible to de-

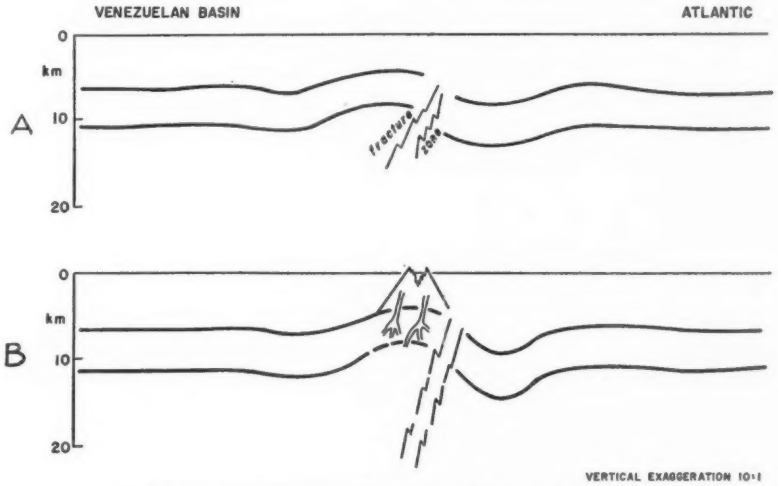

FIGURE 4.—RESULTANT ISLAND-ARC–TRENCH STRUCTURE

A, Origin of an island arc and deep-sea trench through compression. B, Additional developments contemporaneous with the deformation.

from Yucatan through Cuba, northern Hispaniola, Puerto Rico, and the Virgin Islands, and the other from Nicaragua through Jamaica and southern Hispaniola (Hess, 1938). The age along this belt becomes progressively younger to the east, and all of it has been through at least one stage of development. Farther east is the volcanic island arc of the Lesser Antilles, consisting essentially of an older and a younger line of volcanoes emerging from a raised crust. A distinction is made between the orogenic island arc and the volcanic island arc. Outside the arc is the Puerto Rico trench facing on both the older orogenic arc from Puerto Rico to Hispaniola and the younger volcanic arc of the Lesser Antilles. Along the middle portion of the Lesser Antilles, the Puerto Rico trench diminishes in depth toward the southeast and disappears; the Barbados ridge emerges with its axis between that of the trench and the island arc. Along the southern portion, the Lesser Antilles are fronted by the Barbados ridge with total thicknesses of deposited material of geo-

duce what border effects might develop. The seismic results have indicated that the crustal material is raised above its normal level beneath the island arc and depressed beneath the trench. As discussed above, the writers believe that a portion of this elevation has been the direct result of the ascent of a differentiate of lighter material from deep in the mantle. It also seems likely that in this border region there has been strictly structural deformation related directly to the changes that have occurred within the Venezuelan basin and creating a border effect between the altered Venezuelan basin and the undisturbed adjacent Atlantic basin.

Associated with the increased volume of crustal and related material in the Venezuelan basin there may be outward horizontal compression on its borders. As the compression increases, fracturing may occur along zones where rather abrupt changes in crustal properties occur. Along the boundary between the Atlantic and Venezuelan basins the fracturing

would occur in such a manner that the lighter Caribbean crust would override the heavier Atlantic crust. The resultant configuration, resembling Figure 4*A*, would depend upon the proportions of deformation and movement

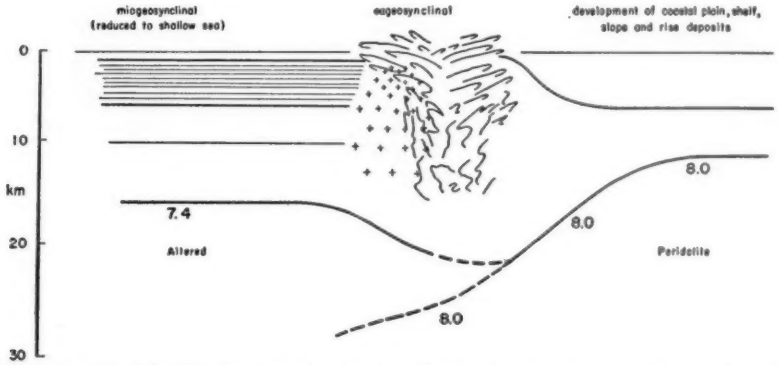

FIGURE 5.—LATER DEVELOPMENTS OF ISLAND-ARC–TRENCH STRUCTURE INTO AN ADDITION TO THE CONTINENTS

The eugeosynclinal belt may include more than one period of trench–island arc and subsequent mountain building developments.

along the fracture zone. This supposition is in agreement with observed seismic and topographic evidence; both infer that the structure is a raised island arc bordered on the Atlantic side by the depressed Puerto Rico trench. It can be argued further that the effect of compression of the Venezuelan basin against the South American continent would be the reverse of that for the Atlantic; the lighter South American continent would tend to override the heavier Venezuelan basin. This provides an explanation for the Los Rocques trench bordering the Venezuelan basin to the south.

During deformation and as a consequence of the deformational stresses an additional effect may take place, as indicated in Figure 4*B*. Along the raised island arc a relaxation of compression will develop in its upper portion. This relaxation of compression will encourage the upward movement of magma from depth. With the supposed alteration of the Venezuelan basin that has occurred it might be expected that the release of the more volatile constituents would be concentrated in such a zone and form a line of volcanoes; as observed, the Lesser Antilles is a chain of volcanic islands.

There is substantial evidence from earthquake seismology for the existence of the fracture zone between the island arc and deep-sea trench. It is the zone of major earthquakes and is well defined for the numerous Pacific island arcs, as well as for the Antilles island arc (Gutenberg and Richter, 1949). The earthquakes describe a zone which starts at the surface between the island arc and the trench and dips down under the island arc at approximately 45°.

LATER DEVELOPMENTS

At present there is extensive igneous activity along the island arc gradually changing from a more extrusive stage in the younger parts to a more intrusive stage in the older. The volcanic islands have been severely eroded, and subsidence of the islands is evident (Davis, 1926). On the subsiding volcanoes lagoon limestones and reefs have been built up, as is well shown by the tilted bevelled-off island of Antigua, where a section of 8000–10,000 feet of Tertiary carbonate deposits overlying the volcanics can be seen (Schuchert, 1935). In addition there has been appreciable offshore deposition into deeper water with thicknesses up to 12,000–14,000 feet, as is shown by the results of the seismic profiles south of Puerto Rico (Pl. 1). The enclosed basin of the Virgin Islands trough appears to be a permanent resting place for sediments from the near-by islands with a present thickness of 7000 feet. For the Puerto Rico trench the sediments are very thin along

the northern boundary but thicken up to about 10,000 feet toward the southern portion of the trench. Along this border region of the island-arc–deep-sea trench area there is ample evidence of extensive igneous activity and intense sedimentation. In the authors' opinion it is one of the more active geologic areas of today.

The island-arc–deep-sea trench area is at present out of isostatic equilibrium. There is a large negative anomaly across the trench and a smaller positive anomaly across the island arc. In time a period of readjustment might begin and lead to an orogeny and formation of a folded and thrust-faulted mountain system.

Complementary to this and probably extending over a longer period of time there would be continued alteration of the crust under the interior (Venezuelan) basin and continued sedimentation from the surrounding land masses through turbidity currents and other depositional mechanisms into the enclosed basin. Essentially flat-lying, structurally undisturbed beds would develop. The total thickness should be less than that for the border regions, and true eolian deposits should be found only at the top of the stratigraphic column. The continued alteration of the crust under the interior basin would produce epeirogenic movements through volume changes.

The suggestion is advanced that through such processes as this additions to the continents are made. The island arc and deep-sea trench with their subsequent orogenies form the eugeosynclinal belts (Kay, 1951), and the interior basin with its continued alteration and sedimentation forms the miogeosynclinal basin. The result might resemble what is illustrated in Figure 5; the final step is presumed to be the development of a coastal plain and continental-shelf, continental-slope, and continental-rise deposits as are found off the east coast of North America (Officer and Ewing, 1954), and off the Gulf coast (Weaver, 1955). The change between the addition to the continent and the ocean is now gradual and gradational.

References Cited

Bentley, C. R., and Worzel, J. L., 1956, Geophysical investigations in the emerged and submerged Atlantic coastal plain. Part X: Continental slope and continental rise south of the Grand Banks: Geol. Soc. America Bull., v. 67, p. 1–18

Birch, F., Schairer, J. F., and Spicer, H. C., 1942, Handbook of physical constants: Geol. Soc. America Special Paper 36, 325 p.

Christman, R. A., 1953, Geology of St. Bartholomew, St. Martin, and Anguilla, Lesser Antilles: Geol. Soc. America Bull., v. 64, p. 65–96

Davis, W. M., 1926, The Lesser Antilles: Am. Geog. Soc. Pub. no. 2, 200 p.

Ewing, J. I., Officer, C. B., Johnson, H. R., and Edwards, R. S., in press, Geophysical investigations in the Eastern Caribbean-Trinidad shelf, Tobago trough, Barbados ridge, Atlantic Ocean: Geol. Soc. America Bull.

Ewing, M., and Heezen, B. C., 1955, Puerto Rico trench topographic and geophysical data, p. 255–267, *in* Poldevaart, A., *Editor*, Crust of the earth: Geol. Soc. America Special Paper 62, 762 p.

Ewing, M., and Worzel, J. L., 1954, Gravity anomalies and structure of the West Indies. Part I: Geol. Soc. America Bull., v. 65, p. 165–173

Ewing, M., Sutton, G. H., and Officer, C. B., 1954, Seismic refraction measurements in the Atlantic ocean, Part VI, Typical deep stations, North America basin: Seismol. Soc. America Bull., v. 44, p. 21–38

Griggs, D. T., 1939, Theory of mountain building: Am. Jour. Sci., v. 237, p. 611–650

Gunn, R., 1936, On the origin of the continents and their motion: Jour. Franklin Inst., v. 222, p. 475–492

—— 1937, A quantitative study of mountain building on an unsymmetrical earth: Jour. Franklin Inst., v. 224, p. 19–53

—— 1947, Quantitative aspects of juxtaposed ocean deeps, mountain chains, and volcanic ranges: Geophysics, v. 12, p. 238–255

—— 1949, Isostasy extended: Jour. Geology, v. 57, p. 263–279

Gutenberg, B., 1955, Channel waves in the earth's crust: Geophysics, v. 20, p. 283–294

Gutenberg, B., and Richter, C. F., 1949, Seismicity of the earth: Princeton, N. J., Princeton Univ. Press, 273 p.

Hersey, J. B., Officer, C. B., Johnson, H. R., and Bergstrom, S., 1952, Seismic refraction observations north of the Brownson deep: Seismol. Soc. America Bull., v. 42, p. 291–306

Hess, H. H., 1938, Gravity anomalies and island arc structure with particular reference to the West Indies: Am. Philos. Soc. Proc., v. 79, p. 71–96

—— 1954, Geological hypotheses and the earth's crust under the oceans: Royal Soc. London Proc., A, v. 222, p. 341–348

—— 1955, Serpentines, orogeny, and epeirogeny, p. 391–407, *in* Poldervaart, A., *Editor*, Crust of the earth: Geol. Soc. America Special Paper 62, 762 p.

Kay, M., 1951, North American geosynclines: Geol. Soc. America Mem. 48, 143 p.

Lawson, A. C., 1932, Insular arcs, foredeeps, and geosynclinal seas of the Asiatic coast: Geol. Soc. America Bull., v. 43, p. 353–381

Marshall, P., 1912, Oceania, *in* Handbook of Regional Geology, v. 7, no. 2, 36 p.

Maxwell, J. C., 1948, Geology of Tobago: Geol. Soc. America Bull., v. 59, p. 801–854

Meyerhoff, H. A., 1933, Geology of Puerto Rico: Univ. Puerto Rico Mon. B, 306 p.

Officer, C. B., and Ewing, M., 1954, Geophysical investigations in the emerged and submerged Atlantic coastal plain. Part VII: Continental shelf, continental slope, and continental rise south of Nova Scotia: Geol. Soc. America Bull., v. 65, p. 653–670

Officer, C. B., Ewing, M., and Wuenschel, P. C., 1952, Seismic refraction measurements in the Atlantic ocean. Part IV: Bermuda, Bermuda rise, and Nares basin: Geol. Soc. America Bull., v. 63, p. 777–808

Raitt, R. W., Fisher, R. I., and Mason, R. G., 1955 Tonga trench, p. 237–254, *in* Poldewaart, A., *Editor*, Crust of the earth: Geol. Soc. America Special Paper 62, 762 p.

Schuchert, C., 1935, Historical geology of the Antillean-Caribbean region: N. Y., John Wiley & Sons, Inc., 767 p.

Trechman, C. T., 1935, Geology and fossils of Carriacou, West Indies: Geol. Mag., v. 72, p. 529–555

Turner, F. J., and Verhoogen, J., 1951, Igneous and metamorphic petrology: N. Y., McGraw-Hill Book Co., 602 p.

U. S. Hydrographic Office, 1939, Bathymetric chart of the Caribbean sea: H. O. Chart 5487

Vening Meinesz, F. A., 1930, Maritime gravity surveys in the Netherlands East Indies, tentative interpretation of the results: Kon. Med. Akad. v. Wetens Proc., v. 33, p. 566–577

—— 1948, Gravity expeditions at sea, 1923–1938, v. 4: Delft, Netherlands Geod. Comm., 233 p.

Vening Meinesz, F. A., Umbgrove, J. H. F., and Kuenen, Ph. H., 1934, Gravity expeditions at sea, 1923–1932, v. 2: Delft, Netherlands Geod. Comm., 208 p.

Weaver, P., 1955, Gulf of Mexico, p. 269–278, *in* Poldervaart, A., *Editor*, Crust of the earth: Geol. Soc. America Special Paper 62, 762 p.

Wilson, J. T., 1949, Origin of continents and Precambrian history: Royal Soc. Canada Trans., v. 43, p. 157–184

Woodring, W. P., 1954, Caribbean land and sea through the ages: Geol. Soc. America Bull., v. 65, p. 719–732

Worzel, J. L., and Ewing, M., 1948, Explosion sounds in shallow water, p. 1–53 *in* Ewing, M., Worzel, J. L., and Pekeris, C. L. Propagation of sound in the ocean: Geol. Soc. America Memoir 27, 205 p.

RICE INSTITUTE, HOUSTON, TEXAS, AND WOODS HOLE OCEANOGRAPHIC INSTITUTION, WOODS HOLE, MASSACHUSETTS; LAMONT GEOLOGICAL OBSERVATORY, PALISADES, NEW YORK; WOODS HOLE OCEANOGRAPHIC INSTITUTION, WOODS HOLE, MASSACHUSETTS; WOODS HOLE OCEANOGRAPHIC INSTITUTION, WOODS HOLE, MASSACHUSETTS

MANUSCRIPT RECEIVED BY THE SECRETARY OF THE SOCIETY, APRIL 16, 1956

WOODS HOLE OCEANOGRAPHIC INSTITUTION CONTRIBUTION NO. 839

LAMONT GEOLOGICAL OBSERVATORY CONTRIBUTION NO. 233

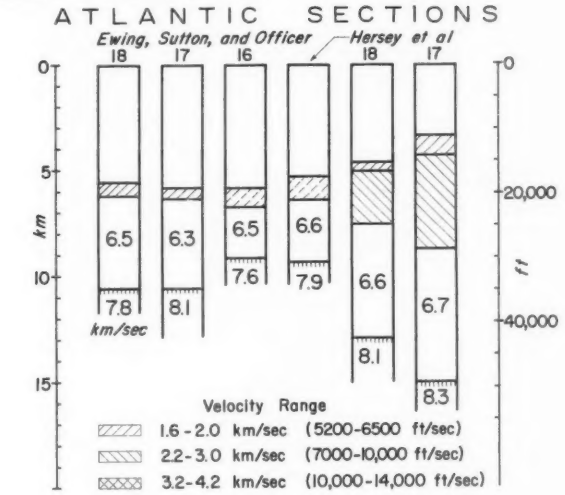

PUERTO R

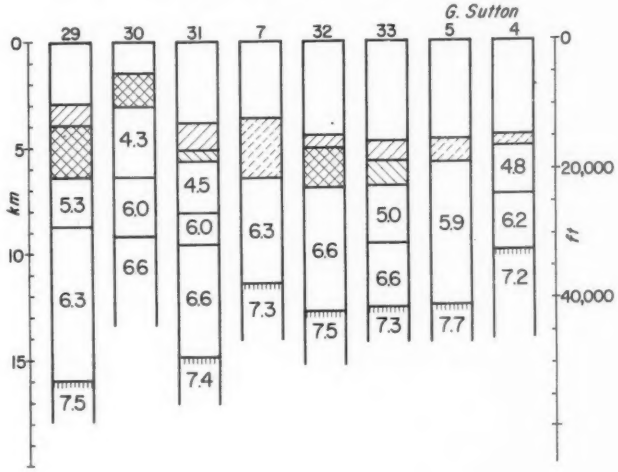

ISLA

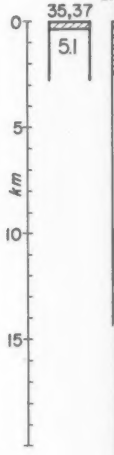

PUERTO RICO TRENCH AND ADJACENT SECTIONS

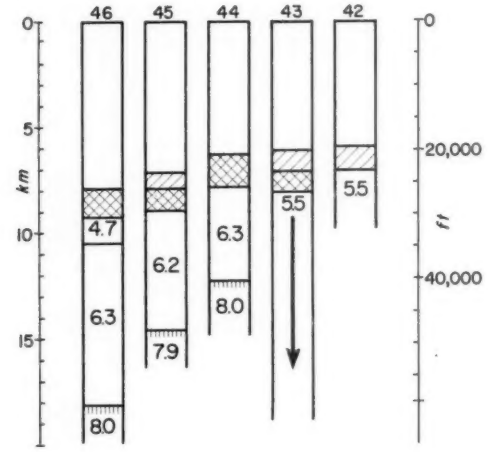

ISLAND ARC SECTIONS

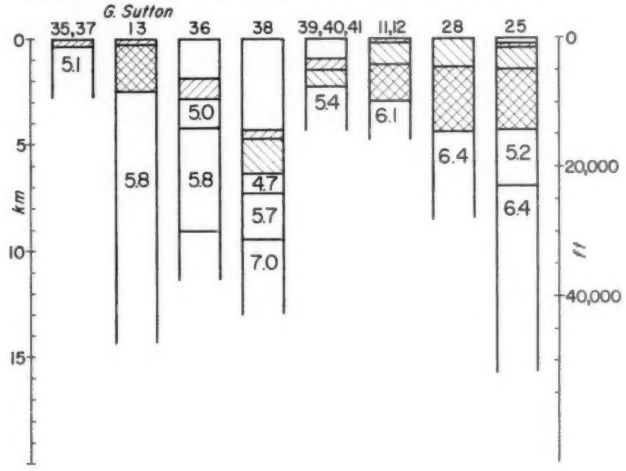

ST. THOMA

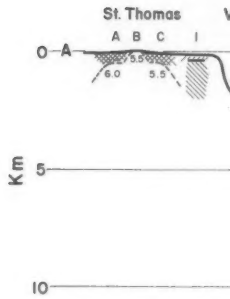

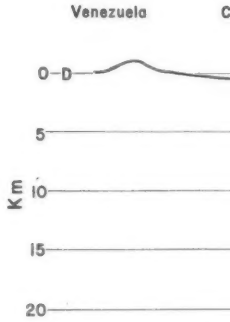

SEISM

Summary of seismic sec
Rico trench and adjacent
structure cross sections pr
Ewing (1948); profiles D,

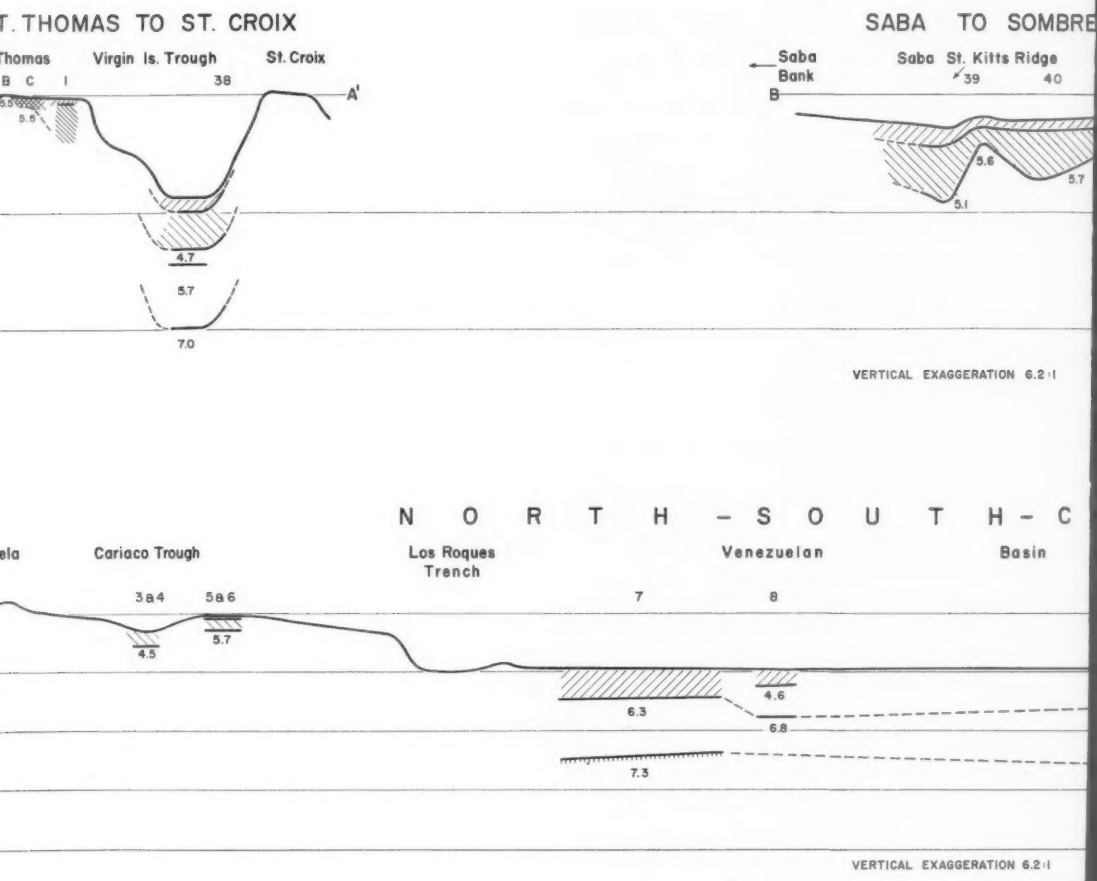

SEISMIC SECTIONS AND STRUCTURE CROSS SECTIONS

seismic sections for Atlantic, Caribbean, Puerto d adjacent area, and island-arc areas. On the sections profiles A, B, and C are from Worzel and rofiles D, E, F, G, and H are from G. H. Sutton (*in* Ewing and Worzel, 1954); and profile I is from E (1952). The locations of the cross sections are shown Unreversed velocities are in parentheses; they are not true seismic velocities.

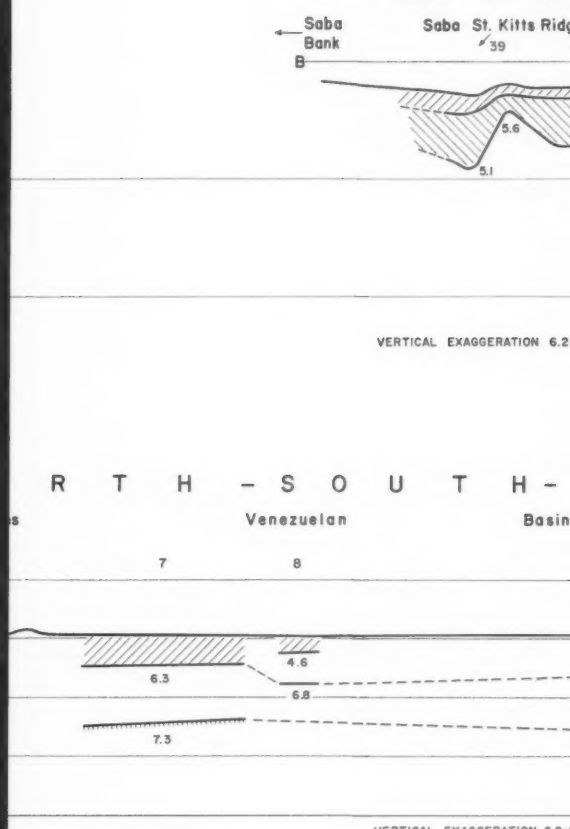

STRUCTURE CROSS SECTIONS

(*in* Ewing and Worzel, 1954); and profile I is from
(1952). The locations of the cross sections are sho
Unreversed velocities are in parentheses; they are
true seismic velocities.

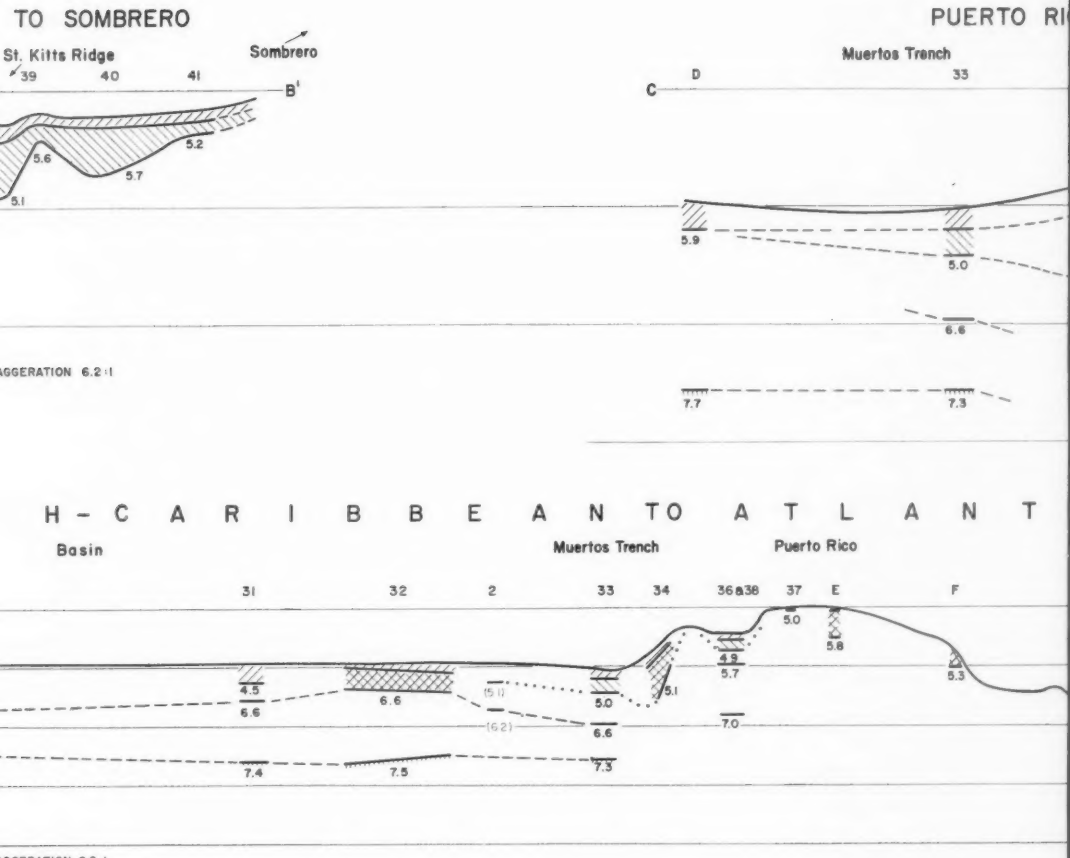

IONS

le I is from Hersey *et al.*
ons are shown in Figure 1.
s; they are not considered

PUERTO RICO SLOPE SOUTH

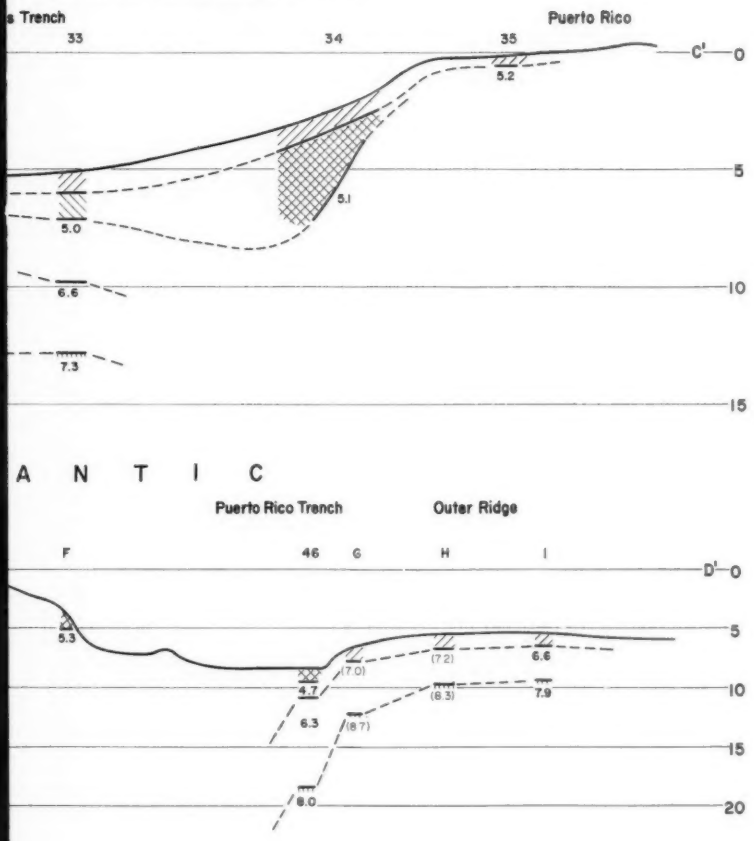

Short Notes

BULLETIN OF THE GEOLOGICAL SOCIETY OF AMERICA
VOL. 68, PP. 379-382, 1 FIG. MARCH 1957

TEST ON THE POSSIBLE CHONDRITIC COMPOSITION OF THE EARTH'S MANTLE AND ITS ABUNDANCE OF URANIUM, THORIUM, AND POTASSIUM

BY PATRICK M. HURLEY

Introduction

Urey (1955) discussed the abundance of U, Th, and K in the earth and concluded that "the Earth's mantle does not contain as much of these radioactive elements as do the meteorites." This conclusion was particularly disturbing because it would have destroyed the only basis for testing the hypothesis that the mantle is of average chondritic composition.

The question of how closely the Earth's mantle approaches the composition of chondritic meteorites can best be answered by the measurement of the principal radioactive elements. These elements alone give evidence of their total abundance in the Earth's mantle by the production of heat which flows to the surface in measurable quantities. If the average heat production by uranium, thorium, and potassium in meteorites matches the requirements for the heat flow in the Earth, substantial evidence will be added in favor of the hypothesis.

Radioactive Heat Production in Chondritic Meteorites

In 1953 the author started the lengthy task of counting alpha particles emitted by powdered surfaces of chondritic meteorites. The

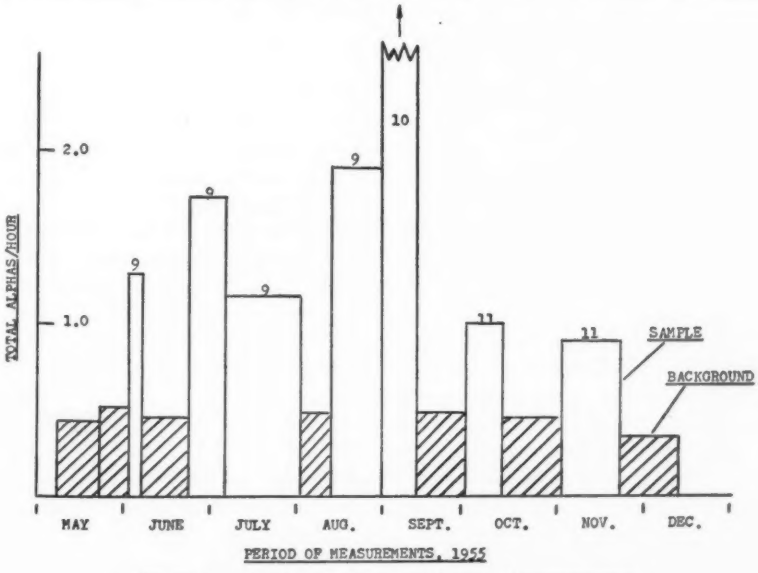

FIGURE 1.—EXAMPLE PERIOD OF ALPHA MEASUREMENTS

major part of the heat production is given by alpha-particle disintegrations, and a measurement of the rate of these disintegrations was considered the most direct method of obtaining values for the heat production.

TABLE 1.—BACKGROUND VARIATIONS, MARCH 1954 TO JUNE 1956

Date, end of run	Av. background α/hr.	Average for period	Remarks
3–12–54	0.67		1 counter, non-mechanical register
3–25–54	0.84		
4–12–54	0.77		
5–8–54	0.60		
7–21–54	0.80		
7–26–54	0.84		
8–12–54	0.60	0.73	
11–24–54	0.47		
5–23–55	0.44		clean chamber, mechanical register
6–2–55	0.52		
6–24–55	0.46		
8–11–55	0.48		
9–28–55	0.48		
11–3–55	0.46		
12–12–55	0.34	0.48	
12–30–55	1.25		changed counter
1–3–56	1.25		
1–20–56	1.12		
3–3–56	1.20	1.20	
5–8–56	0.75		
6–11–56	0.63	0.70	

The alpha-particle emission from the surface of a finely ground sample of chondrite is about 1 particle/day/cm², so that each repetitive comparison against background requires several weeks. An argon-flow proportional counter was used with an unusually low-background chamber (10 alpha counts per 24 hr), and an equivalent source area of 20 cm² with 2 π geometry. Pulses greater than those from alpha particles with a residual range of only about 0.5 cm in argon were relayed to a mechanical register. Tests establishing the precise value of this minimum detactable pulse, and the efficiency of the counter, were made on thick sources of known U and Th content, not from thin-source standards.

During each run the count was recorded every day, so that a plot could be made to indicate spurious events. An example period of measurements is given in Figure 1 showing the relationship between counts on meteorite samples and on background material. Constancy of counter performance is indicated by the data in Table 1.

Table 2 gives the measurements on meteorites to date. The fact that the meteorite samples in Table 2, which were "finds" rather than observed "falls," were still not more than two or three times higher in activity than the Forest City lends support to the average determined for Forest City. The second sample of Forest City (3186) was kindly supplied by Dr. George Reed who has been measuring the uranium content of the same material by neutron activation.

Values for radium equivalent were calculated on the basis of:

$$Ra + .105\ Th = E/915\ \mu\rho$$

where Ra is in 10^{-12} g/g units, Th in 10^{-6} g/g units, E is surface emission of alpha particles per cm² per hr, ρ the density of the meteorite, and μ the ratio of the range of each alpha particle in the mineral to the range in air. A value of 1.68×10^{-3} g/cm² was calculated for $\mu\rho$ by the method described by Nogami and Hurley (1948), which although not precise is well within the needs of this investigation. The calculation of radium equivalent depends to a small extent on the Th/U ratio, which for this purpose was assumed to be 3.5. Reasonable departures from this assumed value will not affect the values for radium equivalent or calculated heat production by more than 5 per cent.

The Forest City value of $.017 \times 10^{-12}$ g/g radium equivalent represents probably the best value as the sample had no chance of contamination by ground water. This value is equal to a heat production of 3.48×10^{-8} cal/gm yr. Table 3 shows the heat production from U, Th, and K assuming a ratio of Th/U

TABLE 2.—THICK-SOURCE ALPHA COUNTS ON CHONDRITIC METEORITES

Chondrite no.	Date, end of run	Total α/hr.	Background α/hr.	Radium equivalent 10^{-12} g/g
9. Bjurböle, Nyland Finland	7–30–54	1.52	0.73	.030
	6–5–55	1.28	0.48	.030
	7–5–55	1.74	0.48	.047
	8–2–55	1.16	0.48	.025
	9–1–55	1.90	0.48	.053
	2–2–56	2.47	1.20	.048
	2–13–56	2.37	1.20	.044
			Average	.040 ± .014
11. Forest City	10–19–55	0.99	0.48	.019
Forest City	11–23–55	0.89	0.48	.015
Forest City	2–28–56	1.735	1.20	.020
3186. Forest City	7–2–56	0.98	0.63	.013
			Average	.017 ± .003
2. Rancom, Ness. Co., Kansas	11–30–54	1.0	0.50	.019
10. Pultusk, Poland	9–7–55	4.05	0.48	.134
	3–13–56	2.03	1.20	.031
	5–21–56	2.58	0.70	.064
21.	5–1–54	0.71	0.73	Very low

= 3.5 and a content of potassium equal to 0.085 per cent (Edwards, 1955).

Content of U, Th, and K in the Earth's Mantle

The value of heat production in chondritic meteorites given above is only 0.3 that used by Urey when he made the conclusions stated in the Introduction above; it agrees well with his desired reduction in the abundances of the radioactive elements by a factor of 0.31 (Urey, 1955, p. 130). His anticipated relative abundances of U, Th, and K in the mantle, however, are not in agreement with our measurements.

The approximate average heat production by radioactive elements in the earth's mantle material may be calculated from surface-heat-flow data if it is assumed that this heat flow is almost entirely due to the radioactive components within the earth. This assumption is probably 90 per cent correct because of the necessary near-surface distribution of the heat sources, if steady-state conductive conditions even approximately exist within the earth.

TABLE 3.—PRESENT RADIOACTIVE HEAT PRODUCTION IN CHONDRITIC METEORITES

Radioactive isotope	Heat reproduction value used cal/gm yr	Content of isotope in chondrites	Heat production in chondrites cal/gm yr ($\times 10^{-6}$)
U 238	0.72	.024 ppm	1.73
U 235	4.7	.00017 ppm	.08
Th 232	0.21	.080 ppm	1.67
K 40	0.21	.....	.....
K (total)	26 × 10	.085%	2.2
		Total	5.68

(Further discussion of this major assumption is beyond the scope of this paper.)

Average surface heat flow (Bullard, 1954):	1.23×10^{-6} cal/cm²sec
Area of earth:	5.10×10^{18} cm²
Total present heat conducted to surface:	8.3×10^{27} ergs/yr
Mass of mantle:	4.1×10^{27} g
Average heat production in mantle material:	2.03 ergs/g yr

This value is to be compared with 2.37 ergs/g yr given in Table 3 for chondritic meteorites. This agreement strongly supports the hypothesis that the earth's mantle was similar in composition to chondritic meteorites originally, although separations of the chemical components have taken place to some extent since the time of origin.

Using the values obtained for U + Th, and the Th/U ratio of 3.5 found in basalts, the total uranium content of the mantle and crust is 1.0×10^{21} grams, and the total thorium is 3.5×10^{21} grams. From Edwards' value of potassium in meteorites, the total potassium in the mantle and crust would be 3.5×10^{24} grams. The use of this value for potassium is supported by the results of this investigation.

Acknowledgments

The author is greatly indebted to Dr. William H. Pinson, Jr., for the loan of his meteorite samples and to Dr. George Reed for his sample of Forest City. This work was supported by the Office of Naval Research, and reproduction in whole or in part is permitted for any purpose of the U. S. Government.

References Cited

Bullard, E. C., 1954, The Earth as a planet) G. P. Kuiper, *Editor*): Univ. Chicago Press, p. 106

Edwards, G., 1955, Sodium and potassium in meteorites: Geochim. et Cosmochim. Acta, v. 8, p. 285–294

Nogami, H. H., and Hurley, P. M., 1948, The absorption factor in counting alpha rays from thick mineral sources: Am. Geophys. Union Trans., v. 29, p. 335–340

Urey, H. C., 1955, The cosmic abundances of potassium, uranium and thorium and the heat balances of the Earth, the Moon, and Mars: Nat. Acad. Sci. Proc., v. 41, p. 127–144

Mass. Inst. Technology, Cambridge, Mass.

Manuscript Received by the Secretary of the Society, November 26, 1956

BULLETIN OF THE GEOLOGICAL SOCIETY OF AMERICA
VOL. 68, PP. 383–388, 2 FIGS., 1 PL. MARCH 1957

APPRAISAL OF RIDGWAY AND GUNNISON "TILLITES," SOUTHWESTERN COLORADO

BY FRANKLYN B. VAN HOUTEN

Introduction

In 1915 Atwood described the Eocene Ridgway "till" on the northwest flank of the San Juan Mountains in southwestern Colorado (Fig. 1), and in 1917 he noted another patch of it on the south flank of the mountains, 100 miles southeast of Ridgway. In 1926 Atwood and his son described the Gunnison "tillite" of Eocene age in the vicinity of Gunnison, Colorado, about 55 miles northeast of Ridgway.

According to Atwood's interpretation, these deposits represent only a modicum of the extensive till the Eocene piedmont glaciers must have made (Atwood and Mather, 1932, p. 16), the postulated Eocene glaciers were more extensive than the Pleistocene glaciers of the San Juan region, and "at no time since mid-Eocene have there existed any ranges comparable in elevation to those in this earlier [Eocene] generation of Rocky Mountains" (Atwood and Atwood, 1926, p. 621).

Largely on the basis of Atwood's reports, early Cenozoic glaciation in the Rocky Mountains has been widely accepted by American geologists (Scott, 1938; Dunbar, 1949, p. 432; Moore, 1949, p. 427; Hunt, 1956, p. 26, 77). Moreover, Larsen and Cross (1956, p. 59) have cited Atwood's data and interpretation in their recent detailed study of the San Juan Mountains, but they have shown that the "tillites" are more reasonably of early Paleocene age.

The implications of extensive glaciation during the early Cenozoic history of the Rocky Mountains are of such paleogeographic significance that the evidence suggesting it should have been evaluated carefully long ago. The present report is principally an attempt to emphasize the need for critical study of the Ridgway and Gunnison deposits.

Gunnison Volcanic Conglomerate

The Gunnison "tillite" is a very poorly sorted volcanic-rich conglomerate lying on Precambrain and Mesozoic rocks and overlain by the Miocene San Juan tuff (Larsen and Cross, 1956, p. 14). At the type locality 3 miles east of Gunnison (Pl. 1, fig. 1; Atwood and Atwood, 1926, fig. 2), angular to subrounded blocks composed chiefly of relatively fresh Tertiary volcanic rocks are set in a slightly calcareous yellowish-gray to light-brownish-gray matrix of reworked crystal-lithic tuff and bentonitic mudstone. Although most of the poorly sorted detritus is less than 18 inches in diameter, some blocks of volcanic rock are as much as 4 feet in diameter.

In most of its outcrops the deposit appears to be unstratified, but locally, especially where giant blocks of volcanic rock are absent and many of the pebbles and cobbles are rather well rounded, the conglomerate is crudely bedded. In these localities, moreover, fragments of nonvolcanic rocks are somewhat more common.

Some fragments in the Gunnison volcanic conglomerate are marked with randomly oriented scratches (Atwood and Atwood, 1926, Fig. 5) which, as preserved, are most common on pieces of Paleozoic chert.

Pebbles of light- to dark-gray volcanic rock examined in thin section contain abundant microporphyritic zoned plagioclase, plus hypersthene, augite, green and brown hornblende, and magnetite, in a glassy or hypocrystalline groundmass (Pl. 1, fig. 2).

In the matrix of the deposit angular lithic volcanic grains are very abundant, crystals and fragments of volcanic minerals are common, and subangular to subrounded grains of quartz, muscovite, chert, quartzose sandstone, and limestone are rare. Most of the lithic fragments are composed of glassy to hypocrystalline groundmass with microlites and dusted with magnetite; some are pieces of pumice. Volcanic minerals in the very fine sand fraction (0.06 to 0.12 mm) occur in the following order of abundance: feldspar—mainly zoned

plagioclase—magnetite, limpid quartz, biotite, hypersthene, augite, oxyhornblende, green hornblende, and apatite.

Atwood and Atwood (1926, p. 615) claimed that the Gunnison volcanic conglomerate at its type locality "exposes all the usual physical characteristics of an unstratified glacial deposit", and Larsen and Cross (1956, p. 59) maintained that it is a typical till. But the evidence is not as convincing as implied, for the Gunnison volcanic conglomerate also resembles poorly sorted stream and mudflow deposits common in Cenozoic volcanic fields throughout the Cordilleran region. In fact, the field relationships and general texture of the conglomerate suggest that it is genetically related to the coarse-grained tuff-breccia or tuff-agglomerate (Larsen and Cross, 1956, p. 70) facies of the overlying San Juan tuff whose lower beds locally contain detritus derived from older formations and overlie Precambrian and Mesozoic rocks except where the Gunnison volcanic conglomerate has been identified below them. At these localities the Gunnison volcanic conglomerate and San Juan tuff-breccia are separated by an unusual convolute surface (Fig. 2) which may have been produced by local channeling and sliding of unconsolidated Gunnison gravel as the tuff-breccia began to accumulate (Atwood and Atwood, 1926, p. 618). The proposition that the Gunnison volcanic conglomerate is closely related to the San Juan tuff-breccia is also supported by the fact that the volcanic rock fragments and the

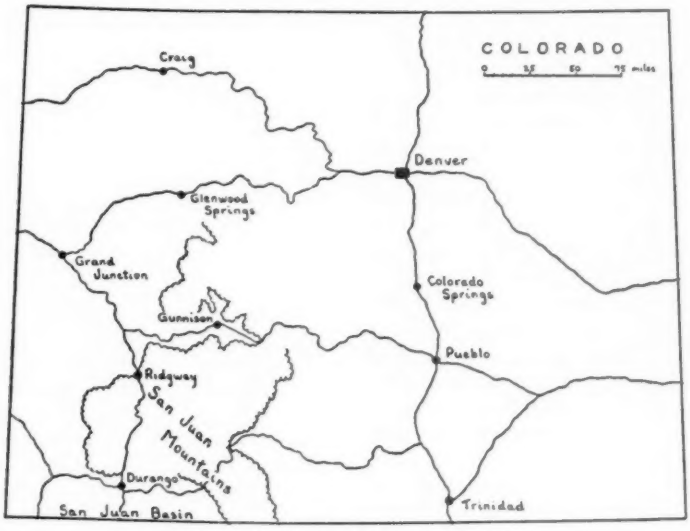

FIGURE 1.—INDEX MAP OF COLORADO

Showing location of Ridgway and Gunnison, San Juan Mountains, northern margin of San Juan Basin, and main highways.

PLATE 1.—GUNNISON AND RIDGWAY CONGLOMERATES

FIGURE 1.—Gunnison volcanic conglomerate at type locality, 3 miles east of Gunnison. Poor sorting, size range, and angularity are typical of deposit. Hammer is scale. *See* Figure 2a.

FIGURE 2.—Photomicrograph of Gunnison volcanic conglomerate from type locality, showing volcanic pebbles and crystal-lithic matrix. Plane light, × 15.

FIGURE 3.—Ridgway conglomerate at type locality on Miller Mesa, 1 mile west of Ridgway, looking westward. R—Ridgway conglomerate; T—Telluride conglomerate; SJ—San Juan tuff.

FIGURE 1

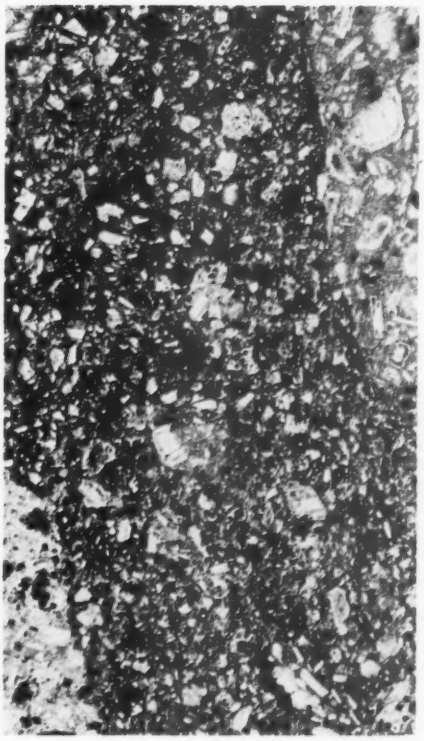

FIGURE 2

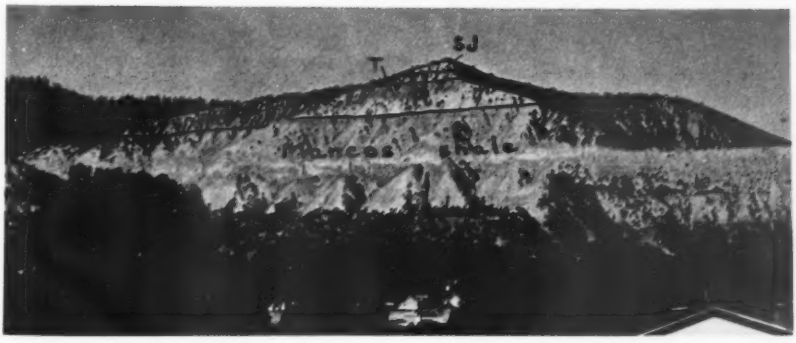

FIGURE 3

GUNNISON AND RIDGWAY
CONGLOMERATES

minerals in the matrix of the conglomerate are like those in a sample of the San Juan tuff-breccia examined in thin section, which is made up almost entirely of hornblende-pyroxene-quartz latite debris (Larsen and Cross, 1956, p. 70–75).

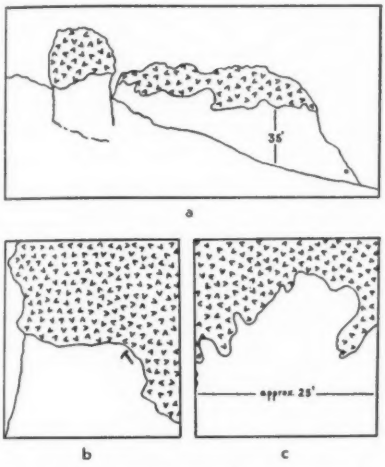

FIGURE 2.—IRREGULAR CONTACT BETWEEN GUNNISON VOLCANIC CONGLOMERATE (blank) AND OVERLYING SAN JUAN TUFF (v)
Sketched from photographs in Atwood and Atwood (1926).
a. Type locality 3 miles east of Gunnison, looking eastward. Dot indicates position of Figure 1 of Plate 1.
b. South side of Tomichi Creek, 2 miles east of Gunnison. Hammer is scale.
c. Palisades on west side of Gunnison River, 1 mile northwest of town.

In view of the similarity of the conglomerate and the tuff-breccia it is of interest to note that the bedding, sorting, and rounding of the San Juan tuff convinced Larsen and Cross (1956, p. 69, 75) that most of the formation was deposited by water. Reasonably, then, the Gunnison volcanic conglomerate, with its less coarse, subrounded detritus, may also have been deposited in part by mudflow and running water, rather than by glaciers.

Ridgway Conglomerate

Regardless of its origin, the Gunnison volcanic conglomerate was assigned an early Cenozoic age because of its supposed equivalence to the coarse-grained facies of the Ridgway "tillite" at its type locality on Miller Mesa, 1 mile west of Ridgway (Pl. 1, fig. 3). Accordingly, the validity of an early Cenozoic episode of glaciation depends primarily upon the status of the conglomerate at Ridgway. This deposit warrants serious reconsideration on both stratigraphic and lithologic grounds, even though Atwood has claimed (1915, p. 16) that it "exhibits all the usual characteristics of glacial till" and has asserted (Atwood and Atwood, 1926, p. 622) that its mid-Eocene age is conclusive.

Stratigraphy: Throughout its identified extent of about 20 square miles the volcanic-rich Ridgway conglomerate rests on the Upper Cretaceous Mancos shale and is overlain in most of its outcrops by the Telluride conglomerate which in turn is overlain by the San Juan tuff. In the original and only detailed discussion of the deposit, Atwood inferred (1915, p. 21) that it probably is of early or middle Eocene age because it accumulated after the Mesaverde formation had been eroded from the San Juan Mountains and before deposition of the Eocene (Cross, 1899) Telluride conglomerate.

Atwood and Mather (1932, p. 16) pointed out that the volcanic debris in the Ridgway conglomerate apparently was derived from the same source as the weathered andesite and rhyolite (Larsen and Cross, 1956, p. 55–56) fragments in the Upper Cretaceous and lower Paleocene Animas formation along the northern margin of the San Juan Basin. Then Cross and Larsen (1935, p. 47, 50, 55) added that the volcanic source was largely eroded from the San Juan Mountains before accumulation of the arkosic Telluride conglomerate overlying the Ridgway conglomerate in the San Juan Mountains and of the Paleocene Nacimiento (Torrejon) and upper Paleocene and lower Eocene San Jose (Wasatch) formations overlying the Animas formation in the northern part of the San Juan Basin. Unfortunately, these important observations were coupled with unfounded assumptions.

(1) A long interval of extensive uplift and deep erosion was assumed to have separated deposition of the Animas and the Ridgway formations. During this postulated episode Mesozoic and Paleozoic sedimentary rocks, as well

as most of the Upper Cretaceous and lower Paleocene volcanic rocks, supposedly were stripped from extensive areas of the San Juan Mountains which were then carved into mountains susceptible to glaciation. Time for this uplift and erosion was provided by continuing to assign the Ridgway conglomerate an Eocene age (Atwood and Mather, 1932, p. 16), despite the fact that its general correlation with the Upper Cretaceous and lower Paleocene Animas formation had been recognized. Similarly, even after Larsen and Cross (1956, p. 58, 59) pointed out that the Ridgway conglomerate is reasonably about the same age as the upper part of the Animas formation, they postulated post-Animas uplift and erosion and cited an unconformity between the Animas and the overlying Nacimiento (Torrejon) formations and one between the Animas and the Ridgway formations. Actually, the upper and lower contacts of the Animas formation in the northern part of the San Juan Basin are gradational (Barnes, 1953), and in the eastern part of the basin the Nacimiento formation grades into the Animas formation (Simpson, 1950, p. 86). Moreover, metamorphic detritus in the McDermott and Animas formations (Larsen and Cross, 1956, p. 55), as well as arkose and pebbles of granite in beds believed to be part of the Animas formation (p. 59), suggest that the San Juan Mountains block had been breached during Late Cretaceous time. Accordingly, there is no evidence of an interval of uplift and erosion separating deposition of the Animas and the Ridgway formations.

(2) Another unfounded assumption was introduced when Cross and Larsen (1935, p. 47) redated the Telluride conglomerate as Oligocene (?) instead of Eocene because the underlying Ridgway conglomerate had been assigned an Eocene age. Present stratigraphic evidence suggests not only that the Ridgway conglomerate is a general correlative of the Animas formation, having accumulated before the Upper Cretaceous and lower Paleocene pile of volcanic rocks was eroded from the source area, but also that the overlying Telluride conglomerate and its probable equivalent, the variegated arkosic Blanco Basin formation on the southern flank of the San Juan Mountains (Cross and Larsen, 1935, p. 48, 49), may correlate with the non-volcanic, variegated arkosic San José (Wasatch) formation in the San Juan Basin.[1]

Lithology: At its type locality the yellowish-gray to yellowish-orange coarse-grained facies of the Ridgway conglomerate is a very poorly sorted deposit 80–100 feet thick. Most of the fragments range from less than an inch to about a foot in diameter, yet some are as much as 15 feet in diameter (Atwood, 1915, Pl. IIIA). Although most are subangular, the degree of rounding varies greatly. Many of the smaller ones and a few of the larger ones are marked by randomly oriented scratches (Atwood, 1915, Pl. IIIB).

In the large-pebble and cobble grades fragments of weathered volcanic rock are abundant; limestone, sandstone, and dark-gray calcareous shale are common; metamorphic rock is rare.

In the coarse-sand and granule grades of the matrix, grains of olive-gray calcareous shale (probably Upper Cretaceous rock) are abundant; fragments of volcanic rock, sandstone, and limestone are common; reddish-brown mudstone and quartz grains are rare. There are also a few fragments of Cretaceous? *Inoceramus* shells.

In the fine-sand grade quartz grains (most are angular, but a few are round) and fragments of soft, light-yellowish-gray limestone are very abundant; weathered lithic volcanic fragments are common; feldspar, magnetite, and pieces of reddish-brown mudstone are rare. In addition there are grains of augite, hornblende, biotite, epidote, apatite, tourmaline, zircon, and garnet, as well as reworked specimens of the Late Cretaceous Foraminifera, *Globigerinella* sp., *Gümbelina* sp., and *Rugoglobigerina* sp. (Richard K. Olsson, personal communication, 1956).

The coloring agent in the matrix is largely concentrated in the "limonite-stained" calcareous clay fraction.

On the basis of these petrographic data the Ridgway conglomerate was derived largely

---

Kelly (1955, p. 86) has also suggested that "certain of the Wasatch–San José beds in the San Juan Basin may have been continuous with the Telluride conglomerate of the western San Juan Mountains . . ."

from Mesozoic and Paleozoic sedimentary rocks and Upper Cretaceous and lower Paleocene volcanic rocks; Precambrian rocks supplied only a minor amount of detritus. There is no petrographic evidence that a pre-Ridgway interval of uplift and erosion exposed extensive areas of Precambrian rocks in the source area (Larsen and Cross, 1956, p. 59).

TABLE 1.—CORRELATION CHART

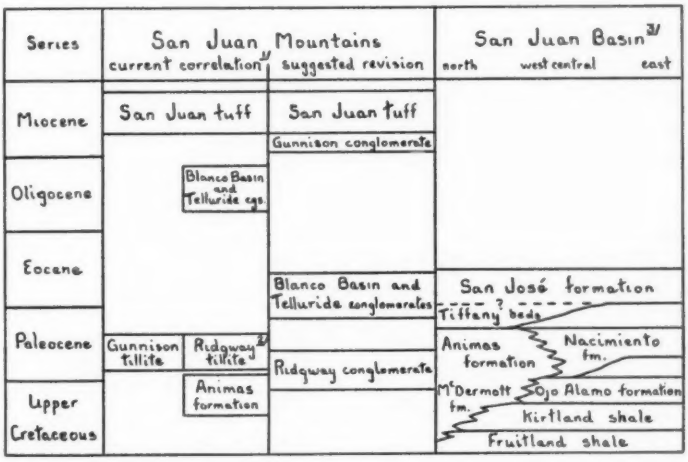

[1] After Larsen and Cross (1956, p. 57–61).
[2] Atwood (1915; 1928) thought that the Ridgway and Gunnison "tillities" were Eocene in age.
[3] After Simpson (1950, p. 87).

Mode of Origin

As Atwood presented his glacial interpretation of the Gunnison and Ridgway conglomerates it is apparent that he was so impressed by the presence of scratched stones as evidence of transportation by ice that he never seriously considered alternative modes of origin. Admittedly, the Ridgway conglomerate may be a tillite. Nevertheless this kind of deposit may also be produced by mudflows.

Numerous studies of recent and ancient mudflows demonstrate not only that they are characteristic features of areas of volcanic activity (Anderson, 1933; Cotton, 1944, p. 239–247; Crandall and Waldron, 1956; Curtis, 1954; Mason and Foster, 1956; Williams, 1932, p. 324–328), but also that their unsorted, unstratified deposits are very difficult to distinguish from glacial till.

"Ancient and dissected mudflow deposits in mountain valleys may be mistaken for glacial deposits because of their lack of assortment and the presence in them of striated rocks. Although pebbles and boulders carried by mudflows may become striatedl they lack the facets which distinguish glacia, boulders" (Thornbury, 1954, p. 92).

Significantly, both the Nirosaki mudflow (Mason and Foster, 1956), composed of blocks and smaller fragments of andesite heterogeneously scattered in a matrix of volcanic ash and dust, and the Osceola mudflow (Crandall and Waldron, 1956), an unsorted, unstratified volcanic-rich mass of boulders and smaller fragments in a matrix of reworked crystal tuff and clay, have been misidentified as glacial till.

In 1926 a mudflow origin of the Ridgway and Gunnison conglomerates was suggested by Tanakadate (Atwood, 1928, p. 1833) in a comment on Atwood's glacial interpretation of these deposits:

"It is a very difficult thing to determine the volcanic boulders as glaciated, specially at the swept zone of mud flow or avalanche area near a volcano. We have striated boulders at the foot of the Volcano Tokati-dake, and also striated pebbles on the top

of the Usa dome. These striated boulders and pebbles are not glaciated but scratched by the volcanic avalanche".

But this alternative mode of origin of the Ridgway and Gunnison conglomerates never received further consideration.

Summary

(1) The Gunnison volcanic conglomerate is a volcanic-rich mudflow and stream deposit that apparently is a basal part of the Miocene San Juan tuff (Table 1).

(2) On stratigraphic evidence the Ridgway conglomerate is a general correlative of the Upper Cretaceous and lower Paleocene Animas formation (Table 1).

(3) On lithologic evidence the Ridgway conglomerate is as reasonably a mudflow and stream deposit as it is a tillite.

(4) There is no good evidence for assigning the Telluride and apparently equivalent Blanco Basin formations an Oligocene (?) age. Instead, they are more probably arkosic border facies of the Upper Paleocene and lower Eocene San José (Wasatch) formation (Table 1).

(5) The Ridgway conglomerate was interpreted to be of glacial origin at a time in the history of American geology when a newly aroused interest in ancient glaciation tended to exaggerate its geologic importance. As a consequence poorly sorted, heterogeneous conglomerates commonly were considered to be tillites, and little attention was given to other possible modes of origin.

References Cited

Anderson, C. A., 1933, The Tuscan formation of Northern California, with a discussion concerning the origin of volcanic breccias: Univ. Calif. Pub., Bull. Dept. Geol. Sci., v. 23, p. 215–276

Atwood, W. W., 1915, Eocene glacial deposits in southwestern Colorado: U.S. Geol. Survey Prof. Paper 95, p. 13–26

—— 1917, Another locality of Eocene glaciation in southern Colorado: Jour. Geology, v. 25, p. 684–686

—— 1928, Eocene glaciation in Colorado: 3d Pan-Pacific Sci. Cong. (1926) Proc., v. II, p. 1826–1833

Atwood, W. W., and Atwood, W. R., 1926, Gunnison tillite of Eocene age: Jour. Geology, v. 34, p. 612–622

Atwood, W. W., and Mather, K. F., 1932, Physiography and Quaternary geology of the San Juan Mountains, Colorado: U. S. Geol. Survey Prof. Paper 166, p. 1–176

Barnes, Harley, 1953, Geology of the Ignacio area, Ignacio and Pagosa Springs quadrangles, La Plata and Archuleta counties, Colorado: U. S. Geol. Survey Oil and Gas Invest. OM 138

Cotton, C. A., 1944, Volcanoes as landscape forms: Wellington, Whitcombe and Tombs Ltd., 416 p.

Crandell, D. R., and Waldron, H. H., 1956, A recent volcanic mudflow of exceptional dimensions from Mt. Rainier, Washington: Am. Jour. Sci., v. 254, p. 349–362

Cross, Whitman, 1899, Telluride folio: U. S. Geol. Survey Geol. Atlas no. 57

Cross, Whitman, and Larsen, E. S., 1935, A brief review of the geology of the San Juan region of southwestern Colorado: U.S. Geol. Survey Bull. 843, p. 1–138

Curtis, G. H., 1954, Mode of origin of pyroclastic debris in the Mehrten formation of the Sierra Nevada: Univ. Calif. Pub., Bull. Dept. Geol. Sci., v. 29, p. 453–502

Dunbar, C. O., 1949, Historical geology: N. Y., John Wiley and Sons, 567 p.

Hunt, C. B., 1956, Cenozoic geology of the Colorado Plateau: U.S. Geol. Survey Prof. Paper 279, p. 1–99

Kelley, V. C., 1955, Regional tectonics of the Colorado Plateau and relationship to the origin and distribution of uranium: Univ. N. Mex. Pub. Geology, no. 5, p. 7–120

Larsen, E. S., Jr., and Cross, Whitman, 1956, Geology and petrology of the San Juan region, southwestern Colorado: U.S. Geol. Survey Prof. Paper 258, p. 1–303

Mason, A. C., and Foster, H. L., 1956, Extruded mudflow hills of Nirasaki, Japan: Jour. Geology, v. 64, p. 74–83

Moore, R. C., 1949, Introduction to Historical Geology: N.Y., McGraw-Hill Book Co., 582 p.

Scott, H. W., 1938, Eocene glaciation in southwestern Montana: Jour. Geology, v. 46, p. 628–636

Simpson, G. G., 1950, Lower Tertiary formations and vertebrate faunas of the San Juan Basin: New Mexico Geol. Soc. Guidebook of San Juan Basin, New Mexico and Colorado, p. 85–89

Thornbury, W. D., 1954, Principles of Geomorphology: N.Y., John Wiley and Sons, 618 p.

Williams, Howel, 1932, Geology of the Lassen Volcanic National Park, California: Univ. Calif. Pub., Bull. Dept. Geol. Sci., v. 21, p. 195–385

PRINCETON UNIVERSITY, PRINCETON, N. J.

MANUSCRIPT RECEIVED BY THE SECRETARY OF THE SOCIETY, OCTOBER 24, 1956

BULLETIN OF THE GEOLOGICAL SOCIETY OF AMERICA
VOL. 68, PP. 389-394, 2 FIGS. MARCH 1957

EVIDENCE OF A PRE-TACONIC OROGENY IN SOUTHEASTERN QUEBEC

BY P. H. RIORDON

Introduction

The earliest geological maps covering the stratigraphy of southern Quebec were those of Ells (1886; 1888; 1894; 1898), who considered the oldest rocks of the region to be Precambrian. These rocks include a belt of schistose sediments, accompanied by some schistose basic volcanics, which have been traced northeastward from the Vermont border for 175 miles to a point 50 miles due east of the city of Quebec (Fig. 1). Later investigators named these rocks the Sutton schists in the southern part of the belt (Clark, 1934, p. 5) and the Bennett schists in the northern portion (R. Harvie, unpublished report, Geol. Survey Canada; Cooke, 1937, p. 11; Tolman, 1936, p. 5; Beland, 1952, p. 4) and described them as Precambrian (?) or Cambrian (?).

A series of quartzites, slates, and volcanic rocks outcropping along the southeast flank of, and overlying, the Sutton-Bennett schists make up the Caldwell group (MacKay, 1921, p. 20; R. Harvie; Tolman, 1936, p. 4). Although the group is commonly in faulted contact with the schists abundant evidence throughout the length of this belt indicates that the schistose sediments grade into the Caldwell rocks (Cooke, 1937, p. 10, 1950, p. 19; Riordon, 1954, p. 4; Tolman, 1936, p. 6). Thus, in the absence of any obvious hiatus between the deposition of the sediments, from which the schists were derived, and the accumulation of the overlying Caldwell rocks, all these rocks presumably belong to the same system.

Cooke (1950, p. 40) presented evidence that the Beauceville group, considered middle Ordovician, is separated from the Caldwell group by an angular uncomformity. He describes another angular uncomformity between the Beauceville and rocks of Silurian age and notes that the latter are conformably overlain by Devonian rocks. The Silurian and Devonian rocks have also been folded.

Thus the region was subjected to three periods of orogeny. The last two are known as the Taconic and Acadian, respectively, and their existence has been confirmed by observations elsewhere in the Appalachian region both in Canada and the United States. Evidence relating to the earliest orogeny has recently been cited by Cooke (1955, p. 113), and the writer here offers supporting evidence.

Thetford-Disraeli Area

All the previous mentioned rock groups, except the Silurian, are represented in the Thetford-Disraeli area (Fig. 2).

The Beauceville group is a sedimentary series composed for the most part of slate; however, in the Thetford-Disraeli area, and to some extent in the Beauceville area (MacKay, 1921, p. 25), these sediments are underlain, apparently conformably, by a series of volcanic rocks. The volcanic rocks were originally included with the Caldwell of the Thetford-Disraeli area (Cooke, 1937, p. 19), but detailed mapping shows a marked distinction between the two. Most of the volcanic rocks interbedded with the Caldwell quartzite and slate are basaltic pillow lavas, whereas the belt of volcanic rocks between the Beauceville and the Caldwell are andesite, dacite, and trachyte flows accompanied by a large proportion of agglomerate and tuff.

The base of this belt of flows and pyroclastic rocks is marked at numerous localities by a distinctive breccia, which, in places, contains a variety of rock types but in most places is composed almost entirely of quartzite fragments. Minor amounts of schist and slate are normally present, and these coarse breccias grade into less coarse material commonly composed of fragments that vary in composition. Besides the metasediments, trachyte, andesite, basalt, gabbro, diorite, and minor amounts of granite may be present. The metasediments, and particularly the quartzite, are identical with those of the Caldwell, and

in view of the extent of the Caldwell rocks in this region it seems reasonable to assume that the fragments were derived from this source.

The breccias, which are predominantly quartzitic, contain fragments with rounded

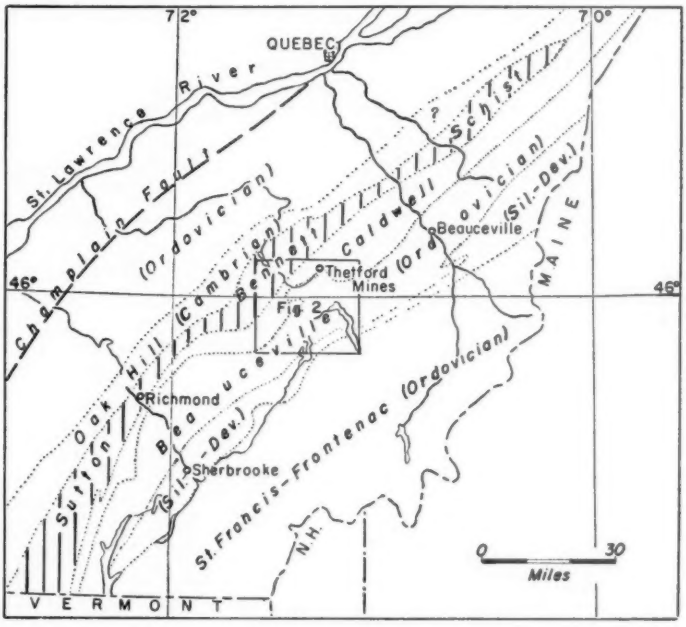

FIGURE 1.—SUTTON-BENNETT SCHIST BELT IN SOUTHEASTERN QUEBEC

corners which range from 1 inch up to blocks 6 feet across. The blocks appear to fit together like the pieces of a jig-saw puzzle with only minor interstitial material of the same composition. Undoubtedly, however, the individual fragments have been moved some distance for it is not possible to match any fragment with its neighbors. The Caldwell quartzite, from which the fragments were derived, is generally well foliated, and stringers of quartz have been injected along the planes of foliation. The attitudes of the foliation in neighboring breccia fragments and the abrupt termination of quartz stringers at the margins of the fragments indicate that intensive metamorphism of the quartzite preceded brecciation.

The irregular distribution of the breccias (Fig. 2) suggests that they do not constitute a stratigraphic unit and were derived through some process other than sedimentation. R. Harvie, who described four of these occurrences, classified them as the Clapham conglomerate; the best exposure is west of Clapham Lake. Cooke (1937, p. 24), on the other hand, considered that most of them were either tectonic or igneous in origin. Certainly, in places, there is some reason for uncertainty concerning their origin, and a brief description of the various occurrences will perhaps emphasize the evidences of sedimentation.

One of the most conspicuous and interesting occurrences of breccia is a belt, in the vicinity of Clapham Lake, that is exposed over a length of nearly 2 miles. It is only a few hundred feet in breadth, yet its outcrops stand up prominently, and it is remarkable in its continuity. It is composed of fragments of quartzite and lesser amounts of schist up to 3 feet across, though most are less than 1 foot, and these have noticeably rounded edges and corners, while the finer interstitial material contains abundant well-rounded pebbles of quartz and quartzite. Near the end of the belt that abuts on the lake and at a point midway in the belt the breccia is exposed in contact with the

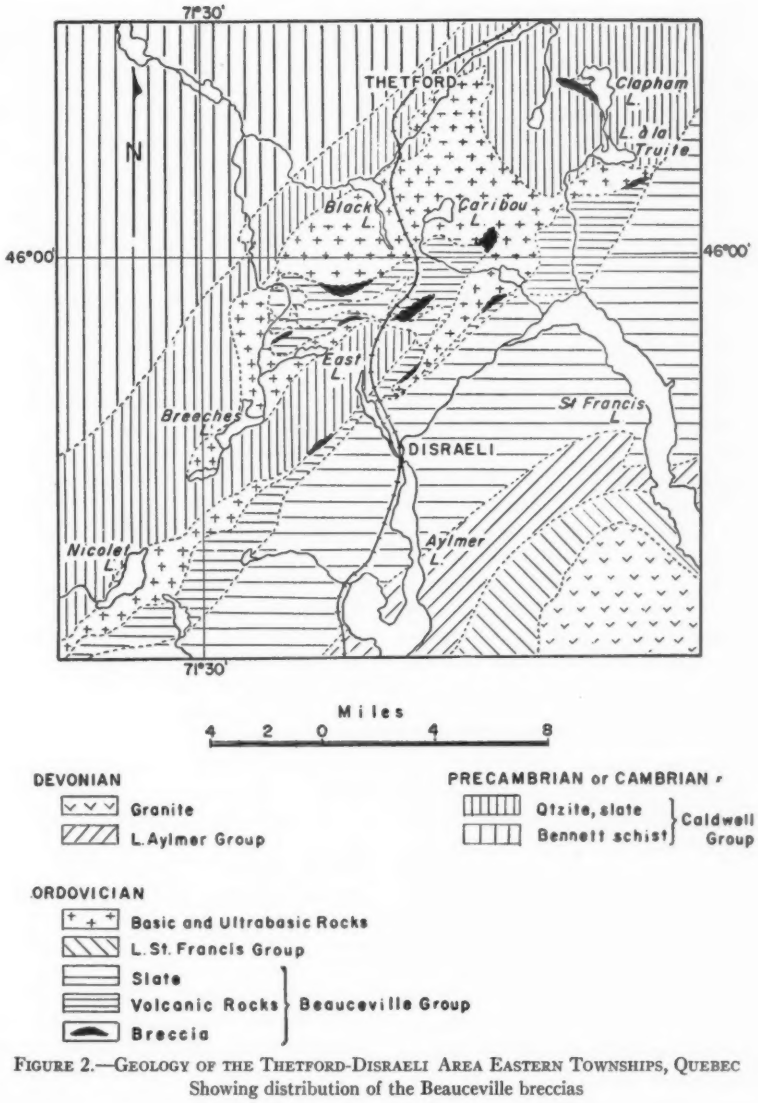

FIGURE 2.—GEOLOGY OF THE THETFORD-DISRAELI AREA EASTERN TOWNSHIPS, QUEBEC
Showing distribution of the Beauceville breccias

Caldwell quartzite; in both places the bedding of the older rock is truncated. There is no evidence of breccia grading into massive quartzite. A small area north of this belt is occupied by trachyte and slate lithologically like the Beauceville. This isolated assemblage of breccia, lava, and slate is evidently an outlier of the Beauceville surrounded by Caldwell rocks.

South of the small lake half way between Lac a la Truite and Disraeli the breccia displays pronounced bedding. The rock is composed of quartzite fragments up to 2 feet across, and locally an abundance of trachyte fragments gives the rock the appearance of an agglomerate. Across the outcrop from north to south, the breccia grades into finer material within a few feet; this is followed by a band of well-

bedded material containing mostly rounded grains of quartzite and quartz from a few millimeters up to 1 cm across. To the south, this bedded rock is in contact with a gray fissile tuff, and this contact parallels the bedding. Grain gradation in the bedded portion, along with flow cleavage in the tuff, indicates that the tops face south; thus the tuff conformably overlies the breccia. Adjacent to the contact, occasional lenses of tuff are interbedded with the breccia. At one point about 5 feet south of the main breccia-tuff contact, fragments of quartzite, up to 4 inches across, are scattered through the tuff. The intermingling of fragments of quartzite and volcanic material and the presence of some bedded material suggest an explosive and sedimentary origin for these rocks.

Fragments of quartzite, along with trachyte and gabbro, constitute the lenticular body of breccia just north of Disraeli on the crest of a prominent ridge. A few small outcrops composed of quartzite fragments occupy the immediate crest. The most northerly one is overlain by pyroclastic rocks; the flat attitude of this contact, and the dips of the tuff beds indicate that the quartzite breccia lies on the axis of an anticline.

The area of breccia near Caribou Lake is made up of two groups of outcrops. The western group is a typical quartzite breccia, with fragments up to 6 feet across, whereas the eastern group is composed of angular fragments, 4–5 mm in diameter, in a fine-grained chloritic groundmass of angular quartz and feldspar. Nothing approaching definite bedding was identified over all these large areas of outcrops. The presence of this fine-grained breccia, however, not far from the commoner coarse variety, is presumably the result of differing conditions of sedimentation in these two localities.

A lenticular body of quartzite breccia outcrops northeast of East Lake and is overlain by thinly bedded tuffs on its northern side. To the south, however, the breccia grades into a gabbro breccia, which in turn appears to grade into gabbro. These relationships are puzzling and at first suggest that all the breccia might be attributed to intrusive activity. Much of the gabbro in other parts of the Thetford-Disraeli area displays marginal zones of brecciation. Probably successive intrusions of gabbroic magma, accompanied by some adjustment and brecciation after the earliest intrusion, gave rise to this condition. Adjustment along the contacts has resulted in a mixture of fragments of gabbro and country rock, and in the vicinity of East Lake in the refragmentation of the quartzite breccia.

The area of breccia south of Black Lake is more like a trachytic to andestic agglomerate but includes many fragments of gabbro, diorite, and quartz. Most of the fragments are moderately well rounded, and in one place distinct bedding was observed.

The area of breccia south of Black Lake is more like a trachytic to andesitic agglomerate but includes many fragments of gabbro, diorite, and quartz. Most of the fragments are moderately well rounded, and in one place distinct bedding was observed.

Another large area of breccia occurs southeast of Black Lake and is made up of a great variety of fragments. In places it is a typical quartzite breccia, in others acid lava and tuff may predominate, and in still others there is a high content of gabbro and basalt. In one place, numerous large fragments of red, green, and gray lava and tuff are imbedded in a gravelly matrix which also contains large fragments of the same material. Parallel alignment of the larger elongated fragments, plus the gravelly matrix, strongly suggest a sedimentary origin.

The other small areas of breccia (Fig 2) are typical quartzite breccias.

Discussion

All the breccias are conformably overlain by the volcanic rocks of the Beauceville group. All the exposures are at the contact between the Beauceville and the Caldwell or between the Beauceville and intrusive rocks which separate them from the Caldwell. The breccias therefore are at the base of the Beauceville group. Because of the frequent association with intrusive contacts it might be inferred that the breccias are the result of intrusive activity. This association, however, does not appear in every case, and the presence of bedding and

well-rounded grains and pebbles of quartz rules out such a possibility. Similarly, a tectonic origin cannot be accepted. The evidence points to an origin due in part to explosive volcanic activity, but also in large part to sedimentary processes.

The prefoliated, quartz-injected fragments in the breccias indicate that the Caldwell rocks were folded and metamorphosed before the accumulation of the Beauceville. Furthermore, in traversing the regional strike from the Caldwell to the Beauceville rocks, there is a distinct contrast in the effects of folding. Interbeds of graywacke in the slates of the Beauceville display little if any foliation, and even the thinnest beds are not broken, whereas the tough Caldwell quartzites are almost everywhere foliated, and in many places the bedding is severely distorted. Where thin beds of quartzite are interbedded with the Caldwell slate boudinage is characteristic.

Thus the Caldwell group was quite evidently folded and metamorphosed before the accumulation of the Beauceville, but this orogeny has yet to be dated precisely. The Beauceville group has been dated as middle Ordovician, although largely on the basis of an isolated fossil occurrence about 2 miles west of Magog. Cooke has shown that rocks of known Silurian age overlie the Beauceville with marked angular unconformity. Thus the Taconic orogeny is accounted for, and the Caldwell folding must therefore be pre-Taconic.

Recent work by Cooke (1954, p. 40) led him to believe that the Sutton schists are Cambrian, for he observed that in the Richmond area these schists grade along their strike into recognizable members of the Oak Hill Series, previously established by Clark (1936, p. 145) as Lower Cambrian. On the other hand, Dresser and Denis (1944, p. 386) have observed that where the Oak Hill Series is found within the belt of Sutton schist it may be infolded remnants.

If the Sutton-Bennett schists, which are presumably a part of the Caldwell group, are Cambrian, and if the extensive belt of rocks termed the Beauceville group are all Ordovician, then an early Paleozoic orogeny must have occurred. On the other hand, the degree of intensity of the pre-Beauceville folding would suggest that the Caldwell rocks were involved in a major mountain-building epoch and are actually Precambrian.

Recent age determinations based on isotope ratios in lead ores (Wilson *et al.*, 1956, p. 553), procured from the Caldwell, indicate that these rocks may be comparable in age to the Grenville, or late Precambrian.

Acknowledgments

The writer wishes to thank the Quebec Department of Mines for permission to release much of the unpublished information incorporated in this paper. He also wishes to express his gratitude to G. S. MacKenzie of the University of New Brunswick and to H. W. McGerrigle of the Quebec Department of Mines for reading the manuscript and offering much helpful criticism.

Selected Bibliography

Beland, J., 1952, St. Magloire area, Montmagny, Bellechasse and Dorchester counties: Quebec Dept. Mines Prelim. Rept. 279

——1954, Rosaire-St. Pamphile area, Montmagny and L'Islet Counties: Quebec Dept. Mines, Prelim. Rept. 294

Burton, F. R., 1930, Vicinity of Lake Aylmer, Eastern Townships: Quebec Bur. Mines Ann. Rept., pt. D, p. 99–146

Clark, T. H., 1934, Structure and stratigraphy of southern Quebec: Geol. Soc. America Bull., v. 45, p. 1–20

——1936, A lower Cambrian series from southern Quebec: Royal Canadian Inst. Trans., v. 21, no. 1, p. 135–151

——1937, Thetford, Disraeli, and eastern half of Warwick map areas, Quebec: Geol. Survey Canada Mem. 211, p. 33–52

Cooke, H. C., 1937, Thetford, Disraeli, and eastern half of Warwick map areas, Quebec: Giol. Survey Canada Mem. 211

——1950, Geology of southwestern part of the Eastern Townships of Quebec: Geol. Survey Canada Mem. 257

——1954, The Green Mountain anticlinorium in Quebec: Geol. Assoc. Canada, v. 6, pt. II, p. 37–48

——1955, An early Palaeozoic orogeny in the Eastern Townships of Quebec: Geol. Assoc. Canada, v. 7, pt. I, p. 113–121

Dresser, J. A., 1912, Reconnaissance along the National Transcontinental Railway in southern Quebec: Geol. Survey Canada Mem. 35

Dresser, J. A., and Denis, T. C., 1944, Geology of Quebec; Quebec Dept. Mines Geol. Rept. 20, v. II

Ells, R. W., 1886, Report on the geology of a portion of the Eastern Townships: Geol. Survey Canada Ann. Rept., v. II, pt. J

——1888, Second report on the geology of a portion of the Province of Quebec: Geol. Survey Canada Ann. Rept., v. III, pt. K
——1894, Report on a portion of the Province of Quebec comprised in the southwest sheet of the "Eastern Townships" map: Geol. Survey Canada Ann. Rept., v. VII, pt. J
——1898, Report on the geology of the Three Rivers map-sheet, or northwestern sheet of the "Eastern Townships" map, Quebec: Geol. Survey Canada Ann. Rept., v. XI, pt. J
MacKay, B. R., 1921, The Beauceville map-area, Quebec: Geol. Survey Canada Mem. 127
Riordon, P. H., 1954, Thetford Mines-Black Lake area: Quebec Dept. Mines Prelim. Rept. 295
Tolman, C., 1936, Lake Etchemin map-area, Quebec: Geol. Survey Canada Mem. 199
Wilson, J. T., Russell, R. D., and Farquhar, R. M., 1956, Economic significance of basement subdivision and structures in Canada: Canad. Min. Metall. Bull., v. 49, p. 550–558

THETFORD MINES, QUEBEC, CANADA
MANUSCRIPT RECEIVED BY THE SECRETARY OF THE SOCIETY, April 2, 1956
PUBLISHED BY PERMISSION OF THE DEPUTY MINISTER, QUEBEC DEPT. OF MINES